



UNIVERSITEIT VAN PRETORIA
UNIVERSITY OF PRETORIA
YUNIBESITHI YA PRETORIA

Denkleiers • Leading Minds • Dikgopolo tša Dihlalefi

**AVIAN ADAPTIVE THERMOREGULATION CORRELATED WITH
TEMPERATURE AND HUMIDITY**

by

Marc Trevor Freeman

Submitted in partial fulfilment of the requirements for the degree

Doctor of Philosophy (Zoology)

in the

Department of Zoology and Entomology
Faculty of Natural and Agricultural Sciences

UNIVERSITY OF PRETORIA

December 2022

**AVIAN ADAPTIVE THERMOREGULATION CORRELATED WITH
TEMPERATURE AND HUMIDITY**

Dulcius ex asperis

SUMMARY

AVIAN ADAPTIVE THERMOREGULATION CORRELATED WITH TEMPERATURE AND HUMIDITY

by

Marc Trevor Freeman

Supervisor: Prof. A.E. McKechnie (DSI-NRF Centre of Excellence at the Percy FitzPatrick Institute, Department of Zoology and Entomology, University of Pretoria, Hatfield 0028, South Africa)

Department: Department of Zoology and Entomology

University: University of Pretoria

Degree: Doctor of Philosophy (Zoology)

Keywords: Avian ecophysiology, adaptive variation, extreme heat, climate change, body temperature, heat tolerance limit, hyperthermia tolerance, humidity

Extreme heat events and increasing global air temperatures pose serious challenges for the persistence of endothermic animals. Physiologically, it remains unclear whether thermoregulatory capacity and mechanisms used to maintain sublethal body temperatures at high environmental temperatures vary among species, particularly those from contrasting climatic regions which may have evolved differently in response to past and current climatic conditions. Moreover, our understanding of how abiotic variables such as humidity affect the thermoregulatory performance of species within such climatic regions and whether

species experience selection for thermal traits to overcome such conditions also remains unexplored. To address these questions, I conducted four related studies (each a chapter in this thesis) to disentangle the effects of air temperature and humidity on avian thermoregulation under hot conditions, and how thermoregulatory performance and limits vary with climate.

In my first chapter, I hypothesised that the maximum tolerable body temperature (T_{bmax}) of birds has evolved in response to climate, with raised T_{bmax} associated with species exposed to high environmental heat loads or humidity-related constraints on evaporative heat dissipation. Making use of flow-through respirometry, I collected thermoregulatory data for 53 bird species at air temperatures between 28-56°C under standardised very dry air from three contrasting climatic regions (hot arid, mesic montane and lowland humid) with varying maximum air temperatures, across South Africa. When analysed in a phylogenetically-informed comparative framework, my data revealed novel macrophysiological patterns supporting recent suggestions that endothermic animals have evolved thermal generalisation vs thermal specialisation analogous to the corresponding continuum among ectothermic animals. Among arid-zone birds, hyperthermia tolerance was relatively low, whereas evaporative cooling was characterised by higher ratios of evaporative heat loss/metabolic heat production (evaporative cooling efficiency). In contrast, among birds from more mesic and particularly humid regions hyperthermia tolerance was elevated but evaporative cooling was modest suggesting thermal generalisation. This study provides evidence that hyperthermia tolerance has evolved in response to climate.

Next, I investigated whether birds from humid habitats had evolved physiological mechanisms to reduce the impact of humidity-impeded scope for evaporative heat dissipation. Using a similar approach to my first chapter, I tested the thermal responses of 30 bird species from three contrasting climatic regions under both dry and humid conditions. I found that the effect of humidity on evaporative cooling and heat tolerance limits was less among birds occupying humid lowlands compared to arid-zone birds. My findings suggest that humid environments have resulted in selection for pronounced hyperthermic tolerance to mitigate the effects of impeded evaporative cooling efficiency, permitting lowland birds to persist during extreme heat coupled with humidity. In contrast, thermoregulatory

performance among birds from less humid habitats was more strongly affected by high humidity and they experienced substantial decreases in heat tolerance limits.

In my third and fourth chapters, I investigated the hyperthermic abilities of a small, highly gregarious passeriform bird, the red-billed quelea (*Quelea quelea*). Red-billed queleas experience extreme heat loads by foraging on the ground in direct solar radiation for long periods, often under conditions of raised humidity. The findings of this study revealed queleas to be capable of extreme hyperthermia well above known limits for endotherms, with average maximum body temperature reaching 48.0 ± 0.7 °C without any apparent ill effects. The highest body temperature recorded in this study was 49.1°C. The study sheds light on the differing hyperthermic capabilities of endotherms which may be beneficial for mitigating the impeding effects of environmental conditions such as humidity on avian thermoregulation. The impressive hyperthermia tolerance of queleas makes them an ideal model species to investigate whether hypothermia can be beneficially used as a thermoregulatory strategy to reduce the effects of extreme heat loads and impeding effects of environmental conditions.

Finally, again using red-billed queleas as a model I assessed whether the evolution of hyperthermia tolerance could be functionally linked to tolerating high heat loads and accommodating humidity-associated curtailment of evaporative cooling. My findings suggest that thermoregulatory response variables under different humidity treatments were largely similar, with queleas essentially becoming poikilothermic at very high T_{air} . No significant difference was detected in maximum tolerable body temperature and limited differences were found for heat tolerance limits. The study provides evidence that hyperthermia tolerance is functionally linked with accommodating the impeding effects of humidity on evaporative water loss and maintaining heat tolerance capacity.

In conclusion, my findings add to an increasing pool of literature regarding adaptive differences in endothermic thermoregulation in response to climate. My thesis also highlights the importance of understanding both avian species-specific thermal capabilities and conducting macro-physiological assessments for making predictions regarding responses to future predicted climatic changes.

RESEARCH OUTPUTS

Publications arising from this thesis

Chapter 1

Freeman, M.T., Czenze, Z.J., Schoeman, K. & McKechnie, A.E. (2022). Adaptive variation in the upper limits of avian body temperature. *Proc Natl Acad Sci U S A*. doi: 10.1073/pnas.2116645119/-/DCSupplemental.Published

Chapter 3

Freeman MT, Czenze ZJ, Schoeman K, McKechnie AE (2020) Extreme hyperthermia tolerance in the world's most abundant wild bird. *Sci Rep* 10:1–6. <https://doi.org/10.1038/s41598-020-69997-7>

Conference presentations and workshops

Freeman, M.T., Czenze, Z.J., Kemp, R., van Jaarsveld, B., Smit, B., Wolf, B.O., McKechnie, A.E. (2020). Regularly drinking desert birds have greater evaporative cooling capacity and higher heat tolerance limits than non-drinking species. Virtual Presentation, North American Ornithological Conference 2020 (Virtual meeting). July 2020

Freeman, M.T., Czenze, Z.J., Schoeman, K. & McKechnie, A.E. (2022). Adaptive variation in the upper limits of avian body temperature. Virtual Presentation, Birdlife South Africa, LAB Conference (Virtual meeting). 2021

Freeman, M.T., Czenze, Z.J., Schoeman, K. & McKechnie, A.E. (2022). Adaptive variation in the upper limits of avian body temperature. Hot Birds Research Project 2021 Workshop. Presentation (Skukuza, Kruger National Park). August 2021

Freeman, M.T., McKechnie, A. E. Incorporating humidity into respirometry heat tolerance protocols. Hot Birds Research Project 2021 Workshop. Facilitated workshop session (Skukuza, Kruger National Park). August 2021

Freeman, M.T., Czenze, Z.J., Schoeman, K. & McKechnie, A.E. (2022). Adaptive variation in the upper limits of avian body temperature. 4th Annual SANBI Research Conference (Virtual meeting). 2022

Freeman, M.T., Czenze, Z.J., Schoeman, K. & McKechnie, A.E. (2022). Adaptive variation in the upper limits of avian body temperature. International Ornithological Conference (Virtual meeting). 2022

LIST OF ABBREVIATIONS

T_b	body temperature
T_{air}	air temperature
HTL	heat tolerance limit
T_{bmax}	maximum body temperature
T_{bnorm}	normothermic body temperature
RMR	resting metabolic rate
EWL	evaporative water loss
EHL/MHP	ratio of evaporative heat loss to metabolic heat production
T_{bslope}	rate of increase in body temperature
EvapScope	evaporative scope
MetabCost	metabolic cost

DECLARATION

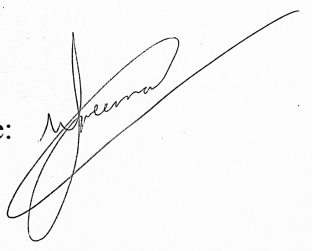
I, Marc Trevor Freeman, declare that the dissertation, which I hereby submit for the degree of Doctor of Philosophy in Zoology at the University of Pretoria, is my own work and has not previously been submitted by me for a degree at this or any other tertiary institution.

ETHICS STATEMENT

The author, whose name appears on the title page of this dissertation/thesis, has obtained, the research described in this work, the applicable research ethics approval.

The author declares that he has observed the ethical standards required in terms of the University of Pretoria's Code of Ethics for Researchers and the Policy guidelines for responsible research.

Signature:

A handwritten signature in black ink, appearing to read 'M. Freeman', is written over a light grey rectangular background.

Name: Marc T. Freeman

DATE: NOVEMBER 2022

ACKNOWLEDGEMENTS

A doctoral thesis is awarded to a single person. However, completing this thesis requires a great many things which are only possible with the help of many other people. I have been fortunate to be surrounded by remarkable people throughout my PhD research, who have provided me with so much more than I could have ever hoped for. I attempt to thank these people here.

I would first and foremost like to thank, Prof. Andrew McKechnie. Thank you for your unwavering intellectual, emotional and financial support. Your guidance and patience throughout this thesis are greatly appreciated and without them, this thesis would not have been possible. Thank you for always encouraging me to take time to think about the problem I am facing and solve it in a structured manner. You have consistently gone out of your way to make sure that I was in a position to learn, grow and complete any task or challenge presented to me. You have allowed me to embark on adventures that I will cherish for a lifetime. I consider you to be so much more than a supervisor, thank you for giving me the opportunity to make a difference.

I would like to give a special thank you to the most important person in my life, my partner, Nevanya. You have stood with me throughout this period of my life, provided endless motivation, been tolerant and shown me that even in the darkest of times there is a way forward to the light. A massive gratitude and thank you to my parents, Diane and Anthony Freeman, without whom all of what I have achieved would have been impossible. You have seen me through massive challenges in life and sacrificed a great deal to see me succeed. Your belief in my abilities has never faltered, I am the person I am today because of you, thank you, Mom and Dad. I would also like to thank my sister Shannon and her husband Deane Kearns, your support during these times has been more valued than you know.

I am extremely grateful for the support and hard work of my field assistants and colleagues namely Dr Zenon Czenze, Keegan Schoeman, Dr Celiwe Ngamphalala, Bianca Coulson, Mathome “Otto” Makola, and James Short who stood firm on the front lines with me during challenging times. Thank you for always helping me catch and assess that one last bird, which was never the last bird. I would also like to thank my past and present colleagues specifically Dr Pieter Olivier, Dr Susan Cunningham, Dr Henry Pollock, Ben Murphy and Barry van Jaarsveld.

A special thank you to the late Prof. Barry Lovegrove, whom I was fortunate to spend time with during my PhD where he taught me a great many lessons in a short space of time that will undoubtedly mould many of my decisions as well as my scientific career in years to come. I would then like to offer a heartfelt thank you to my close friends who were also completing doctoral research with me specifically, Ryno Kemp, Shannon Conradie and Tshepiso Lesedi Majelantle. Your support and willingness to impart knowledge and wisdom during my doctoral research have been colossal.

Finally, I would like to thank the landowners who provided access to their properties for me to conduct research. I would like to specifically thank, Philip Pattinson, the Wild Tomorrow Fund, Kevin Jolliffe, Julian Vickery, Pieter and Verencia Benade, Bill and Gayle Ross-Adams.

FUNDING AND PERMITS

Data collection and experimental protocols were approved by the University of Pretoria Animal Ethics committee (protocol NAS181/2019; protocol NAS141/2020) as well as Research and Scientific Ethics Committee of the South African National Biodiversity Institute (SANBI/RES/P2020/10; SANBI NZG/RES/P19/13). Birds were captured under permit JM 8,057/2019 from the Free State province's Department of Economic, Small Business Development, Tourism and Environmental Affairs, the Northern Cape government (permit number FAUNA 0010/2021) and OP4026/2019 or OP42-2022 from the Ezemvelo KwaZulu-Natal provincial wildlife authority. This work has been funded primarily through the National Research Foundation (Grant No. 119754 to Professor Andrew McKechnie), DSI-NRF Centre of Excellence at the Percy FitzPatrick Institute. The findings, conclusions and opinions do not reflect those of the NRF and are the author's own.

TABLE OF CONTENTS

CHAPTER 1	ADAPTIVE VARIATION IN THE UPPER LIMITS OF AVIAN BODY TEMPERATURE.....	1
1.1	ABSTRACT	2
	Significance Statement	2
1.2	INTRODUCTION.....	3
1.3	METHODS AND MATERIALS	5
	Study areas	5
	Study species	6
	Experimental protocol and measured response variables.....	6
	Data analyses	7
1.4	RESULTS.....	9
	Body temperature	9
	Heat tolerance limits.....	12
	Evaporative heat loss and metabolic heat production	13
1.5	DISCUSSION	16
1.6	CONCLUSION	18
1.7	ACKNOWLEDGMENTS.....	19
1.8	REFERENCES	20
	ADDITIONAL INFORMATION	28
	Appendix S1	28
CHAPTER 2	EVOLUTION OF AVIAN HEAT TOLERANCE: THE ROLE OF ATMOSPHERIC HUMIDITY.....	55
2.1	ABSTRACT	56
2.2	INTRODUCTION.....	56
2.3	MATERIALS AND METHODS	58
	Study areas	58
	Study species	60
	Air and body temperature measurements.....	60
	Experimental protocol	60
	Gas exchange measurements.....	61

Data analyses.....	61
2.4 RESULTS.....	63
Heat tolerance limits and body temperature.....	63
Evaporative water loss (EWL)	65
Maximum resting metabolic rate (RMR).....	68
Maximum evaporative cooling efficiency (EHL/MHP)	68
2.5 DISCUSSION	70
2.6 CONCLUSION	73
2.7 ACKNOWLEDGMENTS.....	73
2.8 REFERENCES.....	74
2.9 ADDITIONAL INFORMATION	80
Appendix M1.....	80
Appendix S1	87
CHAPTER 3 EXTREME HYPERTHERMIA TOLERANCE IN THE WORLD'S MOST ABUNDANT WILD BIRD.....	119
3.1 ABSTRACT	120
3.2 INTRODUCTION.....	120
3.3 METHODS.....	121
Study site and species.....	122
Air and body temperature measurements.....	122
Gas exchange measurements.....	123
Experimental protocol	124
Data analysis.....	125
3.4 RESULTS.....	125
3.5 DISCUSSION	127
3.6 REFERENCES.....	130
3.7 ACKNOWLEDGMENTS.....	135
3.8 ADDITIONAL INFORMATION	136
CHAPTER 4 HEAT AND HUMIDITY: THE ROLE OF HYPERTHERMIA IN AVIAN HEAT TOLERANCE	137
4.1 ABSTRACT	138

4.2	INTRODUCTION.....	138
4.3	MATERIALS AND METHODS	140
	Study sites	140
	Study species	141
	Air and body temperature measurements.....	141
	Gas exchange measurements.....	142
	Experimental protocol	144
	Data analyses.....	144
	Humidity treatment analysis.....	145
4.4	RESULTS.....	146
	Body temperature and heat tolerance limits.....	146
	Evaporative Water loss (EWL)	149
	Resting metabolic rate (RMR)	151
	Evaporative cooling efficiency.....	152
4.5	DISCUSSION	154
4.6	CONCLUSION	156
4.7	ACKNOWLEDGMENTS.....	157
4.8	REFERENCES.....	158
4.9	ADDITIONAL INFORMATION	162

CHAPTER 1 ADAPTIVE VARIATION IN THE UPPER LIMITS OF AVIAN BODY TEMPERATURE

This chapter appears in Proceedings of the National Academy of Sciences of the United States of America volume 119 • 2022 and is formatted in line with the journal's requirements 10.1073/pnas.2116645119/-/DCSupplemental.Published

1.1 ABSTRACT

Physiological performance declines precipitously at high body temperature (T_b), but little attention has been paid to adaptive variation in upper T_b limits among endotherms. We hypothesized that avian maximum tolerable body temperature (T_{bmax}) has evolved in response to climate, with higher T_{bmax} in species exposed to high environmental heat loads or humidity-related constraints on evaporative heat dissipation. To test this hypothesis, we compared T_{bmax} and related variables among 53 bird species at multiple sites in South Africa with differing maximum air temperatures (T_{air}) and humidity using a phylogenetically-informed comparative framework. Birds in humid, lowland habitats had comparatively high T_{bmax} (mean \pm SD = $45.60 \pm 0.58^\circ\text{C}$) and low normothermic T_b (T_{bnorm}), with a significantly greater capacity for hyperthermia ($T_{bmax} - T_{bnorm}$ gradient = $5.84 \pm 0.77^\circ\text{C}$) compared to birds occupying cool montane ($4.97 \pm 0.99^\circ\text{C}$) or hot arid ($4.11 \pm 0.84^\circ\text{C}$) climates. Unexpectedly, T_{bmax} was significantly lower among desert birds ($44.65 \pm 0.60^\circ\text{C}$), a surprising result in light of the functional importance of hyperthermia for water conservation. Our data reveal a novel macrophysiological pattern and support recent arguments that endotherms have evolved thermal generalization *versus* specialization analogous to the continuum among ectothermic animals. Specifically, a combination of modest hyperthermia tolerance and efficient evaporative cooling in desert birds is indicative of thermal specialization, whereas greater hyperthermia tolerance and less efficient evaporative cooling among species in humid lowland habitats suggests thermal generalization.

Significance Statement

We compare body temperatures (T_b) and the associated thermoregulatory traits of 53 bird species from three climatically distinct areas to test the idea that maximum T_b and hyperthermia tolerance evolves in response to climate-related thermoregulatory demands and constraints. The notion of adaptive variation in T_b among endothermic animals has gained traction recently, but the potential role of climate as a correlate of interspecific variation in upper T_b limits has received little attention. Our finding that both maximum

tolerable T_b and normothermic T_b vary significantly among birds occupying sites that vary in humidity and maximum air temperatures provide new insights into avian adaptive thermoregulation.

1.2 INTRODUCTION

Body temperature (T_b) has pervasive effects on physiological function (1, 2) and performance declines when T_b deviates below or above optimal values, constraining the ranges of environmental temperatures animals can tolerate (3, 4). Among ectotherms, considerable adaptive variation correlated with climate in lower thermal limits contrasts with phylogenetic and geographical conservatism in upper thermal limits [e.g., (3, 5, 6)]. Less attention has focused on the adaptive significance of inter- and intraspecific variation in T_b among endotherms, with hypotheses concerning avian and mammalian physiological adaptation to climate typically tested via comparative analyses of metabolic rate [e.g., (7–9)] or evaporative heat loss [e.g., (10, 11)]. Historically, endotherm T_b was viewed as a non-adaptive constant (12), and most comparative analyses of avian or mammalian T_b focused on scaling with body size (13–15). However, the last decade has seen increasing interest in adaptive thermoregulation among endotherms, focusing on whether endotherm thermal performance curves show a continuum from thermal generalization to specialization and whether optimality models can predict patterns of T_b (16–18). Several studies have reported patterns of inter- or intraspecific T_b patterns broadly consistent with predictions arising from this conceptual framework (19–22).

Most investigations of adaptive variation in T_b among endotherms have focused on normothermic T_b [T_{bnorm} - e.g., (23–25)]. Adaptive variation in maximum tolerable body temperature [T_{bmax} , the highest T_b reached before rapid declines in performance and broadly analogous to critical thermal maximum in ectotherms, (26)], on the other hand, has received almost no attention, likely on account of the technical challenges associated with accurately quantifying gas exchange at very high air temperatures while still maintaining low humidity levels in metabolic chambers. Selection favoring high endotherm T_{bmax} might be expected among taxa that regularly experience environmental temperatures approaching or exceeding T_{bnorm} and for which larger thermal safety margins have obvious adaptive value. Selection for hyperthermia tolerance would also be predicted for diurnal taxa occupying hot, arid environments where heat storage is vital for water conservation (27, 28). In addition,

pronounced hyperthermia tolerance likely confers thermal benefits in warm, humid habitats where high atmospheric humidity constrains evaporative heat dissipation (29–32).

Among birds and small mammals, T_{bmax} ranges from ~ 38 °C to 46 °C, with arid-zone birds among the most heat-tolerant taxa in terms of their capacity to maintain T_b at sublethal levels at very high environmental temperatures (33). Avian T_b typically increases above active-phase normothermic values of 39 °C - 41 °C during heat exposure or following intense activity (34–36). Avian T_{bmax} values associated with thermoregulatory failure or the loss of coordinated locomotor capacity are typically 42 °C - 44 °C among non-passerines and 44 °C - 45 °C in passerines [reviewed by McKechnie *et al.* (35)]. Occasionally, however, higher T_{bmax} has been reported with Weathers (29) documenting individual T_{bmax} as high as 47.0 °C in a small passerine from the tropical lowlands of Panama, leading him to hypothesize that elevated T_{bmax} confers adaptive advantages in humid environments where evaporative heat loss is constrained. More recently, even higher T_{bmax} (mean for 20 individuals = 48.0 °C; highest individual value = 49.1 °C) has been reported for an African passerine that forms vast flocks (37). Overall, however, relatively little is known about interspecific variation in avian T_{bmax} beyond ~ 60 arid-zone species [e.g., (38–40)].

In light of increasing evidence for adaptive thermoregulation in endotherms, we hypothesized that avian hyperthermia tolerance has evolved in response to climate, with high environmental temperatures or constraints on evaporative cooling selecting for higher T_{bmax} among inhabitants. To test this hypothesis, we evaluated T_{bmax} associated with thermal endpoints in 53 species at three sites at similar latitudes, but substantially different climate. We predicted a) T_{bmax} is high among arid-zone birds, on account of their evolutionary history of high air temperature (T_{air}) and reduced water access, b) T_{bmax} is high in birds inhabiting humid lowlands, reflecting constraints imposed by high levels of humidity on evaporative cooling (29), and c) T_{bmax} is lower among birds occupying mesic montane regions where T_{air} and humidity values are low and where less selection pressure might be expected for hyperthermia tolerance, relative to deserts and humid lowlands. To elucidate the ecological significance and physiological mechanisms underlying variation in T_{bmax} , we also quantified traits related to evaporative heat loss and metabolic heat production at high T_{air} .

1.3 METHODS AND MATERIALS

Study areas

We obtained data for bird assemblages occurring in three climatically distinct areas (hot arid, mesic montane, humid lowland) at latitudes of S 25.75° – S 29.25° in South Africa (*SI Appendix*, Fig. S1). We measured T_{bmax} and related variables for birds at mesic montane and humid lowland sites and used published data collected using almost identical experimental protocols for a hot, arid region (38, 39, 67, 68). Climatic data (*SI Appendix*, Fig. S1) for all study sites were obtained for the period 1970 – 2000 from the WorldClim2 database (69).

Our mesic montane study site was located near the town of Harrismith (28°11'S, 29°10'E), Free State province, South Africa. Situated in a mountainous area at the eastern edge of the South African escarpment, two main vegetation types prevail: Basotho montane shrub lands on basalt and sandstone mountains and eastern Free State sandy grasslands in valleys (70), although the latter are heavily transformed by agriculture. Mean austral spring/summer (October - March) maximum T_{air} at the site is 26.4 °C, with mean annual precipitation of ~713 mm (69); *SI Appendix*, Fig. S1).

The humid lowland study site was located near the town of Richards Bay (28°46'S, 32°2'E), KwaZulu-Natal, South Africa. The area consists of a mosaic of natural grasslands, woodlands and coastal lowland forest embedded in a matrix of human-modified land use types (60). The climate is humid and subtropical with a mean spring/summer maximum T_{air} of 28.2 °C and mean annual precipitation of ~1126mm (*SI Appendix*, Fig. S1).

We used published data for arid-zone species investigated at multiple sites in the southern Kalahari [(38) - 27°04'S, 21°23'E, (68) - 26°58'S, 21°50'E and (39) - 26°06'S, 22°52'E] and the Koa river valley south of the town of Aggeneys, Northern Cape province, South Africa [(39) and (67) - 29°18'S, 18°51'E]. All arid-zone study sites fall within the arid savanna and Nama Karoo biomes. The mean austral spring/summer maximum T_{air} for all three southern Kalahari sites is 34.9 °C, with mean annual precipitation of ~210mm (*SI Appendix*, Fig. S1). At the Aggeneys site, mean austral spring/summer maximum T_{air} is 31.0°C and mean annual precipitation ~134mm (Fig. 1).

Study species

We measured T_{bmax} and quantified patterns of EHL and MHP at high T_{air} in 346 individuals representing 31 species (some of which occurred at more than one site) at our montane ($n = 16$ species) and lowland ($n = 20$ species) sites during the austral spring/summer of 2019-20. We included published data for *Quelea quelea* (37), collected at the same Harrismith study site. Published data from the arid sites included 199 individuals representing 23 species (*SI Appendix*, Table S1) for which T_{bmax} and all physiological trait values relevant to this study were measured. Body mass (M_b) of the species included in this analysis ranged from 7 – 110 g and did not differ significantly among study areas. Overall, our analysis is based on 53 species, representing 6 orders [Apodiformes (swifts), Coliiformes (mousebirds), Passeriformes (songbirds), Piciformes (barbets and tinkerbirds), Coraciiformes (bee-eaters and kingfishers) and Cuculiformes (cuckoos)] and 22 families. For seven species, data were collected at multiple study areas, with only one species (*Lanius collaris*) investigated at all three study areas ((*SI Appendix*, Table S1).

Experimental protocol and measured response variables

Measurements of gas exchange, T_{air} and T_b and the experimental protocol involved methods identical those described by Czenze *et al.* (39) ; see *SI appendix* for details. These methods and data inclusion criteria were also used in other studies from which we obtained data (38, 67, 68); all data included were collected under standardized conditions. In brief, thermoregulatory responses were assessed using flow-through respirometry. Birds were placed individually in an airtight metabolic chamber fitted with a plastic mesh platform (on which birds could rest) elevated ~10 cm above a ~1 cm layer of mineral oil to prevent evaporation from excreta affecting water vapor pressure readings. An oil-free compressor provided atmospheric air which was subsequently scrubbed of water vapor using a membrane dryer (Champion®CMD3 air dryer and filter; Champion Pneumatic, Princeton, USA), while a mass flow controller (Alicat Scientific Inc., Tucson, AZ, USA) was used to regulate experimental channel flow rates maintaining low humidity levels within the chamber and standardizing experimental chamber conditions experienced by all birds across study sites.

Measurements took place during the day. Relationships between T_b , EWL, MR and EHL/MHP over air temperatures ranging from 28 – 56 °C were quantified by exposing birds to a stepped T_{air} profile involving 4°C increments between $T_{air} = 28$ and $T_{air} = 40$ °C and 2°C increments at $T_{air} > 40$ °C. Temperature-sensitive passive integrated transponder (PIT) tags (Biotherm; Biomark, Idaho, ID, USA) injected intraperitoneally into each bird were used to measure T_b continuously (every second) and quantify T_bmax values and heat tolerance limits (HTL). We recorded T_b values using a portable transceiver system (HPR+; Biomark, Idaho, ID, USA) connected to an antenna placed alongside the metabolic chamber.

Birds were monitored continuously during measurements using an infrared camera and were removed from the chamber only when T_bmax was deemed to have been elicited. Our criteria for T_bmax follow previously used methods (38); these authors identified thermal endpoints as loss of coordination/balance, or rapid uncontrolled increases in T_b associated with declines in EHL or MHP. Birds' activity levels were closely monitored during measurements and only data from calm birds were included in analyses.

Data analyses

1.3.1.1 Within-species patterns of thermoregulation

We quantified physiological response variables for each individual and used these to calculate mean values per species. Species sample sizes (n) for most species were n = 10 individuals, but for seven species varied between n = 6 and n = 10 (*SI Appendix*, Tables S2.1 and S3.1). All analyses were conducted in R 4.0.5 (R Core Team, 2020). The physiological response variables HTL, T_bnorm , T_bslope , EvapScope, MetabCost, maximum EHL/MHP and MR were quantified for each individual. Respective inflection T_{air} values above which T_b , EWL, EHL/MHP and MR increase rapidly were identified using the package *segmented.lme* (71), with individual identity included as a random predictor. We analysed T_b , EWL, and MR above and below inflection points separately using linear mixed-effect models in the R package *nlme* (72), estimating the slopes for the relationships of thermoregulatory response variables as functions of T_{air} . The “dredge” function in the *MuMIn* package was used to conduct model selection (73). Our initial standardised model included T_{air} (or $T_{air}-T_b$), M_b and the $T_{air}:M_b$ interaction. Body mass did not emerge as a significant ($p > 0.05$) predictor for any response variables of any species and did not improve model fit. It was subsequently excluded from analyses. We selected the model with the

highest rank among competing models using Akaike information criterion values corrected for small sample size (AIC_c) and Akaike weights (74). If competing models were within $\Delta AIC_c < 2$, we retained the most parsimonious model. We accounted for pseudoreplication by including individual identity as a random factor in all analyses. Significance was assessed at $\alpha < 0.05$ and values are presented as mean \pm SD.

1.3.1.2 Among-site comparisons

To evaluate the influence of phylogeny on patterns of T_{bmax} and explanatory physiological variables we downloaded 100 phylogenies from www.birdtree.org (75), using the Hackett phylogeny as a back-bone (76). We constructed a maximum-likelihood tree including all study species using *Mesquite* (77). Branch-length transformations were determined using Akaike's information criterion (AIC) by comparing an Ornstein-Uhlenbeck model (78) to a Brownian motion model of trait evolution (79). The Ornstein-Uhlenbeck model was retained as it yielded lower AIC scores.

We tested for phylogenetic signal by estimating Pagel's λ (80) in the residual error of our phylogenetic generalized least-squares regressions (PGLS) while simultaneously estimating regression parameters (81), and rescaled our models using the estimates of λ . Significant phylogenetic signal was detected in T_{bmax} and all related physiological variables, when including M_b and locality as predictor variables (Table 5). We also tested for phylogenetic signal within study areas. Within lowland and montane study sites phylogenetic signal was not detected (Pagel's $\lambda = 0$), whereas it was for our arid study area (Pagel's $\lambda = 0.637$). The significant phylogenetic signal was driven by the inclusion of six closely-related lark (Alaudidae) species (*SI Appendix*, Table S1). The exclusion of larks from the arid-zone dataset resulted in no phylogenetic signal being detected (Pagel's $\lambda = 0$). We therefore present results from both conventional generalized models (GLS) and post hoc multiple comparison tests (Tukey HSD) as well as PGLS analysis and phylogenetically-informed post hoc tests (phylANOVA) where phylogenetic signal occurred. Whereas there were some differences between the results of phylogenetic and conventional analyses, conventional regression and multiple comparison analyses largely confirmed the results of phylogenetic analyses (*SI Appendix*, Table S4 and S6). We included M_b when testing for λ to account for the allometric scaling of physiological traits such as basal metabolic rate (82, 83) and HTL (84).

The ‘pgls’ function in the R package CAPER (85) was used to conduct all regression analysis. To detect differences in T_bmax between study areas and determine significance of physiological variables on patterns of T_bmax , we developed a multivariate additive linear model. We again used the *MuMIn* package and “dredge” function to conduct a model selection procedure (73) using AIC values and weights to identify the model that best explained observed patterns of T_bmax . In conjunction with the model selection approach, we also tested for auto-correlation among predictor variables (*SI Appendix*, Table S7, Durbin Watson test), and assessed the normality of residual distribution for model outputs using a Shapiro-Wilk test. Four competing models were within $\Delta AIC < 2$ (*SI Appendix*, Table S5). We selected model 3.3 ($T_bmax \sim \text{Climate} + \text{HTL} + \text{MaxEHL/MHP} + T_b\text{slope} + T_b\text{norm} + \text{HTL:climate}$; *SI Appendix*, Table S5), as it was most parsimonious. This model excluded EvapScope and M_b , but incorporated all other thermoregulatory variables. Since this model included an interaction between study locality and HTL (*SI Appendix*, Table S5) we investigated each study area separately for the relationship between T_bmax and HTL (PGLS) to unravel the drivers behind the interaction. Residuals for model 3.3 were found to be normally distributed (Shapiro-Wilk normality test: $p=0.34$).

The `anova.pgls` function in the R-package “*caper*” (85) was applied to our multivariate model output to determine significance of predictor variables and assess whether values of T_bmax differed significantly among study localities (*SI appendix*, Table S6). We subsequently conducted a *post-hoc* multiple comparison taking into account phylogenetic relationships using the PhylANOVA function in the R package “*phytools*” (86) to obtain pairwise differences in T_bmax as well as predictor variables between study localities. The PhylANOVA function conducts a simulation-based phylogenetic ANOVA and performs all *post-hoc* comparisons of means among groups providing a p-value by phylogenetic simulation (87).

1.4 RESULTS

Body temperature

Among the 53 study species, T_bmax ranged from 43.2 °C to 48.0 °C. The top multivariate model for T_bmax (*SI Appendix*, Table S5; PGLS/GLS: $F_{8,51} = 19.21$, $p < 0.001$, $R^2=0.72$) revealed the following significant predictors: climate ($p < 0.001$), heat tolerance limit (HTL,

the maximum T_{air} tolerated before the onset of severe hyperthermia; $p < 0.001$), maximum evaporative cooling capacity [MaxEHL/MHP - calculated as maximum evaporative heat loss(EHL) / metabolic heat production (MHP); $p < 0.001$], the slope of T_b as a function of T_{air} above thermoneutrality ($T_b slope$; $p < 0.001$), $T_b norm$ ($p < 0.001$) as well as the interaction between HTL and climate ($p < 0.001$). The $T_b max$ of arid-zone birds ($\bar{x} = 44.65 \pm 0.60^\circ\text{C}$) was significantly lower (by $\sim 0.9^\circ\text{C}$ compared to those of birds from the montane ($\bar{x} = 45.42 \pm 0.78^\circ\text{C}$; PhylANOVA: $t = -3.72$, $p < 0.01$, Tukey: HSD = -0.77 , $p < 0.001$) and lowland ($\bar{x} = 45.60 \pm 0.58^\circ\text{C}$; PhylANOVA: $t = -4.79$, $p < 0.01$, Tukey: HSD = -0.95 , $p < 0.001$) sites. Montane and lowland birds did not differ in $T_b max$ (PhylANOVA: $t = -0.83$, $p = 0.45$; Tukey: HSD = -0.18 , $p = 0.69$) (Fig. 1) in the overall data set. However, the exclusion of two species with atypically high $T_b max$ values (*Quelea quelea*, 48.0°C and *Euplectes orix*, 46.4°C) resulted in $T_b max$ among montane birds ($\bar{x} = 45.18 \pm 0.24^\circ\text{C}$) becoming significantly lower than those of lowland birds (PhylANOVA: $t = -2.36$, $p = 0.02$, Tukey: HSD = -0.42 , $p = 0.56$), but still significantly higher compared to arid-zone birds (PhylANOVA: $t = 3.06$, $p = 0.03$, Tukey: HSD = 0.53 , $p < 0.01$). When included in the multivariate model, M_b was not a significant predictor ($t = -1.88$, $p = 0.07$) of $T_b max$ [model 3.2 (PGLS/GLS: $F_{9,50} = 14.51$, $p < 0.001$, $R^2=0.70$); *SI appendix*, Table S5] and was auto-correlated with other predictor variables (*SI appendix*, Table S7). The rate of increase in T_b (i.e., $T_b slope$) was significantly higher among lowland birds ($\bar{x} = 0.40 \pm 0.07^\circ\text{C}$) than in arid-zone ($\bar{x} = 0.29 \pm 0.07$, PhylANOVA: $t = 4.07$, $p = 0.003$; Tukey: HSD = 0.11 , $p < 0.001$) and montane birds ($\bar{x} = 0.34 \pm 0.09^\circ\text{C}$, PhylANOVA: $t = 2.26$, $p = 0.02$; Tukey: HSD = 0.06 , $p = 0.07$). No significant difference in $T_b slope$ was detected between montane and arid-zone birds (PhylANOVA: $t = 2.2$, $p = 0.15$; Tukey: HSD = 0.05 , $p = 0.08$; Fig. 2B).

Normothermic T_b ranged from $38.5 - 42.2^\circ\text{C}$. The $T_b norm$ of lowland birds ($\bar{x} = 39.76 \pm 0.60^\circ\text{C}$) was significantly lower by $\sim 0.7^\circ\text{C}$ than those of arid-zone ($\bar{x} = 40.55 \pm 0.71^\circ\text{C}$; PhylANOVA: $t = -4.27$, $p = 0.03$; Tukey: HSD = -0.79 , $p < 0.001$) and montane birds ($\bar{x} = 40.45 \pm 0.56^\circ\text{C}$; PhylANOVA: $t = -3.31$, $p = 0.003$; Tukey: HSD = -0.69 , $p < 0.001$). Montane and arid-zone birds' $T_b norm$ did not differ significantly (PhylANOVA: $t = -0.48$, $p = 0.51$; Tukey: HSD = -0.1 , $p = 0.88$). The difference between $T_b max$ and $T_b norm$ was significantly larger among lowland birds ($\bar{x} = 5.84 \pm 0.77^\circ\text{C}$) compared to montane ($\bar{x} = 4.97 \pm 0.99^\circ\text{C}$; PhylANOVA: $t = 0.87$, $p < 0.01$; Tukey: HSD = 0.74 , $p < 0.01$) and arid-zone birds ($\bar{x} = 4.11 \pm 0.84^\circ\text{C}$; PhylANOVA: $t = 1.74$, $p < 0.001$; Tukey: HSD = 1.48 , $p <$

0.01), and was also significantly higher for montane (PhylANOVA: $t = 0.87$, $p < 0.01$; Tukey: $HSD = 0.68$, $p = 0.03$) compared to arid-zone birds (Fig. 1).

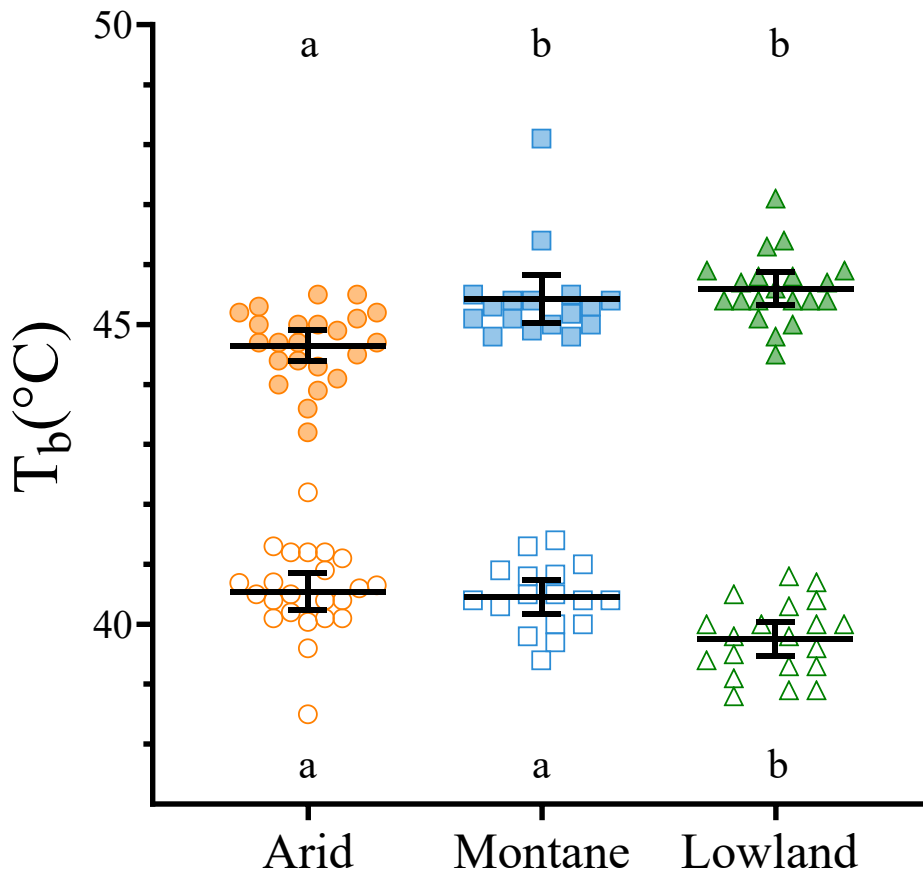


Figure 1 Maximum body temperature (T_{bmax} ; filled symbols) and normothermic body temperature (T_{bnorm} ; white filled symbols) varied significantly among 53 South African bird species across multiple climatic study sites with differing maximum air temperature and humidity. Horizontal lines represent mean values and vertical lines 95% confidence intervals. Letters above plots denote significant differences ($\alpha < 0.05$) in T_{bmax} values between sampling localities; letters at the bottom denote significant differences ($\alpha = 0.05$) in T_{bnorm} values. Significant differences are derived from phylogenetic analysis of variance post-hoc multiple comparison assessments and conventional Tukey multiple comparison assessments regressions. Climate categories are hot arid (orange circles, $n=23$), mesic montane (blue squares, $n=17$) and humid lowland (green triangles, $n=20$).

Heat tolerance limits

Heat tolerance limits (HTL) ranged from 43.3 °C to 56.0 °C ($\bar{x} = 49.09 \pm 2.47$ °C; Fig 3A, *SI Appendix*, Tables S3.1 and S4.1). Regression analysis revealed T_{bmax} was positively correlated with HTL at our montane site (PGLS/GLS: $F_{1,15} = 13.21$, $p < 0.001$, $R^2 = 0.47$), but not at our arid (PGLS: $F_{1,21} = 0.04$, $p = 0.84$, $R^2 = 0.002$, GLS: $F_{1,21} = 0.03$, $p = 0.86$, $R^2 = 0.01$) or lowland sites (PGLS/GLS: $F_{1,18} = 0.84$, $p = 0.36$, $R^2 = 0.001$), explaining the interaction between HTL and climate (study area) in model 3.3 (*SI Appendix*, Table S5). After controlling for the effects of body mass (M_b), post hoc multiple comparative analysis revealed arid-zone birds ($\bar{x} = 50.59 \pm 2.57$ °C) had significantly higher HTL by ~ 2.5 °C than birds from the montane ($\bar{x} = 47.55 \pm 1.56$ °C; PhylANOVA: $t = 4.59$, $p < 0.003$; Tukey: HSD = 3.06, $p < 0.001$) or lowland ($\bar{x} = 48.67 \pm 2.04$ °C; PhylANOVA: $t = 3.25$, $p = 0.004$; Tukey: HSD = 2.06, $p < 0.001$) sites. No significant difference in HTL occurred between montane and lowland birds (PhylANOVA: $t = -1.45$, $p = 0.16$; Tukey: HSD = -0.99, $p = 0.32$; Fig. 2A, *SI Appendix*, Table S6).

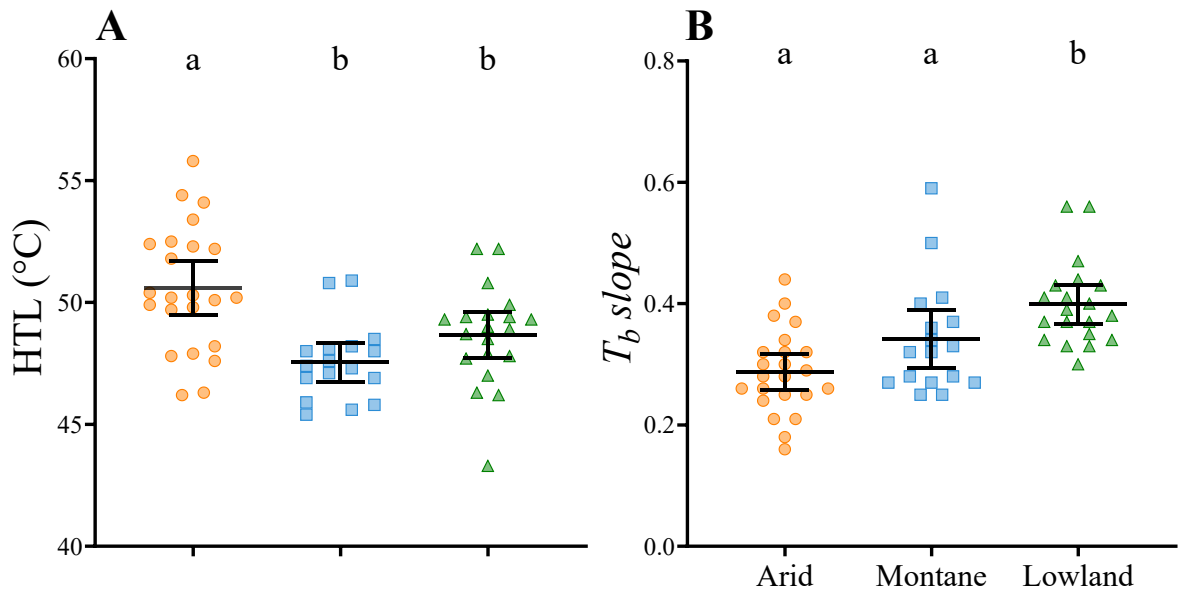


Figure 2 Heat tolerance limits (HTL; i.e., maximum air temperature tolerated; A) and the slope of T_b above the upper critical limit of thermoneutrality (T_b slope; B) among 53 South African bird species across a longitudinal gradient in air temperature and humidity. Horizontal lines represent mean values and vertical lines 95% confidence intervals. Letters above plots denote significant differences ($\alpha = 0.05$) as derived from phylogenetic analysis of variance post hoc multiple comparison assessments. Climatic categories are hot, arid (orange circles, $n=23$), mesic montane (blue squares, $n=17$) and humid lowland (green triangles, $n=20$).

Evaporative heat loss and metabolic heat production

Maximum ratios of evaporative heat loss (EHL) and metabolic heat production (MHP) were significantly ($\sim 26\%$) higher in arid-zone birds ($\bar{x} = 1.91 \pm 0.25$) compared to montane ($\bar{x} = 1.57 \pm 0.25$; PhylANOVA: $t = 3.03$, $p = 0.003$; Tukey: HSD = 0.34, $p = 0.01$) or lowland birds ($\bar{x} = 1.46 \pm 0.26$; PhylANOVA: $t = 4.3$, $p = 0.003$; Tukey: $t = 0.45$, $p < 0.001$), but did not differ between montane and lowland birds (PhylANOVA: $t = -1.05$, $p = 0.33$; Tukey: HSD = 0.12, $p = 0.55$) (Fig. 3A). Conventional and phylogenetic regression analysis revealed T_{bmax} and maximum EHL/MHP were significantly and negatively correlated among arid-birds (PGLS: $F_{1,21} = 4.99$, $p = 0.04$, $R^2 = 0.15$; GLS: $F_{1,21} = 3.77$, $p = 0.07$), but not among montane (PGLS/GLS: $F_{1,15} = 0.55$, $p = 0.47$, $R^2 = 0.04$) or lowland birds (PGLS/GLS: $F_{1,18} = 2.48$, $p = 0.13$, $R^2 = 0.07$; Fig. 3B)

Evaporative scope (EvapScope; maximum EWL/minimum thermoneutral EWL) was not a significant predictor of T_{bmax} in model 3.1 ($t=1.33$, $p=0.19$) and increased AIC values when included in our multivariate regression model (*SI Appendix*, Table S5). Multiple comparison analysis revealed montane birds ($\bar{x} = 7.86 \pm 1.67$) had significantly (~21 %) lower EvapScope than arid-zone ($\bar{x} = 9.07 \pm 2.60$; PhylANOVA: $t = -2.09$, $p = 0.02$; Tukey: HSD = -1.99, $p = 0.1$) or lowland ($\bar{x} = 10.86 \pm 2.78$; PhylANOVA: $t = -2.67$; $p = 0.01$; Tukey: HSD = -2.62, $p = 0.03$) birds. There was no significant difference in EvapScope between lowland and arid-zone birds (PhylANOVA: $t = -0.69$, $p = 0.51$; Tukey: HSD = 0.63, $p = 0.77$ Fig. 3C). Multiple comparison analysis of the metabolic cost of evaporative cooling (MetabCost, maximum metabolic rate (MR) / thermoneutral MR) suggested that lowland birds ($\bar{x} = 1.94 \pm 0.33$) had significantly (~20 %) higher MetabCost than arid ($\bar{x} = 1.62 \pm 0.20$; PhylANOVA: $t = 2.09$, $p = 0.02$; Tukey: HSD = 0.38, $p < 0.001$) and montane birds ($\bar{x} = 1.61 \pm 0.24$; PhylANOVA: $t = 1.97$, $p = 0.04$; Tukey: HSD = 0.38, $p < 0.001$). MetabCost did not differ significantly between arid-zone and montane birds (PhylANOVA: $t = 0.26$, $p = 0.77$; Tukey: HSD = 0.01, $p = 0.99$) (Fig 3D).

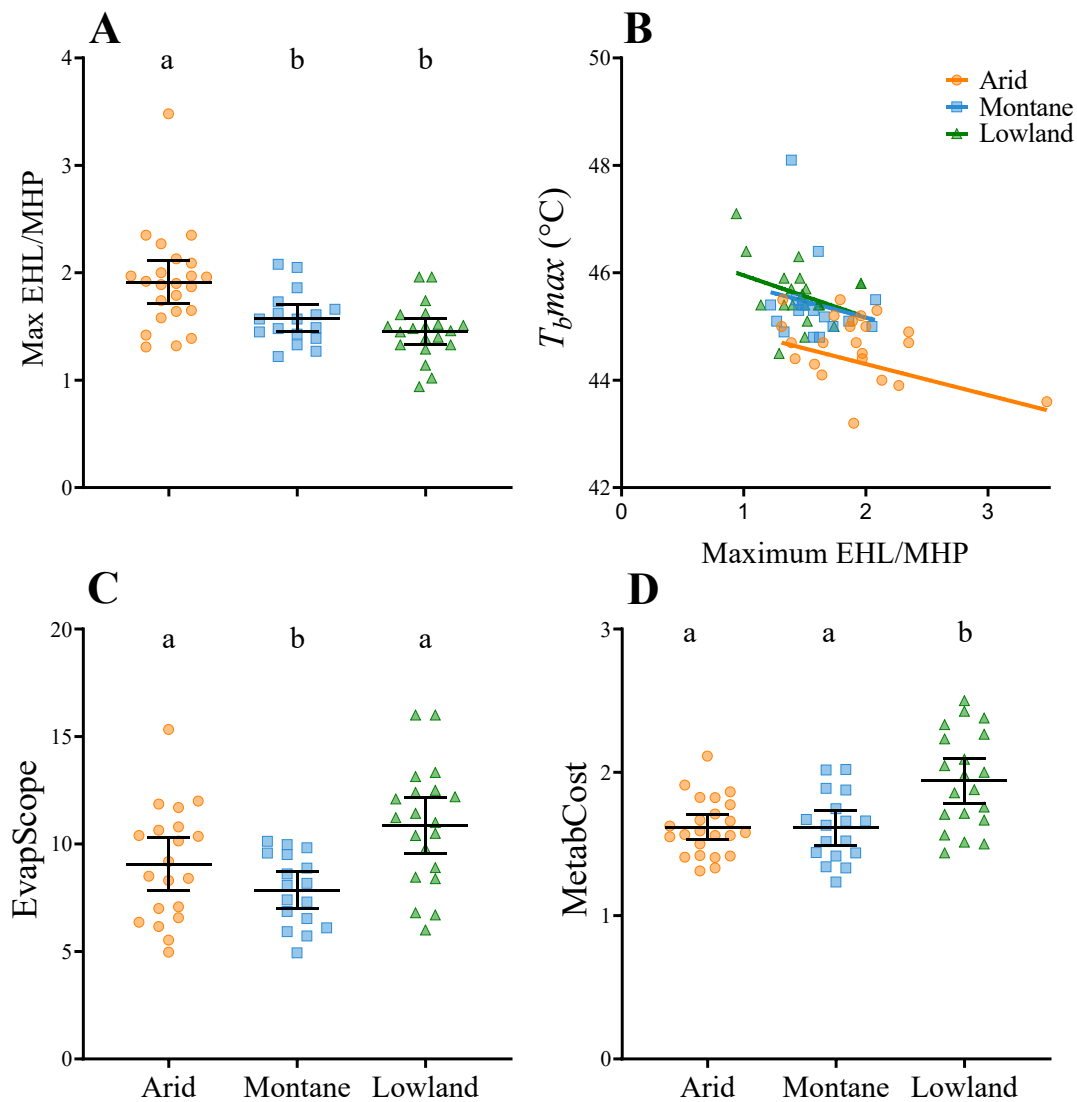


Figure 3 Variation in maximum ratio of evaporative heat loss and metabolic heat production (Max EHL/MHP; A), phylogenetic regressions (pgls) of the relationships between T_{bmax} and maximum EHL/MHP (B), the ratio of maximum to minimum thermoneutral evaporative water loss (EvapScope; C) and the metabolic cost of evaporative cooling calculated as the ratio of maximum to minimum thermoneutral metabolic rate (MetabCost; D) among 53 South African bird species inhabiting hot arid (orange circles, $n=23$), mesic montane (blue squares, $n=17$) or humid lowland (green triangles, $n=20$) climates. Horizontal lines represent mean values and vertical lines 95% confidence intervals. Letters above plots denote significant differences ($\alpha = 0.05$) as identified using phylogenetic analysis of variance post hoc multiple comparison assessments. Max EHL/MHP was significantly higher among arid-zone birds than those from montane and lowland localities, whereas EvapScope was significantly higher in lowland and arid birds to montane birds. MetabCost was significantly higher in lowland birds than species inhabiting arid or montane climates.

1.5 DISCUSSION

Our data support the hypothesis that avian hyperthermia tolerance has evolved in response to climate. Our prediction of high T_bmax in species occupying humid lowlands was confirmed, but the direction of differences between arid and montane species was opposite to what we predicted; arid-zone species had lower T_bmax compared to their montane and lowland counterparts. The combination of comparatively high T_bmax and low T_bnorm in lowland species reveals larger thermal safety margins, permitting greater increases in T_b above normothermic setpoints before the onset of loss of coordinated locomotory capacity and thermoregulatory failure. The climate-correlated variation in T_bmax , T_bnorm , and the gradient between these two variables we report here represents a novel macrophysiological pattern for endotherms, reflecting broad quantitative differences in interactions between evaporative heat loss and metabolic costs during acute heat exposure.

The T_bmax values of some lowland and montane birds in this study were unexpectedly high. Although reports of birds tolerating $T_b \geq 46$ °C without any adverse effects are rare [e.g., (29, 37, 41, 42)] and lethal T_b limits are generally thought to be 46 °C - 48 °C (43–45), many species from the lowland site had T_bmax in the 45.5 °C - 46.0 °C range, and five (3 lowland, 2 montane) had $T_bmax > 46$ °C (Fig. 1). The combination of high T_bmax and low EHL/MHP in lowland species supports Weathers' (29) argument that, among species in humid habitats, the capacity for pronounced hyperthermia tolerance plays a major role in thermoregulation during hot weather. However, the similarly high T_bmax in species inhabiting cooler, drier montane areas is puzzling. This finding is at least partly on account of the inclusion of the *Q. quelea* and *E. orix* in the montane dataset. Both of these species are widespread habitat generalists and, when excluded from the montane data set, T_bmax became significantly lower than that of lowland species, but remained higher than arid-zone species. The atypically high T_bmax in both these euplectids might be the evolutionary product of selection for dehydration tolerance in individuals foraging in large flocks, rather than historical and current climate (37). Regardless, our data reiterate that tolerance of $T_bmax \geq 48$ °C by *Q. quelea* (37) is extreme compared to most birds, rivaled only by recent findings of T_bmax up to 48 °C in common nighthawk chicks (*Chordeiles minor*) (42).

Our most surprising finding is the comparatively low T_bmax of arid-zone birds, despite them experiencing the highest T_{air} maxima, greatest water scarcity, and thus strong selection for water conservation (27, 46). Moreover, compared to species from the other two

sites, arid-zone species had lower T_{bmax} , yet tolerated significantly higher T_{air} values (Fig. 3). It is difficult to offer an adaptive explanation for low T_{bmax} . Instead, we suggest it reflects some physiological constraint associated with arid habitats. One possibility is that cellular heat shock responses involving the rapid synthesis of heat shock proteins (HSPs) in response to high temperatures are blunted in desert birds on account of the energetic costs involved [reviewed by (47)]. This notion is indirectly supported by the reductions in HSP expression associated with experimentally limited resource availability in some plants (48–51) and invertebrates (52). The energetic costs of heat shock responses have not, to the best of our knowledge, been directly quantified, but HSP expression tightly tracking current and past conditions implies that if HSPs were produced cheaply they could always be generously expressed (53). Comparatively low T_{bmax} among arid-zone birds, despite the adaptive value of hyperthermia for water conservation (27, 28), suggests that extreme ($T_b > 45^\circ\text{C}$) hyperthermia tolerance has substantial costs.

The comparatively low T_{bnorm} of lowland birds was also unexpected. We argue that reduced T_{bnorm} increases the scope for hyperthermia, permitting greater increases in T_b during hot, humid weather (Fig. 1) (29, 30, 32). Our findings support this idea, with the gradient between T_{bmax} and T_{bnorm} among lowland birds being significantly larger than among arid-zone species and montane species by 1.74°C and 0.84°C , respectively. The ability of lowland species to accommodate larger increases in T_b above baseline levels, therefore, seems to arise from both lower T_{bnorm} and higher T_{bmax} . These differences are also reflected in the more rapid increases in T_b (Fig 3B - T_{bslope}) compared to species from montane and arid-zone sites. The variation in thermal physiology among lowland and arid-zone species suggests an avoidance *versus* tolerance continuum, whereby lowland birds appear to have experienced selection for hyperthermia tolerance, but arid-zone birds evolved hyperthermia avoidance through more efficient evaporative cooling. The higher metabolic costs and consequently lower maximum evaporative cooling efficiency achievable by birds occupying humid, lowland habitats further support the notion of a greater degree of thermal generalization evolving in birds where high humidity constrains heat dissipation. Generally lower activity levels among desert birds, reflected in the $\sim 50\%$ lower daily energy expenditure of desert birds compared to non-desert birds (54), likely also play a crucial role in minimizing heat loads associated with activity and hence the likelihood of T_b increasing far above normothermic levels.

The data included in the present analysis were collected under standardized conditions of very low humidity so as not to impede evaporative heat dissipation, facilitating direct comparisons across taxa. For lowland birds, the efficiency of evaporative cooling would have been higher under the present experimental conditions than under typical summer conditions at our study site (Fig. 1), so it is very unlikely that their higher T_{bmax} values represent an experimental artefact. Avian evaporative cooling efficiency decreases substantially under humid conditions (30, 32, 55) and a recent heat-related avian mortality event in eastern South Africa at $T_{air} = 43\text{ }^{\circ}\text{C} - 45\text{ }^{\circ}\text{C}$ and a water vapor pressure of $\sim 1.8\text{ kPa}$ (56) underscores the thermoregulatory challenges faced by birds during hot, humid conditions. It is thus likely that birds inhabiting humid lowlands have to rely on cool microsites provided by closed canopy forests where T_{air} is low relative to surrounding areas (57, 58). Human-induced landscape transformations driving the loss of climatic refugia in coastal forests (59, 60) are therefore a concern in light of recent and predicted future increases in T_{air} (61).

1.6 CONCLUSION

The variation in avian thermal physiology at high environmental temperatures and hyperthermia avoidance *versus* tolerance spectrum we report here reveals that the upper limits of endotherm T_b have evolved in response to climate. Although we did not quantify thermal performance curves, our data support the existence of a continuum from thermal specialisation to thermal generalisation among endotherms (16, 17). The combination of reduced capacity for hyperthermia and more efficient evaporative cooling in desert birds *versus* greater capacity for hyperthermia and reduced evaporative cooling capacity in humid lowland birds reveals some of the complex ways in which climate can influence endotherm thermal physiology. The counterintuitive finding of comparatively modest hyperthermia tolerance in desert birds compared to birds from more mesic areas raises questions regarding the costs of hyperthermia tolerance and suggests the historical and recent focus on desert species in the avian thermal physiology literature (27, 35, 44, 62) may have underestimated hyperthermia tolerance among birds in general.

Finally, our findings reiterate that a clearer understanding of adaptive thermoregulation among endotherms is needed for modelling responses to climate change (16). For instance, biophysical models of heat and water exchange (63, 64) need to be

parameterized using species-specific upper and lower boundaries to T_b , which, as shown here, vary geographically as well as phylogenetically. The role of adaptive variation in hyperthermia tolerance in determining the nature of behavioural trade-offs between thermoregulation and foraging and the associated missed-opportunity costs (65) also deserves attention, especially as sublethal fitness costs are anticipated to be the major driver of declines among southern African arid-zone birds (66). All else being equal, species that accommodate larger increases in T_b above normothermic levels before the onset of rapid declines in physiological function may be more buffered from behavioural trade-offs during hot weather.

1.7 ACKNOWLEDGMENTS

We thank Philip Pattinson for access to his farm and home ‘Mooihoek’ in Harrismith and all those who contributed to the fieldwork component of the study, specifically Anna Probert, Nevanya Lubbe, Ryno Kemp and Barry van Jaarsveld. We also thank Tshepiso Majelantle for valuable discussions around statistical approaches used in this study, Barry Lovegrove and Henry Pollock for assistance with phylogenetic analysis, Mylene Mariette for discussions about the energy cost of heat shock responses, and two anonymous reviewers for constructive comments that improved the quality of the manuscript.

Ethics

This work was approved by the Animal Ethics Committee of the University of Pretoria (protocol NAS181/2019) and the Research and Scientific Ethics Committee of the South African National Biodiversity Institute (SANBI NZG/RES /P19/13). Birds were captured under permit JM 8,057/2019 from the Free State province’s Department of Economic, Small Business Development, Tourism and Environmental Affairs and OP 4026/2019 from the Ezemvelo KwaZulu-Natal provincial wildlife authority.

Funding

This work is based on research supported by the DSI-NRF Centre of Excellence at the FitzPatrick Institute and the National Research Foundation of South Africa (grant 119754 to A.E.M.). Any opinions, findings, and conclusions or recommendations expressed in this

material are those of the authors and do not necessarily reflect the views of the National Research Foundation.

1.8 REFERENCES

1. R. B. Huey, R. D. Stevenson, Integrating thermal physiology and ecology of ectotherms: A discussion of approaches. *Integr. Comp. Biol.* **19**, 357–366 (1979).
2. J. F. Gillooly, J. H. Brown, G. B. West, V. M. Savage, E. L. Charnov, Effects of size and temperature on metabolic rate. *Science (80-.)*. **293**, 2248–2251 (2001).
3. A. Addo-Bediako, S. L. Chown, K. J. Gaston, Thermal tolerance, climatic variability and latitude. *Proc. R. Soc. B Biol. Sci.* **267**, 739–745 (2000).
4. A. A. Hoffmann, S. L. Chown, S. Clusella-Trullas, Upper thermal limits in terrestrial ectotherms: How constrained are they? *Funct. Ecol.* **27**, 934–949 (2013).
5. M. B. Araújo, *et al.*, Heat freezes niche evolution. *Ecol. Lett.* **16**, 1206–1219 (2013).
6. J. M. Bennett, *et al.*, The evolution of critical thermal limits of life on Earth. *Nat. Commun.* **12**, 1–9 (2021).
7. B. G. Lovegrove, The zoogeography of mammalian basal metabolic rate. *Am. Nat.* **156**, 201–219 (2000).
8. C. R. White, T. M. Blackburn, G. R. Martin, P. J. Butler, Basal metabolic rate of birds is associated with habitat temperature and precipitation, not primary productivity. *Proc. R. Soc. B Biol. Sci.* **274**, 287–293 (2007).
9. G. A. Londoño, M. A. Chappell, M. del R. Castañeda, J. E. Jankowski, S. K. Robinson, Basal metabolism in tropical birds: Latitude, altitude, and the “pace of life.” *Funct. Ecol.* **29**, 338–346 (2015).
10. B. I. Tieleman, J. B. Williams, The adjustment of avian metabolic rates and water fluxes to desert environments. *Physiol. Biochem. Zool.* **73**, 461–479 (2000).
11. B. I. Tieleman, J. B. Williams, P. Bloomer, Adaptation of metabolism and evaporative water loss along an aridity gradient. *Proc. R. Soc. B Biol. Sci.* **270**, 207–

- 214 (2003).
12. P. F. Scholander, R. Hock, V. Walters, L. Irving, Adaptation to cold in arctic and tropical mammals and birds in relation to body temperature, insulation, and basal metabolic rate. *Biol. Bull.* **99**, 259–271 (1950).
 13. S. Rodbard, Weight and body temperature. *Sci.* **111**, 465–466 (1950).
 14. B. K. McNab, An Analysis of the Body Temperatures of Birds. *Condor* **68**, 47–55 (1966).
 15. A. Clarke, P. Rothery, Scaling of body temperature in mammals and birds. *Funct. Ecol.* **22**, 58–67 (2008).
 16. J. G. Boyles, F. Seebacher, B. Smit, A. E. McKechnie, Adaptive thermoregulation in endotherms may alter responses to climate change. *Integr. Comp. Biol.* **51**, 676–690 (2011).
 17. M. Angilletta, B. S. Cooper, M. S. Schuler, J. G. Boyles, The evolution of thermal physiology in endotherms. *Front. Biosci. (Elite Ed)*. **2**, 861–81 (2010).
 18. H. S. Pollock, J. D. Brawn, Z. A. Cheviron, Heat tolerances of temperate and tropical birds and their implications for susceptibility to climate warming. *Funct. Ecol.* (2020) <https://doi.org/10.1111/1365-2435.13693>.
 19. J. G. Boyles, B. Smit, A. E. McKechnie, Variation in body temperature is related to ambient temperature but not experimental manipulation of insulation in two small endotherms with different thermoregulatory patterns. *J. Zool.* **287**, 224–232 (2012).
 20. J. G. Boyles, L. Verburgt, A. E. Mckechnie, N. C. Bennett, Heterothermy in two mole-rat species subjected to interacting thermoregulatory challenges. *J. Exp. Zool. Part A Ecol. Genet. Physiol.* **317 A**, 73–82 (2012).
 21. E. J. Glanville, S. A. Murray, F. Seebacher, Thermal adaptation in endotherms: Climate and phylogeny interact to determine population-level responses in a wild rat. *Funct. Ecol.* **26**, 390–398 (2012).
 22. G. A. Londoño, M. A. Chappell, J. E. Jankowski, S. K. Robinson, Do thermoregulatory costs limit altitude distributions of Andean forest birds? *Funct.*

-
- Ecol.* **31**, 204–215 (2017).
23. B. G. Lovegrove, The evolution of endothermy in Cenozoic mammals: A plesiomorphic-apomorphic continuum. *Biol. Rev.* **87**, 128–162 (2012).
 24. J. G. Boyles, *et al.*, A global heterothermic continuum in mammals. *Glob. Ecol. Biogeogr.* **22**, 1029–1039 (2013).
 25. B. Smit, C. T. Harding, P. A. R. Hockey, A. E. McKechnie, Adaptive thermoregulation during summer in two populations of an arid-zone passerine. *Ecology* **94**, 1142–1154 (2013).
 26. W. I. Lutterschmidt, V. H. Hutchison, The critical thermal maximum: History and critique. *Can. J. Zool.* **75**, 1561–1574 (1997).
 27. B. I. Tieleman, J. B. Williams, The role of hyperthermia in the water economy of desert birds. *Physiol. Biochem. Zool.* **72**, 87–100 (1999).
 28. A. R. Gerson, *et al.*, The functional significance of facultative hyperthermia varies with body size and phylogeny in birds. *Funct. Ecol.* **33**, 597–607 (2019).
 29. W. W. Weathers, Energetics and Thermoregulation by Small Passerines of the Humid, Lowland Tropics. *Auk* **114**, 341–353 (1997).
 30. M. van Dyk, M. J. Noakes, A. E. McKechnie, Interactions between humidity and evaporative heat dissipation in a passerine bird. *J. Comp. Physiol. B Biochem. Syst. Environ. Physiol.* **189**, 299–308 (2019).
 31. R. M. Edwards, H. Haines, Effects of Ambient Water Vapor Pressure and Temperature on Evaporative Water Loss in *Peromyscus maniculatus* and *Mus musculus*. *J. Comp. Physiol. B* **184**, 177–184 (1978).
 32. A. R. Gerson, B. O. Wolf, E. K. Smith, B. Smit, A. E. McKechnie, The Impact of Humidity on Evaporative Cooling in Small Desert Birds Exposed to High Air Temperatures. *Physiol. Biochem. Zool.* **87**, 782–795 (2014).
 33. A. E. McKechnie, B. O. Wolf, The physiology of heat tolerance in small endotherms. *Physiology* **34**, 302–313 (2019).

34. R. Prinzinger, A. Preßmar, E. Schleucher, Body temperature in birds. *Comp. Biochem. Physiol. -- Part A Physiol.* **99**, 499–506 (1991).
35. A. E. McKechnie, A. R. Gerson, B. O. Wolf, Thermoregulation in desert birds: scaling and phylogenetic variation in heat tolerance and evaporative cooling. *J. Exp. Biol.* **224** (2021).
36. J. Å. Nilsson, A. Nord, Testing the heat dissipation limit theory in a breeding passerine. *Proc. R. Soc. B Biol. Sci.* **285** (2018).
37. M. T. Freeman, Z. J. Czenze, K. Schoeman, A. E. McKechnie, Extreme hyperthermia tolerance in the world's most abundant wild bird. *Sci. Rep.* **10**, 1–6 (2020).
38. M. C. Whitfield, B. Smit, A. E. McKechnie, B. O. Wolf, Avian thermoregulation in the heat: scaling of heat tolerance and evaporative cooling capacity in three southern African arid-zone passerines. *J. Exp. Biol.* **218**, 1705–1714 (2015).
39. Z. J. Czenze, *et al.*, Regularly drinking desert birds have greater evaporative cooling capacity and higher heat tolerance limits than non-drinking species. *Funct. Ecol.* **34**, 1589–1600 (2020).
40. A. E. McKechnie, *et al.*, Avian thermoregulation in the heat: Evaporative cooling in five Australian passerines reveals within-order biogeographic variation in heat tolerance. *J. Exp. Biol.* **220**, 2436–2444 (2017).
41. R. Dmi'el, D. Tel-Tzur, Heat balance of two starling species (*Sturnus vulgaris* and *Onychognathus tristrami*) from temperate and desert habitats. *J. Comp. Physiol. B* **155**, 395–402 (1985).
42. G. N. Newberry, R. S. O' Connor, D. L. Swanson, Urban rooftop-nesting Common Nighthawk chicks tolerate high temperatures by hyperthermia with relatively low rates of evaporative water loss. *Condor* **123** (2021).
43. Z. Arad, J. Marder, Strain differences in heat resistance to acute heat stress, between the bedouin desert fowl, the white leghorn and their crossbreeds. *Comp. Biochem. Physiol. -- Part A Physiol.* **72**, 191–193 (1982).

44. W. R. Dawson, *Temperature regulation and water requirements of the brown and Abert towhees, Pipilo fuscus and Pipilo aberti*. In *University of California publications in zoology*, G. A. Bartholomew, F. Crescitelli, T. H. Bullock, W. H. Furgason, A. M. Schechtman, Eds., vol 59 (University of California Press, 1954).
45. W. C. Randall, Factors influencing the temperature regulation of birds. *Am. J. Physiol. Content* **139**, 56–63 (1943).
46. W. R. J. Dean, J. B. Williams, Adaptations of birds for life in deserts with particular reference to Larks (Alaudidae). *Trans. R. Soc. South Africa* **59**, 79–91 (2004).
47. M. E. Feder, G. E. Hofmann, Heat-shock proteins, molecular chaperones, and the stress response: Evolutionary and ecological physiology. *Annu. Rev. Physiol.* **61**, 243–282 (1999).
48. S. J. Colombo, V. R. Timmer, M. L. Colclough, E. Blumwald, Diurnal variation in heat tolerance and heat shock protein expression in black spruce (*Picea mariana*). *Can. J. For. Res.* **25**, 369–375 (1995).
49. H. Nguyen, *et al.*, The Heat-Shock Response and Expression of Heat-Shock Proteins in Wheat Under Diurnal Heat Stress and Field Conditions. *Funct. Plant Biol.* **21**, 857 (1994).
50. D. Verdaguer, *et al.*, Expression of low molecular weight heat-shock proteins and total antioxidant activity in the Mediterranean tree *Quercus ilex* L. in relation to seasonal and diurnal changes in physiological parameters. *Plant, Cell Environ.* **26**, 1407–1417 (2003).
51. J. J. Burke, J. L. Hatfield, R. R. Klein, J. E. Mullet, Accumulation of Heat Shock Proteins in Field-Grown Cotton. *Plant Physiol.* **78**, 394–398 (1985).
52. M. E. Feder, N. Blair, H. Figueras, Natural thermal stress and heat-shock protein expression in *Drosophila* larvae and pupae. *Funct. Ecol.* **11**, 90–100 (1997).
53. J. Gao, *et al.*, Heat shock protein expression enhances heat tolerance of reptile embryos. *Proc. R. Soc. B Biol. Sci.* **281** (2014).
54. B. I. Tieleman, J. B. Williams, The adjustment of avian metabolic rates and water

- fluxes to desert environments. *Physiol. Biochem. Zool.* **73**, 461–479 (2000).
55. D. R. Powers, Effect of temperature and humidity on evaporative water loss in Anna’s hummingbird (*Calypte anna*). *J. Comp. Physiol. B* **162**, 74–84 (1992).
56. A. E. McKechnie, I. A. Rushworth, F. Myburgh, S. J. Cunningham, Mortality among birds and bats during an extreme heat event in eastern South Africa. *Austral Ecol.*, 687–691 (2021).
57. J. A. Kupfer, G. P. Malanson, S. B. Franklin, Not seeing the ocean for the islands: The mediating influence of matrix-based processes on forest fragmentation effects. *Glob. Ecol. Biogeogr.* **15**, 8–20 (2006).
58. S. R. R. Pinto, *et al.*, Landscape attributes drive complex spatial microclimate configuration of Brazilian Atlantic forest fragments. *Trop. Conserv. Sci.* **3**, 389–402 (2010).
59. P. I. Olivier, R. J. van Aarde, A. T. Lombard, The use of habitat suitability models and species-area relationships to predict extinction debts in coastal forests, South Africa. *Divers. Distrib.* (2013) <https://doi.org/10.1111/ddi.12099>.
60. M. T. Freeman, P. I. Olivier, R. J. van Aarde, Matrix transformation alters species-area relationships in fragmented coastal forests. *Landsc. Ecol.* **33**, 307–322 (2018).
61. IPCC, “Climate Change 2021: The Physical Science Basis. Contribution of Working Group I to the Sixth Assessment Report of the Intergovernmental Panel on Climate Change.” (2021).
62. W. R. Dawson, G. A. Bartholomew, *Temperature regulation and water economy of desert birds* (Academic Press, 1968).
63. M. R. Kearney, W. P. Porter, NicheMapR – an R package for biophysical modelling: the microclimate model. *Ecography (Cop.)*. **40**, 664–674 (2017).
64. E. A. Riddell, K. J. Iknayan, B. O. Wolf, B. Sinervo, S. R. Beissinger, Cooling requirements fueled the collapse of a desert bird community from climate change. *Proc. Natl. Acad. Sci. U. S. A.* **116**, 21609–21615 (2019).
65. S. J. Cunningham, J. L. Gardner, R. O. Martin, Opportunity costs and the response

- of birds and mammals to climate warming. *Front. Biosci. (Elite Ed)*. **19**, 300–307 (2021).
66. S. R. Conradie, S. M. Woodborne, S. J. Cunningham, A. E. McKechnie, Chronic, sublethal effects of high temperatures will cause severe declines in southern African arid-zone birds during the 21st century. *Proc. Natl. Acad. Sci.*, 201821312 (2019).
67. R. Kemp, A. E. McKechnie, Thermal physiology of a range-restricted desert lark. *J. Comp. Physiol. B Biochem. Syst. Environ. Physiol.* **189**, 131–141 (2019).
68. B. Smit, *et al.*, Avian thermoregulation in the heat: phylogenetic variation among avian orders in evaporative cooling capacity and heat tolerance. *J. Exp. Biol.* **221**, jeb174870 (2018).
69. S. E. Fick, R. J. Hijmans, WorldClim 2: new 1-km spatial resolution climate surfaces for global land areas. *Int. J. Climatol.* **37**, 4302–4315 (2017).
70. L. Mucina, M. C. Rutherford, *The vegetation of South Africa, Lesotho and Swaziland.*, L. Mucina, M. Rutherford, Eds. (National Botanical Institute, South Africa, 2006).
71. V. Muggeo, “Segmented mixed models with random changepoints in R” (2016) <https://doi.org/10.13140/RG.2.1.4180.8402>.
72. R. C. T. Pinheiro J, Bates D, DebRoy S, Sarkar D, nlme: Linear and Nonlinear Mixed Effects Models (2015).
73. K. Barton, MuMIn: Multi-Model Inference. R package version 1.43.6. <https://CRAN.R-project.org/package=MuMIn>. (2019).
74. K. P. Burnham, D. R. Anderson, *Model selection and multi-model inference: a practical information-theoretic approach*, 2nd edn (Springer, 2002).
75. W. Jetz, G. H. Thomas, J. B. Joy, K. Hartmann, A. O. Mooers, The global diversity of birds in space and time. *Nature* **491**, 444–448 (2012).
76. S. J. Hackett, *et al.*, A phylogenomic study of birds reveals their evolutionary history. *Science (80-.)*. **320**, 1763–1768 (2008).

-
77. D. R. Maddison, W. P. Maddison, Chromaseq: a Mesquite package for analyzing sequence chromatograms. Version 1.12 (2014).
78. E. P. Martins, T. F. Hansen, Phylogenies and the comparative method: a general approach to incorporating phylogenetic information into the analysis of interspecific data. *Am. Nat.* **149**, 646–667 (1997).
79. A. Grafen, The Phylogenetic Regression Author. *Philos. Trans. R. Soc. B Biol. Sci.* **326**, 119–157 (1989).
80. M. Pagel, Inferring the historical patterns of biological evolution. *Nature* **401**, 877–884 (1999).
81. L. J. Revell, Phylogenetic signal and linear regression on species data. *Methods Ecol. Evol.* **1**, 319–329 (2010).
82. A. E. McKechnie, B. O. Wolf, The allometry of avian basal metabolic rate: Good predictions need good data. *Physiol. Biochem. Zool.* **77**, 502–521 (2004).
83. B. K. McNab, *The physiological ecology of vertebrates: a view from energetics* (Cornell University Press, 2002).
84. B. van Jaarsveld, N. C. Bennett, R. Kemp, Z. J. Czenze, A. E. McKechnie, Heat tolerance in desert rodents is correlated with microclimate at inter- and intraspecific levels. *J. Comp. Physiol. B* (2021) <https://doi.org/10.1007/s00360-021-01352-2>.
85. D. Orme, *et al.*, Caper: comparative analyses of phylogenetics and evolution in R. (2012).
86. L. J. Revell, phytools: An R package for phylogenetic comparative biology (and other things). *Methods Ecol. Evol.* **3**, 217–223 (2012).
87. T. Garland, *et al.*, Phylogenetic Analysis of Covariance by Computer Simulation. *Syst. Biol.* **42**, 265–292 (1993).

ADDITIONAL INFORMATION***Appendix S1*****1.8.1.1 Additional Materials and Methods**

Birds were captured using mist nets or spring traps baited with superworms (*Zophobas morio*). During transportation by road (10–15-minute trip) to field stations, birds were held in cloth bags and upon arrival were transferred to cages (0.8 m³) in holding rooms (T_{air} = 24–27°C). Birds were held in the cages for no more than 12 hours, and provided with an *ad libitum* supply of water and food (seed or superworms), before measurements commenced.

Between 1 October and 17 December 2019, at the montane study site we captured ant-eating chats (AEC, *Myrmecocichla formicivora*: Muscicapidae; n= 10), bokmakieries (BOK, *Telophorus zeylonus*: Malaconotidae; n= 8), buff-streaked chats (BSC, *Campicoloides bifasciata*: Muscicapidae; n= 10), cape robin-chats (CRC, *Cossypha caffra*: Muscicapidae; n= 10), cape white-eyes (CWE, *Zosterops virens*: Zosteropidae; n= 10), dark-capped bulbuls (DCB, *Pycnonotus tricolor*: Pycnonotidae; n= 10), Drakensberg prinias (DPB, *Prinia hypoxantha*: Cisticolidae; n= 7), pied starlings (PST, *Lamprotornis bicolor*: Sturnidae; n= 10), red-capped larks (RCL, *Calandrella cinerea*: Alaudidae; n= 10), South African cliff-swallows (SCS, *Petrochelidon spilodera*: Hirundinidae; n= 10), southern fiscals (SFS, *Lanius collaris*: Lanidae; n= 10), southern masked weavers (SMW, *Ploceus velatus*: Ploceidae; n= 10), southern red bishops (SRB, *Euplectes orix*: Ploceidae; n= 10), speckled mousebirds (SMB, *Colius striatus*: Coliidae; n= 6), spike-heeled larks (SHL, *Chersomanes albobfasciata*: Alaudidae; n= 10) and white-rumped swifts (WRS, *Apus caffer*: Apodidae; n= 10).

Between 5 January and 26 February 2020, at the coastal lowland study site we captured African pygmy kingfishers (APK, *Ispidina picta*: Alcedinidae; n= 10), blue-cheeked bee-eaters (BCB, *Merops persicus*: Meropidae; n= 10), bronze mannikins (BMK, *Spermestes cucullata*: Estrildidae; n= 9), brown-hooded kingfishers (BHK, *Halcyon albiventris*; n= 10), cape white-eyes (CWE, *Zosterops virens*: Zosteropidae; n= 10), collared sunbirds (CSB, *Hedydipna collaris*: Nectariniidae; n= 10), dark-capped bulbuls (DCB, *Pycnonotus tricolor*: Pycnonotidae; n= 10), green-backed camaropteras (GBC, *Camaroptera brachyura*: Cisticolidae; n= 10), little swifts (LSW, *Apus affinis*: Apodidae; n= 10), olive sunbirds (OSB, *Cyanomitra olivacea*: Nectariniidae; n= 10), red-capped robin-chats (RCR,

Cossypha natalensis: Muscicapidae; n= 10), sombre greenbuls (SGB, *Andropadus importunus*: Pycnonotidae; n= 10), southern fiscals (SFS, *Lanius collaris*: Laniidae; n= 10), southern red bishops (SRB, *Euplectes orix*: Ploceidae; n= 10), speckled mousebirds (SPM, *Colius striatus*: Coliidae; n= 10), spectacled weavers (SWE, *Ploceus ocularis*: Ploceidae; n= 10), tawny-flanked prinias (TFP, *Prinia subflava*: Cisticolidae; n= 10), white-eared barbets (WEB, *Stactolaema leucotis*: Lybiidae; n= 10), yellow weavers (YWE, *Ploceus subaureus*: Ploceidae; n= 10) and yellow-rumped tinkerbirds (YRT, *Pogoniulus bilineatus*: Lybiidae; n= 10).

We include data for 12 arid-zone bird species from (1) and a single species - red larks (RLA; *Calendulauda burra*) from (2). We also incorporate unpublished data (M.T. Freeman, Z.J. Czenze, R. Kemp, B. van Jaarsveld and A.E. McKechnie) for three species at the Aggeneys study site between 2 December 2018 and 4 February 2019: little swifts (LSW, *Apus affinis*: Apodidae; n= 10), acacia pied barbets (APB, *Tricholaema leucomelas*: Lybiidae; n= 10) and white-backed mousebirds (WBM, *Colius colius*: Coliidae; n= 10). Previously published data from study sites in the southern Kalahari include scaly-feathered weavers (SFW; *Sporopipes squamifrons*: Ploceidae; n = 6), sociable weavers (SW; *Philetairus socius*: Ploceidae; n = 6) and white-browed sparrow-weavers (WBW; *Plocepasser mahali*: Ploceidae n = 8; (3), and southern pied babbler (SPB; *Turdoides bicolor*: Leiothrichidae; n=10; S.J. Cunningham et al., unpubl. data. Finally, data for African cuckoos (AFC; *Cuculus gularis*: Cuculidae), lilac-breasted rollers (LBR; *Coracias caudatus*: Coraciidae) and Burchell's starling (BST, *Lamprotornis australis*; (4)) were also included in our analysis.

1.8.1.2 Air and body temperature measurements

A temperature-sensitive passive integrated transponder (PIT) tag (Biotherm; Biomark, Idaho, ID, USA) was injected intraperitoneally into each bird to measure T_b . Birds were then placed in a metabolic chamber within receiving range of an antennae connected to a portable transceiver system (HPR+; Biomark, Idaho, ID, USA). PIT tags were calibrated over a temperature range of 35-50 °C within a circulating water bath (model F34, Julabo, Seelbach BW, DE) compared to a thermocouple meter (TC-1000, Sable Systems, Las Vegas, NV, USA), verified against a mercury-in-glass thermometer with NIST-traceable accuracy before and after the PIT tag calibration. Measured PIT tag values deviated from actual temperature by $0.07 \pm 0.08^\circ\text{C}$ ($n = 15$). A thermistor probe (TC-100; Sable Systems) inserted through a

sealed rubber grommet embedded in the wall of the metabolic chamber was used to measure T_{air} during gaseous exchange measurements.

1.8.1.3 Gaseous exchange measurements

We measured carbon dioxide production (\dot{V}_{CO_2}) and EWL with two open flow-through respirometry systems. Birds were placed in a 3-L (dimensions 20 cm high \times 15 cm wide \times 10 cm deep) or 6-L (dimensions 20cm x 28cm wide x 20 cm deep) airtight metabolic chamber. Chamber were fitted with a plastic mesh platform (on which birds could rest) elevated \sim 10 cm above a \sim 1 cm layer of mineral oil to prevent evaporation from excreta. A previous study (Whitfield et al 2015) showed that these metabolic chambers do not adsorb water vapor. Each metabolic chamber was placed inside a \sim 100 L cooler box in which T_{air} was regulated by a Peltier device (AC-162 Thermoelectric Air Cooler, TE Technology, Traverse City MI, USA) and controlled digitally (TC-36–25-RS485 Temperature Controller, TE Technology, Traverse City MI, USA).

An oil-free compressor provided atmospheric air which was subsequently scrubbed of water vapor using a membrane dryer (Champion®CMD3 air dryer and filter; Champion Pneumatic). The dried air was supplied to both systems. For each system, dried air was split into an experimental and baseline channel. Baseline channel air flow rate was regulated at \sim 1.5 L min⁻¹ using a needle valve (Swagelok) while a mass flow controller (Alicat Scientific Inc., Tucson, AZ, USA) calibrated using a soap-bubble flow meter (Gilibrator 2, Sensidyne, St Petersburg, FL, USA) was used to regulate experimental channel flow rates. An air inlet was placed near the top of each metabolic chamber with an elbow joint facing upwards (reducing potential convective cooling at higher flow rates). The air outlet was placed on the opposite side of the chamber below the mesh platform to maximise air mixing. Flow rates ranged from 4 to 36 L min⁻¹, depending on species, behaviour, T_{air} and M_b . Flow rates were also adjusted to maintain water vapor pressures as low as possible (dewpoint $<$ -5 °C) within each chamber while still permitting for accurate measurements of differences between water vapor and CO₂ between incurrent and excurrent air.

A respirometry multiplexer (model MUX3-1,101-18 M, Sable Systems, Las Vegas, NV, USA) in manual mode and a SS-3 Subsampler (Sable Systems, Las Vegas, NV, USA) sequentially subsampled excurrent air from the experimental and baseline channel air in each system. Subsampled air was pulled through a CO₂/H₂O analyser (model LI-840A, LI-COR, Lincoln, NE, USA), zeroed frequently using nitrogen and spanned for CO₂ using a certified

calibration gas with a known CO₂ concentration of 1900 ppm (AFROX, Johannesburg, South Africa). The H₂O sensor was also regularly zeroed using nitrogen and spanned using a dewpoint generator (DG-4, Sable Systems, Las Vegas, NV, USA). Bev-A-Line IV tubing (Thermoplastic Processes Inc.) was used throughout the system. An analogue digital converter (model UI-3; Sable Systems) was used to digitise the voltage outputs from the analysers and thermistor probes. The digital output from the converter was recorded at 5-s intervals using the Expedata software (Sable Systems, Las Vegas, NV, USA)

1.8.1.4 Experimental protocol

Before being placed in a chamber, birds were weighed on an electronic scale (EJ-160, A&D, Tokyo, J.P). To ensure birds were postabsorptive, we estimated food passage rate for each species using the scaling equation provided by (5), and withheld food for at least 1 h (with longer periods for larger species) before beginning measurements. Measurements took place during the day, with relationships between T_b , EWL, MR and metabolic heat production and evaporative heat dissipation (EHL/MHP) quantified over $T_{air} = 28 - 56$ °C by exposing birds to a stepped T_{air} profile involving 4-°C increments between $T_{air} = 28 - 40$ °C and 2-°C increments above $T_{air} = 40$ °C. Measurements began with a baseline air subsample until H₂O and CO₂ readings became stable (~5 min). Thereafter, excurrent air from the chamber was subsampled when T_{air} stabilized at the set value, and CO₂ and H₂O traces were relatively stable for at least 5 min, followed by another 5-min baseline.

Birds were monitored continuously during measurements using an infrared camera and were only removed from the chamber when thermal endpoints were reached (3), or they engaged in sustained escape behaviour. Normally, birds were only removed from the chamber upon reaching their HTL (i.e., T_{air} at which onset of hyperthermia or loss of T_b regulation occurs). After being removed from the chamber birds were immediately placed in front of an air conditioner unit and their bellies dabbed with 90% ethanol to facilitate rapid heat dissipation. Upon returning to normothermic T_b (40 – 42 °C) birds were placed in a cage at room temperature (24-27 °C) and offered *ad libitum* food and water. Birds were later released at the site of capture. Previously this experimental protocol has been used for multiple species and, in one species where individuals were monitored for several weeks post-release, is not associated with any adverse effects (2).

1.8.1.5 Data analysis

Analyser drift and lag were corrected for using the relevant algorithms in Expedata software (Sable Systems, Las Vegas, NV, USA). Lighton (2008) provides two equations 9.5 and 9.6 which were used to calculate \dot{V}_{CO_2} and EWL from the lowest (i.e., resting) stable 5-min periods of CO₂ and H₂O vapor at a given T_{air}, assuming 0.803 mg H₂O mL⁻¹. As individuals were likely postabsorptive, we calculated MR from \dot{V}_{CO_2} assuming a respiratory exchange ratio (RER) = 0.71 (7) and converted rates of \dot{V}_{CO_2} to metabolic rate (W) using 27.8 J mL⁻¹ CO₂ (Withers, 1992). We assumed a latent heat of vaporization of H₂O of 2.406 J mg⁻¹ at 40°C (8) when converting rates of EWL to rates of EHL (W).

1.8.1.6 Additional tables and figures

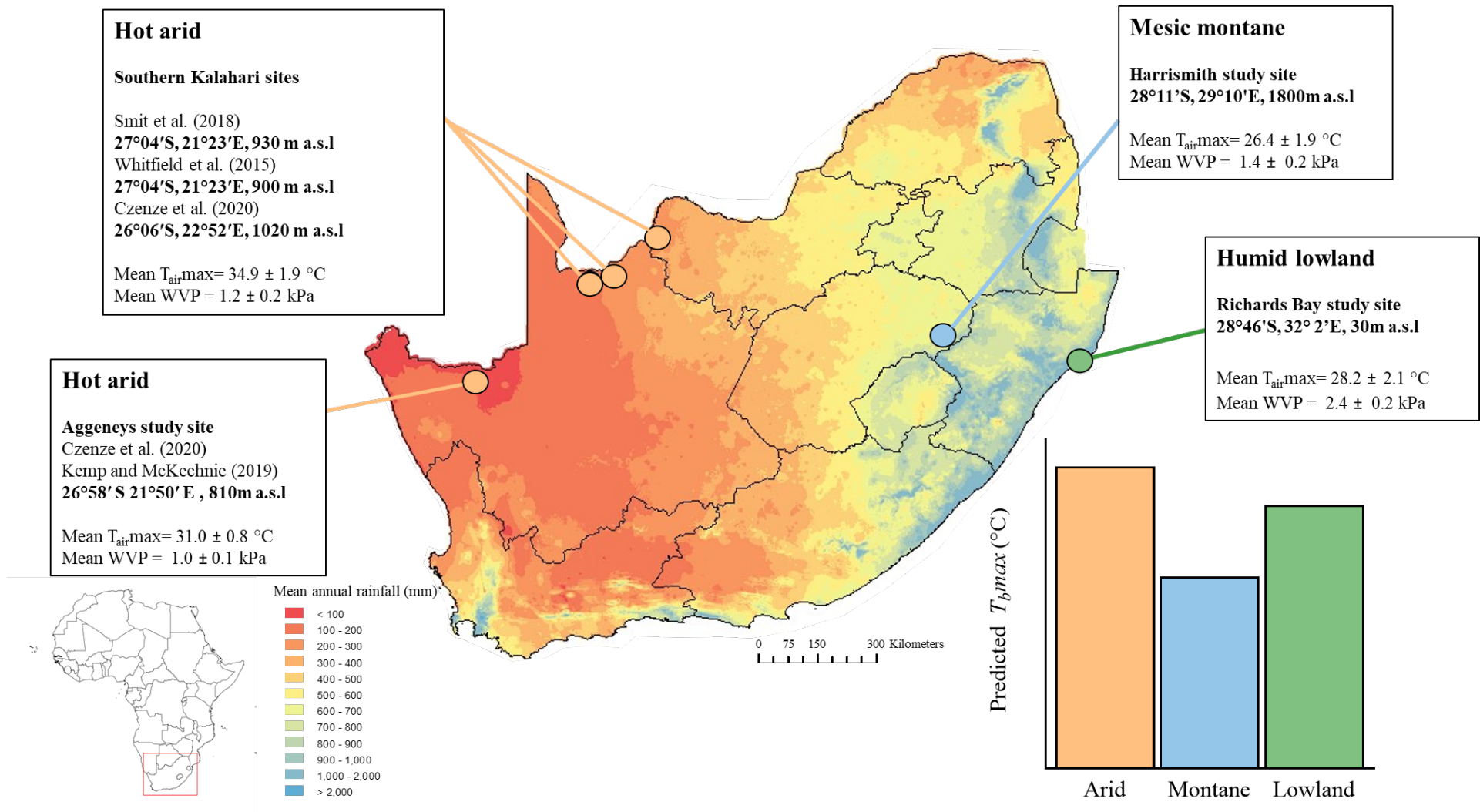


Figure S1

Figure S1 Mean annual precipitation map of South Africa with study site locations, elevation (meters above sea level – a.s.l) and average weather conditions [maximum air temperature (T_{airmax}) and associated water vapor pressure (WVP) as an indication of humidity] during the austral spring/summer obtained from the WorldClim2 dataset. Predictions for relative avian maximum body temperatures (T_{bmax}) within each climatic region are based on concepts of adaptive thermoregulation at each locality calculated using the WorldClim2 dataset. Climatic regions (study localities) are indicated by green (humid lowland), orange (hot arid) and light blue (mesic montane). Map courtesy of SA Atlas of climatology and agrohydrology (9).

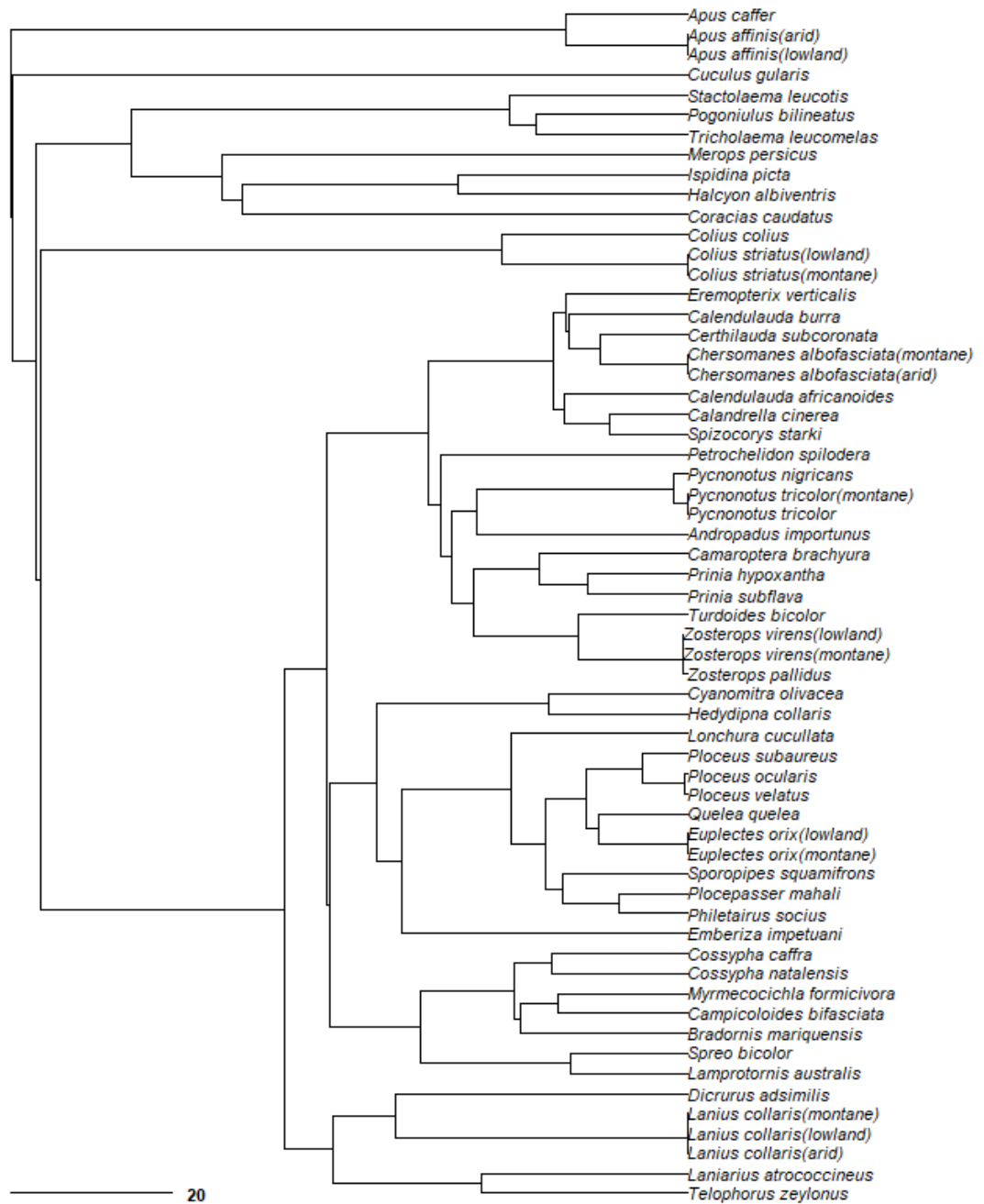


Figure S2 - Phylogenetic tree of the 53 focal species and subspecies, pruned from the maximum-likelihood phylogeny (10)

Table S1. The 53 study species with order, study area and sample size. Also included are data sources for arid-zone species for which body temperature and gas exchange were not measured during the study.

Common Name	Species	Order	Study area (sample size)	Source
Dry assessments (~1g H₂O m⁻³)				
White-rumped swift	<i>Apus caffer</i>	Apodiformes	Montane (<i>n</i> =10)	This study
Speckled mousebird	<i>Colius striatus</i>	Coliiformes	Montane (<i>n</i> =6) Lowland (<i>n</i> =8)	This study
Southern fiscal	<i>Lanius collaris</i>	Passeriformes	Montane (<i>n</i> =10) Lowland (<i>n</i> =10) Arid (<i>n</i> =9)	This study, (1)
Bokmakerie	<i>Telophorus zeylonus</i>	Passeriformes	Montane (<i>n</i> =8)	This study
Pied starling	<i>Spreo bicolor</i>	Passeriformes	Montane (<i>n</i> =10)	This study
Cape robin-chat	<i>Cossypha caffra</i>	Passeriformes	Montane (<i>n</i> =10)	This study
Buff-streaked chat	<i>Campicoloides bifasciatus</i>	Passeriformes	Montane (<i>n</i> =10)	This study
Ant-eating chat	<i>Myrmecocichla formicivora</i>	Passeriformes	Montane (<i>n</i> =10)	This study
Red-billed quelea	<i>Quelea quelea</i>	Passeriformes	Montane (<i>n</i> =20)	(11)
Southern red bishop	<i>Euplectes orix</i>	Passeriformes	Montane (<i>n</i> =10) Lowland (<i>n</i> =9)	This study
Southern masked weaver	<i>Ploceus velatus</i>	Passeriformes	Montane (<i>n</i> =10)	This study
Drakensberg prinia	<i>Prinia hypoxantha</i>	Passeriformes	Montane (<i>n</i> =10)	This study
Cape white-eye	<i>Zosterops virens</i>	Passeriformes	Montane (<i>n</i> =10) Lowland (<i>n</i> =10)	This study
Dark-capped bulbul	<i>Pycnonotus tricolor</i>	Passeriformes	Montane (<i>n</i> =10) Lowland (<i>n</i> =10)	This study
South African cliff swallow	<i>Petrochelidon spilodera</i>	Passeriformes	Montane (<i>n</i> =10)	This study
Red-capped lark	<i>Calandrella cinerea</i>	Passeriformes	Montane (<i>n</i> =10)	This study

Spike-heeled lark	<i>Chersomanes albofasciata</i>	Passeriformes	Montane ($n=10$) Arid ($n=10$)	This study, (1)
Red-capped robin chat	<i>Cossypha natalensis</i>	Passeriformes	Lowland ($n=10$)	This study
Spectacled weaver	<i>Ploceus ocularis</i>	Passeriformes	Lowland ($n=10$)	This study
Yellow weaver	<i>Ploceus subaureus</i>	Passeriformes	Lowland ($n=10$)	This study
Bronze mannikin	<i>Spermestes cucullata</i>	Passeriformes	Lowland ($n=10$)	This study
Collared sunbird	<i>Hedydipna collaris</i>	Passeriformes	Lowland ($n=10$)	This study
Olive sunbird	<i>Nectarinia olivacea</i>	Passeriformes	Lowland ($n=10$)	This study
Tawny-flanked prinia	<i>Prinia subflava</i>	Passeriformes	Lowland ($n=10$)	This study
Green-backed camaroptera	<i>Camaroptera brachyura</i>	Passeriformes	Lowland ($n=10$)	This study
Sombre greenbul	<i>Andropadus importunus</i>	Passeriformes	Lowland ($n=10$)	This study
African pygmy-kingfisher	<i>Ispidina picta</i>	Coraciiformes	Lowland ($n=10$)	This study
Brown-hooded kingfisher	<i>Halcyon albiventris</i>	Coraciiformes	Lowland ($n=10$)	This study
Blue-checked bee-eater	<i>Merops persicus</i>	Coraciiformes	Lowland ($n=10$)	This study
Yellow-rumped tinkerbird	<i>Pogoniulus bilineatus</i>	Piciformes	Lowland ($n=10$)	This study
White-eared barbet	<i>Stactolaema leucotis</i>	Piciformes	Lowland ($n=8$)	This study
Little swift	<i>Apus affinis</i>	Apodiformes	Lowland ($n=10$) Arid ($n=10$)	This study, unpublished data (M.T. Freeman, Z.J. Czenze, R. Kemp, B. van Jaarsveld and A.E. McKechnie)
African cuckoo	<i>Cuculus gularis</i>	Cuculiformes	Arid ($n=6$)	(4)
White-backed mousebird	<i>Colius colius</i>	Coliiformes	Arid ($n=10$)	Unpublished data (M.T. Freeman, Z.J. Czenze, R. Kemp, B. van Jaarsveld and A.E. McKechnie)
Fork-tailed drongo	<i>Dicrurus adsimilis</i>	Passeriformes	Arid ($n=3$)	(1)
Crimson-breasted shrike	<i>Laniarius atrococcineus</i>	Passeriformes	Arid ($n=9$)	(1)

Burchell's starling	<i>Lamprotornis australis</i>	Passeriformes	Arid ($n=5$)	(4)
Marico flycatcher	<i>Melaenornis mariquensis</i>	Passeriformes	Arid ($n=7$)	(1)
Lark-like bunting	<i>Emberiza impetuani</i>	Passeriformes	Arid ($n=10$)	(1)
Stark's lark	<i>Spizocorys starki</i>	Passeriformes	Arid ($n=10$)	(1)
Fawn-coloured lark	<i>Calendulauda africanoides</i>	Passeriformes	Arid ($n=10$)	(1)
Karoo long-billed lark	<i>Certhilauda subcoronata</i>	Passeriformes	Arid ($n=10$)	(1)
Red lark	<i>Calendulauda burra</i>	Passeriformes	Arid ($n=10$)	(2)
Grey-backed sparrow-lark	<i>Eremopterix verticalis</i>	Passeriformes	Arid ($n=10$)	(1)
Orange river white-eye	<i>Zosterops pallidus</i>	Passeriformes	Arid ($n=10$)	(1)
Red-eyed bulbul	<i>Pycnonotus nigricans</i>	Passeriformes	Arid ($n=10$)	(1)
Lilac-breasted roller	<i>Coracias caudatus</i>	Coraciiformes	Arid ($n=11$)	(4)
Acacia pied barbet	<i>Tricholaema leucomelas</i>	Piciformes	Arid ($n=10$)	unpublished data (M.T. Freeman, Z.J. Czenze, R. Kemp, B. van Jaarsveld and A.E. McKechnie)
Southern pied babbler	<i>Turdoides bicolor</i>	Passeriformes	Arid ($n=10$)	(unpublished data, S.J. Cunningham et al.)
Scaly-feathered weaver	<i>Sporopipes squamifrons</i>	Passeriformes	Arid ($n=16$)	(3)
Sociable Weaver	<i>Philetairus socius</i>	Passeriformes	Arid ($n=25$)	(3)
White-browed sparrow weaver	<i>Plocepasser mahali</i>	Passeriformes	Arid ($n=30$)	(3)

Table S2.1. Summary of thermoregulatory performance as a function of chamber air temperature (T_{air}) in seventeen species from the montane study site (Harrismith). T_b = body temperature, T_{air} = ambient temperature, MR = metabolic rate, EWL = evaporative water loss, EHL= evaporative heat loss, MHP = metabolic heat production. Means \pm SD and (N) are reported.

Variable	Ant-eating chat	Bokmakierie	Buff-streaked chat	Cape robin-chat	Cape white-eye	Dark-capped bulbul	Drakensberg prinia
Body mass (g)	48.3\pm3.6 (10)	66.8\pm2.8 (8)	34.8\pm5.8 (10)	25.5\pm3.0 (10)	11.6\pm0.7 (10)	40.2\pm3.1 (10)	9.8\pm0.9 (7)
Body temperature							
Min. T_b ($^{\circ}$ C)	41.0 \pm 1.0 (10)	40.3 \pm 0.9 (8)	40.0 \pm 0.8 (10)	40.5 \pm 1.0 (10)	40.4 \pm 0.9 (10)	40.4 \pm 0.7 (10)	40.5 \pm 1.0 (7)
Inflection T_{air} ($^{\circ}$ C)	36.2	34.3	35	34.4	37.3	33.5	36.1
T_b versus T_{air} slope (per $^{\circ}$ C)	0.37	0.28	0.33	0.32	0.36	0.27	0.41
Max T_b ($^{\circ}$ C)	45.4 \pm 0.4 (9)	45.3 \pm 0.5 (8)	45.2 \pm 0.6 (8)	45.1 \pm 0.7 (10)	44.9 \pm 0.3 (10)	45.0 \pm 0.4 (10)	45.4 \pm 0.4 (7)
Max T_{air} ($^{\circ}$ C)	45.4 \pm 1.0 (9)	48.0 \pm 2.1 (8)	45.9 \pm 1.3 (8)	45.6 \pm 1.9 (10)	47.4 \pm 1.0 (10)	48.1 \pm 3.6 (10)	47.1 \pm 1.3 (7)
T_b at onset of panting ($^{\circ}$ C)	42.9 \pm 0.7 (7)	42.1 \pm 0.9 (8)	43.0 \pm 0.7 (10)	42.5 \pm 1.0 (10)	42.0 \pm 0.7 (10)	42.4 \pm 0.8 (9)	43.1 \pm 1.6 (6)
T_{air} at onset of panting ($^{\circ}$ C)	40.8 \pm 1.9 (8)	39.1 \pm 2 (8)	39.8 \pm 0.8 (10)	38.2 \pm 2.7 (10)	40.1 \pm 1.8 (10)	37.4 \pm 3.6 (9)	41.6 \pm 1.3 (6)
95 th percentile $T_b > T_{air}$ ($^{\circ}$ C)	44.0	43.1	44.1	44.0	42.6	43.3	44.6
Metabolic rate							
Min. MR (W)	0.98 \pm 0.3 (10)	0.98 \pm 0.15 (8)	0.65 \pm 0.13 (10)	0.65 \pm 0.16 (10)	0.34 \pm 0.04 (10)	0.85 \pm 0.20 (10)	0.29 \pm 0.02 (7)
T_{uc} ($^{\circ}$ C)	42	37.5	37.6	32.2	34.1	39.9	36.1
MR slope (mW $^{\circ}$ C ⁻¹)	196.0	85.30	27.74	32.40	6.93	21.0	14.96
Max. MR (W)	1.98 \pm 0.15 (4)	1.84 \pm 0.36 (4)	1.06 \pm 0.32 (10)	1.08 \pm 0.15 (10)	0.42 \pm 0.06 (10)	1.14 \pm 0.29 (6)	0.44 \pm 0.06 (4)
Max. MR/min. MR	2.02	1.87	1.63	1.66	1.23	1.35	1.52
Evaporative water loss							
Min. EWL (g h ⁻¹)	0.37 \pm 0.08 (10)	0.49 \pm 0.13 (8)	0.36 \pm 0.1 (10)	0.30 \pm 0.12	0.16 \pm 0.07 (10)	0.37 \pm 0.14 (10)	0.12 \pm 0.04 (7)
Inflection T_{air} ($^{\circ}$ C)	40.2	38.1	37.2	34.9	37.0	36.0	39.8
EWL slope (g h ⁻¹ $^{\circ}$ C ⁻¹)	0.45	0.33	0.18	0.15	0.06	0.20	0.09
Max. EWL (g h ⁻¹)	3.52 \pm 0.45 (4)	4.22 \pm 0.68 (4)	2.06 (1)	1.96 \pm 0.48 (6)	0.79 \pm 0.12 (6)	2.57 \pm 0.26 (3)	0.98 \pm 0.17 (4)
			1.97 \pm 0.41(6)				
Max. EWL/min. EWL	9.51	8.61	5.72	6.53	4.94	6.86	8.17
Min. EHL/MHP	0.21 \pm 0.06	0.31 \pm 0.10 (8)	0.27 \pm 0.08 (10)	0.28 \pm 0.05	0.29 \pm 0.13 (10)	0.29 \pm 0.09 (10)	0.25 \pm 0.07 (7)
EHL/MHP inflection $T_{air} - T_b$	-5.3	-5.7	-4.5	-5.3	-4.0	-6.0	-3.1
EHL/MHP slope	0.16	0.13	0.14	0.12	0.13	0.14	0.20
Max. EHL/MHP	1.22 \pm 0.21 (10)	1.57 (2)	1.66 (1)	1.27 \pm 0.22 (8)	1.33 \pm 0.17 (6)	1.73 \pm 0.20 (3)	1.49 \pm 0.13 (4)
		1.56 \pm 0.35 (4)	1.35 \pm 0.15 (6)				

Variable	Pied starling	Red-billed quelea	Red-capped lark	South African cliff-swallow	Southern fiscal	Southern masked weaver	Southern red bishop
Body mass (g)	99.3±6.9 (10)	17.9±1.2 (20)	25.5±1.9 (10)	21.0±1.4 (10)	39.7±3.5 (10)	28.9±3.4 (10)	24.2±2.6 (10)
Body temperature							
Min. T_b (°C)	40.4±0.8 (10)	40.8±1.2 (20)	40.9±0.8 (10)	41.4±1.1 (10)	40.83 ±0.74 (10)	39.4±1.1(10)	39.8 ±0.8 (10)
Inflection T_{air} (°C)	32.5	37.6	33.6	34.7	35.5	36.6	37.2
T_b versus T_{air} slope (per °C)	0.25	0.46	0.27	0.25	0.34	0.36	0.40
Max T_b (°C)	45.0±0.4 (9)	48.0±0.7 (20)	44.8±0.3 (10)	44.8±0.3 (10)	45.1±0.5 (10)	45.4±0.6 (9)	46.4±0.4 (10)
Max T_{air} (°C)	48.2±2.2 (9)	50.9±1.4 (20)	46.9±1.6 (10)	47.6±1.3 (10)	47.3±1.6 (10)	48.0±1.3 (9)	50.8±1.5 (10)
T_b at onset of panting (°C)	42.7±0.5 (10)	41.8±1.3 (18)	42.4±0.7 (10)	42.7±0.9 (10)	42.4±0.8 (10)	41.6±0.8 (10)	41.7±0.7 (10)
T_{air} at onset of panting (°C)	39.3±1.2 (10)	40.4±1.5 (18)	38.6±1.6 (10)	40.1±1.0 (10)	39.6±0.9 (10)	38.4±1.6 (10)	39.3±2.2 (10)
95 th percentile $T_b > T_{air}$ (°C)	43.6	44.3	43.5	43.7	44.5	43.0	42.5
Metabolic rate							
Min. MR (W)	1.38±0.40 (10)	0.45±0.07 (20)	0.59±0.11 (10)	0.54±0.06 (10)	0.64±0.15 (10)	0.69±0.23 (10)	0.58±0.13 (10)
T_{uc} (°C)	33.0	43.8	42.5	38.1	37.1	39.8	37.18
MR slope (mW °C ⁻¹)	75.28	43.76	55.29	12.01	50.7	37.9	45.7
Max. MR (W)	2.41±0.52 (6)	0.88 (1)	0.85±0.13 (3)	0.72±0.11 (10)	1.07±0.20 (5)	1.05±0.22 (7)	1.17±0.16 (4)
		0.85±0.1 (10)					
Max. MR/min. MR	1.78	1.89	1.44	1.17	1.67	1.52	2.02
Evaporative water loss							
Min. EWL (g h ⁻¹)	0.67±0.25 (10)	0.18±0.06 (20)	0.25±0.10 (10)	0.20±0.08 (10)	0.29±0.12 (10)	0.39±0.17 (10)	0.26±0.08 (10)
Inflection T_{air} (°C)	37.0	39.0	38.0	39.0	38.9	38.6	38.5
EWL slope (g h ⁻¹ °C ⁻¹)	0.51	0.12	0.15	0.13	0.28	0.19	0.16
Max. EWL (g h ⁻¹)	6.79±1.35 (6)	1.77±0.22 (10)	2.02±0.29 (3)	1.48±0.38 (6)	3.32 (1)	2.31±0.41 (7)	2.31 ± 0.17 (7)
					2.89±0.34 (5)		
Max. EWL/min. EWL	10.13	9.83	8.08	7.40	9.96	5.92	8.88
Min. EHL/MHP	0.31±0.08 (10)	0.22±0.06 (20)	0.28±0.09 (10)	0.19±0.06 (10)	0.24±0.11 (10)	0.35±0.18 (10)	0.29±0.08 (10)
EHL/MHP inflection $T_{air} - T_b$	-5.7	-4.3	-5.1	-4.0	-3.8	-4.6	-4.1
EHL/MHP slope	0.08	0.16	0.15	0.17	0.20	0.15	0.14
Max. EHL/MHP	2.05 (2)	1.71 (1)	1.62±0.39 (3)	1.57±0.28 (6)	2.20 (1)	1.48±0.15 (7)	1.61±0.29 (7)
	1.89±0.20 (6)	1.39±0.13 (10)			1.86±0.42 (5)		

Variable	Speckled mousebird	Spike-heeled lark	White-rumped swift
Body mass (g)	50.8±4.2 (6)	28.0±2.7 (10)	27.3±0.3 (10)
Body temperature			
Min. T_b (°C)	39.7±0.9 (6)	41.3±1.2 (10)	40.0±1.08 (10)
Inflection T_{air} (°C)	40.5	35.9	40.0
T_b versus T_{air} slope (°C)	0.59	0.28	0.50
Max T_b (°C)	45.3±0.3 (5)	45.5±0.3 (10)	45.5±0.3 (10)
Max T_{air} (°C)	45.8±1.1 (5)	48.5±2.2 (10)	46.9±1.0 (10)
T_b at onset of panting (°C)	40.9±0.4 (6)	43.0±0.6 (10)	42.0±0.4 (10)
T_{air} at onset of panting (°C)	37.1±1.3 (6)	40.5±1.5 (10)	36.8±2.2 (10)
95 th percentile $T_b > T_{air}$ (°C)	43.2	44.0	44.1
Metabolic rate			
Min. MR (W)	0.89±0.16 (6)	0.60±0.15 (10)	0.47±0.10 (10)
T_{uc} (°C)	33.8	43.2	40.8
MR slope (mW °C ⁻¹)	37.96	51.43	28.7
Max. MR (W)	1.28±0.40 (4)	0.96±0.26 (10)	0.78±0.13 (3)
Max. MR/min. MR	1.44	1.60	1.66
Evaporative water loss			
Min. EWL (g h ⁻¹)	0.42±0.16 (6)	0.36±0.15 (10)	0.17±0.05 (10)
Inflection T_{air} (°C)	35.2	38.2	35.5
EWL slope (g h ⁻¹ °C ⁻¹)	0.18	0.19	0.11
Max. EWL (g h ⁻¹)	2.56±0.27 (4)	2.63±0.42 (3)	1.63±0.02 (3)
Max. EWL/min. EWL	6.10	7.30	9.58
Min. EHL/MHP	0.30±0.09 (6)	0.33±0.13 (10)	0.23±0.1
EHL/MHP inflection $T_{air} - T_b$	-5.4	-5.2	-5.8
EHL/MHP slope	0.15	0.15	0.12
Max. EHL/MHP	1.45±0.52 (4)	1.90±0.56 (3)	1.43±0.28 (3)

Table S2.2. Mass-specific metabolic rate (MR) and evaporative water loss (EWL) rate at high T_{air} in seventeen bird species from a southern African montane region (Harrismith). Means, SD and N are reported.

Variable	Ant-eating chat	Bokmakierie	Buff-streaked chat	Cape robin chat	Cape white-eye
Min. MR (mW g ⁻¹)	20.4±6.5 (10)	18.0±6.4 (8)	19.2±3.9 (10)	25.8±6.1 (10)	29.0±3.5 (10)
MR slope (mW g ⁻¹ °C ⁻¹)	4.24	1.10	1.21	1.16	0.67
Max. MR (mW g ⁻¹)	41.7±4.1 (4)	28.7±6.0 (6)	30.9±8.4 (10)	42.6±4.3 (6)	36.1±5.3 (9)
Min. EWL (mg h ⁻¹ g ⁻¹)	7.8±1.8 (10)	9.1±4.1 (8)	10.7±3.0 (10)	11.7±4.2 (10)	13.6±6.4 (10)
EWL slope (mg h ⁻¹ g ⁻¹ °C ⁻¹)	9.60	5.43	5.34	5.96	5.47
Max. EWL (mg h ⁻¹ g ⁻¹)	74.1±10.8 (4)	63.3±13.1 (4)	65.4 (1)	76.9±16.0 (6)	68.5±12.9 (6)
			60.9±9.6 (6)		
Variable	Drakensberg prinia	Pied starling	Red-billed quelea	Red-capped lark	South African cliff swallow
Min. MR (mW g ⁻¹)	29.1±4.0 (7)	16.0±7.5 (10)	24.9±4.17 (20)	22.7±4.0 (10)	25.5±3.4 (10)
MR slope (mW g ⁻¹ °C ⁻¹)	1.48	0.84	2.3	1.85	0.56
Max. MR (mW g ⁻¹)	44.0±3.7 (4)	40.04 (2)	47.2±6.7 (10)	31.9±2.6 (3)	34.4±5.9 (10)
		31.5±18.0 (6)	49.2 (1)		
Min. EWL (mg h ⁻¹ g ⁻¹)	12.4±6.1 (7)	7.5±2.8 (10)	9.8±3.2 (20)	9.7±3.2 (10)	9.7±3.9 (10)
EWL slope (mg h ⁻¹ g ⁻¹ °C ⁻¹)	9.16	5.2	6.84	6.14	6.11
Max. EWL (mg h ⁻¹ g ⁻¹)	97.7±8.7 (4)	122 (2)	125.6 (1)	76.6±13.1 (3)	68.3±17.2 (6)
		87.9±47.8 (6)	97.5±11.6 (10)		
Variable	Southern masked weaver	Southern-red bishop	Speckled mousebird	Spike-heeled lark	White-rumped swift
Min. MR (mW g ⁻¹)	24.3±7.5 (10)	24.0±4.3 (10)	18.5±2.1 (6)	21.0±4.6 (10)	17.1±3.6 (10)
MR slope (mW g ⁻¹ °C ⁻¹)	1.48	1.96	0.75	1.79	0.88
Max. MR (mW g ⁻¹)	37.3±5.7 (10)	46.3±7.7 (4)	25.7±7.4 (4)	2.4 (1)	26.7±5.4 (3)
				33.3±9.0 (3)	
Min. EWL (mg h ⁻¹ g ⁻¹)	14.4±7.2 (10)	10.7±3.0 (10)	8.2±2.8 (6)	12.8±7.1 (10)	6.1±1.9 (10)
EWL slope (mg h ⁻¹ g ⁻¹ °C ⁻¹)	7.01	6.63	3.73	6.71	4.04
Max. EWL (mg h ⁻¹ g ⁻¹)	82.0±10.9 (7)	93.0±9.8 (7)	51.5±5.7 (4)	91.9 (1)	62.1±2.02 (3)
				90.1±6.1 (3)	

Table S3.1 Summary of thermoregulatory performance as a function of chamber air temperature (T_{air}) in twenty species from the coastal lowland study site (Richards Bay). T_b = body temperature, T_{air} = ambient temperature, MR = metabolic rate, EWL = evaporative water loss, EHL= evaporative heat loss, MHP = metabolic heat production. Means, SD and N are reported.

Variable	African pygmy-kingfisher	Blue-checked bee-eater	Bronze mannikin	Brown-hooded kingfisher	Cape white-eye	Collared sunbird	Dark-capped bulbul
Body mass (g)	13.3±0.9 (10)	46.3±2.1 (10)	9.1±0.5 (9)	62.1±2.3 (10)	11.0±0.4 (10)	6.9±0.4 (10)	36.8±1.4 (10)
Body temperature							
Min. T_b (°C)	40.5±1.0 (10)	39.5±1.4 (10)	39.6±0.9 (9)	40.0±0.6 (10)	40.8±1.0 (10)	38.9±1.3 (10)	40.0±1.8 (10)
Inflection T_{air} (°C)	34.6	35.2	36.5	35.5	36.8	34.2	35.8
T_b versus T_{air} slope (per °C)	0.37	0.33	0.56	0.33	0.38	0.47	0.30
Max T_b (°C)	45.4±0.3 (10)	45.8±1.4 (10)	47.1±0.4 (9)	45.5±0.3 (10)	45.9±0.4 (10)	44.5±0.7 (10)	45.0±0.5 (10)
Max T_{air} (°C)	46.3±1.1 (10)	52.2±1.4 (10)	47.7±1.3 (9)	49.8±1.5 (10)	47.9±0.8 (10)	43.3±1.8 (10)	49.4±2.6 (10)
T_b at onset of panting (°C)	41.9±1.2 (10)	42.4±1.0 (10)	41.4±0.7 (9)	41.4±0.8 (10)	42.2±0.8 (10)	41.9±1.0 (8)	41.6±1.3 (10)
T_{air} at onset of panting (°C)	39.6±1.6 (10)	41.4±1.3 (10)	39.6±0.4 (9)	39.4±1.5 (10)	39.0±1.1 (10)	39.4±2.1 (8)	38.8±1.9 (10)
95 th percentile $T_b > T_{air}$ (°C)	44.2	42.8	45.1	42.5	44.1	44.1	43.4
Metabolic rate							
Min. MR (W)	0.30±0.05 (10)	0.58±0.07 (10)	0.20±0.03 (9)	0.82±0.13 (10)	0.37±0.07 (10)	0.21±0.04 (10)	0.76±0.14 (10)
T_{ic} (°C)	33.5	38.1	39.3	37.8	37.6	33.3	37.2
MR slope (mW °C ⁻¹)	21.94	63.50	33.60	61.42	21.42	13.91	35.22
Max. MR (W)	0.56±0.07 (6)	1.38±0.22 (8)	0.50±0.15 (5)	1.40±0.1 (5)	0.56±0.07 (7)	0.36±0.05 (9)	1.14±0.11 (3)
Max. MR/min. MR	2.26	2.38	2.50	1.71	1.53	1.71	1.50
Evaporative water loss							
Min. EWL (g h ⁻¹)	0.14±0.02 (10)	0.25±0.06 (10)	0.10±0.03 (9)	0.36±0.1 (10)	0.13±0.06 (10)	0.09±0.02 (10)	0.27±0.06 (10)
Inflection T_{air} (°C)	38.3	39.5	37.5	39.9	37.8	36.2	37.2
EWL slope (g h ⁻¹ °C ⁻¹)	0.10	0.27	0.06	0.30	0.09	0.05	0.18
Max. EWL (g h ⁻¹)	1.07 (2)	4.00±0.78 (3)	0.68±0.09 (5)	4.02 (1)	1.10±0.12 (7)	0.54 (1)	2.97±0.34 (3)
	0.94±0.1 (6)			3.69±0.38 (5)		0.47±0.05 (4)	
Max. EWL/min. EWL	6.7	16.0	6.8	11.17	8.46	6.0	11
Min. EHL/MHP	0.30±0.08 (10)	0.19±0.03 (10)	0.30±0.08 (9)	0.29±0.06 (10)	0.23±0.07 (10)	0.26±0.06 (10)	0.24±0.03 (10)
EHL/MHP inflection $T_{air} - T_b$	-4.3	-3.8	-5.9	-3.4	-5.0	-4.0	-5.5
EHL/MHP slope	0.14	0.15	0.11	0.16	0.13	0.12	0.12
Max. EHL/MHP	1.14±0.20 (6)	1.96±0.17 (3)	0.94±0.21 (5)	1.76±0.22 (10)	1.33±0.13 (7)	1.01±0.15 (4)	1.74±0.09 (3)

Variable	Green-backed camaroptera	Little swift	Olive sunbird	Red-capped robin-chat	Sombre greenbul	Southern fiscal	Southern red bishop
Body mass (g)	11.6±0.5 (10)	25.9±1.5 (10)	11.3±0.9 (10)	29.6±1.4 (10)	30.6±1.7 (10)	40.6±2.2 (10)	16.8±1.8 (9)
Body temperature							
Min. T_b (°C)	40±1.2 (10)	39.3±1.5 (10)	38.9±0.7 (10)	38.8±0.6 (10)	40.4±1.3 (10)	40.3±0.8 (10)	39.8±0.6 (6)
Inflection T_{air} (°C)	33.8	38.5	35.5	36.9	40.3	35.4	38.1
T_b versus T_{air} slope (per °C)	0.35	0.43	0.56	0.34	0.40	0.34	0.39
Max T_b (°C)	45.7±0.4 (10)	45.6±0.5 (10)	46.4±0.6 (10)	45.4±0.4 (10)	45.4±0.6 (10)	45.4±0.5 (10)	46.3±0.5 (9)
Max T_{air} (°C)	48.5±0.9 (10)	49.3±1.4 (10)	46.2±1.0 (10)	49.9±1.4 (10)	49.0±1.8 (10)	49.5±1.2 (10)	50.8±1.2 (9)
T_b at onset of panting (°C)	41.6±0.7 (10)	41.2±0.6 (10)	42.6±1.2 (10)	41.2±0.7 (10)	41.8±1.4 (6)	42.2±0.6 (10)	42.1±1.2 (9)
T_{air} at onset of panting (°C)	38.3±1.6 (10)	38.9±1.5 (10)	39.6±1.6 (10)	39.0±1.6 (10)	37.5±2.2 (6)	40.5±1.0 (10)	39.6±1.9 (9)
95 th percentile $T_b > T_{air}$ (°C)	44.0	42.2	45.3	42.2	42.5	43.0	43.5
Metabolic rate							
Min. MR (W)	0.32±0.05 (10)	0.35±0.07 (10)	0.30±0.04 (10)	0.51±0.15 (10)	0.70±0.12 (10)	0.61±0.07 (10)	0.40±0.06 (9)
T_{uc} (°C)	33.4	39.3	34.6	42.7	41.6	37.5	40.0
MR slope (mW °C ⁻¹)	14.56	45.8	28.5	57.1	67.2	55.3	30.7
Max. MR (W)	0.50 (2)	0.89±0.16 (6)	0.67±0.11 (7)	1.01±0.13 (5)	1.30±0.26 (4)	1.48 (1)	0.80 (2)
	0.49±0.05 (9)					1.13±0.15 (5)	0.67±0.09 (8)
Max. MR/min. MR	1.53	2.54	2.23	1.98	1.86	2.42	2.0
Evaporative water loss							
Min. EWL (g h ⁻¹)	0.10±0.02 (10)	0.11±0.02 (10)	0.11±0.03 (10)	0.21±0.07 (10)	0.23±0.06 (10)	0.28±0.07 (10)	0.13±0.03 (9)
Inflection T_{air} (°C)	37.0	39.1	36.5	38.3	38.4	38.5	38.0
EWL slope (g h ⁻¹ °C ⁻¹)	0.08	0.15	0.09	0.17	0.20	0.25	0.12
Max. EWL (g h ⁻¹)	1.04 (2)	1.84±0.14 (6)	1.01(1)	2.40±0.13 (5)	2.94 (1)	3.14 (1)	1.46±0.25 (8)
	1.02±0.06 (9)		0.98±0.11 (7)		2.86±0.25 (4)	2.74±0.22 (5)	
Max. EWL/min. EWL	10.4	13.14	8.9	11.43	12.4	9.79	11.23
Min. EHL/MHP	0.21±0.05 (10)	0.19±0.04 (10)	0.24±0.06 (10)	0.28±0.06 (10)	0.22±0.05 (10)	0.24±0.09 (10)	0.20±0.04 (9)
EHL/MHP inflection $T_{air} - T_b$	-5.1	-4.0	-4.9	-4.7	-5.70	-3.8	-5.4
EHL/MHP slope	0.14	0.15	0.15	0.14	0.11	0.16	0.12
Max. EHL/MHP	1.39±0.13 (9)	1.48±0.26 (6)	1.02(1)	1.61±0.23 (5)	1.50±0.21 (4)	1.62±0.12 (5)	1.45±0.07 (8)
			0.99±0.18 (7)		1.61 (10)		

Variable	Speckled mousebird	Spectacled weaver	Tawny-flanked prinia	White-eared barbet	Yellow weaver	Yellow-rumped tinkerbird
Body mass (g)	44.2±6.1 (9)	26.1±2.5 (10)	9.1±0.7 (10)	47.4±1.6 (8)	28.5±3.9 (10)	13.5±0.8 (10)
Body temperature						
Min. T_b (°C)	39.1±0.8 (9)	40.0±1.1 (10)	39.4±0.1 (10)	39.3±1.1 (8)	40.7±0.5 (10)	39.8±1.0 (10)39.
Inflection T_{air} (°C)	37.7	38.3	33.8	34.6	37.3	35.2
T_b versus T_{air} slope (per °C)	0.37	0.41	0.44	0.43	0.37	0.41
Max T_b (°C)	44.8±1.4 (9)	45.4±0.8 (10)	45.7±0.4 (9)	45.1±0.5 (8)	45.9±0.4 (10)	45.4±0.5 (10)
Max T_{air} (°C)	49.4±1.1 (9)	49.3±1.5 (10)	48.9±1.5 (9)	47.8±1.6 (8)	48.7±0.7 (10)	47.0±1.3 (10)
T_b at onset of panting (°C)	40.9±0.8 (9)	41.0±1.2 (10)	41.7±0.8 (10)	41.6±1.0 (8)	42.1±0.5 (10)	41.6±1.4 (10)
T_{air} at onset of panting (°C)	37.5±1.9 (9)	37.9±1.7 (10)	39.8±0.6 (10)	40.2±0.7 (8)	39.0±1.2 (10)	38.8±1.4 (10)
95 th percentile $T_b > T_{air}$ (°C)	42.2	42.9	44.1	43.1	43.5	43.6
Metabolic rate						
Min. MR (W)	0.66±0.08 (9)	0.43±0.06 (10)	0.21±0.04 (10)	0.65±0.07 (8)	0.62±0.13 (10)	0.33±0.06 (10)
T_{uc} (°C)	32.5	40.7	34.0	34.5	38.8	34.5
MR slope (mW °C ⁻¹)	27.1	41.6	20.0	46.7	50.8	24.6
Max. MR (W)	1.06±0.15 (4)	0.88±0.05 (10)	0.49±0.04 (10)	1.36 (2) 1.17±0.39 (4)	1.09±0.13 (10)	0.62±1.2 (3)
Max. MR/min. MR	1.61	2.04	2.33	2.09	1.76	1.88
Evaporative water loss						
Min. EWL (g h ⁻¹)	0.28±0.13 (9)	0.15±0.03 (10)	0.09±0.02 (10)	0.24±0.02 (8)	0.18±0.04 (10)	0.12±0.05 (10)
Inflection T_{air} (°C)	34.2	37.6	38.3	37.3	37.7	37.2
EWL slope (g h ⁻¹ °C ⁻¹)	0.14	0.13	0.09	0.21	0.18	0.09
Max. EWL (g h ⁻¹)	2.35±0.26 (4)	1.83±0.09 (7)	1.11±0.1 (4)	2.94 (2) 2.48±0.13 (4)	2.18±0.28 (10)	1.26±0.30 (3)
Max. EWL/min. EWL	8.39	12.20	13.33	12.25	12.1	10.5
Min. EHL/MHP	0.26±0.11 (9)	0.23±0.05 (10)	0.22±0.06 (10)	0.22±0.03 (8)	0.19±0.03	0.23±0.06 (10)
EHL/MHP inflection $T_{air} - T_b$	-5.1	-5.3	-4.2	-4.1	-5.5	-4.4
EHL/MHP slope	0.12	0.12	0.16	0.16	0.14	0.12
Max. EHL/MHP	1.50±0.18 (4)	1.40±0.08 (7)	1.51±0.09 (4)	1.52±0.42 (4)	1.34±0.19 (10)	1.33±0.06 (3)

Table S3.2 Mass-specific metabolic rate (MR) and evaporative water loss (EWL) rate at high T_{air} in twenty bird species from the eastern coastal lowland region of South Africa (Richards Bay). Means, SD and N are reported.

Variable	African pygmy kingfisher	Blue-cheeked bee-eater	Bronze mannikin	Brown-hooded kingfisher	Cape white-eye	Collared sunbird
MR						
Min. MR (mW g ⁻¹)	22.6±3.1 (10)	12.6±1.5 (10)	22.7±3.3 (9)	13.1±2.3 (10)	33.6±5.6 (10)	29.9±5.3 (10)
MR slope (mW g ⁻¹ °C ⁻¹)	1.65	1.38	3.71	0.98	1.94	2.09
Max. MR (mW g ⁻¹)	50.1 (2)	30.0±4.6 (8)	54.7±17.4 (5)	26.1 (1)	50.9±6.2 (7)	46.9±2.9 (4)
	42.1±6.15 (6)			22.3±1.2 (5)		
EWL						
Min. EWL (mg h ⁻¹ g ⁻¹)	10.7±1.7 (10)	5.5±1.1 (10)	11.5±2.5 (9)	5.7±1.8 (10)	12.4±4.8 (10)	13.3±2.6 (10)
EWL slope (mg h ⁻¹ g ⁻¹ °C ⁻¹)	7.30	5.91	6.40	4.74	8.10	6.89
Max. EWL (mg h ⁻¹ g ⁻¹)	77.5 (2)	86.5±13.0 (3)	73.6±11.3 (5)	62.2 (1)	100.2±7.4 (7)	75.7 (1)
	70.6±7.7 (6)			58.5±6.1 (5)		70.7±8.6 (4)
Variable	Dark-capped bulbul	Green-backed camaroptera	Little swift	Olive sunbird	Red-capped robin-chat	Sombre greenbul
MR						
Min. MR (mW g ⁻¹)	20.7±3.3 (10)	27.3±4.0 (10)	14.3±1.8 (10)	26.0±3.6 (10)	17.3±5.3 (10)	22.9±3.52 (10)
MR slope (mW g ⁻¹ °C ⁻¹)	0.95	1.24	1.68	2.40	1.93	2.52
Max. MR (mW g ⁻¹)	30.6±2.3 (3)	42.8 (2)	33.4±5.8 (6)	71.5 (1)	34.5±4.3 (10)	41.61±7.06 (4)
		42.5±4.7 (9)		55.6±11.6 (7)		
EWL						
Min. EWL (mg h ⁻¹ g ⁻¹)	7.4±79.8 (10)	8.5±2.1 (10)	4.1±0.5 (10)	9.3±2.1 (10)	7.0±2.3 (10)	7.59±1.87 (10)
EWL slope (mg h ⁻¹ g ⁻¹ °C ⁻¹)	4.91	7.0	5.52	7.39	5.84	6.46
Max. EWL (mg h ⁻¹ g ⁻¹)	79.8±8.0 (3)	88.3 (2)	69.0±5.0 (6)	110.0 (1)	82.1±2.9 (5)	97.6 (1)
		87.7±5.5 (9)		80.5±10.2 (7)		92.0±4.68 (4)

Variable	Southern fiscal	Southern red bishop	Speckled mousebird	Spectacled weaver	Tawny-flanked prinia	White-eared barbet
MR						
Min. MR (mW g ⁻¹)	15.0±1.7 (10)	23.3±4.4 (9)	15.1±2.3 (9)	17.3±2.1 (10)	29.9±7.8 (10)	13.7±1.2 (8)
MR slope (mW g ⁻¹ °C ⁻¹)	1.35	1.76 (9)	NA	1.61	2.18	0.97
Max. MR (mW g ⁻¹)	35.0 (1)	48.8 (2)	24.1±6.6 (4)	33.8±3.1 (7)	53.0±2.8 (4)	27.9 (2)
	28.5±3.2 (5)	39.7±3.1 (8)				24.1±8.1 (4)
EWL						
Min. EWL (mg h ⁻¹ g ⁻¹)	7.0±1.8 (10)	7.8±2.2 (9)	6.8±3.5 (8)	5.9±1.0 (10)	9.5±2.6 (10)	5.2±0.5 (8)
EWL slope (mg h ⁻¹ g ⁻¹ °C ⁻¹)	6.11	6.30	3.17	4.97	9.53	4.18
Max. EWL (mg h ⁻¹ g ⁻¹)	74.6 (1)	86.3±7.9 (8)	52.8±8.7 (4)	70.6±7.1 (7)	119.8±8.8 (4)	60.2 (2)
	68.5±4.4 (5)					51.2±2.6 (4)
Variable	Yellow weaver	Yellow-rumped tinkerbird				
MR						
Min. MR (mW g ⁻¹)	21.9±3.7 (10)	24.6±4.7 (10)				
MR slope (mW g ⁻¹ °C ⁻¹)	1.94	1.84				
Max. MR (mW g ⁻¹)	38.9±6.0 (10)	44.9±10.0 (3)				
EWL						
Min. EWL (mg h ⁻¹ g ⁻¹)	6.5±1.4 (10)	9.3±4.5 (10)				
EWL slope (mg h ⁻¹ g ⁻¹ °C ⁻¹)	6.70	6.83				
Max. EWL (mg h ⁻¹ g ⁻¹)	77.3±9.1 (10)	90.4±23.9 (10)				

Table S4 Phylogenetic generalized least squares regression and ordinary least square model outputs for heat tolerance limit (HTL), maximum body temperature (T_{bmax}), slope of the relationship between air temperature and T_b (T_{bslope}), upper critical temperature (T_{uc}), ratio between maximum and minimum evaporative water loss (EvapScope) and normothermic body temperature (T_{bnorm}). Main effects for all models included sampling locality (arid, montane and lowland), body mass (M_b), and interaction effect between locality and body mass. A PGLS one way ANOVA was conducted to detect significant differences between physiological responses at different localities. Mean \pm SD for arid, montane, and lowland species for each trait is shown, as well as the phylogenetic signal (λ) and p-value of each main effect. Bold font indicates a significant p-value ($\alpha = 0.05$)

Model (PGLS)	Mean \pm SD ($^{\circ}$ C)			λ	p(locality)	p(M_b)	p(locality: M_b)
	Arid	Montane	Lowland				
HTL~locality+ M_b + locality: M_b	50.59 \pm 2.57	47.55 \pm 1.56	48.67 \pm 2.04	0.67	<0.01	0.01	0.16
T_{bmax} ~locality+ M_b + locality: M_b	44.65 \pm 0.60	45.42 \pm 0.78	45.60 \pm 0.58	0.38	<0.01	<0.01	0.66
T_{bslope} ~locality+ M_b + locality: M_b	0.29 \pm 0.07	0.34 \pm 0.09	0.40 \pm 0.07	0.31	<0.01	<0.01	0.13
T_{UC} ~locality+ M_b + locality: M_b	36.94 \pm 4.45	38.16 \pm 3.60	37.05 \pm 3.07	0	0.59	0.20	0.13
EvapScope~locality+ M_b + locality: M_b	9.07 \pm 2.7	7.86 \pm 1.66	10.86 \pm 2.79	0	0.02	0.49	0.18
T_{bnorm} ~locality+ M_b + locality: M_b	40.55 \pm 0.71	40.45 \pm 0.56	39.76 \pm 0.60	0.40	<0.01	0.31	0.64
Model (OLS)							
HTL~locality+ M_b + locality: M_b	50.59 \pm 2.57	47.55 \pm 1.56	48.67 \pm 2.04	-	<0.01	0.16	0.10
T_{bmax} ~locality+ M_b + locality: M_b	44.65 \pm 0.60	45.42 \pm 0.78	45.60 \pm 0.58	-	<0.01	<0.01	0.80
T_{bslope} ~locality+ M_b + locality: M_b	0.29 \pm 0.07	0.34 \pm 0.09	0.40 \pm 0.07	-	<0.01	<0.01	0.24
T_{UC} ~locality+ M_b + locality: M_b	36.94 \pm 4.45	38.16 \pm 3.60	37.05 \pm 3.07	-	0.59	0.20	0.13
EvapScope~locality+ M_b + locality: M_b	9.07 \pm 2.7	7.86 \pm 1.66	10.86 \pm 2.79	-	0.019	0.49	0.18
T_{bnorm} ~locality+ M_b + locality: M_b	40.55 \pm 0.71	40.45 \pm 0.56	39.76 \pm 0.60	-	<0.01	0.69	0.72

Table S5: Model selection for multivariate additive linear model of maximum body temperature as a function of study locality (Clim), maximum air temperature (T_{air}) tolerated by a species (HTL), evaporative cooling efficiency - evaporative heat loss/metabolic heat production (EHL/MHP), ratio of maximum evaporative water loss (EWL) to minimum thermoneutral EWL (EvapScope), the slope of the relationship between T_b and T_{air} above inflection points ($T_{b\text{slope}}$), T_b at rest at thermoneutral conditions ($T_{b\text{norm}}$) and interaction terms between study locality and HTL, EHL/MHP, EvapScope, $T_{b\text{slope}}$, and $T_{b\text{norm}}$. A “+” indicates inclusion of a predictor variable or interaction from a model formula. Best-performing models are highlighted in bold. If two models were within <2 AIC_c the most parsimonious model was chosen.

Model	Int.	Clim	M_b	HTL	Max EHL/ MHP	Evap Scope	T_b Slope	T_b norm	Clim: Mb	Clim: HTL	Clim: EHL/ MHP	Clim: Evap Scope	Clim: $T_{b\text{slope}}$	Clim: $T_{b\text{norm}}$	df	logLik	AIC	delta	weight
3.2	23.92	+	-0.005	0.15	-0.69		4.40	0.33		+					10	-25.34	70.7	0	0.72
3.3	22.09	+		0.16	-0.81		5.0	0.36		+					9	-27.38	71.0	0.27	0.47
3.1	25.22	+	-0.004	0.13	-0.67	0.02	4.21	0.32		+					11	-24.54	71.1	0.41	0.29
2.1	25.38	+	-0.006	0.14	-0.66	0.02	4.05	0.31	+	+					13	-22.92	71.9	1.18	0.14
2.2	26.76	+	-0.007	0.10	-0.45	0.03	3.67	0.31	+	+	+				15	-21.42	72.9	2.18	0.08
2.4	23.77	+	-0.006	0.15	-0.64	0.02	4.91	0.33	+	+			+		15	-21.71	73.4	2.76	0.06
2.3	25.59	+	-0.007	0.15	-0.68	0.008	3.93	0.30	+	+		+			15	-22.66	75.3	4.64	0.02
2.5	24.12	+	-0.006	0.14	-0.67	0.02	4.16	0.34	+	+				+	15	-22.71	75.4	4.75	0.02
3.4	37.53	+	-0.007	0.16	-0.76		2.60			+					9	-31.07	80.1	9.46	0.002
1.6	24.42	+	-0.006	0.21	-0.82	0.02	3.52	0.25	+						9	-33.21	84.4	13.74	0
2	23.93	+	-0.008	0.23	-0.83	0.01	3.35	0.25							11	-32.16	86.3	15.64	0
3.5	36.08	+	-0.009	0.13	-0.89			0.10		+					9	-34.53	87.1	16.38	0
1.5	35.37	+	-0.007	0.20	-0.85	0.02	2.19								8	-35.90	87.8	17.14	0
1.3	36.89	+	-0.009	0.20	-0.98										6	39.21	90.4	19.75	0
1.4	37.74	+	-0.009	0.17	-0.94	0.03									7	-38.39	90.8	20.10	0
1.2	39.63	+	-0.01	0.11											5	-45.28	100.6	29.89	0
1	45.02	+	-0.01												4	-49.75	107.5	36.83	0
0	44.48	+													3	-53.85	113.7	43.02	0

Table S6 Phylogenetically informed stepwise multiple comparisons (phylogenetic ANOVA post hoc analysis test) and conventional analysis of variance (ANOVA) stepwise multiple comparisons (Tukey HSD post-hoc test) comparing whether body mass, maximum body temperature (T_{bmax}) and the thermoregulatory predictors included in our multivariate additive linear model differed significantly between study localities. Bold values indicate significant differences between study localities ($p < 0.05$). Predictor variables described in table include HTL - the maximum T_{air} tolerated before the onset of severe hyperthermia, EvapScope - maximum EWL (evaporative water loss)/minimum thermoneutral EWL, T_{bslope} - the slope of T_b as a function of T_{air} above thermoneutrality, T_{bnorm} - normothermic T_b , MaxEHL/MHP - maximum evaporative heat loss (EHL)/ metabolic heat production (MHP), MetabCost - maximum metabolic rate (MR) / thermoneutral MR.

	PhylANOVA post hoc			Tukey post hoc		
	t-value	p-value	Diff	lower	upper	p-value
M_b						
Lowland - Arid	-2.06	0.14	-14.56	-31.55	2.41	0.11
Montane - Arid	-0.62	0.45	-4.54	-22.31	13.22	0.81
Mountain - Forest	1.32	0.39	10.03	-8.3	28.35	0.39
HTL						
Lowland - Arid	-3.25	0.004	-2.06	-3.59	-0.53	<0.001
Montane - Arid	-4.59	0.003	-3.06	-4.66	-1.46	<0.001
Mountain - Forest	-1.45	0.16	-0.99	-2.64	0.66	0.32
Tbmax						
Lowland - Arid	4.79	<0.01	0.95	0.47	1.43	<0.001
Montane - Arid	3.72	<0.01	0.77	0.27	1.27	<0.001
Mountain - Forest	-0.83	0.43	-0.18	-0.69	0.34	0.69
Tbnorm						
Lowland - Arid	-4.27	0.03	-0.79	-1.26	-0.33	<0.001
Montane - Arid	-0.48	0.51	-0.10	-0.59	0.39	0.88
Mountain - Forest	3.31	0.03	0.69	0.19	1.2	<0.01
Tbslope						
Lowland - Arid	4.75	0.003	0.11	0.05	0.17	<0.001
Montane - Arid	2.20	0.15	0.05	-0.01	0.11	0.08
Mountain - Forest	-2.26	0.02	-0.06	-0.12	0.01	0.07
Max. EHL/MHP						
Lowland - Arid	-4.30	0.003	-0.45	-0.71	-0.71	<0.001
Montane - Arid	-3.03	0.003	-0.34	-0.61	-0.07	0.01
Mountain - Forest	-1.05	0.33	0.12	-0.16	0.4	0.55
EvapScope						
Lowland - Arid	0.69	0.51	0.63	-1.56	2.82	0.77
Montane - Arid	-2.09	0.02	-1.99	-4.28	0.3	0.1
Mountain - Forest	-2.67	0.01	-2.62	-4.98	-0.26	0.03
MetabCost						
Lowland - Arid	2.09	0.02	0.38	0.18	0.57	<0.001
Montane - Arid	0.26	0.77	0.01	-0.2	0.21	0.99
Mountain - Forest	-1.97	0.04	-0.38	-0.58	-0.16	<0.001

Table S7 Durbin-Watson test outputs assessing autocorrelation between model variables included in the ‘phylogenetic generalised least square’ multivariate additive linear model with maximum body temperature (T_{bmax}) as the response variable. The Durbin Watson test detects autocorrelation based on the independence of residuals of linear regressions output. Values of DW approaching and around two and $p > 0.05$ indicate no significant autocorrelation between variables or within models. Conversely values of DW approaching 0 and $p < 0.05$ indicate significant autocorrelation between variables or within models. Predictor variables described in table include HTL - the maximum T_{air} tolerated before the onset of severe hyperthermia, EvapScope - maximum EWL (evaporative water loss)/minimum thermoneutral EWL, T_{bslope} - the slope of T_b as a function of T_{air} above thermoneutrality, T_{bnorm} - normothermic T_b , MaxEHL/MHP - maximum evaporative heat loss (EHL)/ metabolic heat production (MHP), Climate – dry arid, humid lowland, cool montane.

Input	DW Value	p-value
EvapScope~ M_b	1.91	0.34
EvapScope~ HTL	1.72	0.96
EvapScope~MaxEHL.MHP	1.79	0.21
EvapScope~ T_{bslope}	1.84	0.26
EvapScope~ T_{bnorm}	1.85	0.27
M_b ~HTL	1.11	<0.001
M_b ~MaxEHL.MHP	1.04	<0.001
M_b ~ T_{bslope}	1.35	0.004
M_b ~ T_{bnorm}	1.34	0.003
HTL ~MaxEHL.MHP	1.89	0.34
HTL ~ T_{bslope}	1.92	0.37
HTL ~ T_{bnorm}	2.08	0.61
MaxEHL.MHP~ T_{bslope}	2.36	0.92
MaxEHL.MHP~ T_{bnorm}	2.31	0.88
T_{bslope} ~ T_{bnorm}	2.36	0.92
T_{bmax} ~Climate+HTL+MaxEHL/MHP+ T_{bslope} + T_{bnorm} + HTL: Climate (Model 3.3)	1.83	0.23

1.8.1.7 Appendix S1 References

1. Z. J. Czenze, *et al.*, Regularly drinking desert birds have greater evaporative cooling capacity and higher heat tolerance limits than non-drinking species. *Funct. Ecol.* **34**, 1589–1600 (2020).
2. R. Kemp, A. E. McKechnie, Thermal physiology of a range-restricted desert lark. *J. Comp. Physiol. B Biochem. Syst. Environ. Physiol.* **189**, 131–141 (2019).
3. M. C. Whitfield, B. Smit, A. E. McKechnie, B. O. Wolf, Avian thermoregulation in the heat: scaling of heat tolerance and evaporative cooling capacity in three southern African arid-zone passerines. *J. Exp. Biol.* **218**, 1705–1714 (2015).
4. B. Smit, *et al.*, Avian thermoregulation in the heat: phylogenetic variation among avian orders in evaporative cooling capacity and heat tolerance. *J. Exp. Biol.* **221**, jeb174870 (2018).
5. W. H. Karasov, *Digestion in birds: Chemical and physiological determinants and implications.*, M. L. Morrison, C. J. Ralph, J. Verner, J. R. Jehl, Eds., Studies in (Cooper Ornithological Society, 1990).
6. Lighton, *Measuring Metabolic Rates; A Manual for Scientists* (Oxford University Press, 2008).
7. G. E. Walsberg, B. O. Wolf, Variation in the respiratory quotient of birds and implications for indirect calorimetry using measurements of carbon dioxide production. *J. Exp. Biol.* **219**, 213–219 (1995).
8. C. R. Tracy, W. R. Welch, B. Pinshow, W. P. Porter, *Properties of Air: A Manual for Use in Biophysical Ecology*, 4th Ed. (University of Wisconsin, 2010).
9. R. E. Schulze, *et al.*, “South African atlas of climatology and agrohydrology: Water Research Commission” (2007).
10. M. T. Freeman, Z. J. Czenze, K. Schoeman, A. E. McKechnie, Extreme hyperthermia tolerance in the world’s most abundant wild bird. *Sci. Rep.* **10**, 1–6 (2020).

11. S. J. Hackett, *et al.*, A phylogenomic study of birds reveals their evolutionary history. *Science* (80-.). **320**, 1763–1768 (2008).

CHAPTER 2 EVOLUTION OF AVIAN HEAT TOLERANCE: THE ROLE OF ATMOSPHERIC HUMIDITY

This data chapter has been prepared for submission to Ecology Letters and is formatted in line with the journal's requirements

2.1 ABSTRACT

Raised atmospheric water vapour content (i.e., humidity) is known to affect the thermoregulatory performance of endotherms by impeding evaporative cooling capacity. However, little attention has been directed towards understanding how humidity affects the evolution of heat tolerance and thermoregulatory performance, or whether adaptive thermoregulation is evident among endotherms occupying habitats varying in average humidity. I hypothesized that birds from hot, humid habitats have evolved physiological mechanisms to reduce the impact of humidity-impeded evaporative heat dissipation compared to species occupying dryer habitats. To test this hypothesis, I quantified changes in heat tolerance limit (HTL), maximum body temperatures (T_{bmax}) and associated variables in response to humid ($19.21 \pm 1.20 \text{ g H}_2\text{O m}^{-3}$) versus dry ($1.07 \pm 0.84 \text{ g H}_2\text{O m}^{-3}$) air among 30 southern African bird species occurring at three climatically distinct sites (hot arid, mesic montane and humid lowlands). Making use of a phylogenetically informed comparative framework, I found that raised humidity decreased evaporative water loss (EWL) and resting metabolic rate by 27 - 38% and 21 - 27%, respectively, and did not differ significantly between sites. However, changes in HTL associated with humid air were significantly larger among arid (mean \pm SD = $-3.13 \pm 1.12 \text{ }^\circ\text{C}$) and montane species ($-2.44 \pm 1.0 \text{ }^\circ\text{C}$) compared to lowland species ($-1.23 \pm 1.34 \text{ }^\circ\text{C}$). I also found that, under humid conditions, T_{bmax} among lowland ($46.26 \pm 0.48^\circ\text{C}$) birds was significantly higher than among species at my arid ($45.23 \pm 0.24^\circ\text{C}$) study site. A significant positive relationship for $\text{HTL} \sim T_{bmax}$ under humid conditions highlights the functional importance of hyperthermia tolerance for overcoming the humidity-related constraints placed on evaporative cooling and, subsequently, heat tolerance. The macro-physiological patterns I report here, support the concept of a continuum from thermal specialization to thermal generalization among endotherms, with adaptive variation correlated with prevailing climatic conditions.

2.2 INTRODUCTION

The role of humidity in constraining evaporative heat dissipation has been extensively studied in humans (Sherwood and Huber 2010; Coffel et al. 2018; Sherwood 2018; Raymond et al. 2020; Li et al. 2020), but much less so in other endotherms. The impedance of evaporative heat dissipation by high humidity in laboratory settings has long been

recognized (e.g., Lasiewski et al. 1966), and elevated humidity has been implicated in heat-related mortalities of birds and bats (e.g., Welbergen et al. 2008; Ratnayake et al. 2019; McKechnie et al. 2021). However, the ways in which humidity constrains evaporative cooling capacity and heat tolerance remains poorly understood, primarily because of the technical challenges associated with experimentally manipulating humidity in laboratory settings. Even less attention has been paid to the notion that environmental humidity acts as a source of selection on the thermal physiology of animals (Angilletta et al. 2010); most analyses of environmental correlates of inter- or intraspecific variation have focused on variables such as temperature, aridity, precipitation or primary productivity (Lovegrove 2003; White et al. 2007; Smit et al. 2013; Boyle et al. 2020; Freeman et al. 2022).

Birds are an ideal taxon for investigating the possibility of adaptive variation in thermal physiology (Angilletta et al. 2010; Boyles et al. 2011) correlated with humidity, on account of many species' small size combined with diurnal habits and activity often coinciding with high daytime environmental temperatures. In his seminal paper on how humidity might influence the evolution of avian heat tolerance in humid, lowland environments, Weathers (1997) hypothesised that small birds occupying open, lowland habitats in the tropics have evolved pronounced hyperthermia tolerance to compensate for humidity-imposed constraints on evaporative heat dissipation. By allowing T_b to increase to values as high as $\sim 47^\circ\text{C}$, variable seedeaters (*Sporophila aurita*) maintained a positive $T_b - T_{\text{air}}$ gradient facilitating non-evaporative heat dissipation even at the high operative temperatures they experience in sunlit microsites (Weathers 1997).

Experimental manipulations of humidity in metabolic chambers confirm that elevated humidity impedes the effectiveness of evaporative cooling and increases the costs of offloading heat via evaporative water loss (EWL) (Powers 1992; Gerson et al. 2014b; van Dyk et al. 2019). However, these studies focussed on 1-2 arid-zone species (Gerson et al. 2014b; van Dyk et al. 2019) or were restricted to $T_{\text{air}} < \text{normothermic body temperature}$ ($T_{b\text{norm}}$; e.g., Powers 1992). In a recent comparative analysis of heat tolerance and evaporative cooling capacity measured under standardised conditions of very low humidity, Freeman et al. (2022) found that southern African birds occupying mesic climates, particularly humid coastal habitats, tolerated significantly higher maximum body temperature [$T_{b\text{max}}$ – maximum T_b before rapid declines in performance and broadly analogous to critical thermal maximum in ectotherms (Lutterschmidt and Hutchison 1997)]. Maximum body temperatures were significantly higher compared to arid-zone species,

lending support to the notion of hyperthermia tolerance as a mechanism to mitigate the impeding effects of humidity on evaporative cooling.

Here, I test the hypothesis that birds from hot, humid habitats have evolved physiological mechanisms to reduce the impact of humidity-impeded scope for evaporative heat dissipation. I predicted that a) compared to birds from less humid environments, reductions in heat tolerance limits (HTL – highest T_{air} tolerated before the onset of severe hyperthermia) associated with high humidity are more modest among birds from humid lowlands and b) variation in the effects of humidity on thermoregulation in the heat arise primarily from larger increases in T_{b} above normothermic levels among birds from humid lowlands (Weathers 1997; Freeman et al. 2022). My approach to testing these predictions involved comparing relationships between T_{air} , T_{b} , metabolic heat production and evaporative heat dissipation at an absolute humidity of $\sim 19 \text{ g H}_2\text{O m}^{-3}$ (equivalent to a dewpoint of $22.6 \text{ }^\circ\text{C}$ and relative humidity of 37.2% at $T_{\text{air}} = 40 \text{ }^\circ\text{C}$) to corresponding patterns at $\sim 1 \text{ g H}_2\text{O m}^{-3}$ ($-4.6 \text{ }^\circ\text{C}$ and 5.9%).

2.3 MATERIALS AND METHODS

Study areas

I collected data at three climatically distinct areas (hot arid, mesic montane and humid lowland) between latitudes of 27.90° and 30.04° S in South Africa (see Table 1 for general information and climatic data (Fick & Hijmans 2017, Smit et al. 2011).

Table 1 Location and climatic information relating to my three climatically distinct study areas (hot arid, mesic montane and humid lowland) within South Africa. Means \pm SD and (n) for summer are reported

	Hot arid	Mesic Montane	Humid lowland
Location	Kamiesberg, Mountains of western South Africa	Mooihoek farm, Harrismith, Free State province, South Africa	Hluhluwe, south-eastern South Africa.
Co-ordinates	30° 2'41.58" S, 17°57'12.88" E	28° 11'48.74" S, 29°9'54.70" E	27° 53'19.09" S, 32°21'34.87" E
Climate	hot dry summers and cool wet winters	Cool wet summers and cold dry winters	Hot wet humid summers and moderate winters
Mean summer maximum T_{air}	28.4 \pm 1.36 °C	26.4 \pm 1.50 °C	30.0 \pm 1.85 °C
Mean summer minimum T_{air}	14.63 \pm 2.60 °C	10.3 \pm 1.0 °C	18.82 \pm 1.03°C
Mean summer absolute humidity	7.1 + 0.7 g H ₂ O m ⁻³	10.0 \pm 1.4 g H ₂ O m ⁻³	16.9 \pm 1.4 g H ₂ O m ⁻³
Annual precipitation	~170-220 mm	~713 mm	~895mm

Study species

I analysed data collected under either dry ($\sim 1 \text{ g H}_2\text{O m}^{-3}$) or humid conditions ($\sim 19 \text{ g H}_2\text{O m}^{-3}$). Overall, my analysis includes data from 626 individuals (humid, $n = 307$; dry, $n = 320$) from 30 species, 15 families and three orders – Passeriformes, Piciformes and Coraciiformes (*SI Appendix*, Table S1.1 and 1.2).

Air and body temperature measurements

A temperature-sensitive passive integrated transponder (PIT) tag (Biotherm 13, Biomark, Boise, ID, USA) was injected into the peritoneal cavity of each bird prior to the commencement of experimentation to measure body temperature. Data from the tags were recorded using a reader and transceiver system (HPR +, Biomark, Boise ID, USA). During experimentation, T_{air} within the metabolic chamber was measured using a thermistor probe (TC-100, Sable Systems, Las Vegas, NV, USA) inserted through a small hole in the side of the chamber sealed by a rubber grommet.

Experimental protocol

I measured T_b , EWL and RMR using both the dry and humidity protocols. Measurements typically lasted 2 – 4 h and began with a bird placed in a chamber at $T_{\text{air}} = 28 \text{ }^\circ\text{C}$, and given at least 1 h to habituate to conditions in the metabolic chamber for both the dry and humid assessments. For the dry protocol, T_{air} setpoints beginning from $T_{\text{air}} = 28 \text{ }^\circ\text{C}$ were increased incrementally by $4 \text{ }^\circ\text{C}$ until $T_{\text{air}} = 40 \text{ }^\circ\text{C}$ and then increased incrementally by $2 \text{ }^\circ\text{C}$ until birds reached their thermal endpoint, following Freeman *et al.* (2022). For the humid protocol, T_{air} setpoints started at $34 \text{ }^\circ\text{C}$ and were increased incrementally by $2 \text{ }^\circ\text{C}$ until birds reached their thermal endpoint.. Although the initial T_{air} setpoints differed between dry and humid protocols, the initial habituation periods ($28 \text{ }^\circ\text{C}$) prior to the commencement of data collection were identical, and rates of heating similar between protocols. For these reasons, we do not believe these differences between protocols had any effect on observed patterns of thermoregulation, particularly at T_{air} approaching upper limits of thermoregulation. Transitions between successive T_{air} setpoints took 10–15 min. At each setpoint T_{air} , birds were exposed to stable T_{air} and humidity for a minimum of 15-20 minutes until traces of O_2 , CO_2 and H_2O were stable for at least 5 min. The stepped respirometry protocol involving

brief (15-20 min) exposure to each T_{air} setpoint used in this study has been shown to yield patterns of EWL, RMR and T_b as functions of T_{air} similar to those using a steady-state protocol where birds experience each T_{air} setpoint for several hours (Short et al. 2022).

Gas exchange measurements

Evaporative water loss (EWL) and carbon dioxide production (\dot{V}_{CO_2}) were measured using an open flow-through respirometry system, with my set-up identical to that described by Freeman *et al.* (2020, 2022) and described in full in *SI Appendix M* of the supplementary material.

During dry air measurements, flow rates were adjusted to minimise water vapour pressure within the metabolic chamber (mean chamber humidity across sites = 1.07 ± 0.84 g H₂O m⁻³), and varied between 3 L min⁻¹ and 24 L min⁻¹. Humidity measurements were made following methods similar to the dry protocol, with modifications to the respirometry setup permitting the manipulation of in-chamber humidity (see *SI Appendix M* for a detailed description and Figure M1). During my humidity measurements, mean chamber absolute humidity was 19.21 ± 1.20 g H₂O m⁻³ and varied by < 1.5 g H₂O m⁻³ between sites.

Data analyses

Sample sizes (n) for dry or humidity treatments were generally n = 10 individuals, but for a few species, they were lower (*SI Appendix*, Tables S1.1). All data were analysed in the R 4.0.5 (R Core Team, 2020) environment, using R Studio 1.1.463 (RStudio, Inc.). For each species, respective inflection T_{air} values above which T_b , EWL, EHL/MHP and RMR increased rapidly were identified using the R package *segmented.lme* (Muggeo 2016), with individual identity included as a random effect to account for measurements at multiple T_{air} values per individual and avoid pseudoreplication. Response variables including T_b , EWL, and RMR were analysed above and below inflection points separately using linear mixed-effect models in the R package *nlme* (Pinheiro J, Bates D, DebRoy S, Sarkar D 2015). Slopes for the relationships of thermoregulatory response variables were estimated as functions of T_{air} .

We made use of the “dredge” function from the *MuMIn* package to undertake model selection (Barton 2019). The standardised model used for within-species analysis included

T_{air} (or $T_{air}-T_b$), M_b , the $T_{air}: M_b$ interaction and Bird ID (individual) as a random factor. The model with the highest rank among competing models was selected using the AIC_c (Akaike information criterion values corrected for small sample size) as well as the Akaike weights (Burnham and Anderson 2002). Should the competing models have been within $\Delta AIC_c < 2$, I then selected the most parsimonious model. Significance was assessed at $\alpha < 0.05$ and values are presented as mean \pm SD.

2.3.1.1 Interspecific analyses

I accounted for the effect of phylogenetic non-independence in observed patterns of my thermoregulatory response variables by constructing a maximum-likelihood tree including all study species using Mesquite (Maddison and Maddison 2014). Making use of the Hackett phylogeny as a back-bone (Hackett et al. 2008), I downloaded 100 phylogenies from www.birdtree.org (Jetz et al. 2012). Determining the necessary branch-length transformations was achieved by comparing an Ornstein-Uhlenbeck model (Martins and Hansen 1997) with a Brownian motion model of trait evolution (Grafen 1989) using AIC values. Lower AIC values were attained for the Brownian motion model and it was therefore retained. I used Pagel's λ (Pagel 1999) to test for phylogenetic signal in the residual error of my PGLS (phylogenetic least square regression models) while simultaneously estimating regression parameters (Revell 2010), and rescaled my models using the estimates of λ . When testing for λ , I included mean M_b for species to account for the known allometric scaling of physiological traits such as basal metabolic rate (McNab 2002; McKechnie and Wolf 2004) and HTL (van Jaarsveld et al. 2021). In the data collected using the humidity protocol, I detected significant phylogenetic signal for HTL ($\lambda = 0.50$), RMR ($\lambda = 0.95$), EWL ($\lambda = 0.85$) and EHL_MHP ($\lambda = 0.47$) across climatic study sites, and I therefore present results from my PGLS analysis and phylogenetically informed post hoc tests (PhyloANOVA). The results of conventional analysis (i.e., phylogenetic non-independence not controlled for) are available in the supplementary material (*SI Appendix*, Tables S5). Conventional analyses mostly supported my findings following phylogenetic correction.

The R package *caper* (Orme et al. 2012) along with the “*pgls*” function was used to conduct phylogenetic regression analyses. To detect patterns, quantify differences in HTL between climatic study areas as well as determine which physiological variables were predictors of HTL patterns, I constructed a multivariable additive linear model (*SI Appendix*,

Table S6). The *MuMIn* package and “dredge” function was again used to detect which model selection procedure best explained observed patterns of HTL under humid conditions (Barton 2019). Model selection was conducted using AICc values and weights. In addition to model selection, I ran analyses to detect auto-correlation among predictor variables (*SI Appendix*, Table S7, Durbin Watson test) and assessed the normality of residuals using a Shapiro-Wilk test. Model 328 (HTL ~ Climate + MaxEHL/MHP + EvapScope + T_{bmax} + MaxEHL/MHP:climate; *SI Appendix*, Table S5) was selected. This model excludes EWLslope, MetabCost (maximum RMR/thermoneutral RMR) and RMRSlope. Model 328’s residuals were found to be normally distributed (Shapiro-Wilk normality test: $P=0.13$).

The “anova.pgl” function in the R-package *caper* (Orme et al. 2012) was applied to my multivariable model output to determine the significance of predictor variables and assess whether response variables differed significantly among study localities (*SI Appendix*, Table S5). I conducted post hoc multiple comparison tests taking into account phylogenetic relatedness using the “PhylANOVA” function in the R package *phytools* (Revell 2012) to obtain pairwise differences in both response and predictor between climatic areas. The PhylANOVA function conducts a simulation-based phylogenetic ANOVA and performs all post-hoc comparisons of means among groups providing a p-value by phylogenetic simulation (Garland et al. 1993).

2.4 RESULTS

Heat tolerance limits and body temperature

Among the 30 species included in this study, HTL in humid air ($19 \text{ g H}_2\text{O m}^{-3}$) ranged from 42.3°C to 49.5°C ($\bar{x} = 45.88 \pm 1.81^\circ\text{C}$), whereas HTL in dry air ($\sim 1 \text{ g H}_2\text{O m}^{-3}$) ranged from 43.3°C to 50.9°C ($\bar{x} = 48.02 \pm 1.55^\circ\text{C}$) (*SI Appendix*, Fig S1). Maximum air temperature tolerated was significantly higher under dry compared to humid conditions (t-test: $t = 8.71$, $p < 0.001$). My top multivariate model for HTL_{humid} (*SI Appendix*, Table S6; PGLS: $F_{10,21} = 13.36$, $P < 0.001$, $R^2 = 0.80$) revealed that climate ($F=34.14$, $p<0.001$), T_{bmax} ($F=18.76$, $p<0.01$), maxEHL/MHP ($F=18.20$, $p<0.01$), EvapScope ($F=6.65$, $p=0.02$) and the interaction between climate and maxEHL/MHP ($F= 3.98$, $p=0.03$) were significant predictors of HTL under humid conditions.

Humid HTL was significantly higher for lowland birds ($\bar{x} = 47.11 \pm 1.44$ °C) than arid-zone ($\bar{x} = 44.37 \pm 1.50$ °C; PhylANOVA: $t = 4.52$, $p < 0.01$) or montane ($\bar{x} = 45.45 \pm 1.30$ °C; PhylANOVA: $t = 2.73$, $p = 0.01$) species (*SI Appendix*, Fig S2), but did not differ between arid and montane birds (PhylANOVA: $t = -1.62$, $p = 0.10$) (Fig 1A and Table S5). Changes in HTL associated with humidity (i.e., $HTL_{\text{humid}} - HTL_{\text{dry}}$) were greatest for arid-zone species ($\bar{x} = -3.13 \pm 1.12$ °C), significantly greater than for lowland birds ($\bar{x} = -1.23 \pm 1.34$ °C; PhylANOVA: $t = -3.71$, $p < 0.01$) but not montane birds ($\bar{x} = -2.44 \pm 1.0$ °C; PhylANOVA: $t = -1.21$, $p < 0.22$) (Fig 1A). Humidity-associated decreases in HTL were significantly smaller among lowland birds compared to montane birds (PhylANOVA: $t = 2.37$, $p = 0.02$).

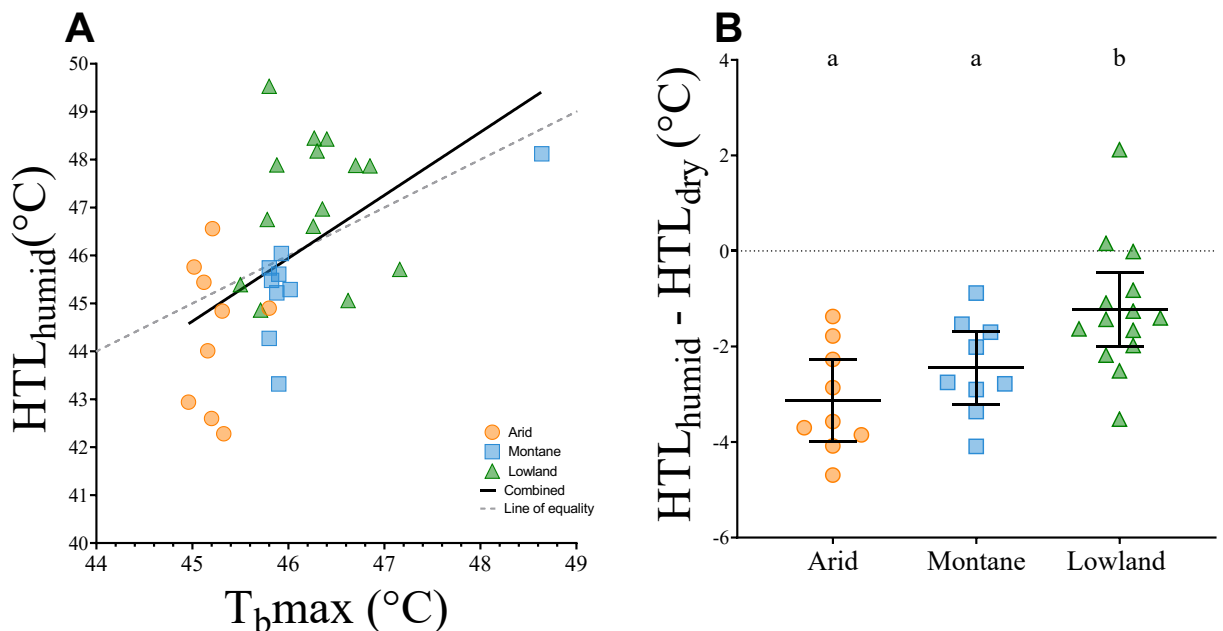


Figure 1 A.) Phylogenetic least square regression analysis (PGLS) of the relationships between HTL and $T_{b\text{max}}$ under humid conditions (~ 19 g H₂O m⁻³). Phylogenetic regression analysis revealed a positive relationship between HTL and $T_{b\text{max}}$ under humid conditions and also found a significant interaction between climatic area and $T_{b\text{max}}$ B.) Phylogenetic comparative analysis for differences in HTL (humid - dry) for birds subjected to a stepped respirometry protocol under dry (~ 1 g H₂O m⁻³) or humid (~ 19 g H₂O m⁻³) conditions in three climatically distinct regions. Climate categories are hot arid (orange circles, $n=9$), mesic montane (blue squares, $n=9$) and humid lowland (green triangles, $n=14$). Horizontal lines represent mean values and vertical lines have 95% confidence intervals. The letters above plots denote significant differences ($\alpha < 0.05$) in HTL (humid - dry) between climatic

areas. Decreases in HTL in response to humidity were significantly less among lowland birds compared to species from the mesic montane and arid climatic areas.

Phylogenetic analysis (PGLS: $F_{3,28} = 11.37$, $P < 0.001$, $R^2 = 0.56$) revealed a significant positive relationship for humid HTL $\sim T_{bmax}$ ($F=16.60$, $p < 0.001$) as well as a significant interaction between climate and T_{bmax} ($F=8.76$, $p < 0.001$; Fig 1B). Humid T_{bmax} was significantly higher among lowland ($\bar{x} = 46.26 \pm 0.48^\circ\text{C}$; PhylANOVA: $t = 4.02$, $p < 0.01$) and montane species [$\bar{x} = 46.19 \pm 0.92^\circ\text{C}$ (excluding *Quelea quelea*, $\bar{x} = 45.88 \pm 0.07^\circ\text{C}$); PhylANOVA: $t = 3.40$, $p < 0.01$] compared to arid-zone species ($\bar{x} = 45.23 \pm 0.24^\circ\text{C}$). Lowland and montane humid T_{bmax} did not differ significantly (PhylANOVA: $t = -0.27$, $p = 0.78$) even when excluding *Q. quelea* from the montane dataset (PhylANOVA: $t = -0.32$, $p = 0.74$).

Normothermic T_b (T_{bnorm}) during the humidity protocol for lowland species ($\bar{x} = 40.31 \pm 0.43^\circ\text{C}$) was significantly lower than arid ($\bar{x} = 41.48 \pm 0.43^\circ\text{C}$; PhylANOVA: $t = -6.11$, $p < 0.01$) or montane ($\bar{x} = 41.80 \pm 0.49^\circ\text{C}$; PhylANOVA: $t = -7.81$, $p < 0.01$) species. Arid-zone and montane T_{bnorm} did not differ significantly (PhylANOVA: $t = 1.53$, $p = 0.01$) (Fig S2 and Table S5). Fractional changes (i.e., humid/dry) in the slope of T_b change above thermoneutrality (i.e. $T_b\text{Slope}$) at my arid (34% increase; $\bar{x} = 1.34 \pm 0.16$ per $^\circ\text{C}$ of T_{air}), montane (28% increase; $\bar{x} = 1.28 \pm 0.32$ per $^\circ\text{C}$ of T_{air}) and lowland sites (26% increase; $\bar{x} = 1.26 \pm 0.24$ per $^\circ\text{C}$ of T_{air}) did not differ significantly (*SI Appendix*, Fig S3 and Table S5).

Evaporative water loss (EWL)

Maximum EWL decreased substantially among arid-zone (~26% decrease), montane (~39% decrease) and lowland birds (~37% decrease) under humid conditions (Fig 2A). However, fractional differences (humid/dry) in maximum EWL did not differ significantly between arid-zone ($\bar{x} = 0.74 \pm 0.19$), montane ($\bar{x} = 0.61 \pm 0.13$; PhylANOVA: $t = 1.58$, $p = 0.27$) and lowland ($\bar{x} = 0.62 \pm 0.15$; PhylANOVA: $t = 1.62$, $p = 0.37$) species (*SI Appendix*, Table S5). Similarly, EvapScope (maximum EWL/minimum EWL) decreased among arid (~19% decrease; $\bar{x} = 0.81 \pm 0.24$), montane (~16% decrease; $\bar{x} = 0.84 \pm 0.28$) and lowland

birds ($\sim 30\%$ decrease; $\bar{x} = 0.70 \pm 0.26$) during the humidity protocol but did not vary significantly with climate (*SI Appendix*, Table S5). Changes in the rate of EWL (i.e., EWL slope) with increasing T_{air} were significantly smaller among arid zone birds [$\bar{x} = 0.92 \pm 0.23$ (8% decrease)] compared to montane [$\bar{x} = 0.61 \pm 0.18$ (39% decrease); PhylANOVA: $t = 3.49$, $p < 0.01$] and lowland birds [$\bar{x} = 0.57 \pm 0.15$ (43% decrease); PhylANOVA: $t = 4.25$, $p < 0.01$] (Fig 2C).

Under humid conditions, a significant difference in T_{air} associated with the onset of panting occurred for montane ($\bar{x} = -1.98 \pm 1.24$ °C; PhylANOVA: $t = -3.54$, $p < 0.01$) and lowland ($\bar{x} = -1.70 \pm 0.70$ °C; PhylANOVA: $t = -3.32$, $p = 0.02$) species, but not arid-zone birds ($\bar{x} = 0.06 \pm 1.20$ °C). Differences in associated with the onset of panting T_b between dry and humid assessments for arid-zone species ($\bar{x} = 0.24 \pm 0.57$ °C) did not differ significantly from those of montane ($\bar{x} = 0.50 \pm 0.51$ °C; PhylANOVA: $t = -0.79$, $p = 0.43$) or lowland birds ($\bar{x} = -0.31 \pm 0.45$ °C; PhylANOVA: $t = 2.38$, $p = 0.12$). However, panting commenced at significantly lower T_b among lowland species than that of the montane species (PhylANOVA: $t = -3.24$, $p < 0.01$) (*SI Appendix*, Fig S6B and Table S5).

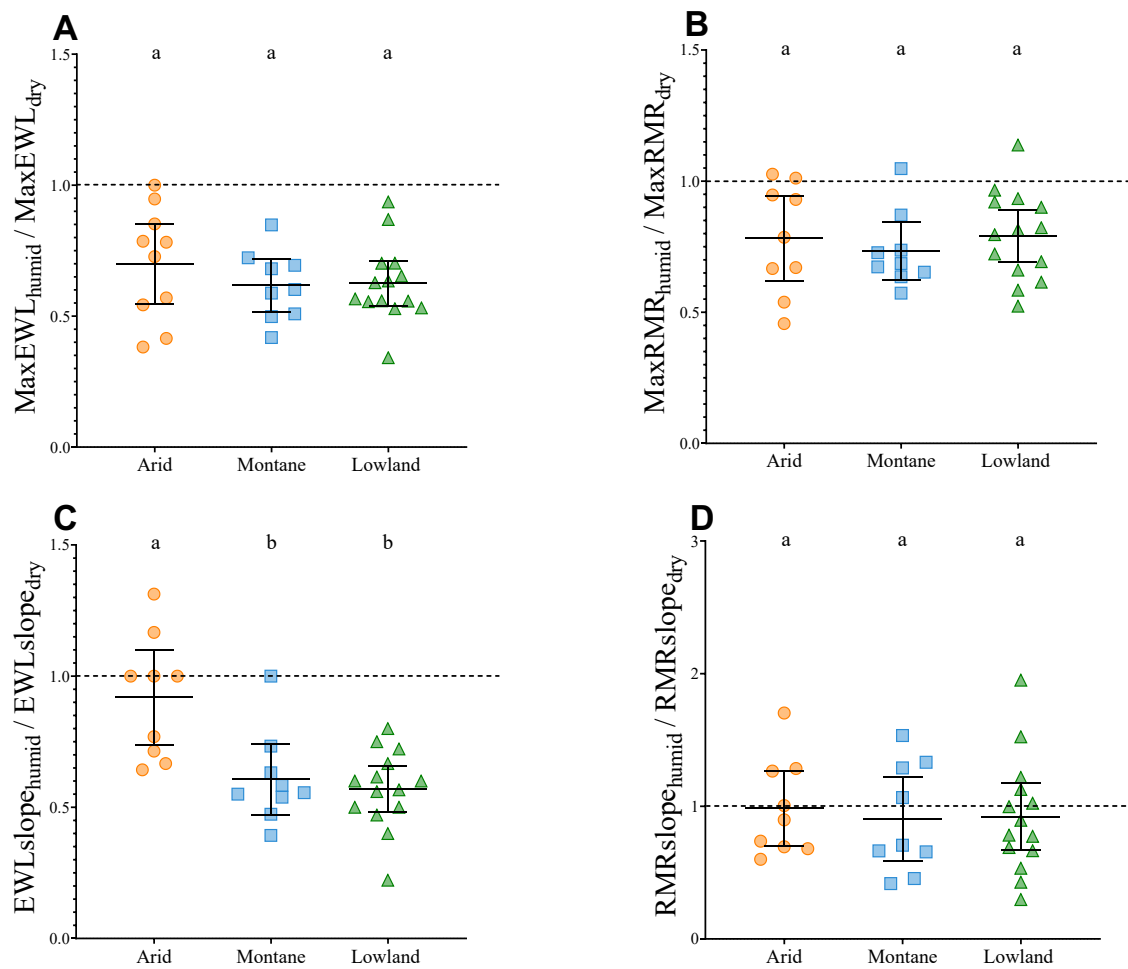


Figure 2 (A–D) Proportional changes (humid/dry) in maximum evaporative water loss [MaxEWL; (A)], maximum resting metabolic rate [MaxEWL: (B)], rate of change in EWL above inflection [EWLslope; (C)] and rate of change in resting metabolic rate above thermoneutral values [RMRslope; (D)] among 30 South African bird species inhabiting hot arid (orange circles, $n=9$), mesic montane (blue squares, $n=9$), or humid lowland (green triangles, $n=14$) climates. Horizontal lines represent mean values, and vertical lines are 95% Confidence intervals. The letters above plots denote significant differences ($\alpha=0.05$) as identified using phylogenetic ANOVA post hoc multiple comparison assessments. Maximum EWL and RMR decreased across climatic areas under humid conditions, but differences but values under dry conditions and humid conditions did not differ significantly between climatic areas. Changes in rates of EWL under humid conditions were significantly lower for arid birds compared to lowland and montane birds which did not differ. No significant differences were detected in proportional changes in the rates of RMR and slopes were similar between dry and humid assessments (A–D).

Maximum resting metabolic rate (RMR)

Under humid conditions, maximum RMR decreased among species from my arid (~22% decrease; $\bar{x} = 0.78 \pm 0.21$ W), montane (~27% decrease; $\bar{x} = 0.73 \pm 0.14$ W) and lowland (~21% decrease; $\bar{x} = 0.79 \pm 0.17$ W) sites. Changes in RMR did not differ significantly between arid and montane (PhylANOVA: $t = 0.58$, $p = 1.0$) or lowland (PhylANOVA: $t = -0.14$, $p = 1.0$) species. Similarly, changes in maximum RMR were similar between lowland and montane (PhylANOVA: $t = 0.78$, $p = 1.0$) species.

Differences in RMR slope (humid/dry – Fig 2D) for my arid (~1% decrease; $\bar{x} = 0.99 \pm 0.36$ W °C⁻¹), montane (~4% increase; $\bar{x} = 1.04 \pm 0.70$ W °C⁻¹) and lowland (~8% decrease; $\bar{x} = 0.92 \pm 0.43$ W °C⁻¹) species were small and vary significantly with climate (*SI Appendix*, Table S5). Differences in MetabCost for arid (~3% increase; $\bar{x} = 1.03 \pm 0.34$), montane (~3% increase; $\bar{x} = 1.03 \pm 0.18$) and lowland (~1% increase; $\bar{x} = 1.01 \pm 0.21$) birds were negligible and did not differ significantly among study areas (*SI Appendix*, Fig S5c and Table S5).

Maximum evaporative cooling efficiency (EHL/MHP)

Maximum humid EHL/MHP did not differ significantly between species from my arid ($\bar{x} = 1.18 \pm 0.19$) and montane ($\bar{x} = 1.31 \pm 0.12$; PhylANOVA: $t = -1.16$, $p = 0.62$) or lowland sites ($\bar{x} = 1.19 \pm 0.34$; PhylANOVA: $t = -0.19$, $p = 0.89$). No significant difference in humid MaxEHL/MHP was detected between lowland and montane sites (PhylANOVA: $t = -1.09$, $p = 0.62$). Fractional differences in MaxEHL/MHP (humid/dry) revealed decreases under humid conditions for arid (~16% decrease; $\bar{x} = 0.84 \pm 0.13$), lowland (~18% decrease; $\bar{x} = 0.82 \pm 0.24$) and montane (~17% decrease; $\bar{x} = 0.83 \pm 0.09$) species (Fig 3A). Subsequent decreases in MaxEHL/MHP did not differ significantly between climatic areas (*SI Appendix*, Table S5).

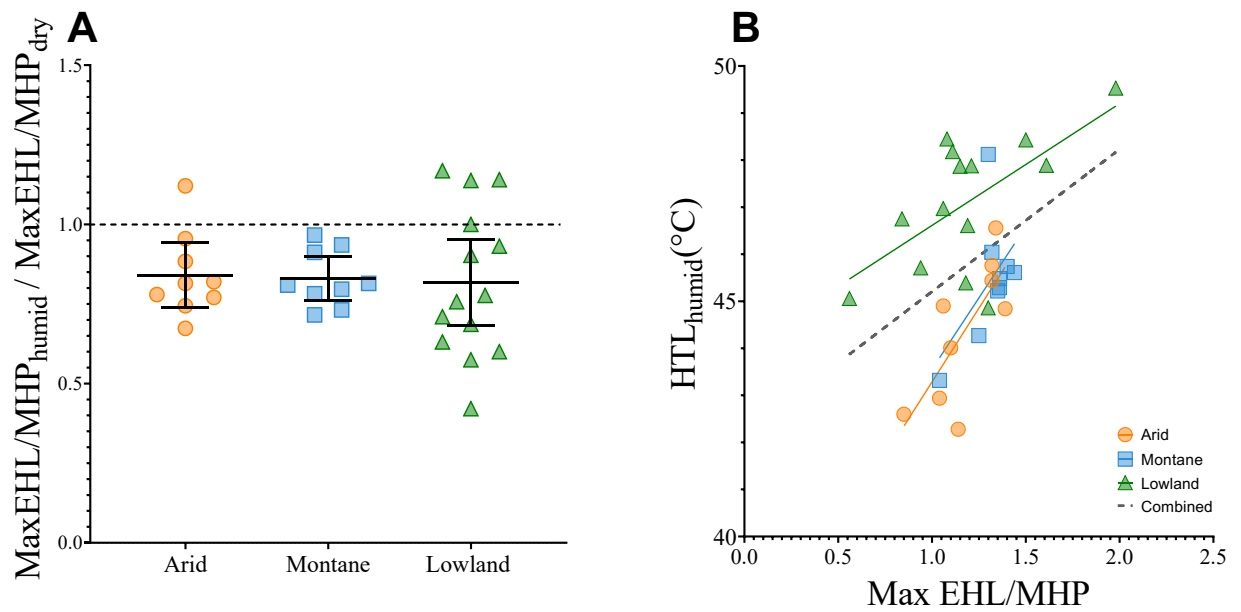


Figure 3 Differences in humid and dry conditions (humid/dry) for the maximum ratio of EHL and MHP [Max EHL/MHP; (A)] Max EHL/MHP decreased in all climatic areas but differences did not differ significantly between sites. Horizontal lines represent mean values and vertical lines 95% confidence intervals. The letters above plots denote significant differences ($\alpha < 0.05$) in MaxEHL/MHP values between sampling localities. Significant differences are derived from phylogenetic analysis of variance post hoc multiple comparison assessments and conventional Tukey multiple comparison assessments regressions. B.) Phylogenetic least square regression analysis (PGLS) of the relationships between HTL and T_{bmax} under humid conditions ($\sim 19 \text{ g H}_2\text{O m}^{-3}$). Under humid conditions increases in Max EHL/MHP were associated with an increase in HTL.

2.5 DISCUSSION

My data reveal that thermoregulatory performance during acute heat exposure is less affected by high atmospheric humidity among birds occupying humid lowlands than is the case for species in environments characterised by drier air. As predicted, the effects of raised humidity on heat tolerance were indeed modest among lowland birds relative to their arid counterparts. The reduced sensitivity of lowland species arises primarily from a greater scope for increasing T_b above normothermic levels, supporting Weathers' (1997) hypothesis that birds in hot, humid environments have evolved more pronounced hyperthermia tolerance to compensate for constraints on evaporative heat dissipation. As expected, arid-zone birds performed relatively poorly under humid conditions, with their HTL reduced by > 3 °C, compared to conditions of very low humidity (Fig 1B).

Across all three sampled bird assemblages, high humidity was associated with large reductions in both maximum EWL (27 - 38% decrease) and maximum RMR (21 - 27% decrease). The latter observation contrasts with a recent study revealing large increases in RMR (~ 40 % at $T_{\text{air}} = 40$ °C) under very humid conditions in an arid-zone passerine (van Dyk et al. 2019). Instead, the blunting of EWL under humid conditions that I observed (Fig 2A) was similar to patterns documented in earlier studies (e.g., Powers 1992; Gerson et al. 2014). As a consequence of the reductions in both EWL and RMR at high humidity in the present study, decreases in maximum EHL/MHP (16-18%) across all three study sites were more modest than anticipated. Moreover, fractional increases in the slope of T_b as a function of T_{air} under humid conditions were similar across study sites, further underscoring the functional importance of adaptative variation in hyperthermia tolerance as the primary mechanism for the observed differences in the effect of humidity on heat tolerance limits.

My data also suggests the capacity for anticipatory responses to high humidity may vary with climate. The smaller decreases in the slope of EWL as a function of T_{air} among arid-zone species compared to montane or lowland species (Fig 2C) appeared to be driven by inflections at lower T_{air} in montane (~ 2.7 °C lower) and lowland (~ 1.2 °C lower) species under humid conditions. Whereas inflections for EWL in arid-zone species remained virtually unchanged (~ 0.1 °C higher). The among-site variation corresponds with changes in T_{air} associated with the onset of panting, where montane ($\bar{x} = 1.97 \pm 1.24$ °C lower) and lowland ($\bar{x} = 1.70 \pm 0.70$ °C lower) species commenced panting at significantly lower T_{air} compared to arid birds ($\bar{x} = 0.06 \pm 1.20$ °C higher) under humid conditions (*SI Appendix*,

Fig S7). In other words, an anticipatory response involving the commencement of panting at lower T_{air} under humid conditions was evident among lowland and montane birds but absent in arid-zone birds. Initiating panting and maximising evaporative cooling at lower T_{air} under humid conditions may delay increases in T_{b} and hence, the onset of a hyperthermic state likely increasing the thermal safety margins under conditions where evaporative heat dissipation is impeded.

In my study, reductions in minimum [(~24% decrease) (*SI Appendix*, Fig S7)] and maximum RMR [(~23% decrease) (Fig 2B)] were observed under humid conditions across climatic areas. Reduced RMR in humid, relative to dry conditions, was unexpected and may represent metabolic suppression (Weathers 1979, 1981). Previous studies speculated that lowered basal and standard metabolic rate (BMR) would have obvious thermal advantages for birds living in hot and particularly humid environments (Bartholomew et al. 1962; Weathers 1979). Suppressed metabolism, and subsequent reductions in endogenous heat production among tropical species, were thought to extend foraging periods when exposed to high operative temperatures (Weathers 1997). In arid zones, another possible example of thermoregulatory benefits brought about by suppressing metabolism is Rufous-cheeked nightjars (*Caprimulgus rufigena*), where O'Connor et al. (2017) found that at $T_{\text{air}} = 55^{\circ}\text{C}$, RMR among *C. rufigena* was only 5% higher than minimum values observed at $T_{\text{air}} = 35^{\circ}\text{C}$, resulting in a concomitant increase in T_{b} of only 2.2 °C. Expected increases in RMR over this T_{air} range are 17-28% ($Q_{10} = 2-3$). While intriguing, the idea of avian metabolic suppression being used as a thermoregulatory mechanism to increase heat tolerance is fairly novel and should receive more attention in future. Among small mammals', metabolic suppression for heat tolerance has also received some attention (e.g., Lovegrove et al. 2014; Reher & Dausmann 2021). Recently, Reher & Dausmann (2021) showed that during hotter periods, a tropical bat species (*Macronycteris commersoni*) made use of adaptive hyperthermia coupled with reduced metabolic heat production (i.e., extended torpor bouts). This allowed for greater environmental heat storage and lowered their dependency on evaporative cooling, thereby increasing heat tolerance ability.

Although pronounced hyperthermia tolerance provides lowland species with a wider thermal safety margin, recent and predicted increases in T_{air} still present a serious thermal challenge (IPCC 2021). Acute and chronic exposure to increasing, frequent heat events is exacerbated by the rapid loss of shady natural vegetation in tropical landscapes (Walsberg 1993; Pinto et al. 2010; Jewitt et al. 2015), reducing the availability of cool microrefugia to which animals can escape. Moreover, many lowland species are sedentary or localised and

cannot move to higher elevations (Sekercioglu et al. 2008). It appears unlikely that many endotherms would have sufficient time to adapt to rapidly changing climates (Loarie et al. 2009) as increasing T_{air} , coupled with raised humidity, may render large areas uninhabitable due to heat stress (Sherwood and Huber 2010). As such, in areas with relatively high humidity, both current and future extreme heat events pose serious acute (McKechnie and Wolf 2010) and chronic challenges (Conradie et al. 2019; Kemp et al. 2020) for preserving avian diversity. For instance, recent heat-related mass mortalities of both birds (McKechnie et al. 2021b) and bats (Welbergen et al. 2008b) have been attributed to raised humidity. Humidity and heat may also indirectly alter the activity and behavioural regimes (Speakman and Król 2010) of endotherms which may have consequences for breeding success and fitness (Walsberg 1993). Admittedly, it is unlikely that arid zone species would experience humidity at T_{air} similar to that in this study. However, the general trends in HTL of my arid species suggest that a singular unprecedented event, or even moderate increases in humidity during a heat wave, could have catastrophic consequences on avifaunal diversity in these regions.

While comprehensive, there are several considerations to be noted from this study. First; comparing thermoregulatory responses of just one very low humidity set point ($\sim 1 \text{ g H}_2\text{O m}^{-3}$) to one relatively high value ($\sim 19 \text{ g H}_2\text{O m}^{-3}$) could potentially mask important non-linear effects. Second, my experimental humidity treatment of $\sim 19 \text{ g H}_2\text{O m}^{-3}$ allowed me to assess southern African birds' responses under conditions characteristic of summer conditions at the humid lowland site ($\sim 18.4 \text{ g H}_2\text{O m}^{-3}$ - January/February). These are similar to that of the highest monthly averages of regions such as the Amazon ($\sim 21.6 \text{ g H}_2\text{O m}^{-3}$ - May) and Congo ($\sim 19.3 \text{ g H}_2\text{O m}^{-3}$ - April) basins and the lowlands of Southeast Asia ($\sim 21.9 \text{ g H}_2\text{O m}^{-3}$ - May) and Panama ($\sim 20.2 \text{ g H}_2\text{O m}^{-3}$ - July). Third, my assessment involves mostly passerines and, hence, most species in my dataset rely on panting as their primary avenue of evaporative heat dissipation. Future research on the effects of humidity on species from other orders that make use of efficient evaporative cooling mechanisms such as gular flutter (e.g., Czenze et al. 2021) to aid in thermoregulation would be valuable for understanding the vulnerabilities of other avian orders to extreme T_{air} coupled with humidity.

2.6 CONCLUSION

Comparing raised hyperthermia tolerance and limited effects on heat tolerance among lowland species to the lowered HTL and hyperthermia avoidance of arid species under humid conditions reinforces the idea that historical contrasting of climatic conditions may have shaped avian thermal physiology (Freeman et al. 2022). Arid-zone species made almost no adjustments to accommodate humidity effects at high T_{air} (i.e., thermal specialisation). Contrastingly, lowland and montane species displayed traits of thermal generalisation (e.g., hyperthermia tolerance, early onset of panting). These findings reiterate the idea of a continuum from thermal specialization to thermal generalization among endotherms (Angilletta et al. 2010; Boyles et al. 2011, Freeman et al. 2022). The evolution of avian T_b is not simple and selection may operate equally on avian T_b as on traits such as RMR and EWL. To gain a clear understanding of the vulnerability of endotherms to predicted changes in T_{air} , it is essential that species-specific responses are taken into account and that climatic variables such as humidity are included in future predictive models (i.e., biophysical models).

2.7 ACKNOWLEDGMENTS

I would like to thank Philip Pattinson for access to his farm and home ‘Mooihoek’ in Harrismith.

Ethics

This work was approved by the Animal Ethics Committee of the University of Pretoria (protocol NAS141/2020) and the Research and Scientific Ethics Committee of the South African National Biodiversity Institute (SANBI NZG/RES /P19/13). Birds were captured under permit JM 8,057/2019 from the Free State province’s Department of Economic, Small Business Development, Tourism and Environmental. At our lowland site research was conducted and birds were captured under permit OP42-2022 from the Ezemvelo KwaZuku-Natal wildlife office. And at my arid site research was conducted under authorisation from the Northern Cape government (permit number FAUNA 0010/2021).

Funding

This work is based on research supported by the DSI-NRF Centre of Excellence at the FitzPatrick Institute and the National Research Foundation of South Africa (grant 119754 to A.E.M.). Any opinions, findings, conclusions or recommendations expressed in this material

are those of the authors and do not necessarily reflect the views of the National Research Foundation.

2.8 REFERENCES

- Angilletta M, Cooper BS, Schuler MS, Boyles JG (2010) The evolution of thermal physiology in endotherms. *Front Biosci (Elite Ed)* 2:861–81
- Bartholomew GA, Hudson JW, Howell TR (1962) Body Temperature, Oxygen Consumption, Evaporative Water Loss, and Heart Rate in the Poor-Will
- Barton K (2019) MuMIn: Multi-Model Inference. R package version 1.43.6. <https://CRAN.R-project.org/package=MuMIn>.
- Bernstein MH, Curtis MB, Hudson DM (1979) Independence of brain and body temperatures in flying American kestrels, *Falco sparverius*. *Am J Physiol Regul Integr Comp Physiol* 6:.. <https://doi.org/10.1152/ajpregu.1979.237.1.r58>
- Boyle WA, Shogren EH, Brawn JD (2020) Hygric Niches for Tropical Endotherms. *Trends Ecol Evol* 35:1–15. <https://doi.org/10.1016/j.tree.2020.06.011>
- Boyles JG, Seebacher F, Smit B, McKechnie AE (2011) Adaptive thermoregulation in endotherms may alter responses to climate change. *Integr Comp Biol* 51:676–690. <https://doi.org/10.1093/icb/icr053>
- Burnham KP, Anderson DR (2002) Model selection and multi-model inference: a practical information-theoretic approach, 2nd edn. Springer, New York, NY
- Campbell GS, Norman JM (1998) An introduction to environmental biophysics. Springer-Verlag, New York
- Coffel ED, Horton RM, de Sherbinin A (2018) Temperature and humidity based projections of a rapid rise in global heat stress exposure during the 21st century. *Environmental Research Letters* 13
- Conradie SR, Woodborne SM, Cunningham SJ, McKechnie AE (2019) Chronic, sublethal effects of high temperatures will cause severe declines in southern African arid-zone birds during the 21st century. *Proceedings of the National Academy of Sciences* 201821312. <https://doi.org/10.1073/pnas.1821312116>
- Czenze ZJ, Freeman MT, Kemp R, et al (2021) Efficient Evaporative Cooling and Pronounced Heat Tolerance in an Eagle-Owl, a Thick-Knee and a Sandgrouse. *Front Ecol Evol* 9:.. <https://doi.org/10.3389/fevo.2021.799302>

- Czenze ZJ, Kemp R, van Jaarsveld B, et al (2020) Regularly drinking desert birds have greater evaporative cooling capacity and higher heat tolerance limits than non-drinking species. *Funct Ecol* 34:.. <https://doi.org/10.1111/1365-2435.13573>
- Dawson WR (1954) Temperature regulation and water requirements of the brown and Abert towhees, *Pipilo fuscus* and *Pipilo aberti*. In University of California publications in zoology, vol 59. University of California Press, Berkeley, CA
- Dawson WR, Schmidt-Nielsen K (1964) “Terrestrial animals in dry heat: desert birds” in *Handbook of Physiology, Adaptation*. American Physiological Society, Washington, DC
- Elliott CCH (1990) The migrations of the Red-billed Quelea *Quelea quelea* and their relation to crop damage. *IBIS* 132:232–237
- Fick SE, Hijmans RJ (2017) WorldClim 2: new 1-km spatial resolution climate surfaces for global land areas. *International Journal of Climatology* 37:4302–4315. <https://doi.org/10.1002/joc.5086>
- Freeman MT, Czenze ZJ, Schoeman K, McKechnie AE (2020) Extreme hyperthermia tolerance in the world’s most abundant wild bird. *Sci Rep* 10:1–6. <https://doi.org/10.1038/s41598-020-69997-7>
- Freeman MT, Czenze ZJ, Schoeman K, McKechnie AE (2022) Adaptive variation in the upper limits of avian body temperature. *Proc Natl Acad Sci U S A* 119:.. <https://doi.org/10.1073/pnas.2116645119/-/DCSupplemental.Published>
- Garland T, Dickerman AW, Janis CM, et al (1993) Phylogenetic Analysis of Covariance by Computer Simulation. *Syst Biol* 42:265–292
- Gerson AR, McKechnie AE, Smit B, et al (2019) The functional significance of facultative hyperthermia varies with body size and phylogeny in birds. *Funct Ecol* 33:597–607. <https://doi.org/10.1111/1365-2435.13274>
- Gerson AR, Smith EK, Smit B, et al (2014a) The impact of humidity on evaporative cooling in small desert birds exposed to high air temperatures. *Physiological and Biochemical Zoology* 87:782–795. <https://doi.org/10.1086/678956>
- Gerson AR, Wolf BO, Smith EK, et al (2014b) The Impact of Humidity on Evaporative Cooling in Small Desert Birds Exposed to High Air Temperatures. *Physiological and Biochemical Zoology* 87:782–795. <https://doi.org/10.1086/678956>
- Grafen A (1989) The Phylogenetic Regression Author. *Philosophical Transactions of the Royal Society B: Biological Sciences* 326:119–157

- Hackett SJ, Kimball RT, Reddy S, et al (2008) A phylogenomic study of birds reveals their evolutionary history. *Science* (1979) 320:1763–1768. <https://doi.org/10.1126/science.1157704>
- Hockey PAR, Dean WRJ, Ryan PG (2005) *Roberts Birds of Southern Africa VII*
- IPCC (2021) *Climate Change 2021: The Physical Science Basis. Contribution of Working Group I to the Sixth Assessment Report of the Intergovernmental Panel on Climate Change.*
- Jetz W, Thomas GH, Joy JB, et al (2012) The global diversity of birds in space and time. *Nature* 491:444–448. <https://doi.org/10.1038/nature11631>
- Jewitt D, Goodman PS, Erasmus BFN, et al (2015) Systematic land-cover change in KwaZulu-Natal, South Africa : implications for biodiversity : research article. *S Afr J Sci* 111:32–40
- Kassambara A (2015) *rstatix: Pipe-friendly framework for basic statistical tests.*
- Kemp R, Freeman MT, van Jaarsveld B, et al (2020) Sublethal fitness costs of chronic exposure to hot weather vary between sexes in a threatened desert lark. *Emu* 120:216–229. <https://doi.org/10.1080/01584197.2020.1806082>
- Kregel KevinC (2002) Heat shock proteins: modifying factors in physiological stress responses and acquired thermotolerance. *J Appl Physiol* 92:2177–2186
- Lasiewski RC, Acosta AL, Bernstein MH (1966) Evaporative water loss in birds-I. Characteristics of the open flow method of determination, and their relation to estimates of thermoregulatory ability. *Comp Biochem Physiol* 19:445–457. [https://doi.org/10.1016/0010-406X\(66\)90153-8](https://doi.org/10.1016/0010-406X(66)90153-8)
- Li D, Yuan J, Kopp RE (2020) Escalating global exposure to compound heat-humidity extremes with warming. *Environmental Research Letters* 15:. <https://doi.org/10.1088/1748-9326/ab7d04>
- Lighton (2008) *Measuring Metabolic Rates; A Manual for Scientists.* Oxford University Press
- Loarie SR, Duffy PB, Hamilton H, et al (2009) The velocity of climate change. *Nature* 462:1052–1055. <https://doi.org/10.1038/nature08649>
- Lovegrove BG (2003) The influence of climate on the basal metabolic rate of small mammals: a slow-fast metabolic continuum. *J Comp Physiol* 173:87–112. <https://doi.org/10.1007/s00360-002-0309-5>
- Lovegrove BG, Lobban KD, Levesque DL (2014) Mammal survival at the Cretaceous–Palaeogene boundary: Metabolic homeostasis in prolonged tropical hibernation in

- tenrecs. *Proceedings of the Royal Society B: Biological Sciences* 281:.
<https://doi.org/10.1098/rspb.2014.1304>
- Lutterschmidt WI, Hutchison VH (1997) The critical thermal maximum: History and critique. *Can J Zool* 75:1561–1574. <https://doi.org/10.1139/z97-783>
- Maddison DR, Maddison WP (2014) Chromaseq: a Mesquite package for analyzing sequence chromatograms.
- Martins EP, Hansen TF (1997) Phylogenies and the comparative method: a general approach to incorporating phylogenetic information into the analysis of interspecific data. *American Naturalist* 149:646–667. <https://doi.org/10.1086/303188>
- McKechnie AE, Gerson AR, Wolf BO (2021a) Thermoregulation in desert birds: scaling and phylogenetic variation in heat tolerance and evaporative cooling. *Journal of Experimental Biology* 224:.
<https://doi.org/10.1242/jeb.229211>
- McKechnie AE, Rushworth IA, Myburgh F, Cunningham SJ (2021b) Mortality among birds and bats during an extreme heat event in eastern South Africa. *Austral Ecol* 687–691.
<https://doi.org/10.1111/aec.13025>
- McKechnie AE, Wolf BO (2004) The allometry of avian basal metabolic rate: Good predictions need good data. *Physiological and Biochemical Zoology* 77:502–521.
<https://doi.org/10.1086/383511>
- McKechnie AE, Wolf BO (2010) Climate change increases the likelihood of catastrophic avian mortality events during extreme heat waves. *Biol Lett* 6:253–256.
<https://doi.org/10.1098/rsbl.2009.0702>
- McNab BKeith (2002) *The physiological ecology of vertebrates: a view from energetics.* Cornell University Press
- Midtgård U (1983) Scaling of the brain and the eye cooling system in birds: A morphometric analysis of the Rete ophthalmicum. *Journal of Experimental Zoology* 225:197–207.
<https://doi.org/10.1002/jez.1402250204>
- Mucina L, Rutherford MC (2006) *The vegetation of South Africa, Lesotho and Swaziland.* National Botanical Institute, South Africa
- Muggeo V (2016) Segmented mixed models with random changepoints in R
- Newberry GN, Swanson DL (2018) Elevated temperatures are associated with stress in rooftop-nesting Common Nighthawk (*Chordeiles minor*) chicks. *Conserv Physiol* 6:1–12. <https://doi.org/10.1093/conphys/coy010>

- O'Connor RS, Wolf BO, Brigham RM, McKechnie AE (2017) Avian thermoregulation in the heat: efficient evaporative cooling in two southern African nightjars. *J Comp Physiol B* 187:477–491. <https://doi.org/10.1007/s00360-016-1047-4>
- Orme D, Freckleton R, Thomas G, et al (2012) Caper: comparative analyses of phylogenetics and evolution in R.
- Pagel M (1999) Inferring the historical patterns of biological evolution. *Nature* 401:877–884. <https://doi.org/10.1038/44766>
- Pinheiro J, Bates D, DebRoy S, Sarkar D RCTeam (2015) nlme: Linear and Nonlinear Mixed Effects Models
- Pinto SRR, Mendes G, Santos AMM, et al (2010) Landscape attributes drive complex spatial microclimate configuration of Brazilian Atlantic forest fragments. *Trop Conserv Sci* 3:389–402. <https://doi.org/10.1177/194008291000300404>
- Powers DR (1992) Effect of temperature and humidity on evaporative water loss in Anna's hummingbird (*Calypte anna*). *Journal of Comparative Physiology B* 162:74–84
- Ratnayake HU, Kearney MR, Govekar P, et al (2019) Forecasting wildlife die-offs from extreme heat events. *Anim Conserv* 22:386–395. <https://doi.org/10.1111/acv.12476>
- Raymond C, Matthews T, Horton RM (2020) The emergence of heat and humidity too severe for human tolerance. *Scientific Advances* 6:eaaw1838
- Reher S, Dausmann KH (2021) Tropical bats counter heat by combining torpor with adaptive hyperthermia. *Proc Biol Sci* 288:20202059. <https://doi.org/10.1098/rspb.2020.2059>
- Revell LJ (2010) Phylogenetic signal and linear regression on species data. *Methods Ecol Evol* 1:319–329. <https://doi.org/10.1111/j.2041-210x.2010.00044.x>
- Revell LJ (2012) phytools: An R package for phylogenetic comparative biology (and other things). *Methods Ecol Evol* 3:217–223. <https://doi.org/10.1111/j.2041-210X.2011.00169.x>
- Scholander PF, Hock R, Walters V, Johnson F (1950) Heat Regulation in Some Arctic and Tropical Mammals and Birds. *Biological Bulletin* 99:237–258
- Sekercioglu CH, Schneider SH, Fay JP, Loarie SR (2008) Climate change, elevational range shifts, and bird extinctions. *Conservation Biology* 22:140–150. <https://doi.org/10.1111/j.1523-1739.2007.00852.x>
- Sherwood SC (2018) How Important Is Humidity in Heat Stress? *Journal of Geophysical Research: Atmospheres* 123:11,808–11,810

- Sherwood SC, Huber M (2010) An adaptability limit to climate change due to heat stress. *Proc Natl Acad Sci U S A* 107:9552–9555. <https://doi.org/10.1073/pnas.0913352107/-/DCSupplemental>
- Short JC, Freeman MT, McKechnie AE (2022) Respirometry protocols for avian thermoregulation at high air temperatures: stepped and steady-state profiles yield similar results. *J Exp Biol* 225:. <https://doi.org/10.1242/jeb.244166>
- Smit B, Harding CT, Hockey PAR, McKechnie AE (2013) Adaptive thermoregulation during summer in two populations of an arid-zone passerine. *Ecology* 94:1142–1154
- Smit B, Whitfield MaxineC, Talbot WA, et al (2018) Avian thermoregulation in the heat: phylogenetic variation among avian orders in evaporative cooling capacity and heat tolerance. *J Exp Biol* 221:jeb174870. <https://doi.org/10.1242/jeb.174870>
- Speakman JR, Król E (2010) Maximal heat dissipation capacity and hyperthermia risk: Neglected key factors in the ecology of endotherms. *Journal of Animal Ecology* 79:726–746. <https://doi.org/10.1111/j.1365-2656.2010.01689.x>
- Tieleman BI, Williams JB (2000) The adjustment of avian metabolic rates and water fluxes to desert environments. *Physiological and Biochemical Zoology* 73:461–479. <https://doi.org/10.1086/317740>
- Tieleman BI, Williams JB, Bloomer P (2003) Adaptation of metabolism and evaporative water loss along an aridity gradient. *Proceedings of the Royal Society B: Biological Sciences* 270:207–214. <https://doi.org/10.1098/rspb.2002.2205>
- Tracy CR, Welch WR, Porter WP (2010) *Properties of air: a manual for use in biophysical ecology*, 4th edn. University of Wisconsin, Madison, USA
- van Dyk M, Noakes MJ, McKechnie AE (2019) Interactions between humidity and evaporative heat dissipation in a passerine bird. *J Comp Physiol B* 189:299–308. <https://doi.org/10.1007/s00360-019-01210-2>
- van Jaarsveld B, Bennett NC, Kemp R, et al (2021) Heat tolerance in desert rodents is correlated with microclimate at inter- and intraspecific levels. *J Comp Physiol B* 191:575–588. <https://doi.org/10.1007/s00360-021-01352-2>
- Walsberg GE (1993) Thermal Consequences of Diurnal Microhabitat Selection in a Small Bird. *Scandinavian Journal of Ornithology* 24:174–182
- Weathers WW (1997) Energetics and Thermoregulation by Small Passerines of the Humid, Lowland Tropics. *Auk* 114:341–353. <https://doi.org/10.2307/4089237>

- Weathers WW (1981) Physiological Thermoregulation in Heat-Stressed Birds: Consequences of Body Size. *Physiol Zool* 54:345–361. <https://doi.org/10.1086/physzool.54.3.30159949>
- Weathers WW (1979) Climatic Adaptation in Avian Standard Metabolic Rate. *Oecologia (Berl)* 42:81–89
- Welbergen JA, Klose SM, Markus N, Eby P (2008a) Climate change and the effects of temperature extremes on Australian flying-foxes. *Proceedings of the Royal Society B: Biological Sciences* 275:419–425. <https://doi.org/10.1098/rspb.2007.1385>
- Welbergen JA, Klose SM, Markus N, Eby P (2008b) Climate change and the effects of temperature extremes on Australian flying-foxes. *Proceedings of the Royal Society B: Biological Sciences* 275:419–425. <https://doi.org/10.1098/rspb.2007.1385>
- White CR, Blackburn TM, Martin GR, Butler PJ (2007) Basal metabolic rate of birds is associated with habitat temperature and precipitation, not primary productivity. *Proceedings of the Royal Society B: Biological Sciences* 274:287–293. <https://doi.org/10.1098/rspb.2006.3727>
- Whitfield MC, Smit B, McKechnie AE, Wolf BO (2015) Avian thermoregulation in the heat: scaling of heat tolerance and evaporative cooling capacity in three southern African arid-zone passerines. *Journal of Experimental Biology* 218:1705–1714. <https://doi.org/10.1242/jeb.121749>
- Withers PC (1992) *Comparative animal physiology*. Saunders College Pub
- Xie S, Tearle R, McWhorter TJ (2018) Heat shock protein expression is upregulated after acute heat exposure in three species of Australian desert birds. *Avian Biol Res* 11:263–273. <https://doi.org/10.3184/175815618X15366607700458>
- Zeileis A, Hothorn T (2002) Diagnostic Checking in Regression Relationships. *R News* 2:7–10

2.9 ADDITIONAL INFORMATION

Appendix M1

2.9.1.1 Study species

I quantified HTL, T_{bmax} and associated thermoregulatory variables at high T_{air} for both dry and humid conditions among 408 individuals representing 29 species (*Pycnonotus tricolor*

and *Lanius collaris* occurred at multiple sites) in this study. All measurements from my arid (n = 9 species), montane (n = 9 species) and lowland (n = 13 species) sites took place during the austral spring/summer of 2021 - 2022 (*SI Appendix*, Table S1.1 and 1.2).

I include published data collected under dry conditions for both montane (n = 9 species, n = 100 individuals) and lowland species (n = 11 species, n = 109 individuals). Data for lowland species were obtained from Freeman et al. (2022), collected near my study site (28°46'S, 32°20'E) following identical protocols to this study (*SI Appendix*, Table S1.1). All data for Rudd's apalis (*Apalis ruddii* – this study) and pink-throated twinspot (*Hypargos margaritatus* – this study) were collected during this study while data for blue waxbills (*Uraeginthus angolensis*) were obtained from Liddle *et al.* (unpublished data) at the same study site. Dry air data for montane species were also obtained from Freeman et al. (2022) and collected at the same site as in the present study (*SI Appendix*, Table S1.1). Overall, my analysis includes data from 626 individuals (humid, n = 307; dry, n = 320) from 30 species, 15 families and three orders - Passeriformes, Piciformes and Coraciiformes.

2.9.1.2 Air and body temperature measurements

Temperature-sensitive passive integrated transponders (PIT) tags (Biotherm 13, Biomark, Boise, ID, USA) were injected into the peritoneal cavity of each bird prior to the commencement of experimentation to measure body temperature. PIT tags were calibrated before use in a circulating water bath (model F34, Julabo, Seelbach BW, DE) from temperatures ranging between 30 and 50 °C against a thermocouple meter (TC-1000, Sable Systems, Las Vegas, NV, USA), which was verified against a mercury-in-glass thermometer with NIST-traceable accuracy before and after the PIT tag calibration. Measured temperatures from pit tags deviated by 0.13 ± 0.05 °C (n = 30) from actual values and I corrected for measured body temperature values accordingly. A reader and transceiver system (HPR +, Biomark, Boise ID, USA) was used to record data from PIT tags. During experimentation T_{air} within the metabolic chamber was measured using a thermistor probe (TC-100, Sable Systems, Las Vegas, NV, USA) which was inserted through a small hole in the side of the chamber sealed by a rubber grommet.

2.9.1.3 Gas exchange measurements

Evaporative water loss (EWL) and carbon dioxide production (\dot{V}_{CO_2}) were measured using an open flow-through respirometry system, with my set up identical to that described by

Freeman *et al.* (2020, 2022). Birds were placed individually into 3-L (200 mm high \times 150 mm wide \times 100 mm deep) plastic metabolic chambers known to not absorb water vapour (Whitfield *et al.* 2015), fitted with a raised mesh platform \sim 10 cm above a \sim 1-cm mineral oil layer into which excreta fell to prevent evaporation affecting measured rates of EWL. Metabolic chambers were then placed inside a modified \sim 100-L cooler box in which T_{air} was regulated by a Peltier device (AC-162 Thermoelectric Air Cooler, TE Technology, Traverse City MI, USA) and adjusted using a digital controller (TC-36–25-RS485 Temperature Controller, TE Technology, Traverse City MI, USA).

For all measurements under dry conditions (hereafter, the dry protocol), methods were identical to those of Freeman *et al.* (2020, 2022). In brief, atmospheric air supplied by an oil-free compressor and scrubbed of water vapour using a membrane dryer (Atlas Copco SD1N air dryer and filter, Atlas Copco, Stockholm, Sweden). Dried air was then split into an experimental, additional dry line and a dry air baseline channel using Bev-A-Line IV tubing (Thermoplastic Processes Inc., Warren, NJ, USA). A needle valve (Swagelok, Solon, OH, USA) maintained flow rates to the baseline channel (“dry baseline”) at $\sim 1 \text{ L min}^{-1}$, whereas the experimental line proceeded directly to the metabolic chamber with flow rates being regulated by a mass flow controller (Alicat Scientific Inc., Tuscon AZ, USA) calibrated using a soap-bubble flow meter (Giliberator 2, Sensidyne, St Petersburg, FL, USA). Flow rates were adjusted to minimise water vapour pressure within the metabolic chamber (mean in chamber humidity across sites = $1.07 \pm 0.84 \text{ g H}_2\text{O m}^{-3}$), and varied between 3 L min^{-1} and 24 L min^{-1} . Freeman *et al.* (2020, 2022)

For measurements at $\sim 19 \text{ g H}_2\text{O m}^{-3}$ (hereafter, humidity protocol) downstream of the compressor the experimental air stream was split into two channels. In one (humid stream), flow rates were regulated at $1000 - 4000 \text{ mL min}^{-1}$ using a mass flow controller (Alicat Scientific Inc., Tuscon AZ, USA) before the air was passed through three water-filled bubblers connected in series. Each bubbler was constructed from a 3-L sealable screw-top bottle (diameter = 14cm, height = 25cm) (Universal Jar, Tupperware, Orlando, FL, USA) with in- and outlet fittings installed in the lid and incurrent air passing through tubing and an aquarium stone positioned $\sim 1 \text{ cm}$ from the bottom of the water column. The first bubbler was kept at ($T_{\text{air}} = \sim 35 \text{ }^\circ\text{C}$). The second and third bubblers were placed in a temperature-controlled chamber (PELT-5, Sable Systems, Las Vegas NV, USA) set to a T_{air} slightly higher than the desired chamber dewpoint ($\sim 22^\circ\text{C}$ or $19 \text{ g H}_2\text{O m}^{-3}$).

The second air stream (dry stream) consisted of dry air and merged with the experimental humid stream downstream of the bubblers, permitting dry air at flow rates

regulated by the second mass flow controller (Alicat Scientific Inc., Tuscon AZ, USA) to be mixed with my humidified air upstream of the metabolic chamber. I found that mixing air humidified to values above the desired chamber values with dry air provided more precise control of chamber humidity than using bubblers alone. Regular adjustments of the dry stream flow rates permitted chamber humidity levels to be regulated precisely (mean chamber humidity across sites = $19.21 \pm 1.20 \text{ g H}_2\text{O m}^{-3}$) despite EWL from the bird increasing with T_{air} . Downstream of the experimental humid stream and dry stream merge, the channel was split into a humid baseline channel with a flow rate regulated using a needle valve ($\sim 1 \text{ L min}^{-1}$) allowing for the precise humidity of the air entering the metabolic chamber to be monitored and recorded. Downstream of this final split, incurrent flow rates were measured upstream of the chamber inlet using a 0-10 L min^{-1} mass flow controller (Alicat Scientific Inc., Tuscon AZ, USA), set to its maximum flow rate, thereby functioning as a mass flow meter at flow rates $< 10 \text{ L min}^{-1}$, also calibrated using a Gilibrator 2 flow meter. Incurrent flow rates varied between 240 - 4000 mL min^{-1} for the humidity protocol. Adjustments of flow rates and/or in current humid air took place during transitional periods ~ 10 -15 minutes before measurements at a set point T_{air} where possible, maximizing the likelihood that equilibrium conditions within the metabolic chamber were reached (Lasiewski et al. 1966). Should humidity values or T_{air} within the chamber have been unstable or still transitioning to the desired set point, additional time was permitted to ensure data were collected from stable O_2 , CO_2 and H_2O traces at the desired humidity level.

By periodically adjusting T_{air} in the temperature-controlled chamber housing the second and third bubblers and flow rates of the humid and dry air streams, I was able to maintain approximately constant values of absolute humidity in the metabolic chamber (i.e., the humidity experienced by a bird). Across study sites, absolute humidity within the metabolic chambers averaged $19.48 \pm 1.19 \text{ g H}_2\text{O m}^{-3}$ ($n=1873$), comparable with that used in previous studies of the effects of humidity on avian thermoregulation (Powers 1992; Gerson et al. 2014b; van Dyk et al. 2019) and similar to the highest monthly (January/February) humidity values experienced by birds at my lowland site (mean maximum absolute humidity $\sim 18.2 \text{ g H}_2\text{O m}^{-3}$ at $30 \text{ }^\circ\text{C}$) (Fick and Hijmans 2017). Site-specific mean chamber humidities varied by $< 1.5 \text{ g H}_2\text{O m}^{-3}$: arid ($19.56 \pm 1.26 \text{ g H}_2\text{O m}^{-3}$, $n = 446$), montane ($18.96 \pm 1.05 \text{ g H}_2\text{O m}^{-3}$, $n = 499$) and lowland sites ($20.37 \pm 1.33 \text{ g H}_2\text{O m}^{-3}$, $n = 928$). As chamber humidities were equivalent to dewpoints of ~ 22 - $23 \text{ }^\circ\text{C}$, I set up all equipment in a controlled climate with $T_{\text{air}} = \sim 35 \text{ }^\circ\text{C}$ to avoid condensation in analysers and tubing. For the dry protocol, incurrent humidity was $\sim 0 \text{ g H}_2\text{O m}^{-3}$, whereas

excurrent humidity (i.e., the humidity experienced by birds in chamber once EWL is taken into account) was maintained at $\sim 1 \text{ g H}_2\text{O m}^{-3}$. For dry runs, the mean absolute humidity within the metabolic chamber was $1.07 \pm 0.84 \text{ g H}_2\text{O m}^{-3}$ ($n = 715$).

For both dry and humid protocols, air from baselines or chamber channels was sequentially subsampled using a respirometry multiplexer (model MUX3-1101-18M, Sable Systems) in manual mode, at a flow rate of $\sim 160 \text{ mL min}^{-1}$ regulated by a subsampling pump (model SS4, Sable Systems, Las Vegas NV, USA) and pulled through a $\text{CO}_2/\text{H}_2\text{O}$ analyser (LI-840A, LI-COR, Lincoln NE, USA) followed by an O_2 analyser (FC-10A, Sable Systems, Las Vegas NV, USA). The $\text{CO}_2/\text{H}_2\text{O}$ analyser was regularly zeroed using pure nitrogen (AFROX, Johannesburg, South Africa) and spanned using a 2000 ppm CO_2 in N_2 gas mix (AFROX) or humidified air with a dewpoint 5 - 6 °C below ambient T_{air} generated using a dew point generator (DG-4, Sable Systems, Las Vegas NV, USA). The O_2 analyser was periodically spanned to 20.95% using dry, CO_2 -free air scrubbed of CO_2 .

Data were acquired every 5 s from analysers using an analog–digital converter (model UI-3, Sable Systems, Las Vegas NV, USA) which converted the voltage inputs to digital values. I then recorded these values using a computer using Expedata software (Sable Systems, Las Vegas NV, USA).

2.9.1.4 Experimental protocol

I measured T_b , EWL and RMR using both the dry and humidity protocols. Measurements typically lasted 2 – 4 h and began with a bird placed in a chamber at $T_{\text{air}} = 28 \text{ °C}$, and given at least 1 h to habituate to conditions in the metabolic chamber for both the dry and humid assessments. For the dry protocol, T_{air} setpoints beginning from $T_{\text{air}} = 28 \text{ °C}$ were increased incrementally by 4 °C until $T_{\text{air}} = 40 \text{ °C}$ and then increased incrementally by 2 °C until birds reached their thermal endpoint, Freeman *et al.* (2022). For the humid protocol, T_{air} setpoints started at 34 °C and were increased incrementally by 2 °C until birds reached their thermal endpoint. Transitions between successive T_{air} setpoints took 10–15 min. At each setpoint T_{air} , birds were exposed to stable T_{air} and humidity for a minimum of 15-20 minutes until traces of O_2 , CO_2 and H_2O were stable for at least 5 min. The stepped respirometry protocol involving brief (15-20 min) exposure to each T_{air} setpoint used in this study has been shown to yield patterns of EWL, RMR and T_b as functions of T_{air} similar to those using a steady-state protocol where birds experience each T_{air} setpoint for several hours (Short et al. 2022).

2.9.1.5 Figures

Figure M1 – Humidity setup; Visual representation of the flow through respirometry setup used in this study to manipulate and regulate levels of absolute humidity within the metabolic chamber and subsequently measure avian thermoregulatory response variables pertaining to evaporative water loss (EWL), resting metabolic rate (RMR), body temperature (T_b) at incrementally increasing air temperatures until birds displayed signs associated with severe hyperthermia. At point A, the dry air line was split into an experimental channel line and a dry air baseline. The dry air baseline and regulatory dry air line are subsequently split at point B. At point C experimental line air has now been humidified by my bubblers (dew point = 22-23 °C) and was split again into a bubbler baseline (which travels to the analysers to determine current absolute humidity) and a continuing experimental “humidified” line. If required at point D, dry air from the regulatory dry air line was mixed with my experimental “humidified” line air to down-regulate to the desired absolute humidity. The humidified air is split one last time at point E into the main humidity baseline (provides a value for incurrent absolute humidity) and the incurrent chamber line which passes through a mass flow meter to measure the exact flow rate of humidified air entering the chamber.

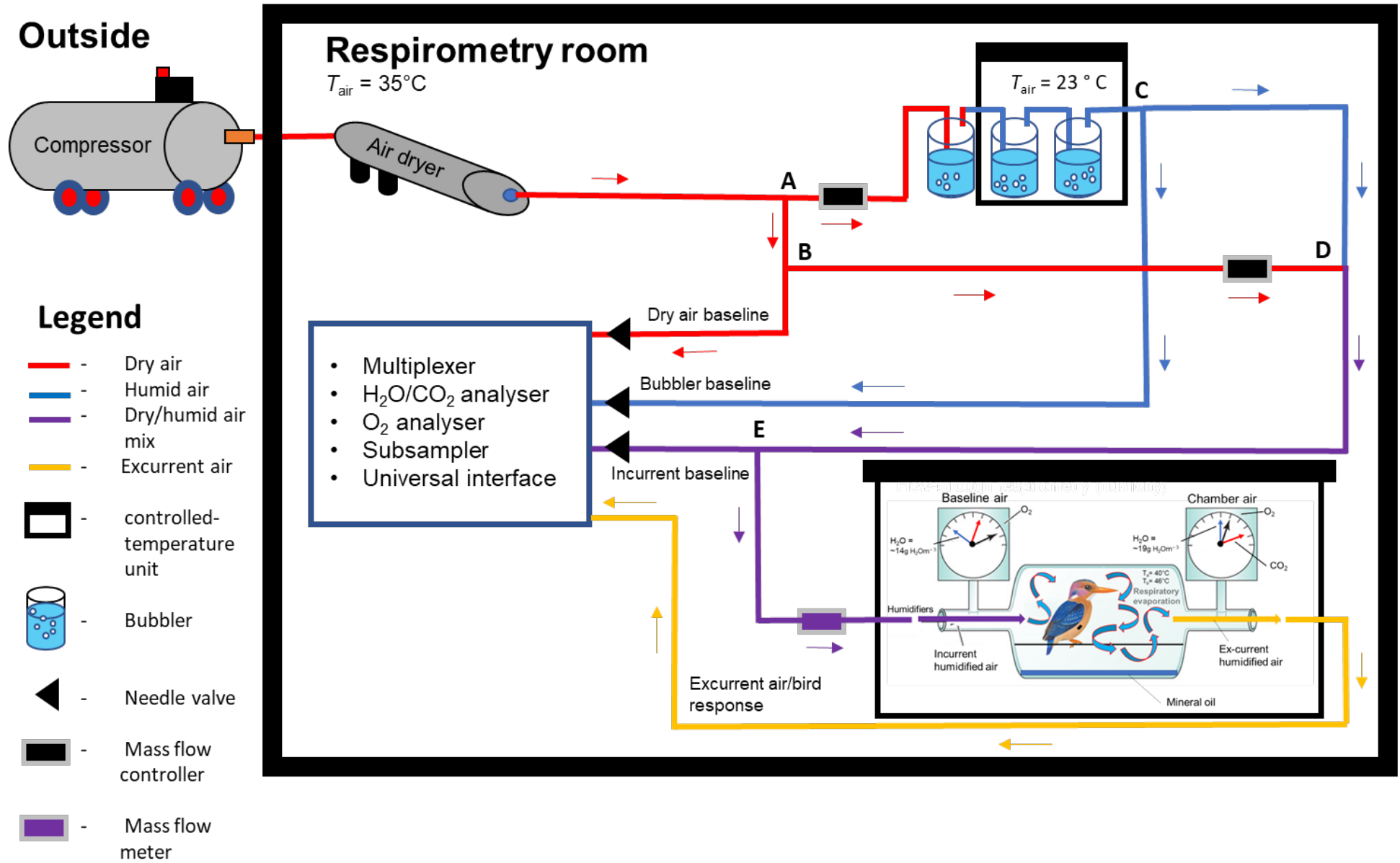


Figure M4

Appendix S1

Figures

Figure S1. Overall heat tolerance limits (HTL; i.e., maximum air temperature tolerated) among 30 South African bird species (two species were assessed at multiple sites) subjected to a stepped respirometry protocol under dry ($\sim 1 \text{ g H}_2\text{O m}^{-3}$) or humid ($\sim 19 \text{ g H}_2\text{O m}^{-3}$) conditions. Horizontal lines represent mean values and vertical lines 95% confidence intervals. Letters above plots denote significant differences ($\alpha = 0.05$) as derived from phylogenetic analysis (PhylANOVA) of variance post hoc multiple comparison assessments. Categories include humid (blue circles, $n = 32$) and dry (orange squares, $n = 32$). HTLs were significantly higher for species under dry conditions.

Figure S2. Maximum body temperature (T_{bmax} ; filled symbols) and normothermic body temperature (T_{bnorm} ; white filled symbols] varied significantly among 30 South African bird species across multiple climatic study sites with differing maximum air temperatures and humidity. Horizontal lines represent mean values and vertical lines represent 95% confidence intervals. Letters above plots denote significant differences ($\alpha < 0.05$) in T_{bmax} values between sampling localities; letters at the bottom denote significant differences ($\alpha = 0.05$) in T_{bnorm} values. Significant differences are derived from phylogenetic analysis of variance post-hoc multiple comparison assessments (PhylANOVA) and conventional Tukey multiple comparison assessments regressions. Climate categories are hot arid (orange circles, $n=9$), mesic montane (blue squares, $n=9$) and humid lowland (green triangles, $n = 14$).

Figure S3. Proportional difference in T_{bslope} (humid/dry) for birds subjected to a stepped respirometry protocol under dry ($\sim 1 \text{ g H}_2\text{O m}^{-3}$) or humid ($\sim 19 \text{ g H}_2\text{O m}^{-3}$) conditions did not differ significantly between my three climatic study areas. Climate categories are hot arid (orange circles, $n=9$), mesic montane (blue squares, $n=9$) and humid lowland (green triangles, $n=14$). Horizontal lines represent mean values and vertical lines 95% confidence intervals. Letters above plots denote significant differences ($\alpha < 0.05$) in T_{bslope} values between sampling localities. Significant differences are derived from phylogenetic analysis of variance post-hoc multiple comparison assessments (PhylANOVA) and conventional Tukey multiple comparison assessments regressions.

Figure S4. The relationship between EvapScope (maximum evaporative water loss (EWL)/minimum evaporative water loss) and heat tolerance limits (HTL - i.e., maximum air temperature tolerated) under my humid protocol ($19 \text{ g H}_2\text{O m}^{-3}$) for birds at the hot arid (orange circles, $n=9$), mesic montane (blue squares, $n=9$) and humid lowland (green triangles, $n=14$) study sites. A combined slope is indicated by the black dotted line to represent the overall response of EvapScope and HTL across all sites. The increasing relationship of HTL in response to increasing EvapScope was mostly driven by lowland species which had lowered minimum EWL, however, support for this pattern was weak among montane and arid species. The increasing relationship within the montane species was driven primarily by *Quelea quelea* (as indicated by the highest blue square), the positive relationship among the other montane species was weak.

Figure S5. (A–D) Variation in the ratio of minimum RMR and Maximum RMR under humid conditions [MetabCost; (A)], the ratio of maximum to minimum thermoneutral evaporative water loss [EvapScope (B)], variation in MetabCost between humid and dry conditions [MetabCost_{humid}/MetabCost_{dry}; (C)], and variation in EvapScope between humid and dry conditions [EvapScope_{humid}/EvapScope_{dry}; (D)] among 30 South African bird species inhabiting hot arid (orange circles, $n = 9$), mesic montane (blue squares, $n = 9$), or humid lowland (green triangles, $n = 14$) climates. Horizontal dotted lines (C - D) represent a ratio of 1:1 of MetabCost and EvapScope between humid and dry conditions, respectively. Horizontal lines represent mean values, and vertical lines 95% confidence intervals. Letters above plots denote significant differences ($\alpha = 0.05$) as identified using phylogenetic ANOVA post hoc multiple (PhylANOVA) comparison assessments. Significant differences were not detected among assemblages from the climatic areas for (A-D).

Figure S6. Onset of panting as a function of (A) air temperature (T_{air}) and (B) body temperature (T_{b}) for birds at the hot arid (orange circles, $n=9$), mesic montane (blue squares, $n = 9$) and humid lowland (green triangles, $n=14$) site. Horizontal dotted lines represent zero-change between humid and dry conditions. Horizontal lines represent mean values and vertical lines 95% confidence intervals. Letters above plots denote significant differences ($\alpha < 0.05$) among climatic areas values between sampling localities. Significant differences are derived from phylogenetic analysis of variance post-hoc multiple comparison assessments (PhylANOVA) and conventional Tukey multiple comparison assessments regressions.

Figure S5. Minimum values recorded for (A) resting metabolic rate (RMR) and (B) evaporative water loss (*EWL*) for birds at the hot arid (orange circles, $n=9$), mesic montane (blue squares, $n=9$) and humid lowland (green triangles, $n=14$) site. Horizontal dotted lines represent zero-change between humid and dry conditions. Horizontal lines represent mean values and vertical lines 95% confidence intervals. Letters above plots denote significant differences ($\alpha < 0.05$) among climatic areas values between sampling localities. Significant differences are derived from phylogenetic analysis of variance post-hoc multiple comparison assessments (PhylANOVA) and conventional Tukey multiple comparison assessments regressions.

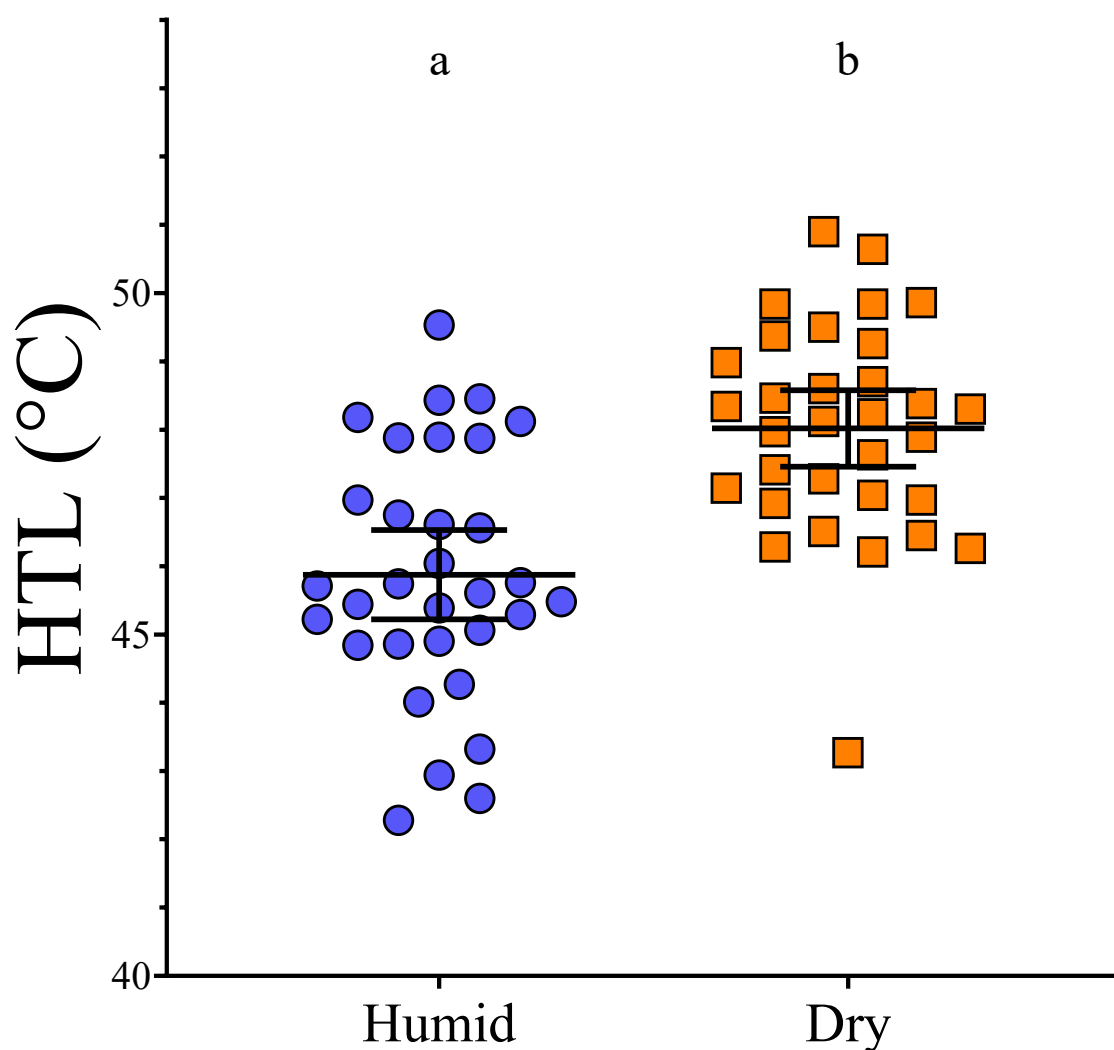


Figure S1

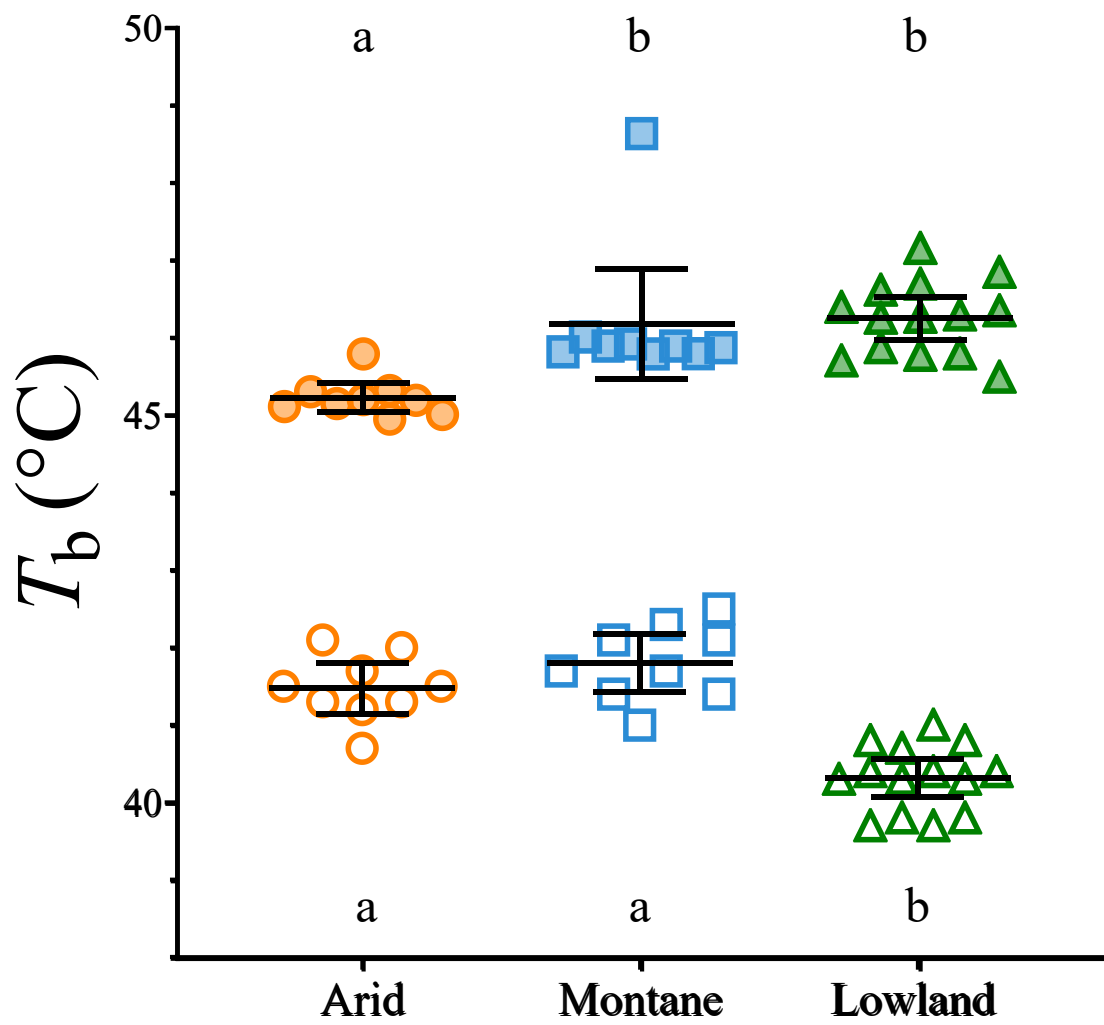


Figure S2

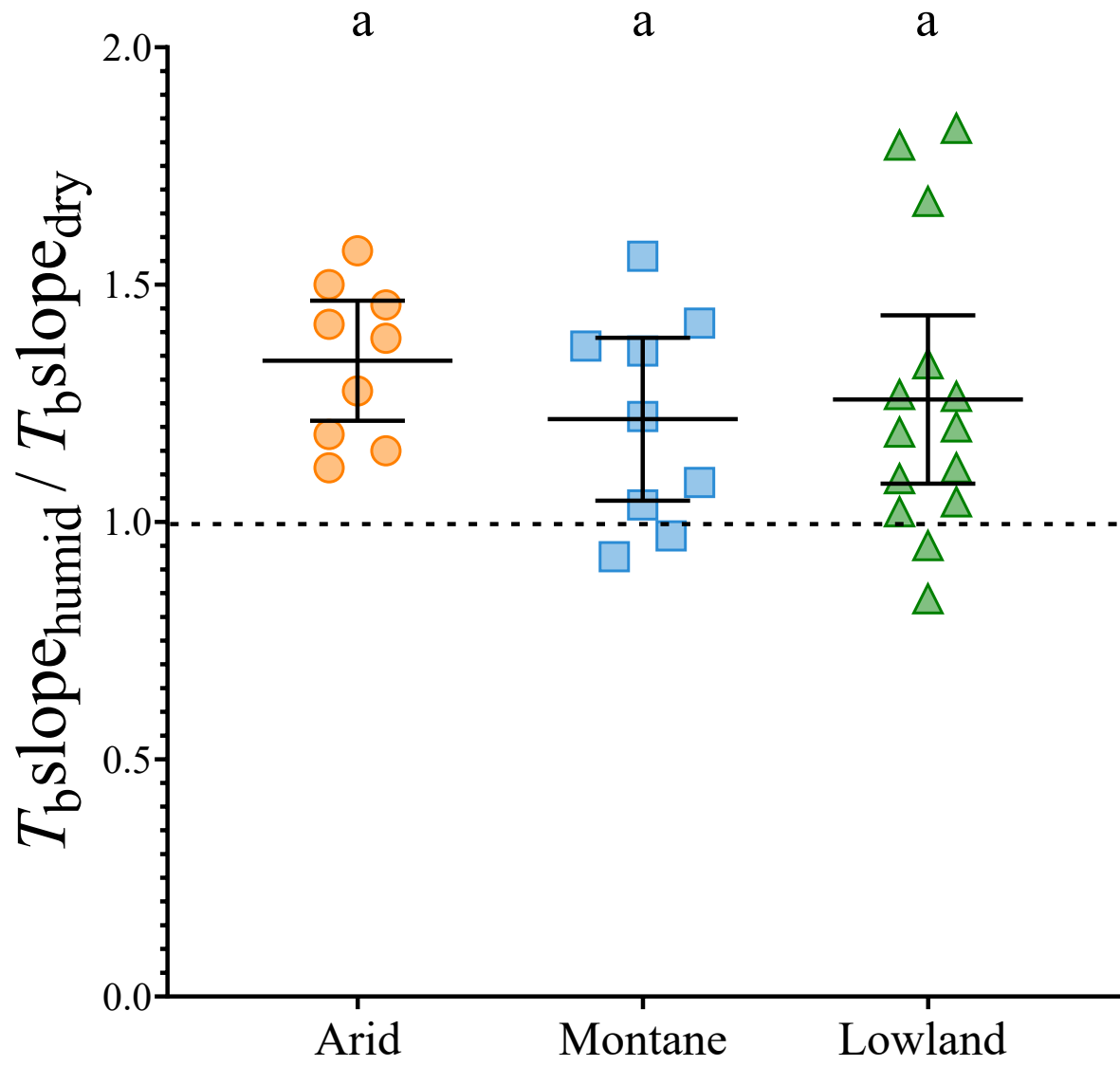


Figure S3

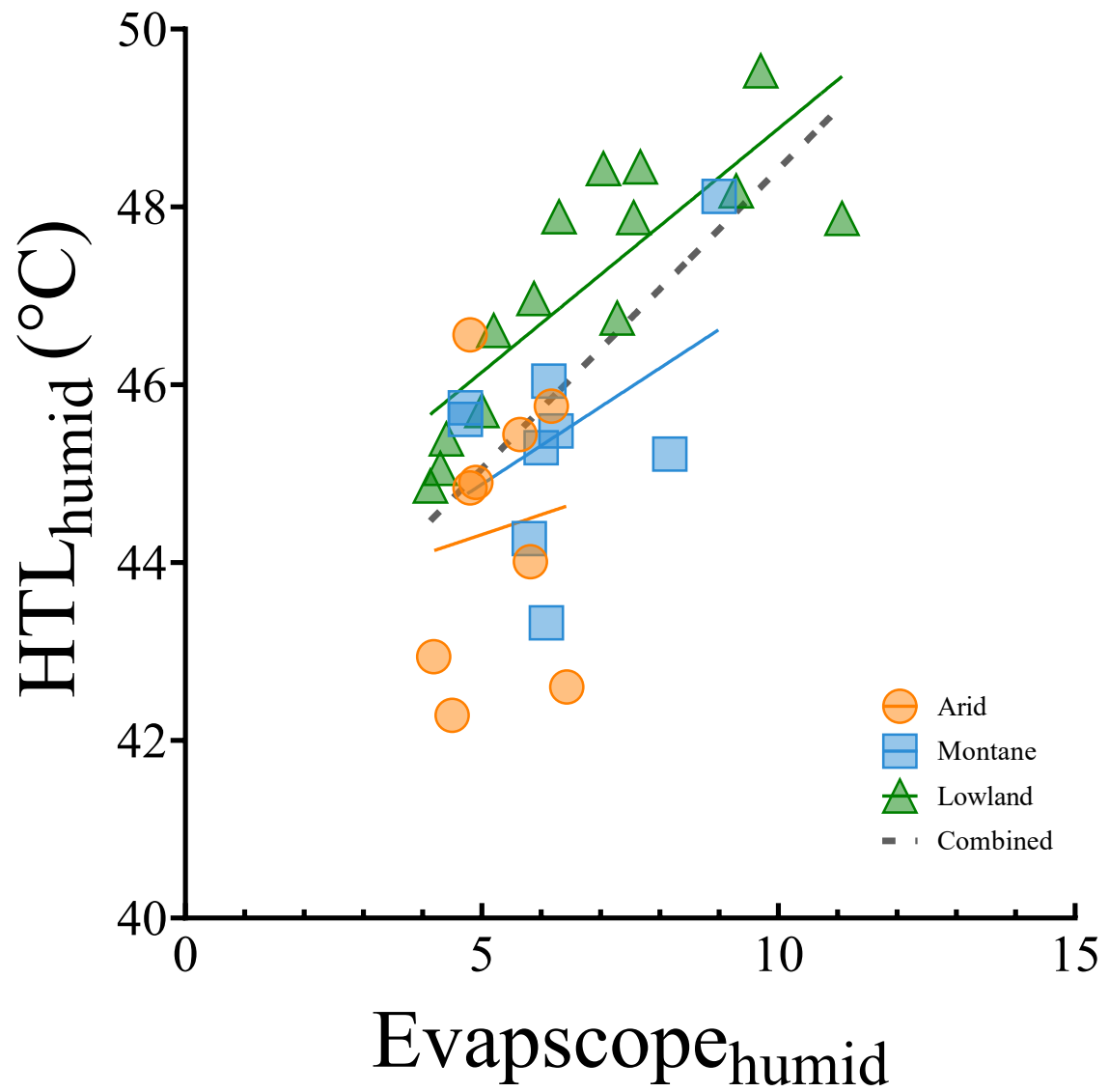


Figure S4

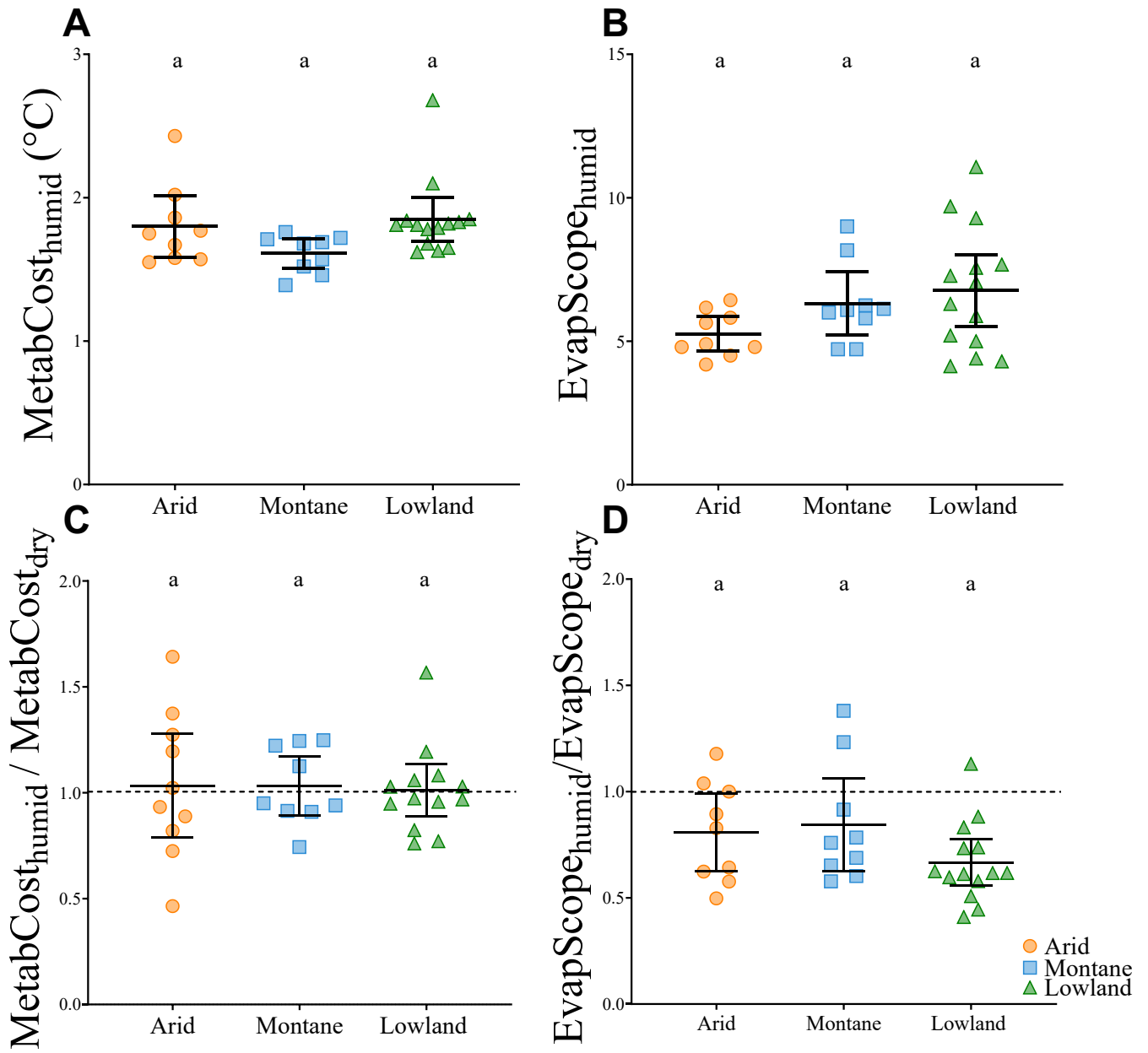


Figure S5 (A-D)

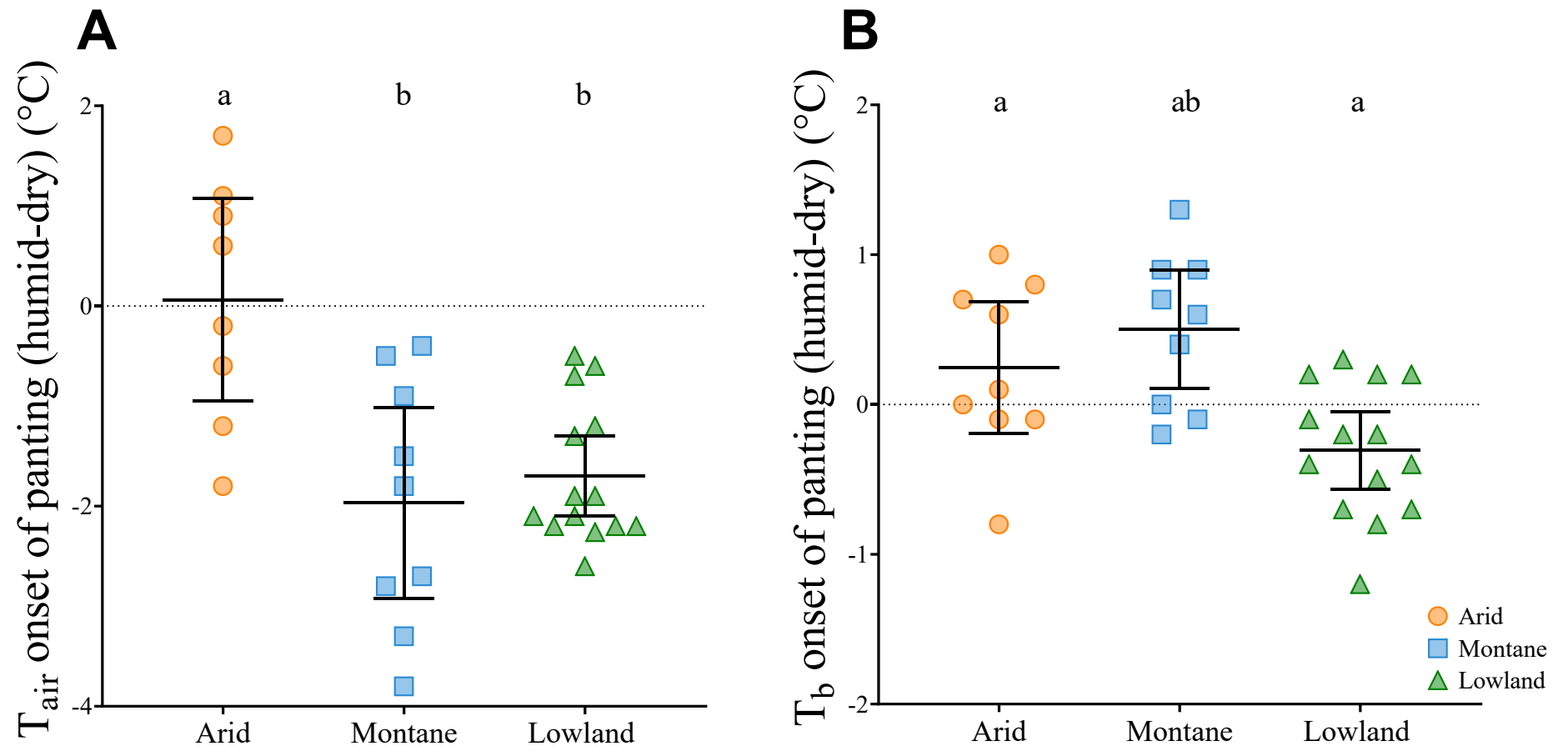


Figure S6

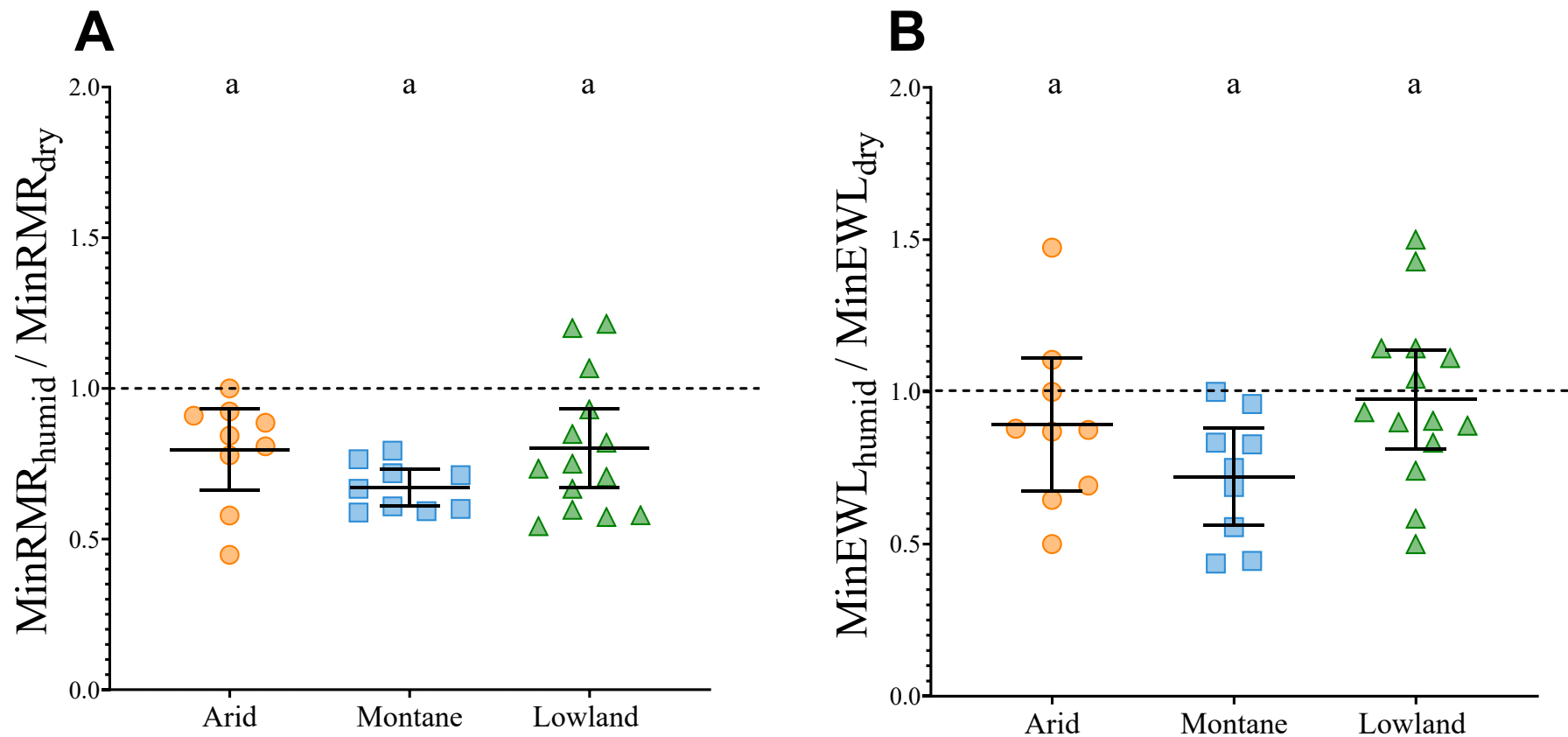


Figure S6

Table S1.1. All 30 species' avian families, orders and sample sizes across the study sites (mesic montane, humid lowland and hot arid) under dry (~1 g H₂O m⁻³) and humid (~19 g H₂O m⁻³) conditions. Also included is the source of the data if individuals were not collected as part of the main study.

Common Name	Species	Family	Order	Study area (sample size)	Source
Dry Assessments (~1 g H ₂ O m ⁻³)	n = 30	n = 15	n = 3	Lowland (n = 139) Montane (n = 100) Arid (n = 81)	
African Pygmy Kingfisher	<i>Ceyx pictus</i>	Alcedinidae	Coraciiformes	Lowland (n = 10)	Freeman <i>et al.</i> 2022
Black-headed Canary	<i>Serinus alario</i>	Fringillidae	Passeriformes	Arid (n = 5)	This study
		Estrelidae	Passeriformes	Lowland (n = 10)	Liddle <i>et al.</i> unpublished
Blue Waxbills	<i>Uraeginthus angolensis</i>				
Brown-hooded Kingfisher	<i>Halcyon albiventris</i>	Alcedinidae	Coraciiformes	Lowland (n = 10)	Freeman <i>et al.</i> 2022
Cape Bulbul	<i>Pycnonotus capensis</i>	Pycnonotidae	Passeriformes	Arid (n = 10)	Freeman <i>et al.</i> 2022
Cape Bunting	<i>Emberiza capensis</i>	Emberizidae	Passeriformes	Arid (n = 10)	This study
Cape White-eye	<i>Zosterops virens</i>	Zosteropidae	Passeriformes	Montane (n = 10)	Freeman <i>et al.</i> 2022
Collared Sunbird	<i>Anthreptes collaris</i>	Nectariniidae	Passeriformes	Lowland (n = 10)	Freeman <i>et al.</i> 2022
Dark-capped Bulbul	<i>Pycnonotus tricolor</i>	Pycnonotidae	Passeriformes	Montane (n = 10) Lowland (n = 10)	Freeman <i>et al.</i> 2022
Drakensberg Prinia	<i>Prinia hypoxantha</i>	Cisticolidae	Passeriformes	Montane (n = 10)	Freeman <i>et al.</i> 2022
Green-backed				Lowland (n = 10)	Freeman <i>et al.</i> 2022
Camaroptera	<i>Camaroptera brachyura</i>	Cisticolidae	Passeriformes		
Karoo Lark	<i>Certhilauda albescens</i>	Alaudidae	Passeriformes	Arid (n = 10)	This study
Karoo Prinia	<i>Prinia maculosa</i>	Cisticolidae	Passeriformes	Arid (n = 10)	This study

CHAPTER 2

SECOND DATA CHAPTER

Lark-like Bunting	<i>Emberiza impetuani</i>	Emberizidae	Passeriformes	Arid (n = 6)	This study
Orange River White-eye	<i>Zosterops pallidus</i>	Zosteropidae	Passeriformes	Arid (n = 10)	This study
Pink-throated Twinspot	<i>Hypargos margaritatus</i>	Estrelidae	Passeriformes	Lowland (n = 10)	This study
Red-billed Quelea	<i>Quelea quelea</i>	Ploceidae	Passeriformes	Montane (n = 20)	Freeman <i>et al.</i> 2020
Red-capped Lark	<i>Calandrella cinerea</i>	Alaudidae	Passeriformes	Montane (n = 10)	Freeman <i>et al.</i> 2022
Red-capped Robin-Chat	<i>Cossypha natalensis</i>	Muscicapidae	Passeriformes	Lowland (n = 10)	Freeman <i>et al.</i> 2022
Rudd's Apalis	<i>Apalis ruddi</i>	Cisticolidae	Passeriformes	Lowland (n = 10)	This study
Sombre Greenbul	<i>Andropadus importunus</i>	Pycnonotidae	Passeriformes	Lowland (n = 10)	Freeman <i>et al.</i> 2022
South African cliff swallow	<i>Hirundo spilodera</i>	Hirundinidae	Passeriformes	Montane (n = 10)	Freeman <i>et al.</i> 2022
Southern Fiscal	<i>Lanius collaris</i>	Laniidae	Passeriformes	Lowland (n = 10) Montane (n = 10)	Freeman <i>et al.</i> 2022
Southern Masked Weaver	<i>Ploceus velatus</i>	Ploceidae	Passeriformes	Montane (n = 10)	Freeman <i>et al.</i> 2022
Spectacled Weaver	<i>Ploceus ocularis</i>	Ploceidae	Passeriformes	Lowland (n = 10)	Freeman <i>et al.</i> 2022
Spike-heeled Lark	<i>Chersomanes albofasciata</i>	Alaudidae	Passeriformes	Montane (n = 10)	Freeman <i>et al.</i> 2022
White-throated Canary	<i>Serinus albogularis</i>	Carduelinae	Passeriformes	Arid (n = 10)	This study
Yellow Bishop	<i>Euplectes capensis</i>	Ploceidae	Passeriformes	Arid (n = 9)	This study
Yellow Weaver	<i>Ploceus subaureus</i>	Ploceidae	Passeriformes	Lowland (n = 9)	Freeman <i>et al.</i> 2022
Yellow-rumped Tinkerbird	<i>Pogoniulus bilineatus</i>	Lybiidae	Piciformes	Lowland (n = 10)	Freeman <i>et al.</i> 2022
Humidity Assessments (~19 g H ₂ O m ⁻³)	n = 30	n = 15	n = 3	Lowland (n = 132) Montane (n = 90) Arid (n = 85)	

African Pygmy Kingfisher	<i>Ceyx pictus</i>	Alcedinidae	Coraciiformes	Lowland (n = 10)	This study
Black-headed Canary	<i>Serinus alario</i>	Fringillidae	Passeriformes	Arid (n = 5)	This study
Blue Waxbills	<i>Uraeginthus angolensis</i>	Estrelidae	Passeriformes	Lowland (n = 10)	This study
Brown-hooded Kingfisher	<i>Halcyon albiventris</i>	Alcedinidae	Coraciiformes	Lowland (n = 10)	This study
Cape Bulbul	<i>Pycnonotus capensis</i>	Pycnonotidae	Passeriformes	Arid (n = 10)	This study
Cape Bunting	<i>Emberiza capensis</i>	Emberizidae	Passeriformes	Arid (n = 10)	This study
Cape White-eye	<i>Zosterops virens</i>	Zosteropidae	Passeriformes	Montane (n = 10)	This study
Collared Sunbird	<i>Anthreptes collaris</i>	Nectariniidae	Passeriformes	Lowland (n = 8)	This study
Dark-capped Bulbul	<i>Pycnonotus tricolor</i>	Pycnonotidae	Passeriformes	Montane (n = 10) Lowland (n = 10)	This study
Drakensberg Prinia	<i>Prinia hypoxantha</i>	Cisticolidae	Passeriformes	Montane (n = 10)	This study
Green-backed Camaroptera	<i>Camaroptera brachyura</i>	Cisticolidae	Passeriformes	Lowland (n = 10)	This study
Karoo Lark	<i>Certhilauda albescens</i>	Alaudidae	Passeriformes	Arid (n = 10)	This study
Karoo Prinia	<i>Prinia maculosa</i>	Cisticolidae	Passeriformes	Arid (n = 10)	This study
Lark-like Bunting	<i>Emberiza impetuani</i>	Emberizidae	Passeriformes	Arid (n = 10)	This study
Orange River White-eye	<i>Zosterops pallidus</i>	Zosteropidae	Passeriformes	Arid (n = 10)	This study
Pink-throated Twinspot	<i>Hypargos margaritatus</i>	Estrelidae	Passeriformes	Lowland (n = 10)	This study
Red-billed Quelea	<i>Quelea quelea</i>	Ploceidae	Passeriformes	Lowland (n = 10) Montane (n = 10)	This study
Red-capped Lark	<i>Calandrella cinerea</i>	Alaudidae	Passeriformes	Montane (n = 10)	This study
Red-capped Robin-Chat	<i>Cossypha natalensis</i>	Muscicapidae	Passeriformes	Lowland (n = 10)	This study

Rudd's Apalis	<i>Apalis ruddi</i>	Cisticolidae	Passeriformes	Lowland (n = 10)	This study
Sombre Greenbul	<i>Andropadus importunus</i>	Pycnonotidae	Passeriformes	Lowland (n = 10)	This study
South African Cliff Swallow	<i>Hirundo spilodera</i>	Hirundinidae	Passeriformes	Montane (n = 10)	This study
Southern Fiscal	<i>Lanius collaris</i>	Laniidae	Passeriformes	Lowland (n = 10) Montane (n = 10)	This study
Southern Masked Weaver	<i>Ploceus velatus</i>	Ploceidae	Passeriformes	Montane (n = 10)	This study
Spectacled Weaver	<i>Ploceus ocularis</i>	Ploceidae	Passeriformes	Lowland (n = 5)	This study
Spike-heeled Lark	<i>Chersomanes albofasciata</i>	Alaudidae	Passeriformes	Montane (n = 10)	This study
White-throated Canary	<i>Serinus albogularis</i>	Carduelinae	Passeriformes	Arid (n = 10)	This study
Yellow Bishop	<i>Euplectes capensis</i>	Ploceidae	Passeriformes	Arid (n = 10)	This study
Yellow Weaver	<i>Ploceus subaureus</i>	Ploceidae	Passeriformes	Lowland (n = 10)	This study
Yellow-rumped Tinkerbird	<i>Pogoniulus bilineatus</i>	Lybiidae	Piciformes	Lowland (n = 9)	This study

Table S1.2. Summary of the number of individuals and species for this study across study sites (Namaqualand, Harrismith and Hluhluwe) under dry ($\sim 1 \text{ g H}_2\text{O m}^{-3}$) and humid ($\sim 19 \text{ g H}_2\text{O m}^{-3}$) conditions and the corresponding ranges of flow-rates (ml min^{-1}) and body mass (grams) across the sites.

Variable	Hot (Namaqualand)	Arid Mesic Montane* (Harrismith)	Humid (Hluhluwe)	Lowland* All sites
No. individuals (dry 0mg^{-3})	81	-	20	101
No. species (dry 0mg^{-3})	9	-	2	11
No. individuals (humid 19mg^{-3})	85	90	132	307
No. species (humid 19mg^{-3})	9	9	13	30
Mb Range Dry (min: max)	7.4: 32.8	-	9.6: 12.5	7.4: 32.8
Mb Range Humid (min: max)	6.9: 32.8	9.3: 42.8	7: 61.7	6.9: 61.7
Flow rate Range Dry (min: max)	600: 17 000	-	3 000: 16 000	3 000: 20 000
Flow rate Range Humid (min: max)	650: 4 000	500: 1 980	840: 2 900	500: 4 000

*Dry assessments for the mesic montane site and several lowland species were not performed for this study, see Freeman *et al.* 2022.

Table S2.1. Summary of thermoregulatory performance as a function of chamber air temperature (T_{air}) at a humidity of $\sim 19\text{g H}_2\text{O m}^{-3}$ in nine bird species from the arid study site (Namaqualand). T_b = body temperature, T_{air} = ambient temperature, RMR = resting metabolic rate, EWL = evaporative water loss, EHL= evaporative heat loss, MHP = metabolic heat production. Means \pm SD and (n) are reported.

Variable	Black-headed Canary	Cape Bulbul	Cape Bunting	Karoo Lark	Karoo Prinia	Lark-like Bunting
Body mass (g)	11.2\pm0.2 (5)	32.8\pm2.1 (10)	19.3\pm1.3 (10)	27.6\pm2.2 (10)	6.9\pm0.6 (10)	13.5\pm0.9 (10)
Body temperature						
Min. T_b ($^{\circ}\text{C}$)	41.5 \pm 0.6 (5)	42.1 \pm 0.4 (10)	42.0 \pm 0.7 (10)	41.3 \pm 0.8 (10)	40.7 \pm 0.4 (10)	41.7 \pm 0.5 (10)
Inflection T_{air} ($^{\circ}\text{C}$)	N/A	40.9	N/A	N/A	N/A	N/A
T_b versus T_{air} slope (per $^{\circ}\text{C}$)	0.41	0.39	0.43	0.39	0.37	0.37
Max T_b ($^{\circ}\text{C}$)	45.2 \pm 0.3 (5)	45.0 \pm 0.8 (10)	45.3 \pm 0.8 (10)	45.2 \pm 0.5 (10)	45.3 \pm 0.7 (10)	45.1 \pm 0.2 (10)
Max T_{air} ($^{\circ}\text{C}$)	42.5 \pm 1.6 (5)	45.8 \pm 2.2 (10)	42.3 \pm 1.9 (10)	46.6 \pm 1.4 (10)	44.8 \pm 1.1 (10)	45.4 \pm 0.9 (10)
T_b at onset of panting ($^{\circ}\text{C}$)	43.6 \pm 0.4 (5)	42.4 \pm 0.5 (10)	43.9 \pm 0.6 (8)	42.1 \pm 1.1 (10)	44.2 \pm 0.7 (10)	43.08 \pm 0.7 (10)
T_{air} at onset of panting ($^{\circ}\text{C}$)	38.3 \pm 0.8 (4)	37.6 \pm 2.1 (10)	39.1 \pm 1.1 (8)	38.8 \pm 1.8 (10)	41.8 \pm 0.7 (10)	40.3 \pm 1.7 (10)
Metabolic rate						
Min. RMR (W)	0.20 \pm 0.01 (5)	0.37 \pm 0.14 (10)	0.30 \pm 0.07 (10)	0.31 \pm 0.03 (10)	0.14 \pm 0.03 (10)	0.24 \pm 0.06 (10)
T_{uc} ($^{\circ}\text{C}$)	N/A	N/A	N/A	N/A	N/A	N/A
RMR slope (mW $^{\circ}\text{C}^{-1}$)	16.64	35.39	31.45	19.2	7.82	24.95
Max. RMR (W)	0.35 \pm 0.07 (3)	0.90 \pm 0.18 (5)	0.53 \pm 0.21 (4)	0.48 \pm 0.12 (8)	0.22 \pm 0.01 (3)	0.40 \pm 0.06 (3)
Max. RMR/min. RMR	1.75	2.43	1.77	1.55	1.57	1.67
Evaporative water loss						
Min. EWL (g h $^{-1}$)	0.07 \pm 0.04 (5)	0.29 \pm 0.11 (10)	0.20 \pm 0.09 (10)	0.20 \pm 0.07 (10)	0.09 \pm 0.03 (10)	0.14 \pm 0.08 (10)
Inflection T_{air} ($^{\circ}\text{C}$)	N/A	40.01	N/A	40.13	39.3	38.29
EWL slope (g h $^{-1}$ $^{\circ}\text{C}^{-1}$)	0.06	0.21	0.09	0.11	0.05	0.09
Max. EWL (g h $^{-1}$)	0.45 \pm 0.13 (3)	1.79 \pm 0.38 (5) 2.20 (1)	0.90 \pm 0.43 (4)	0.96 \pm 0.30 (8)	0.46 \pm 0.70 (3)	0.79 \pm 0.15 (3)
Max. EWL/min. EWL	6.43	6.17	4.5	4.80	5.11	5.64
Min. EHL/MHP	0.23 \pm 0.13 (5)	0.53 \pm 0.14 (10)	0.44 \pm 0.10 (10)	0.44 \pm 0.15 (10)	0.40 \pm 0.13 (10)	0.39 \pm 0.20 (10)
EHL/MHP inflection $T_{air} - T_b$	-6.0	N/A	N/A	N/A	N/A	N/A
EHL/MHP slope	0.19	0.11	0.14	0.14	0.16	0.16
Max. EHL/MHP	0.85 \pm 0.12 (3)	1.32 \pm 0.18 (5) 1.75 (1)	1.14 \pm 0.13 (4)	1.34 \pm 0.18 (8) 1.63 (1)	1.39 \pm 0.20 (3)	1.32 \pm 0.05 (3)

Table S2.1. Cont.

Variable	Orange-river White-eye	White-throated Canary	Yellow Bishop
Body mass (g)	9.5±0.5 (10)	22.6±1.4 (10)	29.5±4.9(10)
Body temperature			
Min. T_b (°C)	41.2±2.0 (10)	41.5±0.6 (10)	41.3±0.7 (10)
Inflection T_{air} (°C)	38.5	N/A	37.0
T_b versus T_{air} slope (per °C)	0.54	0.51	0.45
Max T_b (°C)	45.2±0.2 (10)	45.0±0.9 (10)	45.8±0.4 (10)
Max T_{air} (°C)	44.0±1.1 (10)	42.9±1.9 (10)	44.9±1.3 (10)
T_b at onset of panting (°C)	43.2±0.8 (9)	42.2±2.3 (10)	43.0±1.2 (10)
T_{air} at onset of panting (°C)	38.8±1.2 (9)	39.6±1.0 (10)	40.6±1.1 (10)
Metabolic rate			
Min. RMR (W)	0.21±0.03 (10)	0.36±0.06 (10)	0.43±0.11 (10)
T_{uc} (°C)	N/A	38.77	37.0
RMR slope (mW °C ⁻¹)	21.03	33.73	45.95
Max. RMR (W)	0.39±0.07 (8)	0.57±0.10 (5) 0.64 (1)	0.87±0.16 (3)
Max. RMR/min. RMR	1.86	1.58	2.02
Evaporative water loss			
Min. EWL (g h ⁻¹)	0.11±0.04 (10)	0.21±0.10 (10)	0.28±0.08 (10)
Inflection T_{air} (°C)	38.0	39.1	38.5
EWL slope (g h ⁻¹ °C ⁻¹)	0.07	0.10	0.13
Max. EWL (g h ⁻¹)	0.64±0.14 (8)	0.88±0.18 (5) 1.12 (1)	1.38±0.20 (3)
Max. EWL/min. EWL	5.82	4.19	4.9
Min. EHL/MHP	0.37±0.12 (10)	0.38±0.15 (10)	0.45±0.14 (10)
EHL/MHP inflection $T_{air} - T_b$	N/A	N/A	N/A
EHL/MHP slope	0.11	0.42	0.12
Max. EHL/MHP	1.10±0.11 (8)	1.04±0.17(5) 1.17 (1)	1.06±0.09 (3)

Table S2.2. Summary of thermoregulatory performance as a function of chamber air temperature (T_{air}) at a humidity of ~ 1 g H₂O m⁻³ (dry air) in nine bird species from the arid study site (Namaqualand). T_b = body temperature, T_{air} = ambient temperature, RMR = resting metabolic rate, EWL = evaporative water loss, EHL = evaporative heat loss, MHP = metabolic heat production. Means \pm SD and (n) are reported.

Variable	Black-headed Canary	Cape Bulbul	Cape Bunting	Karoo Lark	Karoo Prinia	Lark-like Bunting	Orange-river White-eye
Body mass (g)	10.4\pm0.6 (5)	32.8\pm2.1 (10)	19.7\pm1.8 (10)	28.2\pm3.2 (10)	7.4\pm0.5 (10)	13.5\pm0.8 (6)	9.6\pm0.5 (10)
Body temperature							
Min. T_b ($^{\circ}$ C)	41.3 \pm 0.9 (5)	41.4 \pm 0.6 (10)	40.60 \pm 0.8 (10)	40.5 \pm 0.8 (10)	40.5 \pm 1.5 (10)	40.1 \pm 0.7 (6)	40.66 \pm 0.95(10)
Inflection T_{air} ($^{\circ}$ C)	32.5	38.9	32.5	37.3	34.4	35.7	32.9
T_b versus T_{air} slope (per $^{\circ}$ C)	0.26	0.26	0.31	0.36	0.32	0.29	0.36
Max T_b ($^{\circ}$ C)	44.8 \pm 0.4 (4)	45.2 \pm 0.3 (9)	45.2 \pm 0.3 (9)	45.0 \pm 0.7 (10)	45.3 \pm 0.5 (10)	45.2 \pm 0.2 (6)	45.3 \pm 0.3 (10)
Max T_{air} ($^{\circ}$ C)	46.5 \pm 0.5 (4)	49.8 \pm 1.4 (9)	47.0 \pm 1.5 (9)	48.3 \pm 1.3 (10)	46.2 \pm 1.1 (10)	48.3 \pm 1.0 (6)	46.3 \pm 1.1 (10)
T_b at onset of panting ($^{\circ}$ C)	44.2 \pm 0.4 (4)	42.3 \pm 0.9 (10)	43.2 \pm 1.5 (10)	42.9 \pm 0.8 (10)	44.3 \pm 0.9 (9)	42.3 \pm 0.8 (5)	43.3 \pm 1.1 (10)
T_{air} at onset of panting ($^{\circ}$ C)	40.4 \pm 1.1 (4)	36.7 \pm 3.3 (10)	38.9 \pm 2.1 (10)	40.6 \pm 2.1 (10)	41.7 \pm 1.1 (9)	38.6 \pm 2.1 (5)	40.0 \pm 1.7 (10)
Metabolic rate							
Min. RMR (W)	0.33 \pm 0.07 (4)	0.64 \pm 0.14 (10)	0.67 \pm 0.12 (10)	0.35 \pm 0.05 (10)	0.18 \pm 0.02 (10)	0.24 \pm 0.03 (6)	0.26 \pm 0.04 (10)
T_{uc} ($^{\circ}$ C)	32.5	38.50	33.94	37.71	35.17	37.2	38.0
RMR slope (mW $^{\circ}$ C ⁻¹)	27.7	27.96	35.02	19.13	11.5	14.6	16.37
Max. RMR (W)	0.65 \pm 0.16 (4)	0.95 \pm 0.15 (9)	1.16 \pm 0.25 (6)	0.66 \pm 0.09 (4)	0.27 \pm 0.03 (10)	0.43 \pm 0.10 (4)	0.38 \pm 0.04 (9)
	0.84 (2)						
Max. RMR/min. RMR	1.97	1.48	1.73	1.89	3.38	1.79	1.46
Evaporative water loss							
Min. EWL (g h ⁻¹)	0.14 \pm 0.07 (4)	0.33 \pm 0.11 (10)	0.31 \pm 0.11 (10)	0.23 \pm 0.07 (10)	0.13 \pm 0.05 (10)	0.16 \pm 0.06 (6)	0.11 \pm 0.03 (10)
Inflection T_{air} ($^{\circ}$ C)	36.45	39.25	34.96	38.25	39.03	39.15	37.5
EWL slope (g h ⁻¹ $^{\circ}$ C ⁻¹)	0.09	0.16	0.14	0.11	0.07	0.09	0.06
Max. EWL (g h ⁻¹)	0.79 \pm 0.18 (4)	2.45 \pm 0.60 (5)	2.17 \pm 0.41 (6)	1.77 \pm 0.22 (4)	0.61 \pm 0.12 (7)	1.01 \pm 0.15 (4)	0.64 \pm 0.13 (9)
	0.87 (2)	2.55 (1)	2.36 (2)				0.70 (1)
Max. EWL/min. EWL	5.64	7.42	7	7.70	4.62	6.31	5.82
Min. EHL/MHP	0.25 \pm 0.14 (4)	0.35 \pm 0.09 (10)	0.29 \pm 0.10 (10)	0.41 \pm 0.13 (10)	0.45 \pm 0.18 (10)	0.42 \pm 0.13 (6)	0.31 \pm 0.09 (10)
EHL/MHP inflection $T_{air} - T_b$	-4.07	-7.46	-7.80	-5.96	-4.07	-5.46	-6.44
EHL/MHP slope	0.05	0.13	0.10	0.12	0.17	0.15	0.12
Max. EHL/MHP	0.89 \pm 0.34 (4)	1.96 \pm 0.25 (5)	1.29 \pm 0.30 (6)	1.80 \pm 0.30 (4)	1.24 \pm 0.70 (7)	1.61 \pm 0.29 (4)	1.35 \pm 0.17 (7)
	0.94 (1)	2.20 (1)	1.63 (2)		1.81 (1)		

Table S2.2. Cont.

Variable	White-throated Canary	Yellow Bishop
Body mass (g)	22.1±1.5 (10)	30.6±4.4 (9)
Body temperature		
Min. T_b (°C)	40.19±0.6 (10)	40.6±0.7 (9)
Inflection T_{air} (°C)	30.33	38.2
T_b versus T_{air} slope (per °C)	0.35	0.38
Max T_b (°C)	45.3±0.3 (10)	45.4±0.3 (9)
Max T_{air} (°C)	46.5±1.5 (10)	48.7±1.2 (9)
T_b at onset of panting (°C)	42.2±1.2 (10)	42.0±0.7 (9)
T_{air} at onset of panting (°C)	39.0±2.0 (10)	39.5±0.6 (10)
Metabolic rate		
Min. RMR (W)	0.39±0.06 (10)	0.51±0.11 (9)
T_{uc} (°C)	36.98	41.77
RMR slope (mW °C ⁻¹)	48.56	62.32
Max. RMR (W)	0.85±0.05 (4)	0.86±0.27 (6)
Max. RMR/min. RMR	2.18	1.69
Evaporative water loss		
Min. EWL (g h ⁻¹)	0.19±0.05 (10)	0.19±0.05 (9)
Inflection T_{air} (°C)	38.0	37.8
EWL slope (g h ⁻¹ °C ⁻¹)	0.14	0.13
Max. EWL (g h ⁻¹)	1.60±0.22 (4)	1.62±0.42 (6)
Max. EWL/min. EWL	8.42	8.52
Min. EHL/MHP	0.31±0.09 (10)	0.24±0.11 (9)
EHL/MHP inflection $T_{air} - T_b$	-4.60	-6.21
EHL/MHP slope	0.13	0.11
Max. EHL/MHP	1.35±0.17 (7)	1.28±0.10 (6)
		1.36 (2)

Table S2.3a. Mass-specific resting metabolic rate (RMR) and evaporative water loss (EWL) rate at high T_{air} in ten bird species thermoregulatory performance as a function of chamber air temperature (T_{air}) coupled with humidity of $\sim 19\text{g H}_2\text{O m}^{-3}$ within a southern African arid region (Namaqualand). Means, SD and (n) are reported.

Variable	Black-headed Canary	Cape Bulbul	Cape Bunting	Karoo Lark	Karoo Prinia
Min. RMR (mW g^{-1})	17.78±2.35 (5)	11.30±3.75 (10)	15.23±3.84 (10)	10.52±2.53 (10)	20.59±3.86 (10)
RMR slope ($\text{mW g}^{-1} \text{ }^\circ\text{C}^{-1}$)	1.22	1.37	1.55	1.96	1.13
Max. RMR (mW g^{-1})	31.49±6.04 (3)	26.66±5.39 (5)	26.89±11.22 (4)	16.70±3.63 (8)	32.32±6.84 (3)
				17.58 (1)	
Min. EWL ($\text{mg h}^{-1} \text{ g}^{-1}$)	6.21±3.45 (5)	8.75±3.06 (10)	10.03±4.07 (10)	7.06±2.44 (10)	12.63±5.36 (10)
EWL slope ($\text{mg h}^{-1} \text{ g}^{-1} \text{ }^\circ\text{C}^{-1}$)	0.96		4.59		4.49
Max. EWL ($\text{mg h}^{-1} \text{ g}^{-1}$)	40.36±11.07 (3)	52.53±10.27 (5)	45.64±20.97 (4)	33.79±9.45 (8)	66.35±8.17 (3)
		62.44 (1)		42.89 (1)	
Variable	Lark-like Bunting	Orange-river eye	White-White-throated Canary	Yellow Bishop	
Min. RMR (mW g^{-1})	17.54±4.21 (11)	21.20±1.81 (10)	15.69±2.46 (10)	14.64±4.64 (10)	
RMR slope ($\text{mW g}^{-1} \text{ }^\circ\text{C}^{-1}$)	1.84	1.54	1.16	0.53	
Max. RMR (mW g^{-1})	32.78±10.27 (11)	40.14±6.08 (8)	24.25±3.40 (5)	29.11±10.78 (3)	
			29.88(1)		
Min. EWL ($\text{mg h}^{-1} \text{ g}^{-1}$)	10.27±5.32 (11)	11.82±4.0 (10)	9.05±3.90 (10)	9.41±2.70 (10)	
EWL slope ($\text{mg h}^{-1} \text{ g}^{-1} \text{ }^\circ\text{C}^{-1}$)	5.65	4.96	3.98	2.15	
Max. EWL ($\text{mg h}^{-1} \text{ g}^{-1}$)	58.91±14.85 (3)	66.21±14.07 (8)	37.51±6.69 (5)	46.01±16.50 (3)	
			52.11 (1)		

Table S2.3b. Mass-specific resting metabolic rate (RMR) and evaporative water loss (EWL) rate at high T_{air} in nine bird species thermoregulatory performance as a function of chamber air temperature (T_{air}) coupled with humidity of $\sim 1 \text{ g H}_2\text{O m}^{-3}$ (dry air) within a southern African arid region (Namaqualand). Means, SD and (n) are reported.

Variable	Black-headed Canary	Cape Bulbul	Cape Bunting	Karoo Lark	Karoo Prinia
Min. RMR (mW g^{-1})	30.43±9.07 (5)	18.27±2.34 (10)	34.87±6.22 (10)	12.30±2.24 (10)	14.66±66.6 (7)
RMR slope ($\text{mW g}^{-1} \text{ }^\circ\text{C}^{-1}$)	2.51	0.91	1.68	0.69	1.59
Max. RMR (mW g^{-1})	61.02±19.9 (4)	29.1±4.31 (9)	55.69±11.39 (6)	22.22±5.34 (4)	37.61±5.63 (10)
	43.46 (2)				
Min. EWL ($\text{mg h}^{-1} \text{ g}^{-1}$)	12.73±9.77 (5)	10.19±3.30 (10)	15.31±5.38 (10)	7.95±1.48 (10)	17.86±6.98 (10)
EWL slope ($\text{mg h}^{-1} \text{ g}^{-1} \text{ }^\circ\text{C}^{-1}$)	1.06	5.08	7.21	4.01	9.13
Max. EWL ($\text{mg h}^{-1} \text{ g}^{-1}$)	73.05±18.00 (4)	78.42±22.21 (5)	104.55±17.88 (6)	59.31±14.99 (4)	83.67±23.07 (7)
	87.62 (2)	82.17 (1)	114.21 (2)		
Variable	Lark-like Bunting	Orange-river White-eye	White-throated Canary	Yellow Bishop	
Min. RMR (mW g^{-1})	17.69±2.33 (6)	27.20±4.33 (10)	17.40±2.70 (10)	16.79±3.75 (9)	
RMR slope ($\text{mW g}^{-1} \text{ }^\circ\text{C}^{-1}$)	1.44	1.70	2.43	0.19	
Max. RMR (mW g^{-1})	31.02±8.06 (4)	39.65±3.78 (9)	36.27±4.46 (4)	27.60±6.21 (6)	
Min. EWL ($\text{mg h}^{-1} \text{ g}^{-1}$)	11.94±4.39 (6)	11.62±3.31 (10)	8.21±2.08 (10)	6.41±2.21 (9)	
EWL slope ($\text{mg h}^{-1} \text{ g}^{-1} \text{ }^\circ\text{C}^{-1}$)	5.76	6.12	6.21	1.92	
Max. EWL ($\text{mg h}^{-1} \text{ g}^{-1}$)	73.10±10.30 (4)	65.76±11.81 (9)	67.88±15.10 (4)	54.64 (2)	
		74.21 (1)		52.46±10.08 (6)	

Table S3.1. Summary of thermoregulatory performance as a function of chamber air temperature (T_{air}) at a humidity of $\sim 19\text{g H}_2\text{O m}^{-3}$ in 13 bird species from the lowland study site (Hluhluwe). T_b = body temperature, T_{air} = ambient temperature, RMR = resting metabolic rate, EWL = evaporative water loss, EHL= evaporative heat loss, MHP = metabolic heat production. Means \pm SD and (n) are reported.

Variable	African Pygmy Kingfisher	Brown-hooded Kingfisher	Collared Sunbird	Southern Fiscal	Dark-capped Bulbul	Green-backed Camaroptera
Body mass (g)	13.4 \pm 1.1 (10)	61.7 \pm 3.3 (10)	7.0 \pm 0.6 (8)	40.9 \pm 1.8 (10)	36.4 \pm 2.8 (10)	11.7 \pm 0.4 (10)
Body temperature						
Min. T_b ($^{\circ}\text{C}$)	40.8 \pm 0.7 (10)	40.4 \pm 0.7 (10)	39.8 \pm 0.7 (8)	40.8 \pm 0.7 (10)	39.8 \pm 1.1 (9)	40.4 \pm 0.5 (10)
Inflection T_{air} ($^{\circ}\text{C}$)	N/A	N/A	N/A	NA	N/A	N/A
T_b versus T_{air} slope (per $^{\circ}\text{C}$)	0.44	0.39	0.49	0.43	0.36	0.39
Max T_b ($^{\circ}\text{C}$)	45.7 \pm 0.5 (10)	46.3 \pm 0.4 (10)	45.9 \pm 0.6 (7)	46.9 \pm 0.3 (10)	45.8 \pm 0.5 (10)	46.3 \pm 0.5 (10)
Max T_{air} ($^{\circ}\text{C}$)	44.9 \pm 0.7 (10)	48.2 \pm 1.1 (10)	45.4 \pm 1.7 (8)	47.9 \pm 1.0 (10)	49.5 \pm 1.6 (10)	48.5 \pm 0.7 (10)
T_b at onset of panting ($^{\circ}\text{C}$)	42.1 \pm 0.8 (10)	41.7 \pm 0.6 (10)	41.8 \pm 1.3 (8)	42.4 \pm 0.8 (10)	40.8 \pm 1.6 (10)	41.2 \pm 0.8 (10)
T_{air} at onset of panting ($^{\circ}\text{C}$)	38.2 \pm 0.6 (10)	38.2 \pm 0.6 (10)	38.7 \pm 0.9 (8)	38.4 \pm 1.0 (10)	36.7 \pm 1.3 (10)	36.4 \pm 1.3 (10)
Metabolic rate						
Min. RMR (W)	0.22 \pm 0.01 (10)	0.47 \pm 0.04 (10)	0.14 \pm 0.01 (8)	0.50 \pm 0.07 (10)	0.44 \pm 0.05 (10)	0.24 \pm 0.02 (10)
T_{uc} ($^{\circ}\text{C}$)	N/A	N/A	34.34	38.83	41.34	N/A
RMR slope (mW $^{\circ}\text{C}^{-1}$)	14.6	61.26	10.89	49.49	36.05	11.27
Max. RMR (W)	0.37 \pm 0.03 (10)	1.26 \pm 0.22 (8) 1.85 (1)	0.26 \pm 0.03 (4)	0.92 \pm 0.22 (10)	0.79 \pm 0.20 (9) 0.83 (1)	0.39 \pm 0.03 (8)
Max. RMR/min. RMR	1.68	3.93	1.85	1.84	1.79	1.62
Evaporative water loss						
Min. EWL (g h $^{-1}$)	0.16 \pm 0.03 (10)	0.21 \pm 0.07 (10)	0.10 \pm 0.04 (8)	0.14 \pm 0.03 (10)	0.20 \pm 0.05 (10)	0.09 \pm 0.03 (10)
Inflection T_{air} ($^{\circ}\text{C}$)	36.3	37.215	34.61	38.93	39.231	37.42
EWL slope (g h $^{-1}$ $^{\circ}\text{C}^{-1}$)	0.06	0.17	0.03	0.14	0.13	0.04
Max. EWL (g h $^{-1}$)	0.66 \pm 0.14 (10)	1.95 \pm 0.59 (8) 3.18 (1)	0.44 \pm 0.09 (4)	1.55 \pm 0.48 (5)	1.94 \pm 0.22 (3) 2.40 (1)	0.64 \pm 0.13 (8) 0.69 (1)
Max. EWL/min. EWL	4.13	9.29	4.4	11.07	9.7	7.67
Min. EHL/MHP	0.49 \pm 0.07 (10)	0.31 \pm 0.12 (10)	0.42 \pm 0.18 (8)	0.19 \pm 0.06 (10)	0.30 \pm 0.10 (10)	0.26 \pm 0.08 (10)
EHL/MHP inflection $T_{air} - T_b$	-5.51	-5.579	N/A	-4.13	N/A	N/A
EHL/MHP slope	0.16	0.107	0.15	0.14	0.12	0.11
Max. EHL/MHP	1.30 \pm 0.27 (10)	1.11 \pm 0.26 (10) 1.14 (1)	1.18 \pm 0.19 (6)	1.15 \pm 0.34 (5)	1.98 \pm 0.08 (3)	1.08 \pm 0.24 (8) 1.18 (1)

Table S3.1. Cont.

Variable	Pink-throated Twinspot	Red-capped Robin-Chat	Rudd's Apalis	Sombre Greenbul	Spectacled Weaver
Body mass (g)	12.5 ± 1.2 (10)	27.8 ± 2.4 (10)	9.5 ± 0.4 (10)	27.3 ± 1.8 (10)	26.7 ± 1.3 (5)
Body temperature					
Min. T_b (°C)	40.3 ± 1.1 (10)	40.3 ± 0.7 (10)	39.7 ± 1.1 (10)	40.3 ± 0.9 (10)	40.4 ± 0.9 (5)
Inflection T_{air} (°C)	N/A	43.0	N/A	N/A	40.84
T_b versus T_{air} slope (per °C)	0.48	0.61	0.48	0.38	0.75
Max T_b (°C)	46.4 ± 0.4 (10)	46.4 ± 0.4 (10)	46.3 ± 1.2 (10)	45.9 ± 0.6 (10)	46.7 ± 0.9 (4)
Max T_{air} (°C)	46.9 ± 0.8 (10)	48.4 ± 1.1 (10)	46.6 ± 2.1 (10)	47.9 ± 2.1 (10)	46.8 ± 1.8 (4)
T_b at onset of panting (°C)	41.3 ± 0.9 (10)	41.0 ± 1.2 (10)	41.8 ± 1.0 (10)	40.6 ± 1.1 (10)	40.6 ± 0.6 (5)
T_{air} at onset of panting (°C)	37.7 ± 0.9 (10)	36.8 ± 1.5 (10)	38.7 ± 1.1 (10)	35.3 ± 1.4 (10)	35.6 ± 0.7 (5)
Metabolic rate					
Min. RMR (W)	0.18 ± 0.01 (10)	0.36 ± 0.03 (10)	0.16 ± 0.02 (10)	0.38 ± 0.03 (10)	0.40 ± 0.03 (5)
T_{uc} (°C)	40.74	N/A	N/A	41.56	40.735
RMR slope (mW °C ⁻¹)	24.43	16.94	10.03	28.76	63.39
Max. RMR (W)	0.33 ± 0.04 (9)	0.59 ± 0.04 (3)	0.29 ± 0.07 (7)	0.68 ± 0.01 (4)	0.81 ± 0.01 (3) 0.84 (1)
Max. RMR/min. RMR	1.83	1.63	1.81	1.78	2.10
Evaporative water loss					
Min. EWL (g h ⁻¹)	0.09 ± 0.04 (10)	0.19 ± 0.06 (10)	0.10 ± 0.03 (10)	0.24 ± 0.09 (10)	0.14 ± 0.03 (5)
Inflection T_{air} (°C)	36.93	35.93	37.14	N/A	37.93
EWL slope (g h ⁻¹ °C ⁻¹)	0.04	0.08	0.04	0.08	0.08
Max. EWL (g h ⁻¹)	0.53 ± 0.09 (9)	1.34 ± 0.13 (3)	0.52 ± 0.17 (7)	1.52 ± 0.11 (4)	1.02 ± 0.29 (3) 1.20 (1)
Max. EWL/min. EWL	5.88	7.05	5.2	6.3	7.28
Min. EHL/MHP	0.35 ± 0.09 (10)	0.36 ± 0.13 (10)	0.41 ± 0.12 (10)	0.41 ± 0.14 (10)	0.24 ± 0.06 (5)
EHL/MHP inflection $T_{air} - T_b$	-4.95	-5.64	-4.841	N/A	N/A
EHL/MHP slope	0.12	0.14	0.12	0.11	0.08
Max. EHL/MHP	1.06 ± 0.14 (9)	1.50 ± 0.06 (3)	1.19 ± 0.28 (5)	1.61 ± 0.12 (4)	0.84 ± 0.22 (3) 0.95 (1)

Table S3.1. Cont.

Variable	Yellow-rumped Tinkerbird	Yellow Weaver
Body mass (g)	14.2 ± 1.1 (10)	25.7 ± 2.6 (10)
Body temperature		
Min. T_b (°C)	40.7 ± 0.8 (10)	41.0 ± 0.5 (10)
Inflection T_{air} (°C)	N/A	40.9
T_b versus T_{air} slope (per °C)	0.52	0.6
Max T_b (°C)	46.6 ± 0.2 (10)	46.7 ± 0.5 (10)
Max T_{air} (°C)	45.1 ± 0.8 (10)	47.9 ± 1.1 (10)
T_b at onset of panting (°C)	41.8 ± 0.8 (10)	41.4 ± 0.9 (10)
T_{air} at onset of panting (°C)	38.2 ± 3.4 (10)	36.4 ± 1.9 (10)
Metabolic rate		
Min. RMR (W)	0.28 ± 0.05 (10)	0.37 ± 0.04 (10)
T_{ic} (°C)	36.55	39.63
RMR slope (mW °C ⁻¹)	27.72	35.03
Max. RMR (W)	0.51 ± 0.05 (2)	0.67 ± 0.12 (8)
Max. RMR/min. RMR	1.82	1.81
Evaporative water loss		
Min. EWL (g h ⁻¹)	0.10 ± 0.02 (10)	0.16 ± 0.04 (10)
Inflection T_{air} (°C)	N/A	37.08
EWL slope (g h ⁻¹ °C ⁻¹)	0.02	0.09
Max. EWL (g h ⁻¹)	0.43 ± 0.03 (2)	1.21 ± 0.38 (8)
Max. EWL/min. EWL	4.3	7.56
Min. EHL/MHP	0.25 ± 0.04 (10)	0.29 ± 0.08 (10)
EHL/MHP inflection $T_{air} - T_b$	-4.59	-5.65
EHL/MHP slope	0.08	0.12
Max. EHL/MHP	0.56 ± 0.01 (2)	1.21 ± 0.35 (8)

Table S3.2. Summary of thermoregulatory performance as a function of chamber air temperature (T_{air}) at a humidity of ~ 0 g H₂O m⁻³ (dry air) in two bird species from the lowland study site (Hluhluwe). T_b = body temperature, T_{air} = ambient temperature, RMR = resting metabolic rate, EWL = evaporative water loss, EHL = evaporative heat loss, MHP = metabolic heat production. Means \pm SD and (n) are reported.

Variable	Pink-throated Twinspot	Rudd's Apalis
Body mass (g)	12.5 \pm 0.6 (10)	9.6 \pm 0.6 (10)
Body temperature		
Min. T_b ($^{\circ}$ C)	39.1 \pm 0.8 (10)	38.9 \pm 1.0 (10)
Inflection T_{air} ($^{\circ}$ C)	34.8	34.55
T_b versus T_{air} slope (per $^{\circ}$ C)	0.47	0.44
Max T_b ($^{\circ}$ C)	46.6 \pm 0.4 (10)	46.4 \pm 1.2 (10)
Max T_{air} ($^{\circ}$ C)	48.2 \pm 0.6 (10)	50.6 \pm 1.7 (10)
T_b at onset of panting ($^{\circ}$ C)	42.0 \pm 1.6 (10)	42.0 \pm 1.4 (9)
T_{air} at onset of panting ($^{\circ}$ C)	39.9 \pm 1.8 (10)	39.2 \pm 2.4 (9)
95 th percentile $T_b > T_{air}$ ($^{\circ}$ C)		
Metabolic rate		
Min. RMR (W)	0.15 \pm 0.01 (10)	0.15 \pm 0.02 (10)
T_{uc} ($^{\circ}$ C)	36.55	33.577
RMR slope (mW $^{\circ}$ C ⁻¹)	12.52	8.24
Max. RMR (W)	0.29 \pm 0.03 (10)	0.28 \pm 0.05 (10)
Max. RMR/min. RMR	1.93	1.86
Evaporative water loss		
Min. EWL (g h ⁻¹)	0.06 \pm 0.01 (10)	0.07 \pm 0.02 (10)
Inflection T_{air} ($^{\circ}$ C)	37.56	37.93
EWL slope (g h ⁻¹ $^{\circ}$ C ⁻¹)	0.05	0.06
Max. EWL (g h ⁻¹)	0.61 \pm 0.09 (9)	0.82 \pm 0.15 (6)
Max. EWL/min. EWL	10.16	11.7
Min. EHL/MHP	0.23 \pm 0.03 (10)	0.30 \pm 0.05 (10)
EHL/MHP inflection $T_{air} - T_b$	-4.57	-3.492
EHL/MHP slope	0.16	0.21
Max. EHL/MHP	1.40 \pm 0.19 (9)	2.07 \pm 0.18 (6)

Table S3.3A. Mass-specific metabolic rate (RMR) and evaporative water loss (EWL) rate at high T_{air} in 13 bird species thermoregulatory performance as a function of chamber air temperature (T_{air}) coupled with humidity of $\sim 19\text{g H}_2\text{O m}^{-3}$ within a southern African lowland region (Hluhluwe). Means, SD and (n) are reported.

Variable	African Kingfisher	Pygmy Kingfisher	Brown-hooded Kingfisher	Collared Sunbird	Common Fiscal	Dark-capped Bulbul	Green-backed Camaroptera	Pink-throated Twinspot
Min. RMR (mW g^{-1})	16.81 \pm 1.7 (10)	7.65 \pm 0.5 (10)	20.38 \pm 2.7 (8)	12.36 \pm 2.0(10)	12.17 \pm 1.6 (10)	21.30 \pm 2.0 (10)	14.84 \pm 1.8 (10)	
RMR slope ($\text{mW g}^{-1} \text{ }^\circ\text{C}^{-1}$)	1.09	1.12	1.39	1.21	0.95	0.96	1.99	
Max. RMR (mW g^{-1})	27.64 \pm 1.9 (10)	20.34 \pm 3.4 (8)	36.68 \pm 4.7 (4)	21.96 \pm 3.3 (10)	22.10 \pm 6.3 (9)	33.91 \pm 3.4 (8)	27.08 \pm 3.0 (9)	
Min. EWL ($\text{mg h}^{-1} \text{ g}^{-1}$)	12.44 \pm 2.3 (10)	30.99 (1)	3.54 \pm 1.3 (10)	12.82 \pm 4.7 (8)	3.50 \pm 0.8 (10)	22.76 (1)	35.64 (1)	7.89 \pm 2.69 (10)
EWL slope ($\text{mg h}^{-1} \text{ g}^{-1} \text{ }^\circ\text{C}^{-1}$)	4.14	2.84	5.36	3.58	3.58	4.13	3.71	
Max. EWL ($\text{mg h}^{-1} \text{ g}^{-1}$)	50.04 \pm 12.2 (10)	31.44 \pm 9.5 (8)	61.74 \pm 8.4 (4)	37.53 \pm 12.1 (5)	51.98 \pm 7.8 (3)	54.98 \pm 12.4 (8)	42.82 \pm 5.5 (9)	
		53.22 (1)			65.91 (1)	63.12 (1)		
Variable	Red-capped Chat	Robin-	Rudd's Apalis	Sombre Greenbul	Spectacled Weaver	Yellow-rumped Tinkerbird	Yellow Weaver	
Min. RMR (mW g^{-1})	13.18 \pm 1.5 (10)	17.50 \pm 2.2 (10)	14.13 \pm 1.3 (10)	15.23 \pm 0.76 (5)	20.02 \pm 3.45 (10)	14.75 \pm 1.96 (10)		
RMR slope ($\text{mW g}^{-1} \text{ }^\circ\text{C}^{-1}$)	0.60	1.04	1.05	2.15	1.95	1.31		
Max. RMR (mW g^{-1})	20.74 \pm 1.3 (3)	30.06 \pm 7.8 (7)	25.59 \pm 1.7 (4)	29.68 \pm 0.82 (3)	37.27 \pm 1.10 (2)	25.49 \pm 2.18 (8)		
Min. EWL ($\text{mg h}^{-1} \text{ g}^{-1}$)	7.15 \pm 2.8 (10)	10.83 \pm 3.5 (10)	0.24 \pm 0.1 (10)	5.45 \pm 1.34 (5)	29.93 (1)	7.53 \pm 1.83 (10)	6.44 \pm 1.73 (10)	
EWL slope ($\text{mg h}^{-1} \text{ g}^{-1} \text{ }^\circ\text{C}^{-1}$)	3.12	4.219	3.25	3.54	2.07	3.63		
Max. EWL ($\text{mg h}^{-1} \text{ g}^{-1}$)	46.82 \pm 4.8 (3)	54.32 \pm 19.1 (5)	1.52 \pm 0.1 (4)	37.39 \pm 9.89 (3)	31.36 \pm 0.05 (2)	46.06 \pm 13.5 (8)		
				42.58 (1)				

Table S4.1. Summary of thermoregulatory performance as a function of chamber air temperature (T_{air}) at water vapour pressures of $\sim 19\text{g H}_2\text{O m}^{-3}$ in nine bird species from the montane study site (Harrismith). T_b = body temperature, T_{air} = ambient temperature, RMR = metabolic rate, EWL = evaporative water loss, EHL = evaporative heat loss, MHP = metabolic heat production. Means \pm SD and (n) are reported.

Variable	Cape White-eye	Dark-capped Bulbul	Drakensberg Prinia	Red-billed Quelea	Red-capped Lark	South African Cliff-swallow
Body mass (g)	11.9\pm0.5 (10)	42.4\pm3.6 (10)	9.3\pm0.8 (10)	17.1\pm0.8 (10)	26.7\pm1.5 (10)	19.1 \pm 1.2 (10)
Body temperature						
Min. T_b ($^{\circ}\text{C}$)	41.7 \pm 0.8 (10)	42.1 \pm 0.5 (10)	41.4 \pm 1.0 (10)	41.0 \pm 0.7 (10)	42.3 \pm 0.5 (9)	41.7 \pm 0.6 (7)
Inflection T_{air} ($^{\circ}\text{C}$)	NA	40.7	N/A	44.8	37.6	N/A
T_b versus T_{air} slope (per $^{\circ}\text{C}$)	0.44	0.51	0.38	0.88	0.37	0.39
Max T_b ($^{\circ}\text{C}$)	45.9 \pm 0.9 (10)	45.8 \pm 0.2 (10)	45.9 \pm 0.3 (10)	48.6 \pm 0.7 (10)	45.9 \pm 0.4 (10)	45.8 \pm 0.4 (10)
Max T_{air} ($^{\circ}\text{C}$)	43.3 \pm 1.6 (10)	45.7 \pm 1.4 (10)	45.6 \pm 1.0 (10)	48.1 \pm 1.1 (10)	46.0 \pm 0.6 (10)	44.3 \pm 0.8 (10)
T_b at onset of panting ($^{\circ}\text{C}$)	42.9 \pm 0.5 (10)	42.4 \pm 0.5 (10)	42.9 \pm 0.6 (10)	43.1 \pm 0.9 (10)	43.0 \pm 0.6 (10)	42.6 \pm 0.7 (10)
T_{air} at onset of panting ($^{\circ}\text{C}$)	37.3 \pm 0.9 (10)	37.0 \pm 1.0 (10)	37.8 \pm 0.8 (10)	38.9 \pm 1.3 (10)	38.1 \pm 2.3 (10)	37.4 \pm 1.2 (10)
Metabolic rate						
Min. RMR (W)	0.26 \pm 0.05 (10)	0.50 \pm 0.09 (10)	0.23 \pm 0.06 (10)	0.30 \pm 0.04 (10)	0.42 \pm 0.11 (10)	0.32 \pm 0.07 (7)
T_{uc} ($^{\circ}\text{C}$)	~ 34	32.21	36.14	41.90	38.28	41.58
MR slope ($\text{mW }^{\circ}\text{C}^{-1}$)	18.24	47.81	9.93	19.92	36.28	45.88
Max. RMR (W)	0.44 \pm 0.09 (4)	0.84 \pm 0.10 (6)	0.32 \pm 0.07 (7)	0.54 \pm 0.10 (6)	0.74 \pm 0.26 (5)	0.47 \pm 0.1 (9)
Max. RMR/min. RMR	1.69	1.68	1.39	1.7	1.76	1.46
Evaporative water loss						
Min. EWL (g h^{-1})	0.11 \pm 0.05 (10)	0.37 \pm 0.11 (10)	0.10 \pm 0.05 (10)	0.1 \pm 0.03 (10)	0.24 \pm 0.12 (10)	0.15 \pm 0.04 (10)
Inflection T_{air} ($^{\circ}\text{C}$)	NA	N/A	35.27	~ 35.6	37.70	38.47
EWL slope ($\text{g h}^{-1} ^{\circ}\text{C}^{-1}$)	0.06	0.11	0.05	0.07	0.11	0.07
Max. EWL (g h^{-1})	0.67 \pm 0.13 (4)	1.75 \pm 0.21 (6)	0.68 \pm 0.15 (7)	0.9 \pm 0.20 (10)	1.46 \pm 0.52 (5)	0.87 \pm 0.23 (9)
Max. EWL/min. EWL	6.09	4.72	6.81	9.0	6.13	5.80
Min. EHL/MHP	0.27 \pm 0.08 (10)	0.51 \pm 0.16 (10)	0.27 \pm 0.10 (10)	0.2 \pm 0.10 (10)	0.37 \pm 0.16 (9)	0.33 \pm 0.15 (7)
EHL/MHP inflection $T_{air} - T_b$	-7.1	N/A	N/A	-6.2	N/A	N/A
EHL/MHP slope	0.17	0.10	0.16	0.19	0.12	0.15
Max. EHL/MHP	1.04 \pm 0.25 (4)	1.40 \pm 0.11 (6)	1.44 \pm 0.31 (7)	1.3 \pm 0.2 (10)	1.32 \pm 0.13 (5)	1.25 \pm 0.19 (9)

Table S4.1. Cont.

Variable	Southern Fiscal	Southern Masked Weaver	Spike-heeled Lark
Body mass (g)	42.8±1.9 (10)	28.9±3.4 (10)	30.35±3.59 (10)
Body temperature			
Min. T_b (°C)	42.1±1.0 (8)	41.4±0.9 (10)	42.5±0.4 (8)
Inflection T_{air} (°C)	N/A	N/A	N/A
T_b versus T_{air} slope (per °C)	0.33	0.39	0.29
Max T_b (°C)	46.0±0.6 (10)	45.9±0.2 (10)	45.8±0.4 (10)
Max T_{air} (°C)	45.3±1.4 (10)	45.2±0.9 (10)	45.5±0.9 (10)
T_b at onset of panting (°C)	43.1±0.6 (10)	42.5±0.8 (10)	43.4±0.6 (10)
T_{air} at onset of panting (°C)	37.8±0.5 (10)	37.5±0.7 (10)	37.2±1.4 (10)
Metabolic rate			
Min. RMR (W)	0.46±0.06 (8)	0.42±0.10 (10)	0.36±0.06 (8)
T_{uc} (°C)	N/A	39.78	41.53
RMR slope (mW °C ⁻¹)	21.14	50.41	36.35
Max. RMR (W)	0.72±0.15 (5)	0.72±0.17 (10)	0.55±0.05 (6)
Max. RMR/min. RMR	1.57	1.71	1.52
Evaporative water loss			
Min. EWL (g h ⁻¹)	0.24±0.15 (10)	0.17±0.07 (10)	0.16±0.07 (8)
Inflection T_{air} (°C)	N/A	N/A	36.68
EWL slope (g h ⁻¹ °C ⁻¹)	0.11	0.12	0.09
Max. EWL (g h ⁻¹)	1.44±0.16 (5) 1.54±0.36 (2)	1.39±0.05 (3)	1.10±0.27 ()
Max. EWL/min. EWL	6.0	8.17	6.25
Min. EHL/MHP	0.32±0.19 (10)	0.27±0.08 (10)	0.29±0.12 (8)
EHL/MHP inflection $T_{air} - T_b$	N/A	N/A	N/A
EHL/MHP slope	0.15	0.16	0.13
Max. EHL/MHP	1.36±0.26 (5) 1.50±0.06 (2)	1.35±0.30 (3)	1.36±0.21 (9)

Table S4.2. Mass-specific metabolic rate (RMR) and evaporative water loss (EWL) rate at high T_{air} in nine bird species as a function of chamber air temperature (T_{air}) coupled with humidity of $\sim 19\text{g H}_2\text{O m}^{-3}$ within a southern African montane region (Harrismith). Means, SD and (n) are reported.

Variable	Cape White-eye	Dark-capped Bulbul	Drakensberg Prinia	Red-billed Quelea	Red-capped Lark	South African Cliff Swallow
Min. RMR (mW g^{-1})	21.99±4.55 (10)	12.41±2.68 (10)	24.59±5.34 (10)	16.4±2.7 (10)	15.14±4.67 (10)	15.85±2.94 (10)
RMR slope ($\text{mW g}^{-1} \text{ }^\circ\text{C}^{-1}$)	1.55	1.21	1.09	1.4	1.25	2.44
Max. RMR (mW g^{-1})	37.58±8.99 (4)	20.68±2.18 (6)	35.14±7.86 (7)	27.2±4.4 (6)	26.00±11.6 (5)	24.47±5.69 (9)
Min. EWL ($\text{mg h}^{-1} \text{ g}^{-1}$)	9.11±3.96 (10)	9.05±2.69 (10)	10.40±5.01 (10)	5.7±2.0 (6)	9.08±4.66 (9)	7.83±1.73 (10)
EWL slope ($\text{mg h}^{-1} \text{ g}^{-1} \text{ }^\circ\text{C}^{-1}$)	5.22	2.93	5.97	4.11	4.26	5.02
Max. EWL ($\text{mg h}^{-1} \text{ g}^{-1}$)	57.21±13.09 (4)	43.16±5.32 (6)	74.04±16.57 (7)	52.4±8.1 (10)	51.20±22.2 (5)	45.91±14.85 (9)

Variable	Southern Fiscal	Southern Masked Weaver	Spike-heeled Lark
Min. RMR (mW g^{-1})	10.92±1.52 (8)	15.39±4.37 (10)	12.18±1.70 (8)
	8.71 (1)		
RMR slope ($\text{mW g}^{-1} \text{ }^\circ\text{C}^{-1}$)	0.49	1.92	1.41
Max. RMR (mW g^{-1})	16.82±3.62 (5)	26.99±8.43 (10)	19.24±2.57 (6)
			21.61 (1)
Min. EWL ($\text{mg h}^{-1} \text{ g}^{-1}$)	5.56±3.33 (10)	6.24±2.84 (10)	5.23±1.81 (8)
EWL slope ($\text{mg h}^{-1} \text{ g}^{-1} \text{ }^\circ\text{C}^{-1}$)	2.74	4.74	2.84
Max. EWL ($\text{mg h}^{-1} \text{ g}^{-1}$)	36.02±8.88 (2)	49.76±7.90 (3)	37.80±4.93 (6)
			43.49 (1)

Table S5. Phylogenetically informed stepwise multiple comparisons (PhylANOVA post hoc analysis test) and conventional analysis of variance (ANOVA) stepwise multiple comparisons (Tukey HSD post-hoc test) comparing whether body mass, maximum body temperature (T_{bmax}) and the thermoregulatory predictors included in my multivariate additive linear model differed significantly between study localities. Bold values indicate significant differences between climatic localities ($p < 0.05$). Variables described in the table include HTL - the maximum T_{air} tolerated before the onset of severe hyperthermia, EvapScope - maximum EWL (evaporative water loss)/minimum thermoneutral EWL, T_{bslope} - the slope of T_b as a function of T_{air} above thermoneutrality, T_{bnorm} - normothermic T_b , MaxEHL/MHP - maximum evaporative heat loss(EHL)/ metabolic heat production(MHP), MetabCost - maximum resting metabolic rate (RMR)/thermoneutral resting metabolic rate, Pant – T_{air} or T_b at which panting began.

	PhylANOVA post hoc		Tukey post hoc	
	t-value	p-value	HSD	p-value
HTL (humid-dry)				
Montane - Arid	1.21	0.22	0.69	0.46
Lowland - Arid	3.71	<0.01	1.90	<0.01
Lowland - Montane	2.37	0.02	1.22	0.06
HTL (humid)				
Montane - Arid	1.62	0.10	1.08	0.25
Lowland - Arid	4.52	<0.01	2.74	<0.001
Lowland - Montane	2.73	0.01	1.66	0.03
T_{bmax} (humid-dry)				
Montane - Arid	3.73	<0.01	0.72	<0.01
Lowland - Arid	3.12	0.01	0.54	0.01
Lowland - Montane	-0.99	0.31	-0.17	0.58
T_{bmax} (humid)				
Montane - Arid	3.40	<0.01	0.95	<0.01
Lowland - Arid	4.02	<0.01	1.02	<0.01
Lowland - Montane	0.27	0.78	0.07	0.96
T_{bnorm} (humid)				
Montane - Arid	1.53	0.11	0.32	0.29
Lowland - Arid	-6.11	<0.01	-1.16	<0.001
Lowland - Montane	-7.81	<0.01	-1.48	<0.001
T_{bSlope} (humid/dry)				
Montane - Arid	-0.08	1.0	-0.01	0.99
Lowland - Arid	-0.59	1.0	-0.08	0.82
Lowland - Montane	-0.51	1.0	-0.07	0.87

MaxEWL (humid/dry)				
Montane - Arid	-1.58	0.27	-0.12	0.27
Lowland - Arid	-1.62	0.37	-0.11	0.25
Lowland - Montane	0.11	0.90	0.01	0.99
MaxRMR (humid/dry)				
Montane - Arid	-0.58	1.0	-0.05	0.83
Lowland - Arid	0.14	1.0	0.01	0.99
Lowland - Montane	0.78	1.0	0.06	0.72
MaxEHL/MHP (humid)				
Montane - Arid	1.16	0.62	0.14	0.49
Lowland - Arid	0.19	0.89	0.02	0.98
Lowland - Montane	-1.09	0.62	-0.12	0.52
MaxEHL/MHP (humid/dry)				
Montane - Arid	-0.13	1.0	-0.01	0.99
Lowland - Arid	-0.31	1.0	-0.02	0.94
Lowland - Montane	-0.16	1.0	-0.012	0.99
EvapScope (humid/dry)				
Montane - Arid	0.28	0.86	0.03	0.96
Lowland - Arid	-0.94	0.86	-0.11	0.62
Lowland - Montane	-1.26	0.67	-0.14	0.43
MetabCost (humid/dry)				
Montane - Arid	-0.92	0.94	0.11	0.63
Lowland - Arid	-0.03	0.98	-0.002	0.99
Lowland - Montane	-1.04	0.94	-0.11	0.56
EWLSlope (humid/dry)				
Montane - Arid	-3.49	<0.01	-0.37	<0.01
Lowland - Arid	-4.25	<0.01	-0.41	<0.001
Lowland - Montane	-0.39	0.70	0.04	0.92
RMRSlope (humid/dry)				
Montane - Arid	-0.08	1.0	-0.02	0.99
Lowland - Arid	-0.85	1.0	-0.23	0.67
Lowland - Montane	-0.76	1.0	-0.21	0.72
PantT_{air}				
Montane - Arid	-3.54	<0.01	-1.79	<0.01
Lowland - Arid	-3.32	0.02	-1.52	<0.01
Lowland - Montane	0.58	0.63	0.27	0.83
PantT_b				
Montane - Arid	0.79	0.43	0.19	0.71
Lowland - Arid	-2.38	0.12	-0.52	0.06
Lowland - Montane	-3.24	<0.01	-0.71	<0.01

Table S6. Model selection for the multivariate additive linear model of humid heat tolerance limit as a function of study locality (Clim), maximum body temperature tolerated by a species (T_{bmax}), maximum evaporative cooling efficiency - evaporative heat loss/metabolic heat production (MaxEHL/MHP), a ratio of maximum evaporative water loss (EWL) to minimum thermoneutral EWL (EvapScope), ratio of maximum resting metabolic rate (RMR) to minimum RMR (MetabCost), the slope of the relationship between T_b and T_{air} above inflection points (T_{bslope}), and interaction terms between study locality and MaxEHL/MHP. A “+” indicates and inclusion of a predictor variable or interaction from a model formula. Best-performing models are highlighted in bold. If two models were within < 2 AIC_c the most parsimonious model was chosen.

Model	Int.	Clim	MaxEHL/MHP	EvapScope	EWLslope	MetabCost	RMRSlope	T_{bmax}	T_{bslope}	Clim: EHL/MHP	df	logLIK	AICc	delta	weight
328	-0.62	+	6.61	0.24				0.80		+	8	-33.83	89.81	0.00	0.50
76	-10.16	+	3.19		11.23			1.10			6	-38.38	92.12	2.20	0.27
72	-0.20	+	3.47	0.21				0.87			6	-38.41	92.18	2.27	0.16
456	6.66	+	7.13	0.25				0.61	1.59	+	9	-33.20	92.57	2.66	0.12
360	-5.13	+	6.84	0.19			0.01	0.89		+	9	-33.28	92.74	2.82	0.05
100	-13.92	+	4.02				0.03	1.17			6	-38.71	92.78	2.87	0.05
392	32.43	+	7.66	0.29					3.38	+	8	-35.34	92.95	3.04	0.04
336	-3.16	+	6.35	0.19	3.91			0.86		+	9	-33.48	93.15	3.23	0.04
332	-11.75	+	5.82		11.06			1.06		+	8	-35.63	93.53	3.62	0.03
344	-1.80	+	6.60	0.22		0.24		0.81		+	9	-33.77	93.73	3.81	0.03
356	-16.10	+	7.10				0.03	1.13		+	8	-35.77	93.81	3.89	0.03
104	-6.06	+	3.70	0.13			0.02	0.99			7	-37.57	93.81	3.90	0.03
80	-4.52	+	3.24	0.12	6.69			0.97			7	-37.62	93.90	3.98	0.03
84	-12.01	+	4.05			1.52		1.08			6	-39.59	94.54	4.62	0.02
108	-12.05	+	3.50		7.22		0.01	1.13			7	-38.04	94.75	4.84	0.02
88	-3.26	+	3.64	0.16		0.60		0.92			7	-38.14	94.95	5.03	0.02
200	2.43	+	3.54	0.21				0.81	0.56		7	-38.35	95.37	5.45	0.01
92	-10.45	+	3.27		10.25	0.20		1.10			7	-38.36	95.39	5.47	0.01

Table S7. Durbin-Watson test outputs assessing autocorrelation between model variables included in the ‘phylogenetic generalised least square’ multivariate additive linear model with heat tolerance limit (HTL) as the response variable. The Durbin-Watson test detects autocorrelation based on the independence of residuals of linear regressions output. Values of DW approaching and around two and $p > 0.05$ indicate no significant autocorrelation between variables or within models. Conversely, values of DW approaching zero and $p < 0.05$ indicate significant autocorrelation between variables or within models. Predictor variables described in the table include HTL - the maximum T_{air} tolerated before the onset of severe hyperthermia, EvapScope - maximum EWL (evaporative water loss)/minimum thermoneutral EWL, MetabCost - maximum resting metabolic rate (RMR)/minimum RMR, T_b slope - the slope of T_b as a function of T_{air} above thermoneutrality, MaxEHL/MHP - maximum evaporative heat loss (EHL)/ metabolic heat production (MHP), Climate – dry arid, humid lowland, mesic montane.

Input	DW Value	p-value
EvapScope ~ Mass	1.92	0.41
MetabCost ~ Mass	1.41	0.04
T_b max ~ Mass	1.43	0.05
MaxEHL_MHP ~ Mass	1.85	0.33
T_b slope ~ Mass	1.87	0.36
EWLslope ~ Mass	1.21	<0.001
RMRslope ~ Mass	1.89	0.38
EvapScope ~ MaxEHL_MHP	1.91	0.41
EvapScope ~ T_b slope	2.1	0.61
EvapScope ~ MetabCost	2.04	0.54
T_b max ~ EvapScope	1.5	0.07
T_b max ~ MetabCost	1.49	0.07
T_b slope ~ MetabCost	2.06	0.56
HTLhumid~Climate+Mass+EHL_MHPmax+EvapScope+ T_b max+Climate: EHL_MHPmax	1.94	0.30

**CHAPTER 3 EXTREME
HYPERthermia
TOLERANCE IN THE
WORLD'S MOST
ABUNDANT WILD BIRD**

This chapter appears in Scientific Reports volume 10 • 2020 and is formatted in line with the journal's requirements doi.org/10.1038/s41598-020-69997-7

3.1 ABSTRACT

The thermal tolerances of vertebrates are generally restricted to body temperatures below 45–47 °C, and avian and mammalian critical thermal maxima seldom exceed 46 °C. We investigated thermoregulation at high air temperatures in the red-billed quelea (*Quelea quelea*), an African passerine bird that occurs in flocks sometimes numbering millions of individuals. Our data reveal this species can increase its body temperature to extremely high levels: queleas exposed to air temperature > 45 °C increased body temperature to 48.0 ± 0.7 °C without any apparent ill-effect, with individual values as high as 49.1 °C. These values exceed known avian lethal limits, with tolerance of body temperature > 48 °C unprecedented among birds and mammals.

3.2 INTRODUCTION

Survival and reproduction in hot environments are constrained by the upper limits to organisms' thermal tolerances. Under high environmental heat loads, the avoidance of lethal body temperature (T_b) drives fundamental behavioural trade-offs between thermoregulation and activities such as foraging (1,2), and constraints on the evolution of upper thermal limits have important consequences for predicting responses to climate change (3). Upper thermal limits also constrain performance under conditions of high metabolic heat production (4) in contexts that include livestock production and food security under hotter future conditions (5,6).

Body temperatures (T_b) of vertebrates are thought to be limited to below 45–47 °C by the thermal sensitivity of cellular macromolecules (7–10) and oxygen supply limitation (11,12). Among terrestrial vertebrates, critical thermal maxima for squamate reptiles, rodents and birds are usually below 46 °C (13–16). The same is generally true of maximum T_b values observed in birds, rodents and small bats in studies involving acute heat exposure but where critical thermal maxima were not quantified (17–20). Typical lethal avian T_b values are 46.2–47.7 °C in two species of towhees (21) and 46–47.8 °C in barred-rock chickens (16), although the latter author reported lethal values as high as 48.8 °C associated with tracheal administration of 100% oxygen

However, T_b above the typical vertebrate range has occasionally been documented. Critical thermal maxima above 47 °C have been reported in a small number of desert lizards [reviewed by Clusella-Trullas et al. (13)], with a value of 51.0 °C observed in ten adult *Aspidoscelis sexlineata* (22). Among birds, three variable seed-eaters (*Sporophila aurita*), a passerine from the humid lowlands of Panama, survived $T_b = 46.8\text{--}47.0$ °C without any apparent ill-effects (23). In a pioneering study of the use of surgically-implanted transmitters to measure avian T_b , Southwick (24) recorded $T_b = 47.7$ °C in a single white-crowned sparrow (*Zonotrichia leucophrys gambelli*). However, cloacal T_b measured simultaneously was 44.1 °C, and the 3.6 °C difference between this pair of measurements was the largest reported in the study (24).

As part of a study of adaptive variation in avian heat tolerance, we investigated thermoregulation during acute heat exposure in the red-billed quelea (*Quelea quelea*). This small (18-g) African passerine is widely considered the most abundant non-domesticated bird on Earth, with post-breeding population estimates of ~ 1.5 billion individuals (25). It is highly gregarious and forms huge flocks that may consist of several million individuals (26). The peculiar natural history of this species led us to hypothesize that its thermal physiology differs from that of typical small songbirds. Red-billed queleas drink regularly (26). However, the timing of flocks' visits to water sources is presumably determined by the average hydration status of large numbers of flock members rather than that of single individuals. Under conditions where hydration status potentially varies substantially across individuals within a vast flock, selection should favour the capacity for water conservation via facultative hyperthermia. Accordingly, we predicted pronounced facultative hyperthermia buffers individual queleas from dehydration risk. To test this prediction, we quantified relationships between body temperature, evaporative heat loss and metabolic heat production in red-billed queleas in South Africa.

3.3 METHODS

All experimental procedures were approved by the University of Pretoria's Animal Ethics Committee (NAS181/2019) and the Research Ethics and Scientific Committee of the South African National Biodiversity Institute (SANBI NZG/RES/P19/13) and birds were captured

under permit JM 8,057/2019 from the Free State province's Department of Economic, Small Business Development, Tourism and Environmental Affairs. The methods we used for quantifying the upper limits of evaporative cooling capacity and heat tolerance followed those of a recent series of studies of avian heat tolerance (27–30).

Study site and species

We trapped 20 red-billed queleas (body mass = $17.94 \pm \text{SD } 1.19$ g) using mist nets in agricultural fields near the town of Harrismith in South Africa ($28^{\circ} 06' \text{ S}$, $29^{\circ} 10' \text{ E}$, 1754 m asl) during November 2019 (early austral summer). After capture, birds were transported by road (approximately 20-min trip) in cloth bags to a field laboratory, where they were held in cages ($600 \times 400 \times 400$ mm) for 1–16 h with ad libitum access to water and wild bird seed. Food was removed at least one hour prior to gas exchange and body temperature measurements, allowing individuals to habituate and ensure they were post-absorptive (31).

Air and body temperature measurements

Body temperature was measured using a temperature-sensitive passive integrated transponder (PIT) tag (Biotherm 13, Biomark, Boise, ID, USA) injected intraperitoneally in each bird. Prior to injection, all PIT tags were calibrated in a circulating water bath (model F34, Julabo, Seelbach BW, DE) over temperatures ranging 35 to 50 °C against a thermocouple meter (TC-1000, Sable Systems, Las Vegas, NV, USA), the output of which was verified against a mercury-in-glass thermometer with NIST-traceable accuracy before and after the PIT tag calibration. Temperatures measured by PIT tags deviated by 0.28 ± 0.23 °C ($n = 23$) from actual values and we corrected all measured values accordingly. Data from the PIT tags were recorded using a reader and transceiver system (HPR +, Biomark, Boise ID, USA). To measure air temperature during the gas exchange measurements, we inserted a thermistor probe (TC-100, Sable Systems, Las Vegas, NV, USA) through a hole sealed with a rubber grommet in the side of each metabolic chamber.

Gas exchange measurements

An open flow-through respirometry system was used to measure evaporative water loss (EWL) and carbon dioxide production (V_{CO_2}) during measurements. Queleas were placed individually in 3-L (approximate dimensions 20 cm high \times 15 cm wide \times 10 cm deep) plastic chambers, previously shown to not absorb water vapour (27), equipped with a mesh platform \sim 10 cm above a 1-cm layer of mineral oil into which excreta fell to prevent evaporation. The chambers were placed in a \sim 100 L ice chest modified such that temperature inside the chest was regulated using a Peltier device (AC-162 Thermoelectric Air Cooler, TE Technology, Traverse City MI, USA) controlled via a digital controller (TC-36–25-RS485 Temperature Controller, TE Technology, Traverse City MI, USA).

Atmospheric air supplied by an oil-free compressor was scrubbed of water vapour using a membrane dryer (Champion CMD3 air dryer and filter, Champion Pneumatic, Quincy IL, USA). The dried air was split into an experimental and baseline channel. A mass flow controller (Alicat Scientific Inc., Tuscon AZ, USA), calibrated using a soap-bubble flow meter (Gilibrator 2, Sensidyne, St Petersburg, FL, USA), regulated experimental flow rates to the animal chamber. The flow rate of the baseline channel was controlled using a needle valve (Swagelok, Solon, OH, USA). Within each chamber, the air inlet was positioned close to the lid with an elbow joint facing upwards (to minimize any potential convective cooling at higher flow rates) and the air outlet below the mesh platform to maximize air mixing. We used flow rates of 10.1–18.3 L min⁻¹, depending on air temperature and individual behaviour, with flow rate regularly adjusted during measurements to maintain chamber humidity below a dewpoint of -7.7 °C.

A respirometry multiplexer (model MUX3-1,101-18 M, Sable Systems, Las Vegas, NV) in manual mode and an SS-3 Subsamplere (Sable Systems) sequentially subsampled excurrent air from the chamber and baseline air. Subsampled air was pulled through a CO₂/H₂O analyzer (model LI-840A, LI-COR, Lincoln, NE, USA), which was regularly zeroed using nitrogen and spanned for CO₂ using a certified calibration gas with a known CO₂ concentration of 1900 ppm (AFROX, Johannesburg, South Africa). The H₂O sensor of the Li-840A was regularly zeroed using nitrogen and spanned using a dewpoint generator (DG-4, Sable Systems, Las Vegas NV). Voltage outputs from the analyzers and thermistor

probes were digitized using an analog–digital converter (model UI-3, Sable Systems) and recorded with a sampling interval of 5 s using Expedata software (Sable Systems). All tubing in the system was Bev-A-Line IV tubing (Thermoplastic Processes Inc., Warren, NJ, USA).

Experimental protocol

Measurements occurred during the day, and we quantified relationships between body temperature, metabolic heat production and evaporative heat dissipation over air temperatures of 28–52 °C by exposing birds to the same stepped air temperature profile involving 4-°C increments below 40 °C and 2-°C increments above 40 °C as used in previous studies (27–30). Measurements commenced with a baseline air subsample until water and CO₂ readings were stable (5 min). Birds spent a minimum of 10 min at each air temperature, with stable average values over the last 5 min at each air temperature value included in subsequent analyses, followed by another 5 min baseline. This approach to quantifying physiological responses to heat exposure is functionally analogous to the sliding cold exposure protocol used to elicit maximum metabolic rates during cold exposure (32).

During measurements, individuals were continuously monitored using a video camera with an infrared light source. Only data from birds that remained calm during measurements (i.e., no sign of agitation or sustained escape behaviour) were included in analyses. Trials were terminated and individuals immediately removed from the chamber when a bird reached its thermal endpoint characterized by sustained escape behaviour (i.e., agitated jumping) or a loss of coordination or balance, often associated with a sudden decrease in EWL or resting metabolic rate. Individual critical thermal maximum was taken as the body temperature associated with the onset of loss of balance and or uncoordinated movement. Immediately after each bird was removed from the chamber, its belly feathers were dabbed with 80% ethanol to accelerate heat loss and it was placed in a recovery cage with ad libitum water and food. Each bird was later released at the site of capture. This experimental protocol has been used previously for multiple species and, in one study with opportunistic monitoring for several weeks post-release, no adverse effects were observed (33).

Data analysis

We corrected for analyzer drift and lag using the relevant algorithms in Expedata software (Sable Systems, Las Vegas NV, USA). Eqs. 9.5 and 9.6 from Lighton (34) were used to calculate V_{CO_2} and EWL from the lowest stable 5-min periods of CO_2 and water vapour at a given air temperature, assuming $0.803 \text{ mg H}_2\text{O mL}^{-1}$ vapour. As individuals were likely post-absorptive, we estimated resting metabolic rate from V_{CO_2} assuming respiratory exchange ratio (RER) = 0.71 and converted rates of V_{CO_2} to metabolic rate (W) using $27.8 \text{ J mL}^{-1} \text{ CO}_2$ (35). Rates of EWL were converted to rates of evaporative heat loss (EHL, W) assuming a latent heat of vaporization of water of 2.406 J mg^{-1} at $40 \text{ }^\circ\text{C}$ (36). Body temperatures, rates of EWL and resting metabolic rates at thermoneutral air temperatures (Supplementary Fig. S1) were considered normothermic values.

All analyses were conducted in R 3.5.2 (37). Relationships between physiological response variables and air temperature as a predictor were analyzed using linear mixed-effects models (“lme” command) in the R package nlme 3.1–140 (38) after using segmented 1.1–0 (39) to identify inflection points. We accounted for pseudoreplication (multiple measurements per individual) by including individual identity as a predictor (random factor) in all analyses. We assessed significance at $p < 0.05$ and values are presented as mean \pm s.d.

3.4 RESULTS

The normothermic body temperature of queleas was $40.9 \pm 0.9 \text{ }^\circ\text{C}$ ($n = 20$), a value typical for small passerines (Fig. 1). Above an inflection air temperature of $38.0 \pm \text{SE } 0.6 \text{ }^\circ\text{C}$, body temperature increased by $0.5 \text{ }^\circ\text{C}$ per $1 \text{ }^\circ\text{C}$ increase in air temperature. Body temperature reached an estimated critical thermal maximum (i.e., maximum values associated with a loss of coordination and motor function) of $48.0 \pm 0.7 \text{ }^\circ\text{C}$ ($n = 20$) at an air temperature of $50.9 \pm 1.5 \text{ }^\circ\text{C}$. Individual maximum values were $46.4\text{--}49.1 \text{ }^\circ\text{C}$, with 75% of individuals reaching body temperature $\geq 48.0 \text{ }^\circ\text{C}$ (Fig. 1). Concurrent measurements of metabolic heat production (MHP) and evaporative heat loss (EHL) (Supplementary Fig. S1) revealed that EHL/MHP reached a maximum value of 1.49 at air temperature $> 46.9 \pm \text{SE } 0.5 \text{ }^\circ\text{C}$ (Fig. 1), confirming the queleas’ maximum evaporative cooling capacity had been attained.

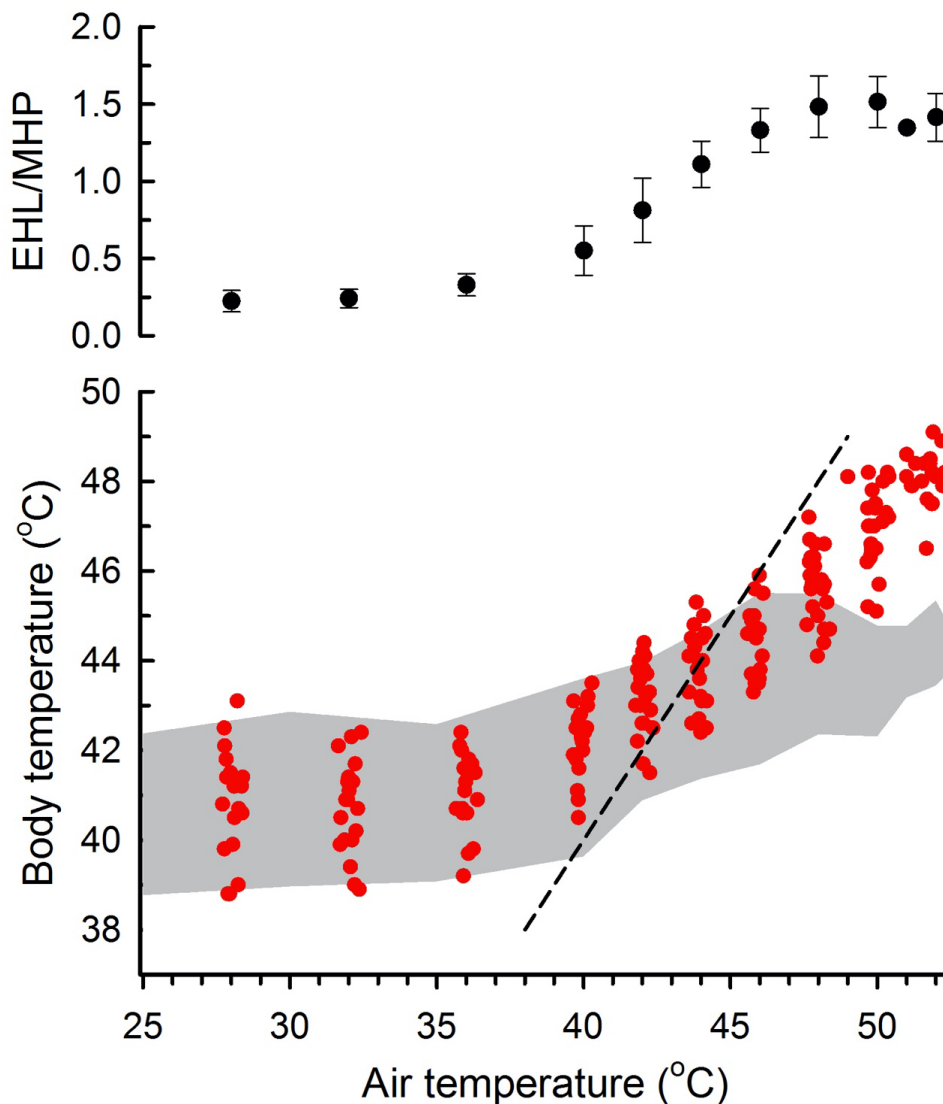


Figure 1. During acute heat exposure, the body temperature of red-billed queleas (*Quelea quelea*, red circles, lower panel) remained largely within the range reported in other passerine birds at air temperatures below 45°C but increased well above previously-documented values at higher air temperatures. The grey band is the range of individual values in five Australian species (40) and three southern African species (27) in studies using the same experimental protocol. The dashed line indicates equality between air and body temperatures. The ratio of evaporative heat loss (EHL) to metabolic heat production (MHP) increased to an average maximum value of 1.49 at air temperatures above 46.9 °C (upper panel).

3.5 DISCUSSION

Patterns of T_b during acute heat exposure supported our prediction that red-billed queleas have a pronounced capacity to tolerate hyperthermia. The species' critical thermal maximum is substantially higher than the known avian range (Fig. 2), exceeding by 2–3 °C the values associated with breakdown of respiratory function in poultry (15,16) and the body temperatures associated with loss of motor function in wild birds (27–30,40,41). Moreover, the body temperature range tolerated by the queleas exceeds known avian lethal values for passerines (21) and domestic fowls (15,16). Tolerance of body temperature > 48 °C is unprecedented among birds and mammals, with higher values having been reported only in ectothermic vertebrates (13) and invertebrates (42).

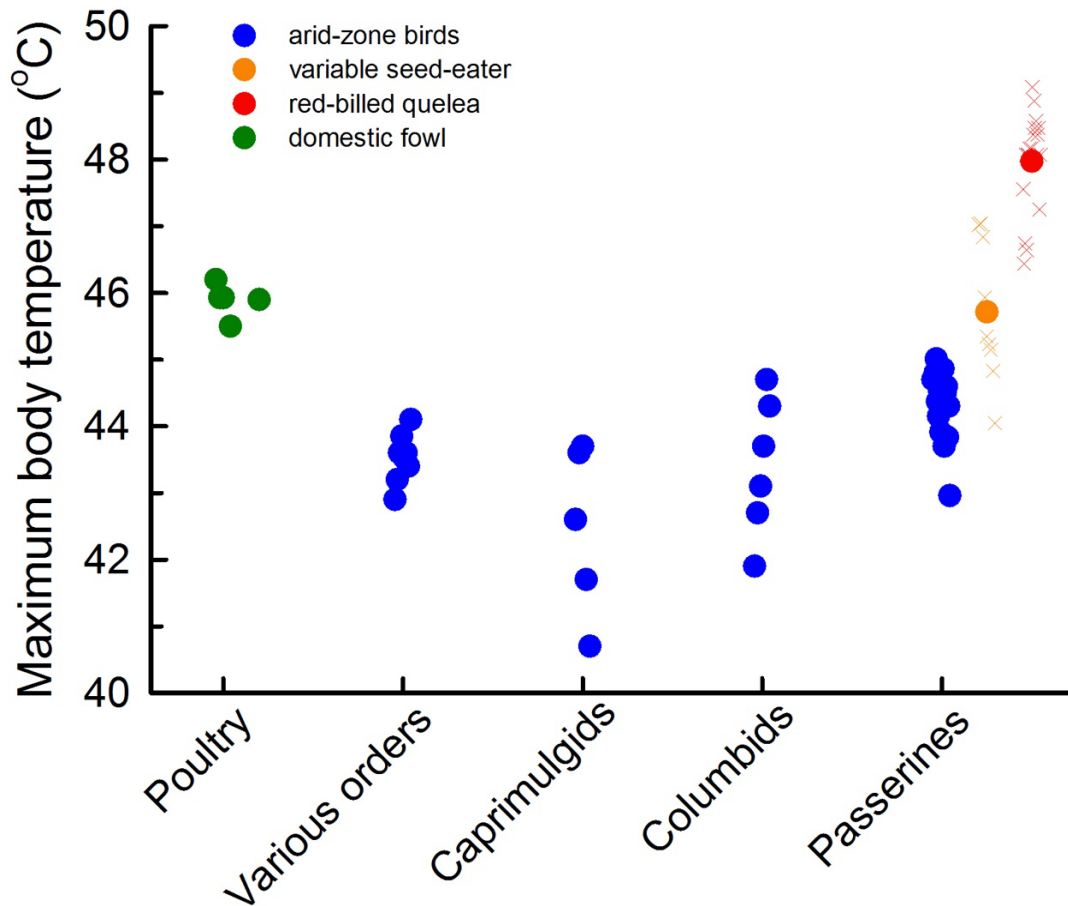


Figure 2. Maximum body temperatures attained during acute heat exposure in red-billed queleas (*Quelea quelea*) exceeded by a substantial margin those previously reported for birds. Species averages (in the case of domestic fowls, averages for breeds) are indicated using filled circles. Data for poultry are from (15,16), and data for non-domesticated species from (27-30,40,41,50-54). For variable seed-eaters (*Sporophila aurita*, data from (23) and red-billed queleas (present study), both species averages (filled circles) and individual values (crosses) are shown.

The methods we used here to establish the upper limits of queleas' heat tolerance and evaporative cooling capacity are identical to those of recent studies involving ~ 55 bird species, including three arid-zone representatives of the Ploceidae (27), the family to which *Q. quelea* belongs. Extreme hyperthermia tolerance comparable to that of the queleas appears to be absent among small passerines inhabiting arid regions where air temperature

maxima may approach or exceed 50 °C (27,29,40). That desert birds apparently lack the ability to tolerate comparably high body temperatures, despite strong selection for water conservation (43), suggests there are substantial costs to such extreme hyperthermia tolerance. These costs could potentially be related the synthesis of heat shock proteins (HSPs) and interactions with stress responses via the modification of glucocorticoid receptor function (9,44).

The capacity of queleas to dissipate evaporatively a maximum of ~ 150% of metabolic heat production is relatively modest for a passerine; among 30 species, maximum EHL/MHP was 1.75 ± 0.31 (27,29,30,40,45). Among arid-zone passerines, regular-drinking species are capable of greater fractional increases in EWL and have higher heat tolerance limits compared to non-drinking species (45). Our finding here of modest evaporative cooling capacity accompanied by extreme hyperthermia tolerance in a regularly-drinking species raises the possibility that coevolution of thermal physiology and water-dependence follows a different trajectory in species that form large flocks. Our hypothesis that avian social systems involving large flocks are associated with selection for pronounced hyperthermia tolerance could be tested further in gregarious species inhabiting hot, arid climates, particularly Australian species such as budgerigars (*Melopsittacus undulatus*) or cockatiels (*Nymphicus hollandicus*).

Our findings reveal it is possible for birds to evolve short-term tolerance of very high body temperature. Moreover, they identify red-billed queleas as a model for future studies of the physiological and molecular bases of extreme hyperthermia tolerance. We speculate that this species' ability to tolerate T_b as high as 48–49 °C arises from an array of anatomical and molecular mechanisms, including a well-developed rete opthalmicum to maintain brain temperature well below core T_b (46–48) and pronounced heat shock protein expression (44,49). Understanding the processes underlying the queleas' ability to tolerate T_b values lethal to other endotherms may, we suspect, prove useful for biotechnology aimed at developing greater heat tolerance in birds and other organisms.

3.6 REFERENCES

- 1 Sears, M. W., Raskin, E. & Angilletta Jr, M. J. The world is not flat: defining relevant thermal landscapes in the context of climate change. *Integrative and Comparative Biology* **51**, 666-675 (2011).
- 2 du Plessis, K. L., Martin, R. O., Hockey, P. A. R., Cunningham, S. J. & Ridley, A. R. The costs of keeping cool in a warming world: implications of high temperatures for foraging, thermoregulation and body condition of an arid-zone bird. *Global Change Biology* **18**, 3063-3070 (2012).
- 3 Araújo, M. B. *et al.* Heat freezes niche evolution. *Ecology Letters* **16**, 1206-1219 (2013).
- 4 Speakman, J. R. & Król, E. Maximal heat dissipation capacity and hyperthermia risk: neglected key factors in the ecology of endotherms. *Journal of Animal Ecology* **79**, 726-746 (2010).
- 5 Dagher, N. J. *Poultry production in hot climates. 2nd Edition.*, (CAB International, 2008).
- 6 Nyoni, N. M. B., Grab, S. & Archer, E. R. M. Heat stress and chickens: climate risk effects on rural poultry farming in low-income countries. *Climate and Development* **11**, 83-90, doi:10.1080/17565529.2018.1442792 (2018).
- 7 Laszlo, A. The effects of hyperthermia on mammalian cell structure and function. *Cell Prolif.* **25**, 59-87 (1992).
- 8 Roti Roti, J. L. Cellular responses to hyperthermia (40–46 C): Cell killing and molecular events. *Int. J. Hyperthermia* **24**, 3-15 (2008).
- 9 Feder, M. E. & Hofmann, G. E. Heat-shock proteins, molecular chaperones, and the stress response: evolutionary and ecological physiology. *Annual review of physiology* **61**, 243-282 (1999).
- 10 Hochachka, P. W. & Somero, G. N. *Biochemical adaptation.*, (Princeton University Press, 1984).
- 11 Pörtner, H. Climate change and temperature-dependent biogeography: oxygen limitation of thermal tolerance in animals. *Naturwissenschaften* **88**, 137-146 (2001).

- 12 Pörtner, H.-O. Oxygen-and capacity-limitation of thermal tolerance: a matrix for integrating climate-related stressor effects in marine ecosystems. *Journal of Experimental Biology* **213**, 881-893 (2010).
- 13 Clusella-Trullas, S., Blackburn, T. M. & Chown, S. L. Climatic predictors of temperature performance curve parameters in ectotherms imply complex responses to climate change. *The American naturalist* **177**, 738-751 (2011).
- 14 McKechnie, A. E. & Wolf, B. O. The physiology of heat tolerance in small endotherms. *Physiology* **34**, 302-313 (2019).
- 15 Arad, Z. & Marder, J. Strain differences in heat resistance to acute heat stress, between the bedouin desert fowl, the white leghorn and their crossbreeds. *Comp Biochem Physiol A* **72**, 191-193 (1982).
- 16 Randall, W. C. Factors influencing the temperature regulation of birds. *American Journal of Physiology* **139**, 56-63 (1943).
- 17 Tieleman, B. I., Williams, J. B., LaCroix, F. & Paillat, P. Physiological responses of Houbara bustards to high ambient temperatures. *Journal of Experimental Biology* **205**, 503-511 (2002).
- 18 Chappell, M. A. & Bartholomew, G. A. Activity and thermoregulation of the antelope ground squirrel *Ammospermophilus leucurus* in winter and summer. *Physiol Zool* **54**, 215-223 (1981).
- 19 Lovegrove, B. G., Heldmaier, G. & Ruf, T. Perspectives of endothermy revisited: the endothermic temperature range. *Journal of Thermal Biology* **16**, 185-197 (1991).
- 20 Cory Toussaint, D. & McKechnie, A. E. Interspecific variation in thermoregulation among three sympatric bats inhabiting a hot, semi-arid environment. *J Comp Physiol B* **182**, 1129-1140 (2012).
- 21 Dawson, W. R. in *University of California Publications in Zoology* Vol. 59 (eds G.A. Bartholomew *et al.*) 81-123 (University of California Press, 1954).
- 22 Paulissen, M. A. Ontogenetic comparison of body temperature selection and thermal tolerance of *Cnemidophorus sexlineatus*. *Journal of herpetology* **22**, 473-476 (1988).

- 23 Weathers, W. W. Energetics and thermoregulation by small passerines of the humid, lowland tropics. *Auk* **114**, 341-353 (1997).
- 24 Southwick, E. E. Remote sensing of body temperature in a captive 25-g bird. *Condor* **75**, 464-466 (1973).
- 25 Elliott, C. C. H. in *Quelea quelea: Africa's bird pest* (eds R.L. Bruggers & C.C.H. Elliott) (Oxford University Press, 1989).
- 26 Craig, A. J. F. K. in *Roberts birds of southern Africa*. (eds P.A.R. Hockey, W.R.J. Dean, & P.G. Ryan) 1025-1026 (The Trustees of the John Voelcker Bird Book Fund, 2005).
- 27 Whitfield, M. C., Smit, B., McKechnie, A. E. & Wolf, B. O. Avian thermoregulation in the heat: scaling of heat tolerance and evaporative cooling capacity in three southern African arid-zone passerines. *Journal of Experimental Biology* **218**, 1705-1714 (2015).
- 28 McKechnie, A. E. *et al.* Avian thermoregulation in the heat: efficient evaporative cooling allows for extreme heat tolerance in four southern Hemisphere columbids. *Journal of Experimental Biology* **219**, 2145-2155 (2016).
- 29 Smith, E. K., O'Neill, J. J., Gerson, A. R., McKechnie, A. E. & Wolf, B. O. Avian thermoregulation in the heat: resting metabolism, evaporative cooling and heat tolerance in Sonoran Desert songbirds. *Journal of Experimental Biology* **220**, 3290-3300 (2017).
- 30 Smit, B. *et al.* Avian thermoregulation in the heat: phylogenetic variation among avian orders in evaporative cooling capacity and heat tolerance. *Journal of Experimental Biology* **221**, jeb174870 (2018).
- 31 Karasov, W. H. in *Studies in Avian Biology No. 13*. (eds M.L. Morrison, C.J. Ralph, J. Verner, & J.R. Jehl) 391-415 (Cooper Ornithological Society, 1990).
- 32 Swanson, D. L., Drymalski, M. W. & Brown, J. R. Sliding vs static cold exposure and the measurement of summit metabolism in birds. *Journal of Thermal Biology* **21**, 221-226 (1996).
- 33 Kemp, R. & McKechnie, A. E. Thermal physiology of a range-restricted desert lark. *J Comp Physiol B* **189**, 131-141, doi:10.1007/s00360-018-1190-1 (2019).

- 34 Lighton, J. R. B. *Measuring metabolic rates: a manual for scientists.*, (Oxford University Press, 2008).
- 35 Walsberg, G. E. & Wolf, B. O. Variation in the respirometry quotient of birds and implications for indirect calorimetry using measurements of carbon dioxide production. *Journal of Experimental Biology* **198**, 213-219 (1995).
- 36 Tracy, C. R., Welch, W. R., Pinshow, B. & Porter, W. P. Properties of air: a manual for use in biophysical ecology. 4th Ed. *The University of Wisconsin Laboratory for Biophysical Ecology: Technical Report* (2010).
- 37 Team, R. C. R: *A language and environment for statistical computing.*, (R Foundation for Statistical Computing, 2018).
- 38 Pinheiro, J., Bates, D., DebRoy, S., Sarkar, D. & RDevelopmentCoreTeam. *nlme: Linear and nonlinear mixed effects models.* R package version 3. 57. (2009).
- 39 Muggeo, V. M. R. *Segmented: an R package to fit regression models with broken-line relationships.* (2009).
- 40 McKechnie, A. E. *et al.* Avian thermoregulation in the heat: evaporative cooling in five Australian passerines reveals within-order biogeographic variation in heat tolerance. *Journal of Experimental Biology* **220**, 2436-2444 (2017).
- 41 O'Connor, R. S., Wolf, B. O., Brigham, R. M. & McKechnie, A. E. Avian thermoregulation in the heat: efficient evaporative cooling in two southern African nightjars. *J Comp Physiol B* **187**, 477-491 (2017).
- 42 Hoffmann, A. A., Chown, S. L. & Clusella-Trullas, S. Upper thermal limits in terrestrial ectotherms: how constrained are they? *Functional Ecology* **27**, 934-949 (2013).
- 43 Tieleman, B. I., Williams, J. B. & Bloomer, P. Adaptation of metabolic rate and evaporative water loss along an aridity gradient. *Proceedings of the Royal Society of London* **270**, 207-214 (2003).
- 44 Xie, S., Tearle, R. & McWhorter, T. J. Heat shock protein expression is upregulated after acute heat exposure in three species of Australian desert birds. *Avian Biology Research* **11**, 263-273 (2018).

- 45 Czenze, Z. J. *et al.* Regularly-drinking desert birds have greater evaporative cooling capacity and higher heat tolerance limits than non-drinking species. *Functional Ecology* **in press** (2020).
- 46 Midtgård, U. Scaling of the brain and the eye cooling system in birds: a morphometric analysis of the rete ophthalmicum. *Journal of Experimental Zoology* **225**, 197-207 (1983).
- 47 Kilgore, D. L., Bernstein, M. H. & Hudson, D. M. Brain temperatures in birds. *J Comp Physiol* **110**, 209-215 (1976).
- 48 Bernstein, M. H., Curtis, M. B. & Hudson, D. M. Independence of brain and body temperatures in flying American kestrels, *Falco sparverius*. *American Journal of Physiology-Regulatory, Integrative and Comparative Physiology* **237**, R58-R62 (1979).
- 49 Kregel, K. C. Invited review: heat shock proteins: modifying factors in physiological stress responses and acquired thermotolerance. *Journal of applied physiology* **92**, 2177-2186 (2002).
- 50 McKechnie, A. E. *et al.* Avian thermoregulation in the heat: evaporative cooling capacity in an archetypal desert specialist, Burchell's sandgrouse (*Pterocles burchelli*). *Journal of Experimental Biology* **219**, 2137-2144 (2016).
- 51 Talbot, W. Z.A., McWhorter, T. J., Gerson, A. R., McKechnie, A. E. & Wolf, B. O. Avian thermoregulation in the heat: evaporative cooling capacity of arid-zone Caprimulgiformes from two continents. *Journal of Experimental Biology* **220**, 3488-3498 (2017).
- 52 McWhorter, T. J. *et al.* Avian thermoregulation in the heat: evaporative cooling capacity and thermal tolerance in two Australian parrots. *Journal of Experimental Biology* **221**, jeb168930 (2018).
- 53 Talbot, W. A., Gerson, A. R., Smith, E. K., McKechnie, A. E. & Wolf, B. O. Avian thermoregulation in the heat: metabolism, evaporative cooling and gular flutter in two small owls. *Journal of Experimental Biology* **221**, jeb171108 (2018).
- 54 Smith, E. K., O'Neill, J., Gerson, A. R. & Wolf, B. O. Avian thermoregulation in the heat: resting metabolism, evaporative cooling and heat tolerance in Sonoran Desert doves and quail. *Journal of Experimental Biology* **218**, 3636-3646 (2015).

3.7 ACKNOWLEDGMENTS

We thank Philip Pattinson for his accommodation and permission to work on his property and three anonymous reviewers whose comments improved the manuscript. This work was supported by funding from the DST-NRF Centre of Excellence at the FitzPatrick Institute and the National Research Foundation of South Africa (grant 119754 to A.E.M). Any opinions, findings, conclusions, or recommendations expressed in this article are those of the authors and do not necessarily reflect the views of the National Research Foundation.

3.8 ADDITIONAL INFORMATION

3.8.1.1 Additional figures

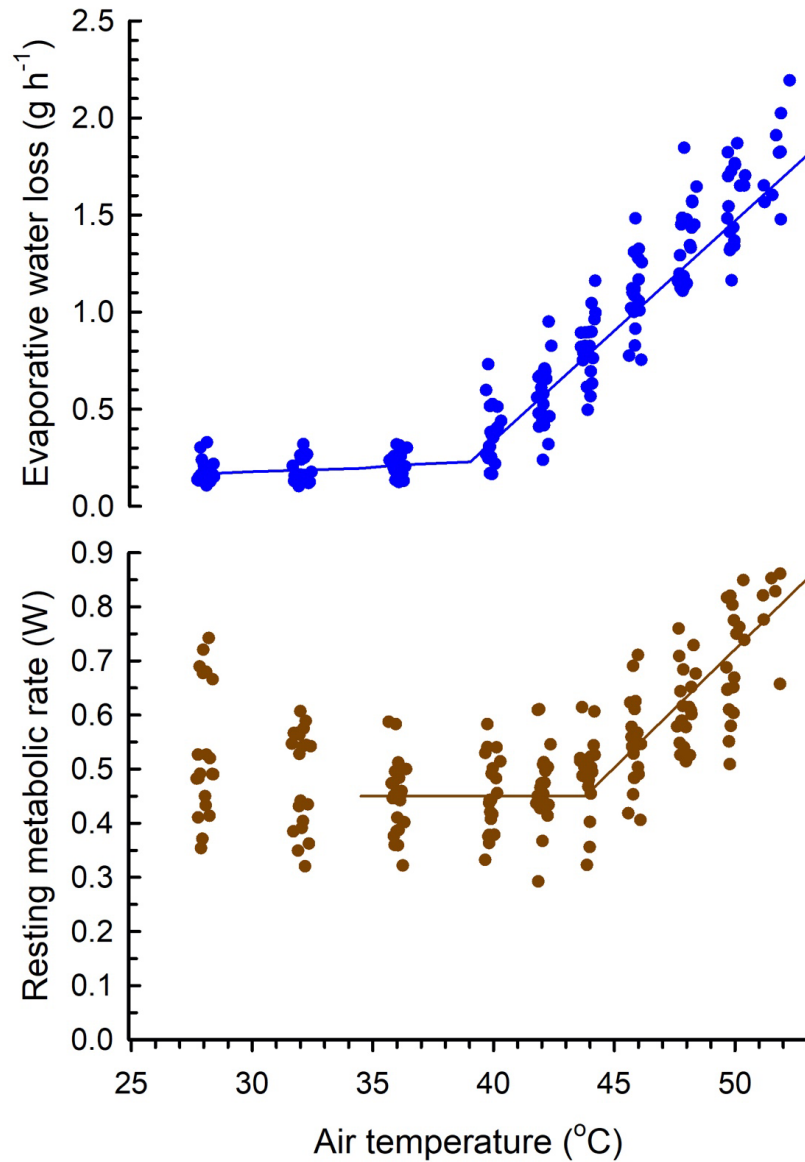


Figure S1. Relationships between air temperature and evaporative water loss (upper panel) and resting metabolic rate (lower panel) during acute heat exposure in red-billed queleas (*Quelea quelea*; $n = 20$). The solid lines are the relationships above and below inflection points from linear mixed-effects models that included individual as a random effect to account for multiple measurements per individual.

**CHAPTER 4 HEAT AND HUMIDITY:
THE ROLE OF
HYPERTHERMIA IN
AVIAN HEAT TOLERANCE**

This chapter is prepared for submission to the Journal of Experimental Biology and is formatted in line with the journal's requirements

4.1 ABSTRACT

Evaporative heat dissipation is fundamentally important among endotherms for maintaining sub-lethal body temperatures (T_b) during extreme heat exposure. However, high atmospheric humidity impedes the effectiveness of evaporative heat dissipation, subsequently reducing heat tolerance capacity. The evolution of increased hyperthermia tolerance has been hypothesized as being functionally linked to tolerating high heat loads and accommodating humidity-associated constraints on evaporative cooling. To test this hypothesis, I examined how varying absolute humidity at air temperatures (T_{air}) $>$ T_b affects the thermoregulatory performance of red-billed queleas (*Quelea quelea*), a species known to tolerate extreme hyperthermia ($T_b > 48$ °C) during acute heat exposure. Using a modified flow-through respirometry technique I was able to precisely manipulate humidity conditions within metabolic chambers and exposed birds to set point T_{air} between 34 °C and 50 °C at four humidity treatments (6, 13, 19 or 25 g m⁻³). I found that thermoregulatory response variables such as resting metabolic rate, evaporative water loss and evaporative cooling efficiency were largely similar across increasing T_{air} regardless of absolute humidity. I also found no significant difference in maximum tolerable body temperature (T_{bmax} ; mean \pm SD = 48.60 \pm 0.40 °C) and limited effects on heat tolerance limits (HTL: 48.41 \pm 1.03 °C). Across humidity treatments, at 44°C $>$ T_{air} , rates of increase in T_b (T_b slope) tracked increases in T_{air} , suggesting that for 3-4 °C, rates of T_b increase were proportional to T_{air} increases. My study provides evidence that hyperthermia tolerance is functionally linked with accommodating the impeding effects of humidity on evaporative water loss and maintaining heat tolerance capacity.

4.2 INTRODUCTION

A large fraction of Earth's avian biodiversity inhabits warm, humid climates in the tropics and subtropics. Although often perceived as climatically benign and among the least challenging of physical environments for endotherms to occupy, high atmospheric humidity may exacerbate the thermoregulatory challenges of hot weather (Gerson et al., 2014; Powers, 1992), particularly for species that experience high solar heat loads while foraging in open

microsites (Weathers 1981, 1997). Indeed, high humidity is thought to be a contributing factor in recent mortality events involving birds and bats (Welbergen et al. 2008b; Ratnayake et al. 2019; McKechnie et al. 2021b). However, understanding of the evolution of avian thermal physiology in humid habitats lags far behind that for environments such as deserts and highly seasonal temperate and boreal latitudes.

For endothermic animals, evaporative heat loss (EHL) is critical for defending body temperatures (T_b) when the temperature (T_{air}) of an animal's immediate environment exceeds their T_b (Dawson 1954; Dawson and Schmidt-Nielsen 1964). The thermoregulatory role of evaporative water loss (EWL) has been assessed in numerous species, however, most of these measurements involved dry air or unspecified humidities (Scholander et al. 1950; Powers 1992; Weathers 1997; Tieleman and Williams 2000; Whitfield et al. 2015; Czenze et al. 2020; Freeman et al. 2020). Whereas assessing thermoregulatory performance and capacity in dry air is informative and provides data collected under standardized conditions, in reality outside of arid climates animals seldom experience conditions of very low humidity comparable to those associated with dry air laboratory conditions. Rather, experienced atmospheric humidity by animals outside of arid climates is normally relatively higher. Humidity drives reductions in evaporative cooling efficiency [evaporative heat loss (EHL)/metabolic heat production (MHP)] in most species investigated so far (Powers 1992; Gerson et al. 2014b; van Dyk et al. 2019). One of the effects of these reductions in EHL/MHP is a subsequent downward shift in heat tolerance limits (HTL- maximum T_{air} tolerated before the onset of severe hyperthermia). For example, in Chapter 2 I found that HTL's among 30 southern African bird species decreased on average by $>2^{\circ}\text{C}$ between dry and humid conditions, while Gerson et al. (2014b) found that rates of evaporative water loss (EWL) in sociable weavers (*Philetairus socius*), an arid savannah species, decreased by approximately 50% as humidity increased from relatively dry conditions to a maximum of $26 \text{ g H}_2\text{O m}^{-3}$.

Gaining an understanding of how hot and humid conditions influence thermoregulatory performance is important for making accurate predictions regarding species vulnerabilities to predicted increases in global air temperatures (IPCC 2021). Weathers (1997) hypothesised that birds in humid environments may benefit by using pronounced hyperthermia to mitigate the effects of humidity on heat tolerance, and showed

that Variable Seed eaters (*Sporophila aurita*) were capable of surviving T_bmax of 46.7 - 47 °C and maintaining a large $T_b - T_{air}$ gradient, allowing for heat to be dissipated passively. More recent findings support this idea and suggest some species may have indeed evolved an increased capacity to tolerate hyperthermia to accommodate humidity-associated constraints on evaporative cooling (Freeman, unpublished – Chapter 2) or extreme operative temperatures (Weathers 1997; Freeman et al. 2020). Birds, specifically those inhabiting humid environments, often have a combination of higher T_bmax and smaller humidity-associated reductions in HTL (Chapter 2), strongly suggesting a functional link between the capacity for hyperthermia and lower sensitivity of heat tolerance to humidity.

To test the hypothesis that pronounced hyperthermia tolerance is functionally linked to accommodating high heat loads in humid environments, I examined how humidity affects thermoregulation at $T_{air} > T_b$ in the bird species with the most extreme hyperthermia tolerance yet described, the red-billed quelea (*Q. quelea*) (Chapter 3). I predicted that 1.) increases in absolute humidity decrease thermoregulatory performance, specifically reducing rates of EWL, evaporative cooling efficiency (EHL/MHP- evaporative heat loss (EHL) / metabolic heat production) and RMR; 2.) heat tolerance limits are similar between different humidity treatments primarily due to birds relying more heavily on hyperthermia tolerance than thermoregulation to manage raised absolute humidity, specifically at extreme T_{air} (>40 °C); 3.) T_bmax remains unaffected by increasing humidity.

4.3 MATERIALS AND METHODS

Study sites

I captured birds at Mooihoek farm (28°11'48.74"S, 29° 9'54.70"E, 1754 m asl) near the town of Harrismith, Free State province, South Africa. Situated in a mountainous region at the eastern edge of the South African escarpment, the study area comprises predominantly of eastern Free State sandy grasslands in wide valleys (Mucina and Rutherford 2006) (Mucina and Rutherford 2006), although much of these grasslands have been anthropogenically transformed for agricultural cultivations. Mean austral spring/summer (September - March)

maximum T_{air} at the study site is 26.4 °C while minimum T_{air} is 10.3°C with mean annual precipitation of ~713 mm (Fick and Hijmans 2017). Average mean austral spring/summer atmospheric humidity is $10.0 \pm 1.4 \text{ g H}_2\text{O m}^{-3}$.

Study species

During September/October 2021 (austral spring) I captured 40 red-billed queleas [*Quelea quelea*, body mass [(mean \pm SD) = $17.33 \pm 0.88 \text{ g}$], a small granivorous Passeriformes bird, using mist nets. Following capture, each bird was placed in a cloth bag and transported to a field laboratory (approximately 20 minutes away). At the field station birds were housed in cages ($\sim 600 \times 400 \times 400 \text{ mm}$) for 1–16 h with ad libitum access to water and seed. Approximately two hours before experimentation commenced food was removed from the cage to ensure that birds were post-absorptive during experimental measurements.

Air and body temperature measurements

A temperature-sensitive passive integrated transponders (PIT) tag (Biotherm 13, Biomark, Boise, ID, USA) was injected into the peritoneal cavity of each bird prior to the commencement of experimentation to measure body temperature. PIT tags were calibrated before use in a circulating water bath (model F34, Julabo, Seelbach BW, DE) at temperatures between 30 and 50 °C against a thermocouple meter (TC-1000, Sable Systems, Las Vegas, NV, USA), verified against a mercury-in-glass thermometer with NIST-traceable accuracy before and after the PIT tag calibration. Measured temperatures from PIT tags deviated by $0.13 \pm 0.05 \text{ °C}$ ($n = 30$) from actual values and I corrected for measured body temperature values accordingly. A reader and transceiver system (HPR +, Biomark, Boise ID, USA) was used to record data from PIT tags. During experimentation T_{air} within the metabolic chamber was measured using a thermistor probe (TC-100, Sable Systems, Las Vegas, NV, USA) which was inserted through a small hole in the side of the chamber sealed by a rubber grommet.

Gas exchange measurements

Evaporative water loss (EWL) and carbon dioxide production (V_{CO_2}) were measured using an open flow-through respirometry system. Birds were placed individually into 3-L (200 mm high \times 150 mm wide \times 100 mm deep) plastic metabolic chambers known to not absorb water vapour (Whitfield et al. 2015) (Whitfield et al. 2015), fitted with a raised mesh platform \sim 10 cm a mineral oil layer (\sim 1 cm) into which excreta could fall to prevent evaporation effects on rates of EWL. Metabolic chambers were then placed inside a modified \sim 100L cooler box in which T_{air} was regulated by a Peltier device (AC-162 Thermoelectric Air Cooler, TE Technology, Traverse City MI, USA) and adjusted using a digital controller (TC-36–25-RS485 Temperature Controller, TE Technology, Traverse City MI, USA).

Atmospheric air was supplied by an oil-free compressor and which was scrubbed of water vapour using a membrane dryer (Atlas Copco SD1N air dryer and filter, Atlas Copco, Stockholm, Sweden). Dried air was then split into an in chamber (experimental), additional dry line and a dry air baseline channel using Bev-A-Line IV tubing (Thermoplastic Processes Inc., Warren, NJ, USA). A needle valve (Swagelok, Solon, OH, USA) maintained flow rates to the baseline channel (“dry baseline”) at \sim 1 L min⁻¹, while flow rates to the experimental channel were maintained between 1-4 L min⁻¹ using a mass flow controller (Alicat Scientific Inc., Tuscon AZ, USA) calibrated using a soap-bubble flow meter (Giliblator 2, Sensidyne, St Peters- burg, FL, USA). Downstream of the mass flow controller, experimental channel air passed through three water-filled bubblers connected in series each constructed from a 3-L (200 mm high \times 150 mm wide \times 100 mm deep) sealable Tupperware screw-top bottles (universal jar, Tupperware, Orlando, FL, USA) with in- and outlet fittings installed in the lid and incurrent air passing through an aquarium stone. The first bubbler was placed at room temperature ($T_{air} = \sim$ 35 °C). The other two bubblers were placed in a temperature-controlled chamber (PELT-5, Sable Systems, Las Vegas NV, USA) set to a T_{air} slightly higher than the desired in chamber dewpoint. This was done as it was more practical to lower humidity levels before reaching the chamber than to try and increase levels of humidity post-bubblers. Downstream of the bubblers, an additional line of dry air (“regulatory dry air line”), merged with the humid channel which allowed for the mixing of dry air with the humidified air should we have needed to lower the saturation of the air before it reached the metabolic

chamber. Flow rates for a regulatory dry air line were controlled by another mass flow controller (Alicat Scientific Inc., Tuscon AZ, USA) and adjusted in response to in chamber humidity which allowed for in chamber humidity levels to be regulated to the desired absolute humidity treatment while also compensating for increased water vapour pressure brought about by EWL from the bird in the chamber. Downstream of the regulatory dry air line and the humid channel merge the channel was again split into a secondary “humid” baseline channel with flow rate regulated using a needle valve allowing for the exact water vapour pressure of the air entering the channel to be monitored and recorded. The humid channel continued to the chamber. Before entering the chamber, the humid air line passed through a flow meter [(10 SLPM mass flow controller set to maximum (Alicat Scientific Inc., Tuscon AZ, USA)], also calibrated using a Gilibrator 2 flow meter. The exact flow rate through the mass flow meter was recorded manually at each sampled set T_{air} . Incurrent flow rates to the chamber varied between 570 and 3998 mL min⁻¹. Where possible, adjustments of flow rates and/or incurrent humid air took place during a transitional period of ~10-15 minutes before measurements at a set point T_{air} to maximize the likelihood that equilibrium conditions (Lasiewski et al. 1966) were reached. Should conditions within the chamber have been unstable or transitioning to the desired humidity set point, additional time was permitted to ensure data were collected from stable O₂, CO₂ and H₂O traces.

By periodically adjusting the set T_{air} within my temperature-controlled chamber where bubblers were housed, flow rates of incurrent air into bubblers and flow rate of the regulatory dry air line I was able to maintain fairly consistent values of absolute humidity in the metabolic chamber (i.e., the humidity experienced by a bird) at one of four set point values (mean \pm SD): 6.13 \pm 0.50 g H₂O m⁻³ (n = 78), 12.69 \pm 0.57 g H₂O m⁻³ (n = 81), 18.60 \pm 0.91 g H₂O m⁻³ (n = 76) and 24.68 \pm 0.79 g H₂O m⁻³ (n = 78) in line with that of previous studies on the effects of humidity on avian thermoregulation (Powers 1992; Gerson et al. 2014a; van Dyk et al. 2019). I refer to these values, hereafter as 6, 13, 19 and 25 g m⁻³. On account of 25 g m⁻³ being equivalent to a dewpoint of ~ 27 °C, I set up the equipment in a controlled climate within a mobile lab to regulate T_{air} at ~ 35 °C to avoid condensation within analysers and tubing.

Air from either of the baselines or chamber channel was sequentially subsampled using a respirometry multiplexer (model MUX3-1101-18M, Sable Systems) in manual

mode, at a flow rate $\sim 160 \text{ mL min}^{-1}$ regulated by a subsampling pump (model SS4, Sable Systems, Las Vegas NV, USA) and pulled through a $\text{CO}_2/\text{H}_2\text{O}$ analyser (LI-840A, LI-COR, Lincoln NE, USA) followed by an O_2 analyser (FC-10A, Sable Systems, Las Vegas NV, USA). The $\text{CO}_2/\text{H}_2\text{O}$ analyser was regularly zeroed using pure nitrogen (AFROX, Johannesburg, South Africa) and spanned using a 2000 ppm CO_2 in N_2 gas mix (AFROX) or humidified air with a dewpoint 5 - 6 °C below ambient T_{air} generated using a dew point generator (DG-4, Sable Systems, Las Vegas NV, USA). The O_2 analyser was periodically spanned to 20.95% using dry, CO_2 -free air scrubbed of CO_2 .

Data were acquired every 5 seconds from analysers and SS-4 using an analog–digital converter (model UI-3, Sable Systems, Las Vegas NV, USA) which converted the voltage inputs to digital values. I then recorded these values using a computer with the Expedata software (Sable Systems, Las Vegas NV, USA) installed on it.

Experimental protocol

I measured T_b , EWL and RMR at each of the four humidity set points at T_{air} values beginning from 34 °C and increasing incrementally by 2 °C. Until birds reached their thermal endpoint following the same protocol as that of (Freeman et al. 2020). Measurements typically lasted 2–3 hours and began with a bird placed in a chamber at $T_{\text{air}} = 28 \text{ °C}$, after which it was given at least an hour to habituate to conditions in the metabolic chamber. Following the habituation period, humidity values were held constant at the desired treatment while T_{air} increased to 34 °C, and then incrementally increased by 2 °C with transitions between treatments taking a maximum of 10–15 min to achieve. Birds were exposed to T_{air} /humidity conditions for a minimum of 15 min until traces of O_2 , CO_2 and H_2O were deemed to be stable.

Data analyses

Analyser drift and lag were corrected using the relevant Expedata algorithms. Equation [9.3] of Lighton (2008) was used to calculate excurrent flow rates while equations [9.4]— [9.6] were used to calculate VO_2 , V_{CO_2} and EWL. Selecting the lowest 5-min period of V_{CO_2} per

trace I calculated the RMR and EWL. Respiratory exchange ratio ($RER = V_{CO_2} / V_{O_2}$), and thermal equivalence data (Withers 1992) were used to convert rates from respiratory gas exchange to metabolic rates (W). Assuming $2.406 \text{ J mg H}_2\text{O}^{-1}$ (Tracy et al. 2010), rates of evaporative water loss rates were converted to EHL (W). Equations provided by (Campbell and Norman 1998) were used to convert water vapour pressure (kPa) values to absolute humidity ($\text{g H}_2\text{O m}^{-3}$) and to calculate saturation water vapour pressures.

Humidity treatment analysis

I quantified physiological response variables for each individual and used these to calculate mean values per humidity treatment (i.e., 6, 13, 19, 25 g m^{-3}). All statistical analyses were computed in the R 4.0.5 (R Core Team, 2020) environment, using R Studio 1.1.463 (RStudio, Inc.). Sample sizes (n) at each absolute humidity treatment were $n = 10$ individuals (*SI Appendix*, Tables S2.1 and S3.1). Respective inflection T_{air} values above which T_b , EWL, EHL/MHP and RMR increased rapidly, were identified using the package *segmented.lme* (Muggeo 2016), with individual identity at each treatment, included as a random effect. I analysed T_b , EWL, and RMR above and below inflection points separately using linear mixed-effect models in the R package *nlme* (Pinheiro J, Bates D, DebRoy S, Sarkar D 2015), estimating the slopes for the relationships of thermoregulatory response variables as functions of T_{air} .

The “dredge” function in the *MuMIn* package was used to conduct model selection (Barton 2019). My standardised model included T_{air} (or $T_{air} - T_b$), M_b and the $T_{air}:M_b$ interaction. I selected the model with the highest rank among competing models using Akaike information criterion values corrected for small sample size (AIC_c) and Akaike weights (Burnham and Anderson 2002). If competing models were within $\Delta AIC_c < 2$, I retained the most parsimonious model. I accounted for pseudoreplication by including individual identity as a random factor in all analyses. Significance was assessed at $\alpha < 0.05$ and values are presented as mean \pm SD.

Breusch-Pagan Test tests implanted in the R package *lmtest* (Zeileis and Hothorn 2002) were used to confirm that no significant heteroscedasticity existed in T_b , EWL or RMR data among humidity or temperature categories. After confirming that no obvious deviations

from normality or homoscedasticity were evident in residual plots, I fitted linear mixed effect models using the nlme package (Pinheiro et al. 2009). I modelled the responses of T_b , EWL, RMR and EHL/MHP to the continuous predictor variables T_{air} , absolute humidity, bird mass, sex and the T_{air} X absolute humidity interaction term. Individual identity was included as a random fixed effect in all models. To select the models with the highest explanatory power, I used the model.sel function of the R package *MuMIn* (Bartoń 2013) to identify the best model for each response variable on the basis of Akaike information criterion values corrected for small sizes (AICc). For T_b , RMR, EWL and EHL/MHP, the best models included T_{air} , absolute humidity, T_{air} X absolute humidity but not body mass (Mb) and sex. However, models including Mb and sex difference in values of AICc < 2 and I, therefore, decided to include both variables in my model to ensure they were not predictors of any of the response variables.

To compare maximum values recorded for T_b , RMR, EWL and EHL/MHP I used post hoc multiple comparisons Tukey HSD tests to compare between humidity treatments. I also compared values associated with the relationship between each response variable (T_b , EWL, RMR and EHL/MHP) and T_{air} between absolute humidity treatments using a pairwise.t.test function fitted with a Bonferroni adjustment correction in the R package *rstatix* (Kassambara 2015).

4.4 RESULTS

Body temperature and heat tolerance limits

Quelea T_b varied from 41.0 °C at $T_{air} = 34$ °C and reached a mean maximum value of 48.6 ± 0.4 °C at $T_{air} = 48.5 \pm 1.1$ °C (*SI Appendix*, Table S1). The highest individual T_{bmax} recorded was 49.6 °C at $T_{air} = 49.8$ °C (19 g m^{-3} , Figure 1b). Values of T_{bmax} did not differ significantly between absolute humidity treatments (*SI Appendix*, Table S2.1, Tukey HSD). Heat tolerance limits (HTL) did not differ between the 6 g m^{-3} ($\bar{x} = 48.4 \pm 0.9^\circ\text{C}$), 19 g m^{-3} ($\bar{x} = 48.1 \pm 0.8^\circ\text{C}$) and 25 g m^{-3} ($\bar{x} = 47.9 \pm 0.9^\circ\text{C}$) treatments, but mean HTL at 13 g m^{-3} ($\bar{x} = 49.3 \pm 0.6^\circ\text{C}$) was significantly higher than those for 19 g m^{-3} (Tukey: HSD = 1.23, $p=0.01$) and 25 g m^{-3} (Tukey: HSD = 1.43, $p=0.002$) (Figure 1c, *SI Appendix*, Table S2.2).

Segmented linear mixed-effect models detected inflections in T_b at $T_{air} = 43.9 - 45.2$ °C (*SI Appendix*, Table S1), above which T_b increased rapidly at all humidity treatments (Figure 1a). I, therefore, report results for T_b below (T_b slope 1) and above (T_b slope 2) respective T_b inflection points separately (Figure 1a).

At T_{air} below the inflection points, T_b increased linearly (6 g m^{-3} : 0.31 °C T_b °C T_{air}^{-1} , 13 g m^{-3} : 0.28 °C T_b °C T_{air}^{-1} , 19 g m^{-3} : 0.39 °C T_b °C T_{air}^{-1} and 25 g m^{-3} : 0.28 °C T_b °C T_{air}^{-1}). There were significant effects of T_{air} ($F_{1,220} = 2237.44$, $p < 0.001$), humidity ($F_{1,220} = 6.78$, $p < 0.001$) and the $T_{air} \times$ humidity interaction ($F_{1,220} = 9.68$, $p < 0.001$) on T_b . Sex ($F_{1,220} = 0.15$, $p = 0.69$) and M_b ($F_{1,220} = 2.04$, $p = 0.16$) did not significantly affect T_b (Figure 1B). Pairwise t-tests indicated that T_b in the 19 g m^{-3} humidity treatment was significantly higher compared to the 13 g m^{-3} treatment ($t = 3.94$, $p < 0.01$). No other significant differences between humidity treatments were detected (Figure 1 and Table S3.1, *SI appendix*).

At T_{air} above the inflection points, there was a significant influence of T_{air} ($F_{1,82} = 234.83$, $p < 0.001$) on T_b , but no significant effect of humidity ($F_{1,82} = 0.70$, $p = 0.56$), the $T_{air} \times$ humidity interaction ($F_{1,82} = 0.74$, $p = 0.54$), sex ($F_{1,82} = 0.13$, $p = 0.72$) or M_b ($F_{1,82} = 1.33$, $p = 0.26$) (Figure 1B). Slopes of T_b were approximately three-fold steeper than at T_{air} below the inflections (6 g m^{-3} : 1.06 °C T_b °C T_{air}^{-1} , 13 g m^{-3} : 0.93 °C T_b °C T_{air}^{-1} , 19 g m^{-3} : 0.77 °C T_b °C T_{air}^{-1} and 25 g m^{-3} : 0.91 °C T_b °C T_{air}^{-1}). Pairwise t-tests indicated no significant differences among humidity treatments between values of T_b as T_{air} increased (Figure 1a; *SI appendix*, Table S3.2).

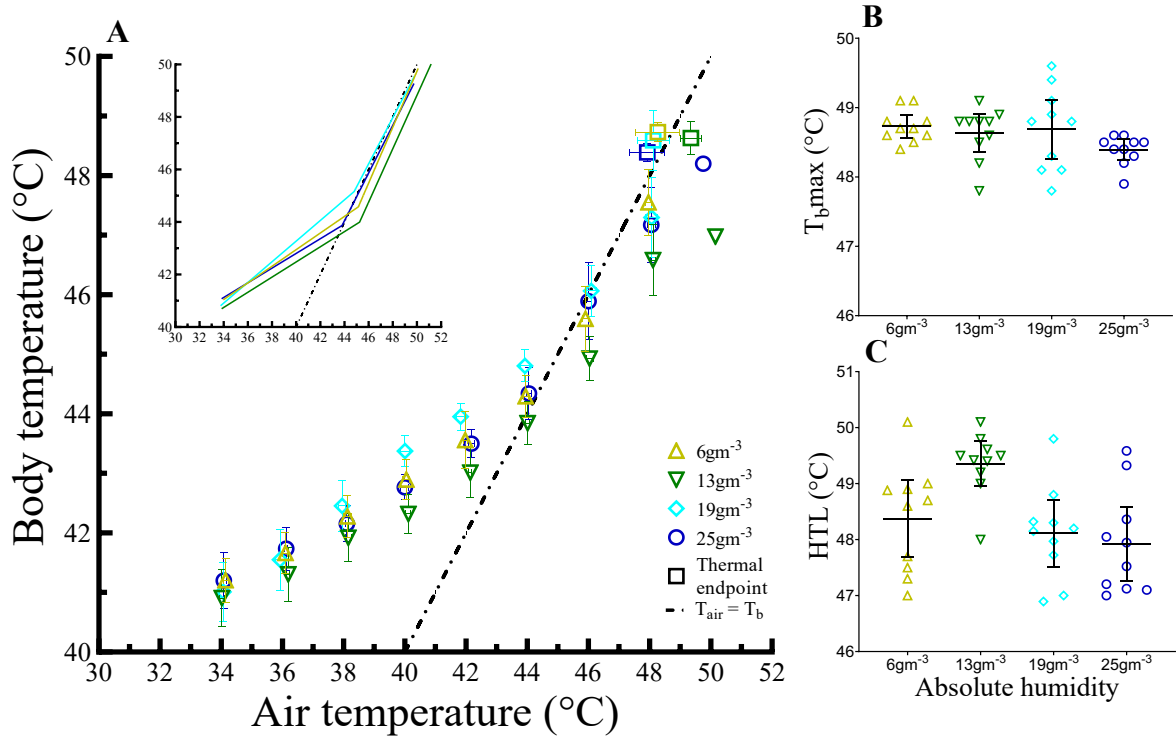


Figure 1 a.) Relationship between body temperature (T_{b}) and air temperature (T_{air}) over four different treatments of absolute humidity [6 g m^{-3} (gold triangles), 13 g m^{-3} (green upside-down triangles), 19 g m^{-3} (light blue diamonds), 25 g m^{-3} (dark blue circles)] in red-billed queleas (*Quelea quelea*). Values are means with vertical lines representing 95% confidence limits shown by error bars whenever sample sizes were large enough. The dashed line shows $T_{\text{b}} = T_{\text{air}}$. Thermal endpoints (mean T_{bmax} with 95% confidence limits) for each treatment are indicated by a square. The inset graph shows segmented linear model relationships of $T_{\text{b}} \sim T_{\text{air}}$ for each treatment. **b.)** Mean maximum body temperature (T_{bmax}) did not differ significantly between my four absolute humidity treatments. **c.)** Heat tolerance limits (HTL) did not differ between 6 g m^{-3} , 19 g m^{-3} and 25 g m^{-3} but values at 13 g m^{-3} were found to be significantly higher than that at 19 g m^{-3} and 25 g m^{-3}

Evaporative Water loss (EWL)

Values of EWL were predicted by T_{air} ($F_{1,303} = 2388.79$, $p < 0.001$), humidity ($F_{1,303} = 7.13$, $p < 0.001$) and $T_{\text{air}} \times$ humidity ($F_{1,303} = 6.91$, $p < 0.001$), whereas neither body mass ($F_{1,303} = 0.12$, $p = 0.73$) nor sex ($F_{1,303} = 1.78$, $p = 0.19$) had a significant effect. Mean rates of EWL were minimal at 34 °C ($\sim 0.1 \text{ g h}^{-1}$, Table 1). At all humidity treatments, EWL increased with T_{air} (6 g m^{-3} : $0.06 \text{ g h}^{-1} \text{ }^{\circ}\text{C}^{-1}$, 13 g m^{-3} : $0.07 \text{ g h}^{-1} \text{ }^{\circ}\text{C}^{-1}$, 19 g m^{-3} : $0.07 \text{ g h}^{-1} \text{ }^{\circ}\text{C}^{-1}$ and 25 g m^{-3} : $0.05 \text{ g h}^{-1} \text{ }^{\circ}\text{C}^{-1}$) while $\text{EWL} \sim T_{\text{air}}$ at each treatment did not differ significantly (Figure 2a, *SI appendix*, Table S3.3). I could not identify inflections in EWL, as EWL increased from the lowest experimental T_{air} of 34°C across all humidity treatments and reached maximum values of $T_{\text{air}} = 45\text{-}47^{\circ}\text{C}$ before flattening out. At higher T_{air} , EWL in the 19 g m^{-3} and 25 g m^{-3} humidity treatments began to decrease (Figure 2a). Maximum values of EWL did not differ among humidity treatments (*SI appendix*, Table S2.2).

Table 2 Body temperature (T_b), evaporative water loss (EWL), resting metabolic rate (RMR) and evaporative cooling efficiency [ratio of evaporative heat loss (EHL)/metabolic heat production (MHP)] in red-billed queleas (*Quelea quelea*) exposed to incrementally increased air temperatures (T_{air}) and four humidity treatments (6 g m^{-3} , 13 g m^{-3} , 19 g m^{-3} and 25 g m^{-3}). Values are presented as means \pm SD, with sample size (number of individuals) in parentheses.

T_{air} ($^{\circ}\text{C}$)	Body temperature ($^{\circ}\text{C}$)				Evaporative water loss (g h^{-1})			
	6g m^{-3}	13g m^{-3}	19g m^{-3}	25g m^{-3}	6g m^{-3}	13g m^{-3}	19g m^{-3}	25g m^{-3}
34	41.20 ± 0.51 (10)	40.91 ± 0.67 (10)	41.01 ± 0.69 (10)	41.20 ± 0.66 (10)	0.14 ± 0.05 (10)	0.08 ± 0.02 (10)	0.10 ± 0.03 (10)	0.14 ± 0.18 (10)
36	41.66 ± 0.48 (10)	41.31 ± 0.64 (10)	41.55 ± 0.71 (10)	41.74 ± 0.50 (10)	0.18 ± 0.07 (10)	0.14 ± 0.05 (10)	0.12 ± 0.03 (10)	0.18 ± 0.04 (10)
38	42.28 ± 0.50 (10)	41.92 ± 0.56 (10)	42.45 ± 0.60 (10)	42.15 ± 0.42 (10)	0.29 ± 0.07 (10)	0.30 ± 0.06 (10)	0.25 ± 0.11 (10)	0.29 ± 0.05 (10)
40	42.89 ± 0.47 (10)	42.31 ± 0.46 (10)	43.38 ± 0.36 (10)	42.77 ± 0.30 (10)	0.45 ± 0.10 (10)	0.44 ± 0.08 (10)	0.44 ± 0.12 (10)	0.41 ± 0.06 (10)
42	43.56 ± 0.67 (10)	43.01 ± 0.59 (10)	43.95 ± 0.32 (10)	43.50 ± 0.33 (10)	0.56 ± 0.09 (10)	0.52 ± 0.06 (10)	0.58 ± 0.10 (10)	0.54 ± 0.05 (10)
44	44.29 ± 0.50 (10)	43.84 ± 0.51 (10)	44.80 ± 0.38 (10)	44.34 ± 0.61 (10)	0.64 ± 0.11 (10)	0.69 ± 0.10 (10)	0.76 ± 0.16 (10)	0.71 ± 0.08 (10)
46	45.59 ± 0.76 (10)	44.93 ± 0.51 (10)	46.06 ± 0.60 (10)	45.89 ± 0.91 (10)	0.83 ± 0.13 (10)	0.83 ± 0.09 (10)	0.91 ± 0.15 (10)	0.87 ± 0.15 (10)
48	47.55 ± 0.61 (7)	46.58 ± 0.82 (10)	47.30 ± 0.64 (6)	47.17 ± 0.68 (7)	0.89 ± 0.14 (7)	1.00 ± 0.07 (10)	0.86 ± 0.13 (6)	0.80 ± 0.22 (7)
50		46.97 (1)		48.20 (1)		1.00 (1)		0.77 (1)
	Resting metabolic rate (W)				Evaporative heat loss/metabolic heat production			
34	0.27 ± 0.04 (10)	0.26 ± 0.02 (10)	0.28 ± 0.05 (10)	0.28 ± 0.04 (10)	0.35 ± 0.11 (10)	0.22 ± 0.05 (10)	0.24 ± 0.11 (10)	0.33 ± 0.05 (10)
36	0.29 ± 0.04 (10)	0.27 ± 0.02 (10)	0.29 ± 0.04 (10)	0.28 ± 0.04 (10)	0.41 ± 0.13 (10)	0.35 ± 0.12 (10)	0.28 ± 0.06 (10)	0.44 ± 0.12 (10)
38	0.31 ± 0.05 (10)	0.29 ± 0.03 (10)	0.31 ± 0.04 (10)	0.28 ± 0.04 (10)	0.62 ± 0.15 (10)	0.71 ± 0.14 (10)	0.53 ± 0.18 (10)	0.70 ± 0.16 (10)
40	0.30 ± 0.05 (10)	0.31 ± 0.03 (10)	0.33 ± 0.04 (10)	0.29 ± 0.05 (10)	1.01 ± 0.16 (10)	0.95 ± 0.16 (10)	0.87 ± 0.19 (10)	0.95 ± 0.18 (10)
42	0.32 ± 0.05 (10)	0.33 ± 0.04 (10)	0.35 ± 0.05 (10)	0.31 ± 0.05 (10)	1.18 ± 0.19 (10)	1.08 ± 0.16 (10)	1.12 ± 0.14 (10)	1.19 ± 0.18 (10)
44	0.35 ± 0.06 (10)	0.37 ± 0.06 (10)	0.40 ± 0.08 (10)	0.37 ± 0.05 (10)	1.24 ± 0.16 (10)	1.27 ± 0.16 (10)	1.27 ± 0.13 (10)	1.31 ± 0.13 (10)
46	0.41 ± 0.05 (10)	0.41 ± 0.07 (10)	0.46 ± 0.08 (10)	0.45 ± 0.06 (10)	1.38 ± 0.21 (10)	1.39 ± 0.21 (10)	1.32 ± 0.15 (10)	1.31 ± 0.16 (10)
48	0.47 ± 0.09 (7)	0.47 ± 0.08 (6)	0.47 ± 0.09 (10)	0.48 ± 0.10 (7)	1.28 ± 0.29 (7)	1.37 ± 0.22 (10)	1.24 ± 0.20 (6)	1.10 ± 0.20 (7)
50		0.46 (1)		0.45 (1)		1.46 (1)		1.13 (1)

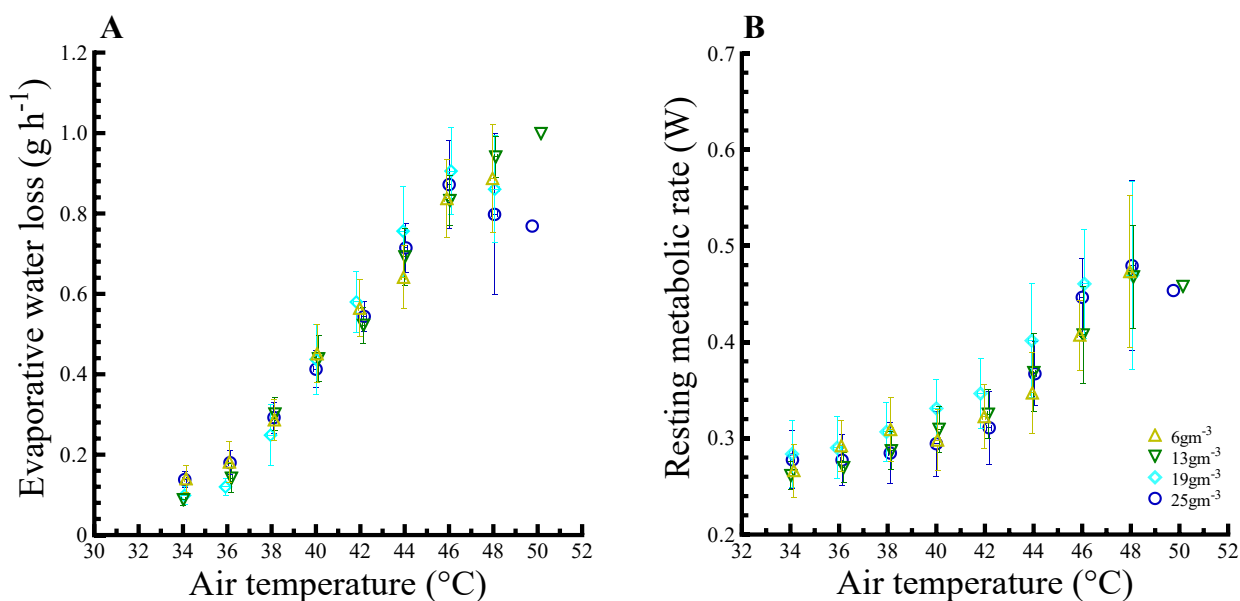


Figure 2 a.) Relationship between evaporative water loss (EWL) and air temperature (T_{air}) and **b.)** relationship between resting metabolic rate (RMR) and air temperature (T_{air}) over four different treatments of absolute humidity [6 g m^{-3} (gold triangles), 13 g m^{-3} (green upside-down triangles), 19 g m^{-3} (light blue diamonds), 25 g m^{-3} (dark blue circles)] in red-billed queleas (*Quelea quelea*). Values for both **2a.)** and **2b.)** are mean values per set point T_{air} with vertical and horizontal lines representing 95% confidence limits shown by error bars whenever sample sizes were large enough. Graphs with calculated segmented linear regressions are available in supplementary material, appendix 1, figure S1. Pairwise t-tests indicated that values of $\text{RMR} \sim T_{\text{air}}$ and $\text{EWL} \sim T_{\text{air}}$ did not differ significantly between absolute humidity treatments. Tukey HSD tests indicated that maximum values of RMR and EWL [where sample sizes were sufficient ($T_{\text{air}} = 48\text{ }^{\circ}\text{C}$)] did not differ significantly between absolute humidity treatments.

Resting metabolic rate (RMR)

Mixed-effect models revealed T_{air} ($F_{1,123} = 164.33, p < 0.001$) as the only significant predictor of RMR above inflection points. Humidity treatment ($F_{1,123} = 2.04, p = 0.11$), the interaction between humidity treatment and T_{air} ($F_{1,123} = 1.78, p = 0.15$), sex ($F_{1,123} = 0.68, p = 0.41$) and M_b ($F_{1,123} = 0.19, p = 0.66$) were not significant predictors of RMR. Maximum values of RMR did not differ among humidity treatments (*SI appendix*, Table S2.3). Pairwise t-tests indicated that values of RMR did not differ with increasing T_{air} (Figure 2B and Table S3.4, *SI appendix*).

Evaporative cooling efficiency

Significant predictors of EHL/MHP included T_{air} ($F_{11, 328}=2208.20, p < 0.001$) and humidity treatment ($F_{11, 328}= 69.03, p < 0.001$) but not M_b ($F_{11, 328}=0.292, p =0.75$), sex ($F_{11, 328}=2.44, p =0.25$) or the interaction between humidity treatment and T_{air} ($F_{11, 328}=4.13, p = 0.38$). Slopes of $\text{EHL/MHP} \sim T_{\text{air}}$ did not vary significantly among humidity treatments (Figure 3; *SI appendix*, Table S3.5). At $T_{\text{air}} = \sim 44$ °C, maximum values of EHL/MHP (1.3 – 1.5) were achieved at all humidity treatments, and significant inflections were detected (Table 1 and *SI appendix*, Table S1), with EHL/MHP either reaching a plateau (6 g m⁻³: -0.06 per °C, 13 g m⁻³: -0.005 per °C) or decreasing (19 g m⁻³: -0.05 per °C and 25 g m⁻³: -0.05 per °C) at T_{air} higher than the inflections (Figure 3b).

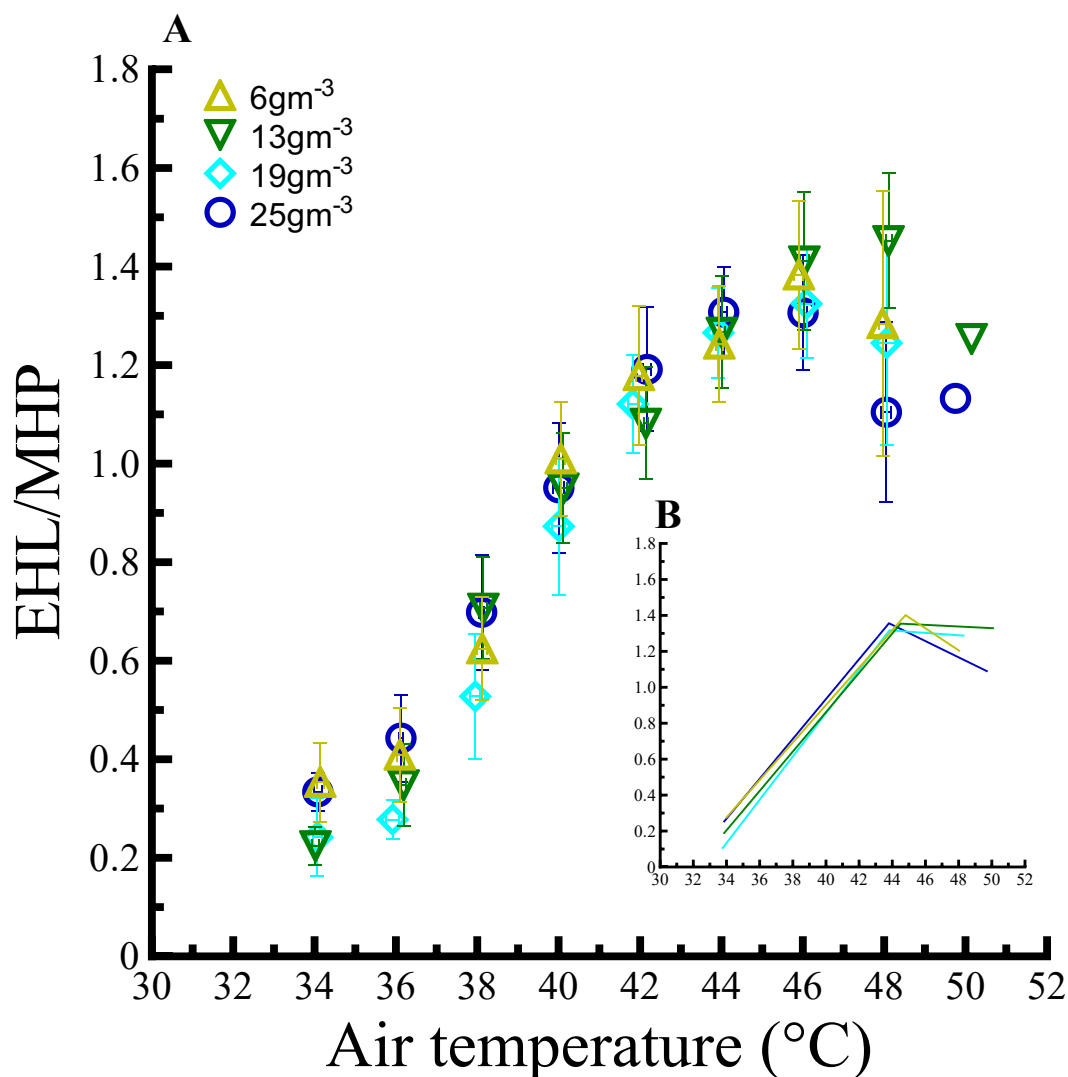


Figure 3 a.) Relationship between evaporative cooling efficiency [(EHL/MHP) - calculated as the ratio of evaporative heat loss (EHL) /metabolic heat production (MHP)] and air temperature (T_{air}) over four different treatments of absolute humidity [6 $g\ m^{-3}$ (gold triangles), 13 $g\ m^{-3}$ (green upside-down triangles), 19 $g\ m^{-3}$ (light blue diamonds), 25 $g\ m^{-3}$ (dark blue circles)] in red-billed queleas (*Quelea quelea*). Values are means with vertical lines representing 5% confidence limits shown by error bars whenever sample sizes were large enough. **b.)** The inset graph illustrates the segmented linear relationship of EHL/MHP at each of the four absolute humidity treatments.

4.5 DISCUSSION

My findings support the hypothesis that pronounced hyperthermia tolerance is functionally linked to thermoregulation under humid conditions, as proposed by Weathers (1997). Increases in absolute humidity, coupled with increasing T_{air} , did not affect the thermoregulatory performance of *Q. quelea* to the extent, nor as predictably, as has been the case in previous studies relating to the impeding effect of humidity on evaporative cooling (Powers 1992; Gerson et al. 2014b; van Dyk et al. 2019). Response variables including EWL, RMR, EHL/MHP and T_b at each of my four humidity treatments were largely similar in relation to T_{air} and did not differ significantly in terms of maxima. At the upper thermal limits, $T_{b\text{max}}$ did not differ significantly between treatments and HTL was also similar between treatments. However, other thermoregulatory variables often reached maximum values and then either decreased or plateaued (e.g., EHL/MHP, and EWL). One of my more unexpected findings was the patterns in $T_b \sim T_{\text{air}}$, where across humidity treatments, rates of T_b increase ($T_{b\text{slope}}$) at $T_{\text{air}} > 44\text{C}$ were $\sim 1^\circ\text{C}$ per 1°C T_{air} . Over this T_{air} range ($44^\circ\text{C} - 48^\circ\text{C}$), queleas were poikilothermic.

Pronounced hyperthermia tolerance is undoubtedly an important physiological mechanism for the occupation of hot, humid regions and is likely more widespread than currently appreciated, particularly among tropical species. Queleas maintained $T_b > T_{\text{air}}$ until $T_{\text{air}} \sim 44^\circ\text{C}$, likely losing some heat non-evaporatively and thereby reducing evaporative heat loss demands and conserving water (Tieleman et al. 2003; Gerson et al. 2019). Across humidity treatments, HTLs were high ($48.40 \pm 1.02^\circ\text{C}$), with most birds reaching the set point of $T_{\text{air}} = 48^\circ\text{C}$. Only two individuals at the 13 g m^{-3} and 25 g m^{-3} treatments reached and were stable (i.e., did not display signs associated with severe hyperthermia) at a $T_{\text{air}} = 50^\circ\text{C}$. Similar to my findings in Chapter 3, queleas in the present study displayed a pronounced capacity to tolerate extreme hyperthermia (mean $T_{b\text{max}} = 48.6 \pm 0.40^\circ\text{C}$). Only $T_{b\text{max}}$ among common nighthawk chicks (*Chordeiles minor*) is comparable to that of the queleas (Newberry and Swanson 2018). The capacity for extreme hyperthermia tolerance is still poorly understood and likely involves both molecular mechanisms [pronounced heat shock protein expression (Kregel 2002; Xie et al. 2018)] and anatomical features such as a

well-developed *rete ophthalmicum* (Bernstein et al. 1979; Midtgård 1983) for brain temperature maintenance below hyperthermic levels. Regardless of the underlying mechanisms, pronounced facultative hyperthermia has obvious benefits for avian thermoregulation and water conservation (Gerson et al. 2019). The impressive hyperthermic tolerance capacity of queleas offered a buffering effect on heat tolerance, which otherwise would have been lowered substantially, as seen in Chapter 2, among species that avoid hyperthermia, such as arid-specialised species. In this study, arid zone species attempted to avoid hyperthermia and experienced $>3^{\circ}\text{C}$ decreases in HTLs under raised humidity conditions compared to dry air.

The use of hyperthermia by queleas to mitigate the impeding effects of humidity on evaporative cooling supports arguments that selection may act strongly on thermoregulatory traits such as T_b , particularly at upper thermal limits. These findings suggest that inter- and/or intraspecific variation in heat tolerance correlated with climate should be expected (Angilletta et al. 2010; Boyles et al. 2011; Smit et al. 2013; Freeman et al. 2022). Furthermore, my findings support the notion that the thermal performance of endotherms, similar to ectotherms, should be viewed as a continuum from thermal specialization to generalization (Angilletta et al. 2010). According to this, hyperthermia tolerance should be more common among species, or populations which inhabit hot humid environments, where the effectiveness of evaporative cooling is reduced, or within taxa that experience extreme environmental temperature loads, for instance, small birds exposed to direct solar radiation while foraging (Weathers 1979, 1997).

Above $T_{\text{air}} \sim 44^{\circ}\text{C}$, EWL and EHL/MHP began to plateau or decrease slightly (19 g m^{-3} and 25 g m^{-3}). During the 4°C increase in T_{air} towards HTL's ($T_{\text{air}} > 44^{\circ}\text{C}$), T_b was approximately proportional to T_{air} . The reliance on hyperthermia among queleas was therefore manifested as poikilothermy at high T_b . This finding was unexpected as it deviates from patterns normally associated with endothermic thermoregulation and contrasts with other passerine birds where T_b always remained below T_{air} at $T_{\text{air}} > 45^{\circ}\text{C}$ (e.g., Czenze et al., 2020; Freeman et al., 2022; Smit et al., 2018, Review - McKechnie et al., 2021b). Proportional increases in $T_b \sim T_{\text{air}}$ lasted for on average ~ 30 -60 minutes among birds. The reaching of maximal values in rates of EHL/MHP (at $T_{\text{air}} = \sim 44^{\circ}\text{C}$) and EWL (at $T_{\text{air}} = \sim 45^{\circ}\text{C}$) at all treatments correlate closely with where these proportional increases in T_b

began (*SI appendix*, fig S1D). Moreover, rates of increase in RMR were similar among humidity treatments and did not increase to accommodate increased thermoregulatory efforts to lower T_b below T_{air} . I consider it unlikely that this is an indication of thermoregulatory failure. This is primarily due to the time periods that the birds resorted to such a pattern and displayed little to no visible symptoms associated with severe hyperthermia (Whitfield et al. 2015) and survived assessments. Finally, maximum values of EHL/MHP, normally recorded at $T_{air} = 46$ °C (EHL/MHP = 1.35), were comparable with that of other passerine birds (reviewed by McKechnie et al., 2021b) as well as that recorded in Chapter 3. However, at $T_{air} > 46$ °C values of EHL/MHP began to decrease for all treatments. Similar maximum values of EHL/MHP among treatments were surprising and provide further support to the idea of hyperthermia tolerance reliance among queleas to reduce the effects of humidity in lowering HTL's.

4.6 CONCLUSION

I present red-billed queleas as a model species to illustrate how hyperthermia tolerance can be beneficially used as a thermoregulatory strategy to reduce the effects of extreme heat loads and impeding effects of environmental conditions (i.e., atmospheric humidity on evaporative cooling) on heat tolerance. However, further research into the extent of hyperthermia tolerance and the mechanisms which make it possible are required. Hyperthermia tolerance is an important consideration for making accurate predictions when assessing and/or modelling the vulnerabilities of endothermic species to potential future climatic conditions (IPCC 2021). Therefore, gaining a comprehensive understanding of whether and how this trait varies phylogenetically may be important for understanding how future climates will shape avifaunal communities. In conclusion, hyperthermia tolerance among queleas may be a selected trait associated with thermal generalisation, along with broad-scale expansions in agriculture where this species is often considered a pest (Elliott, 1990), which may also explain this species' success and wide distribution across multiple climatic regions over sub-Saharan Africa (Hockey et al. 2005).

4.7 ACKNOWLEDGMENTS

I would like to thank Philip Pattinson for access to his farm and home ‘Mooihoek’ in Harrismith as well as Bill and Gayle Ross-Adams for providing accommodation and access to their property.

Ethics

This work was approved by the Animal Ethics Committee of the University of Pretoria (protocol NAS141/2020) and the Research and Scientific Ethics Committee of the South African National Biodiversity Institute (SANBI NZG/RES /P19/13). Birds were captured under permit JM 8,057/2019 from the Free State province’s Department of Economic, Small Business Development, Tourism and Environmental.

Funding

This work is based on research supported by the DSI-NRF Centre of Excellence at the FitzPatrick Institute and the National Research Foundation of South Africa (grant 119754 to A.E.M.). Any opinions, findings, and conclusions or recommendations expressed in this material are those of the authors and do not necessarily reflect the views of the National Research Foundation.

4.8 REFERENCES

- Angilletta, M., Cooper, B. S., Schuler, M. S. and Boyles, J. G.** (2010). The evolution of thermal physiology in endotherms. *Front Biosci (Elite Ed)* **2**, 861–81.
- Barton, K.** (2019). MuMIn: Multi-Model Inference. R package version 1.43.6. <https://CRAN.R-project.org/package=MuMIn>.
- Bernstein, M. H., Curtis, M. B. and Hudson, D. M.** (1979). Independence of brain and body temperatures in flying American kestrels, *Falco sparverius*. *Am J Physiol Regul Integr Comp Physiol* **6**,
- Boyles, J. G., Seebacher, F., Smit, B. and McKechnie, A. E.** (2011). Adaptive thermoregulation in endotherms may alter responses to climate change. *Integr Comp Biol* **51**, 676–690.
- Burnham, K. P. and Anderson, D. R.** (2002). *Model selection and multi-model inference: a practical information-theoretic approach*. 2nd edn. New York, NY: Springer.
- Campbell, G. S. and Norman, J. M.** (1998). *An introduction to environmental biophysics*. New York: Springer-Verlag.
- Czenze, Z. J., Kemp, R., van Jaarsveld, B., Freeman, M. T., Smit, B., Wolf, B. O. and McKechnie, A. E.** (2020). Regularly drinking desert birds have greater evaporative cooling capacity and higher heat tolerance limits than non-drinking species. *Funct Ecol* **34**,
- Dawson, W. R.** (1954). *Temperature regulation and water requirements of the brown and Abert towhees, Pipilo fuscus and Pipilo aberti*. In *University of California publications in zoology*. vol 59. (ed. Bartholomew, G. A.), Crescitelli, F.), Bullock, T. H.), Furgason, W. H.), and Schechtman, A. M.) Berkeley, CA: University of California Press.
- Dawson, W. R. and Schmidt-Nielsen, K.** (1964). “*Terrestrial animals in dry heat: desert birds*” in *Handbook of Physiology*. Adaptation. Washington, DC: American Physiological Society.
- Elliott, C. C. H.** (1990). The migrations of the Red-billed Quelea *Quelea quelea* and their relation to crop damage. *IBIS* **132**, 232–237.
- Fick, S. E. and Hijmans, R. J.** (2017). WorldClim 2: new 1-km spatial resolution climate surfaces for global land areas. *International Journal of Climatology* **37**, 4302–4315.
- Freeman, M. T., Czenze, Z. J., Schoeman, K. and McKechnie, A. E.** (2020). Extreme hyperthermia tolerance in the world’s most abundant wild bird. *Sci Rep* **10**, 1–6.

- Freeman, M. T., Czenze, Z. J., Schoeman, K. and McKechnie, A. E.** (2022). Adaptive variation in the upper limits of avian body temperature. *Proc Natl Acad Sci U S A* **119**,.
- Gerson, A. R., Wolf, B. O., Smith, E. K., Smit, B. and McKechnie, A. E.** (2014a). The Impact of Humidity on Evaporative Cooling in Small Desert Birds Exposed to High Air Temperatures. *Physiological and Biochemical Zoology* **87**, 782–795.
- Gerson, A. R., Smith, E. K., Smit, B., McKechnie, A. E. and Wolf, B. O.** (2014b). The impact of humidity on evaporative cooling in small desert birds exposed to high air temperatures. *Physiological and Biochemical Zoology* **87**, 782–795.
- Gerson, A. R., McKechnie, A. E., Smit, B., Whitfield, M. C., Smith, E. K., Talbot, W. A., McWhorter, T. J. and Wolf, B. O.** (2019). The functional significance of facultative hyperthermia varies with body size and phylogeny in birds. *Funct Ecol* **33**, 597–607.
- Hockey, P. A. R., Dean, W. R. J. and Ryan, P. G.** (2005). Red-billed Quelea. In *Roberts Birds of Southern Africa VII*, pp. 1025–1026.
- IPCC** (2021). *Climate Change 2021: The Physical Science Basis. Contribution of Working Group I to the Sixth Assessment Report of the Intergovernmental Panel on Climate Change.*
- Kassambara, A.** (2015). rstatix: Pipe-friendly framework for basic statistical tests.
- Kregel, Kevin. C.** (2002). Heat shock proteins: modifying factors in physiological stress responses and acquired thermotolerance. *J Appl Physiol* **92**, 2177–2186.
- Lasiewski, R. C., Acosta, A. L. and Bernstein, M. H.** (1966). Evaporative water loss in birds-I. Characteristics of the open flow method of determination, and their relation to estimates of thermoregulatory ability. *Comp Biochem Physiol* **19**, 445–457.
- Lighton** (2008). *Measuring Metabolic Rates; A Manual for Scientists.* Oxford University Press.
- McKechnie, A. E., Rushworth, I. A., Myburgh, F. and Cunningham, S. J.** (2021). Mortality among birds and bats during an extreme heat event in eastern South Africa. *Austral Ecol* 687–691.
- Midtgård, U.** (1983). Scaling of the brain and the eye cooling system in birds: A morphometric analysis of the Rete ophthalmicum. *Journal of Experimental Zoology* **225**, 197–207.
- Mucina, L. and Rutherford, M. C.** (2006). *The vegetation of South Africa, Lesotho and Swaziland.* (ed. Mucina, L.) and Rutherford, M.) National Botanical Institute, South Africa.
- Muggeo, V.** (2016). *Segmented mixed models with random changepoints in R.*

- Newberry, G. N. and Swanson, D. L.** (2018). Elevated temperatures are associated with stress in rooftop-nesting Common Nighthawk (*Chordeiles minor*) chicks. *Conserv Physiol* **6**, 1–12.
- Pinheiro J, Bates D, DebRoy S, Sarkar D, R. C. Team.** (2015). nlme: Linear and Nonlinear Mixed Effects Models.
- Powers, D. R.** (1992). Effect of temperature and humidity on evaporative water loss in Anna's hummingbird (*Calypte anna*). *Journal of Comparative Physiology B* **162**, 74–84.
- Ratnayake, H. U., Kearney, M. R., Govekar, P., Karoly, D. and Welbergen, J. A.** (2019). Forecasting wildlife die-offs from extreme heat events. *Anim Conserv* **22**, 386–395.
- Scholander, P. F., Hock, R., Walters, V. and Johnson, F.** (1950). Heat Regulation in Some Arctic and Tropical Mammals and Birds. *Biological Bulletin* **99**, 237–258.
- Smit, B., Harding, C. T., Hockey, P. A. R. and McKechnie, A. E.** (2013). Adaptive thermoregulation during summer in two populations of an arid-zone passerine. *Ecology* **94**, 1142–1154.
- Tieleman, B. I. and Williams, J. B.** (2000). The adjustment of avian metabolic rates and water fluxes to desert environments. *Physiological and Biochemical Zoology* **73**, 461–479.
- Tieleman, B. I., Williams, J. B. and Bloomer, P.** (2003). Adaptation of metabolism and evaporative water loss along an aridity gradient. *Proceedings of the Royal Society B: Biological Sciences* **270**, 207–214.
- Tracy, C. R., Welch, W. R. and Porter, W. P.** (2010). *Properties of air: a manual for use in biophysical ecology*. 4th ed. Madison, USA: University of Wisconsin.
- van Dyk, M., Noakes, M. J. and McKechnie, A. E.** (2019). Interactions between humidity and evaporative heat dissipation in a passerine bird. *J Comp Physiol B* **189**, 299–308.
- Weathers, W. W.** (1979). Climatic Adaptation in Avian Standard Metabolic Rate. *Oecologia (Berl.)* **42**, 81–89.
- Weathers, W. W.** (1997). Energetics and Thermoregulation by Small Passerines of the Humid, Lowland Tropics. *Auk* **114**, 341–353.
- Welbergen, J. A., Klose, S. M., Markus, N. and Eby, P.** (2008). Climate change and the effects of temperature extremes on Australian flying-foxes. *Proceedings of the Royal Society B: Biological Sciences* **275**, 419–425.

- Whitfield, M. C., Smit, B., McKechnie, A. E. and Wolf, B. O.** (2015). Avian thermoregulation in the heat: scaling of heat tolerance and evaporative cooling capacity in three southern African arid-zone passerines. *Journal of Experimental Biology* **218**, 1705–1714.
- Withers, P. C.** (1992). *Comparative animal physiology*. Saunders College Pub.
- Xie, S., Tearle, R. and McWhorter, T. J.** (2018). Heat shock protein expression is upregulated after acute heat exposure in three species of Australian desert birds. *Avian Biol Res* **11**, 263–273.
- Zeileis, A. and Hothorn, T.** (2002). Diagnostic Checking in Regression Relationships. *R News* **2**, 7–10.

4.9 ADDITIONAL INFORMATION

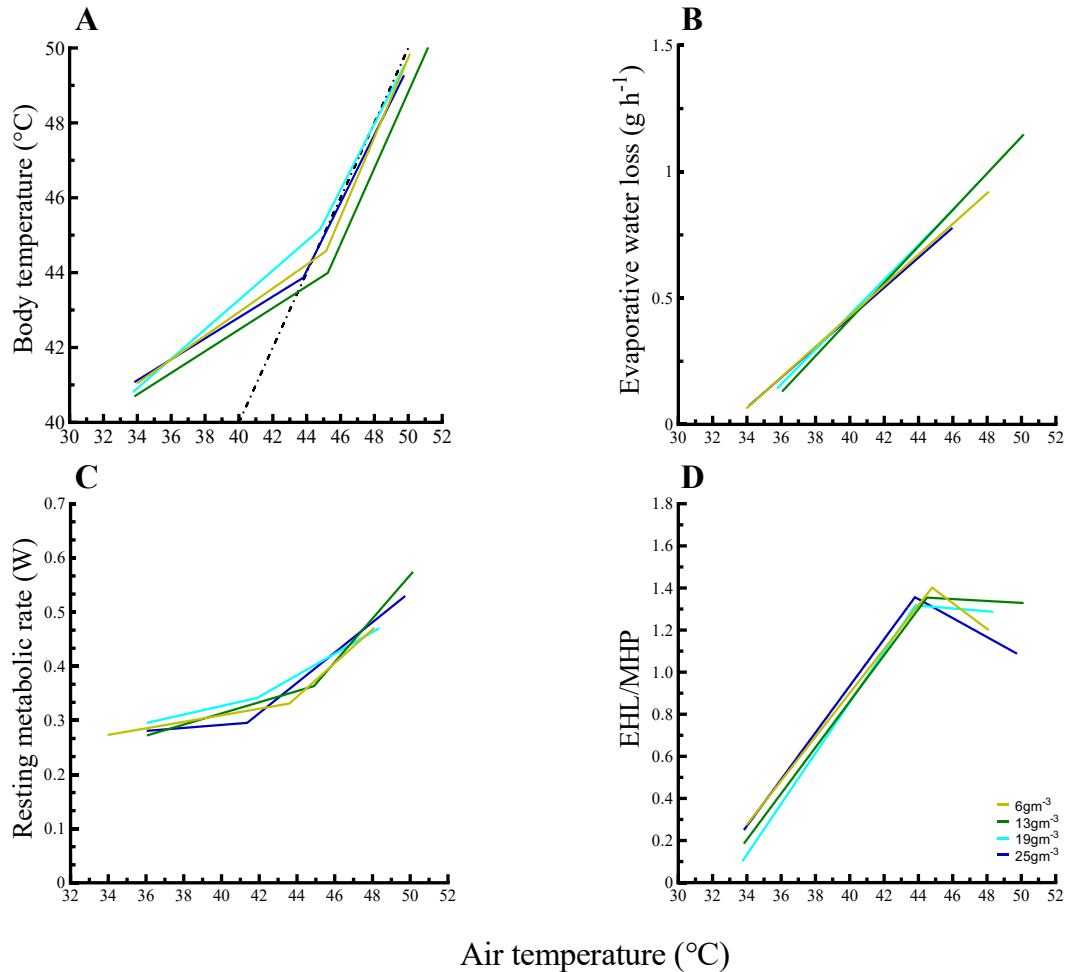


Figure S7 Segmented linear relationship between a.) body temperature (T_b), b.) evaporative water loss (EWL), c.) resting metabolic rate (RMR) and d.) evaporative cooling efficiency (EHL/MHP) with air temperature (T_{air}) over four different treatments of humidity [6 g m^{-3} (gold line), 13 g m^{-3} (green line), 19 g m^{-3} (light blue line), 25 g m^{-3} (dark blue line)] in red-billed queleas (*Quelea quelea*). The dashed line in a.) shows $T_b = T_{air}$.

Table S1.1 Summary of thermoregulatory performance as a function of chamber air temperature (T_a) and four absolute humidity treatments (6 g m^{-3} , 13 g m^{-3} , 19 g m^{-3} , 25 g m^{-3}) for red-billed quelea (*Q.quelea*). T_b = body temperature, T_{air} = ambient temperature, RMR = resting metabolic rate, EWL = evaporative water loss, EHL= evaporative heat loss, MHP = metabolic heat production. Means, SD and N are reported. Humidity treatment birds (6 g m^{-3} , 13 g m^{-3} , 19 g m^{-3} , 25 g m^{-3}) began respirometry protocols at $T_{air} = 34\text{ }^\circ\text{C}$.

Variable	6 g m^{-3}	13 g m^{-3}	19 g m^{-3}	25 g m^{-3}
Body mass (g)	17.3±0.6 (10)	17.8±1.2 (10)	17.1±0.8 (10)	17.2±0.5 (10)
Body temperature				
Min. T_b ($^\circ\text{C}$)	41.2±0.5 (10)*	40.9±0.7*	41.0±0.7 (10)*	41.2±0.7 (10)*
Inflection 1				
Inflection T_{air} ($^\circ\text{C}$)	~34.0	<34.0	<34.0	<34.0
T_b versus T_{air} slope ($^\circ\text{C}$)	0.31	0.28	0.39	0.28
Inflection 2				
Second inflection T_{air} ($^\circ\text{C}$)	45.2	45.2	44.8	43.9
Second T_b versus T_{air} slope ($^\circ\text{C}$)	1.06	0.93	0.88	0.91
Max T_b ($^\circ\text{C}$)	48.7±0.2 (10)	48.6±0.4 (10)	48.6±0.7 (10)	48.4±0.2 (10)
Max T_{air} ($^\circ\text{C}$)	48.3±0.8 (10)	49.8±0.8 (10)	48.1±1.1 (10)	47.8±0.9 (10)
T_b at onset of panting ($^\circ\text{C}$)	43.8±1.1 (10)	41.8±0.6 (10)	42.1±0.6 (10)	42.05±0.5 (10)
T_a at onset of panting ($^\circ\text{C}$)	38.9±1.3 (10)	37.7±0.7 (10)	37.4±0.7 (10)	37.8±0.7 (10)
Resting metabolic rate				
Min. RMR (W)	0.3±0.04 (10)	0.3±0.02 (10)	0.3±0.04 (10)	0.3±0.04 (10)
T_{inc} ($^\circ\text{C}$)	43.6	43.1	41.9	41.4
RMR slope ($\text{mW } ^\circ\text{C}^{-1}$)	31.1	24.02	19.9	28.0
Max. RMR (W)	0.5±0.1 (7)	0.5±0.1 (10)	0.5±0.1 (6)	0.5±0.1 (7)
Max. RMR/min. RMR	1.7	1.7	1.7	1.7
Evaporative water loss				
Min. EWL (g h^{-1})	0.1±0.1 (10)	0.1±0.02 (10)	0.1±0.03 (10)	0.1±0.03 (10)
Inflection T_a ($^\circ\text{C}$)	~34.2	~34.8	~35.6	< 34
EWL slope 1 ($\text{g h}^{-1} ^\circ\text{C}^{-1}$)	0.06	0.07	0.07	0.05
Max. EWL (g h^{-1})	0.9±0.2 (7)	1.0 (1)	0.9±0.2 (10)	0.8±0.2 (7)
		0.9±0.07 (10)		
Max. EWL/min. EWL	9.0	10.0	9.0	8.0
Evaporative cooling efficiency (EHL/MHP)				
Min. EHL/MHP	0.4±0.1 (10)	0.2±0.1 (10)	0.2±0.1 (10)	0.3±0.1 (10)
EHL/MHP inflection $T_a - T_b$	-6.6	-5.7	-6.2	-6.4
EHL/MHP slope	0.15	0.15	0.19	0.20
Inflection 2				
Second EHL/MHP inflection $T_a - T_b$	NA	NA	-1.23	-0.72
Second EHL/MHP slope	NA	NA	0.02	-0.02
Second EHL/MHP inflection T_a	44.8	44.5	43.7	43.8
Second EHL/MHP inflection T_a Slope	-0.06	-0.005	-0.05	-0.05
Max. EHL/MHP	1.4±0.2 (10)	1.5±0.2 (10)	1.3±0.2 (10)	1.3±0.2 (7)

Table S1.2 Mass-specific resting metabolic rates (RMR) and evaporative water loss (EWL) rate at high T_a in red-billed Quelea subjected to four treatments of varying absolute humidity. Means, SD and N are reported

Variable	6 g m ⁻³	13 g m ⁻³	19 g m ⁻³	25 g m ⁻³
RMR				
Min. RMR (mW g ⁻¹)	15.6±2.2 (10)	14.7±1.4 (10)	16.4±2.7 (10)	16.1±2.1 (10)
RMR slope (mW g ⁻¹ °C ⁻¹)	1.8	1.7	1.4	0.7
Max. RMR (mW g ⁻¹)	27.8±4.7 (7)	32.1 (1) 16.8±6.0 (10)	27.2±4.4(6)	27.7±5.3 (7)
Min. EWL (mg h ⁻¹ g ⁻¹)	8.2±2.8 (10)	5.0±1.3 (10)	5.7±2.0 (10)	8.0±1.5 (10)
EWL slope (mg h ⁻¹ g ⁻¹ °C ⁻¹)	3.6	2.18	4.11	3.63
Max. EWL (mg h ⁻¹ g ⁻¹)	51.8±7.2 (7)	60.3 (1) 57.4±10.0 (10)	52.4±8.1 (10)	45.9±11.9 (7)

Table S2.1 Tukey HSD post-hoc test comparing maximum body temperature values (T_{bmax}) for *Q.quelea* exposed to increasing T_{air} at four different absolute humidity treatments (6, 13, 19 and 25 g m⁻³). Significant difference is indicated by bold p-values ($p < 0.05$). Upper and lower confidence limits (95%) of the honest significant difference (HSD) are provided.

	HSD	95% CI lower	95% CI upper	p-value
6gm ⁻³ vs. 13gm ⁻³	0.1	-0.36	0.56	0.94
6gm ⁻³ vs. 19gm ⁻³	0.04	-0.43	0.51	0.99
6gm ⁻³ vs. 25gm ⁻³	0.34	-0.13	0.80	0.22
13gm ⁻³ vs. 19gm ⁻³	-0.06	-0.53	0.41	0.99
13gm ⁻³ vs. 25gm ⁻³	0.24	-0.23	0.71	0.52
19gm ⁻³ vs. 25gm ⁻³	0.3	-0.17	0.77	0.33

Table S2.2 Tukey HSD post-hoc test comparing heat tolerance limit (HTL) for *Q.quelea* exposed to increasing T_{air} at four different absolute humidity treatments (6, 13, 19 and 25 g m⁻³). Significant difference is indicated by bold p-values ($p < 0.05$). Upper and lower confidence limits (95%) of the honest significant difference (HSD) are provided.

	HSD	95% CI lower	95% CI upper	p-value
6gm ⁻³ vs. 13gm ⁻³	-0.99	-1.99	0.02	0.06
6gm ⁻³ vs. 19gm ⁻³	0.25	-0.76	1.26	0.91
6gm ⁻³ vs. 25gm ⁻³	0.45	-0.56	1.46	0.64
13gm ⁻³ vs. 19gm ⁻³	1.24	0.23	2.25	0.01
13gm ⁻³ vs. 25gm ⁻³	1.43	0.42	2.44	<0.01
19gm ⁻³ vs. 25gm ⁻³	0.19	-0.81	1.20	0.95

Table S2.3 Tukey HSD post-hoc test comparing maximum rates of evaporative water loss (EWL) for *Q.quelea* exposed to increasing T_{air} at four different absolute humidity treatments (6, 13, 19 and 25 g m⁻³). Significant difference is indicated by bold p-values ($p < 0.05$). Upper and lower confidence limits (95%) of the honest significant difference (HSD) are provided.

	HSD	95% CI lower	95% CI upper	p-value
6gm ⁻³ vs. 13gm ⁻³	-0.1	-0.35	0.15	0.69
6gm ⁻³ vs. 19gm ⁻³	0	-0.25	0.25	1
6gm ⁻³ vs. 25gm ⁻³	0.1	-0.17	0.37	0.75
13gm ⁻³ vs. 19gm ⁻³	0.1	-0.13	0.33	0.63
13gm ⁻³ vs. 25gm ⁻³	0.2	-0.05	0.45	0.15
19gm ⁻³ vs. 25gm ⁻³	0.1	-0.15	0.35	0.70

Table S2.4 Tukey HSD post-hoc test comparing maximum rates of resting metabolic rate (RMR) for *Q.quelea* exposed to increasing T_{air} at four different absolute humidity treatments (6, 13, 19 and 25 g m⁻³). Significant difference is indicated by bold p-values ($p < 0.05$). Upper and lower confidence limits (95%) of the honest significant difference (HSD) are provided.

	HSD	95% CI lower	95% CI upper	p-value
6gm ⁻³ vs. 13gm ⁻³	0	-0.14	0.14	1
6gm ⁻³ vs. 19gm ⁻³	0	-0.15	0.15	1
6gm ⁻³ vs. 25gm ⁻³	0	-0.15	0.15	1
13gm ⁻³ vs. 19gm ⁻³	0	-0.14	0.14	1
13gm ⁻³ vs. 25gm ⁻³	0	-0.14	0.14	1
19gm ⁻³ vs. 25gm ⁻³	0	-0.16	0.15	1

Table S2.5 Tukey HSD post-hoc test comparing maximum rates of maximum values of evaporative cooling efficiency (EHL/MHP) for *Q.quelea* exposed to increasing T_{air} at four different absolute humidity treatments (6, 13, 19 and 25 g m⁻³). Significant difference is indicated by bold p-values (p<0.05). Upper and lower confidence limits (95%) of the honest significant difference (HSD) are provided.

	HSD	95% CI lower	95% CI upper	p-value
6g m ⁻³ vs. 13 g m ⁻³	-0.1	-0.34	0.14	0.68
6 g m ⁻³ vs. 19 g m ⁻³	0.1	-0.14	0.34	0.68
6 g m ⁻³ vs. 25 g m ⁻³	0.1	-0.17	0.36	10.74
13 g m ⁻³ vs. 19 g m ⁻³	0.2	-0.04	0.44	1
13 g m ⁻³ vs. 25 g m ⁻³	0.2	-0.07	0.46	1
19 g m ⁻³ vs. 25 g m ⁻³	0	-0.26	0.26	1

Table S3.1 Pairwise t-test comparing slope 1 of body temperature $\sim T_{\text{air}}$ for *Q.quelea* at four different absolute humidity treatments (6, 13, 19 and 25 g m⁻³). Significant difference is indicated by bold p-values (p<0.05). Test statistics, degrees of freedom (df), sample size for each treatment (n), p-value and adjusted p-value (Bonferroni correction) are provided.

Treatment 1	Treatment 2	n1	n2	t-statistic	df	p-value	adjusted p-value
13 g m ⁻³	19 g m ⁻³	56	50	-3.94	98.98	0.000	0.001
13 g m ⁻³	25 g m ⁻³	56	56	-1.67	109.58	0.098	0.68
13 g m ⁻³	6 g m ⁻³	56	58	-1.78	111.99	0.077	0.46
19 g m ⁻³	25 g m ⁻³	50	56	2.30	101.27	0.023	0.09
19 g m ⁻³	6 g m ⁻³	50	58	2.26	101.30	0.026	0.15
25 g m ⁻³	6 g m ⁻³	56	58	-0.08	111.70	0.94	1.000

Table S3.2 Pairwise t-test comparing slope 2 of body temperature $\sim T_{\text{air}}$ for *Q.quelea* at four different absolute humidity treatments (6, 13, 19 and 25 g m⁻³). Significant difference is indicated by bold p-values (p<0.05). Test statistics, degrees of freedom (df), sample size for each treatment (n), p-value and adjusted p-value (Bonferroni correction) are provided.

Treatment 1	Treatment 2	n1	n2	t-statistic	df	p-value	adjusted p-value
13 g m ⁻³	19 g m ⁻³	31	26	-1.60	54.89	0.115	1
13 g m ⁻³	25 g m ⁻³	31	28	-1.25	55.85	0.216	1
13 g m ⁻³	6 g m ⁻³	31	28	-1.22	56.98	0.229	1
19 g m ⁻³	25 g m ⁻³	26	28	0.42	51.47	0.675	1
19 g m ⁻³	6 g m ⁻³	26	28	0.33	51.80	0.742	1
25 g m ⁻³	6 g m ⁻³	28	28	-0.06	52.61	0.954	1

Table S3.3 Pairwise t-test comparing evaporative water loss (EWL) $\sim T_{\text{air}}$ for *Q.quelea* at dry air (0 g m⁻³) and four different absolute humidity treatments (6, 13, 19 and 25 g m⁻³). Significant difference is indicated by bold p-values (p<0.05). Test statistics, degrees of freedom (df), sample size for each treatment (n), p-value and adjusted p-value (Bonferroni correction) are provided.

Treatment 1	Treatment 2	n1	n2	t-statistic	df	p-value	adjusted p-value
13 g m ⁻³	19 g m ⁻³	80	66	-0.36	142.24	7.18E-01	1
13 g m ⁻³	25 g m ⁻³	80	78	0.72	153.12	4.70E-01	1
13 g m ⁻³	6 g m ⁻³	80	79	0.75	154.02	4.53E-01	1
19 g m ⁻³	25 g m ⁻³	66	78	1.11	133.73	2.71E-01	1
19 g m ⁻³	6 g m ⁻³	66	79	1.13	134.55	2.59E-01	1
25 g m ⁻³	6 g m ⁻³	78	79	0.03	154.99	9.73E-01	1

Table S3.4 Pairwise t-test comparing resting metabolic rate (RMR) $\sim T_{\text{air}}$ for *Q.quelea* at dry air (0 g m^{-3}) and four different absolute humidity treatments (6, 13, 19 and 25 g m^{-3}). Significant difference is indicated by bold p-values ($p < 0.05$). Test statistics, degrees of freedom (df), sample size for each treatment (n), p-value and adjusted p-value (Bonferroni correction) are provided.

Treatment 1	Treatment 2	n1	n2	t-statistic	df	p-value	adjusted p-value
13 g m^{-3}	19 g m^{-3}	21	36	1.50	40.32	0.14	1
13 g m^{-3}	25 g m^{-3}	21	38	2.24	39.58	0.31	0.308
13 g m^{-3}	6 g m^{-3}	21	28	1.84	39.35	0.07	0.73
19 g m^{-3}	25 g m^{-3}	36	38	0.87	71.76	0.39	1
19 g m^{-3}	6 g m^{-3}	36	28	0.42	60.58	0.68	1
25 g m^{-3}	6 g m^{-3}	38	28	-0.43	61.26	0.67	1

Table S3.5 Pairwise t-test comparing evaporative cooling efficiency (EHL/MHP) $\sim T_{\text{air}}$ for *Q.quelea* at dry air (0 g m^{-3}) and four different absolute humidity treatments (6, 13, 19 and 25 g m^{-3}). Significant difference is indicated by bold p-values ($p < 0.05$). Test statistics, degrees of freedom (df), sample size for each treatment (n), p-value and adjusted p-value (Bonferroni correction) are provided.

Treatment 1	Treatment 2	n1	n2	t-statistic	df	p-value	adjusted p-value
13 g m^{-3}	19 g m^{-3}	59	50	2.22	106.06	0.029	0.29
13 g m^{-3}	25 g m^{-3}	59	50	0.68	106.88	0.498	1
13 g m^{-3}	6 g m^{-3}	59	61	-0.29	117.71	0.773	1
19 g m^{-3}	25 g m^{-3}	50	50	-1.60	97.65	0.113	1
19 g m^{-3}	6 g m^{-3}	50	61	-2.54	106.80	0.013	0.13
25 g m^{-3}	6 g m^{-3}	50	61	-0.99	108.24	0.326	1